68

INUNDATION AND SUBSTRATE STABILITY STUDY TO SUPPORT VERDE RIVER VEGETATION ANALYSIS

Prepared for:

Salt River Project
P.O. Box 52025
Phoenix, Arizona 85072-2025

Prepared by:

Mussetter Engineering, Inc.
1730 S. College Avenue, Suite 100
Fort Collins, Colorado 80525

May 20, 2004

TABLE OF CONTENTS

Page

LIST OF FIGURES

LIST OF PLATES

LIST OF TABLES

1. INTRODUCTION

1.1. Background

The Salt River Project (SRP) operates two dams on the Verde River (Horseshoe Dam and Bartlett Dam) to provide water to municipal and agricultural users in the area of metropolitan Phoenix (**Figure 1.1**). The effects of these dams on cottonwood-willow habitat for bald eagles, southwestern willow flycatchers, and yellow-billed cuckoos along the lower Verde River were discussed during approval of the Roosevelt Habitat Conservation Plan (RHCP), which is part of SRP's Incidental Take Permit (ITP) under Section 10 of the Endangered Species Act (ESA). More recently, SRP has initiated preparation of an ITP application for continued operation of Horseshoe and Bartlett Dams, and is evaluating several alternatives to modify the operation of the dams in order to create and maintain habitat for bald eagles, flycatchers and cuckoos. In addition, the indirect effects of alternative dam operations on Verde River reservoir levels and releases would be evaluated in the Environmental Impact Statement (EIS) that would be issued by the U.S. Fish and Wildlife Service (USFWS) on consideration of a Section 10 permit for Horseshoe and Bartlett Dams.

In order to evaluate the effects of the dams on woody riparian vegetation such as cottonwood-willow habitat, it is first necessary to quantify the effects of various dam operations on the frequency and duration of inundation of likely areas for the establishment and maintenance of the vegetation, and to determine the flows necessary to mobilize the channel bed and bar sediments that form the substrate for the vegetation. This information can then be used by plant ecologists to evaluate the likely effects of various dam operations on the establishment and maintenance of the vegetation.

1.2. Study Objectives and Scope of Work

Mussetter Engineering, Inc. (MEI) was retained by SRP to assist plant ecologists from ERO Resources Corporation (ERO) in addressing the issue of whether re-operation of the dams on the Verde River could significantly improve downstream conditions for establishment and maintenance of woody riparian vegetation. MEI's work involved assistance to ERO in selecting study sites for the analysis, preparation of one-dimensional (1-D) hydraulic models each of the three selected sites (Figure 1.1), and use of the models to evaluate the extent and frequency at which various geomorphic surfaces are inundated and the range of flows that are required to mobilize the sediment that makes up the in-channel bars and channel margins within the riparian zone. This information was then provided to ERO for use in their analysis of the vegetation.

Specific tasks that were carried out to meet the objectives of the study included the following:

1. An aerial reconnaissance of Verde River from the confluence with the Salt River to near the Verde River near Tangle Creek gage, upstream from Horseshoe Reservoir, was conducted on November 11, 2002, to observe the characteristics of the study reach and to select sites for more detailed study. Participants in the aerial reconnaissance included Craig Sommers and Liz Payson (ERO) and Bob Mussetter and Stuart Trabant (MEI).

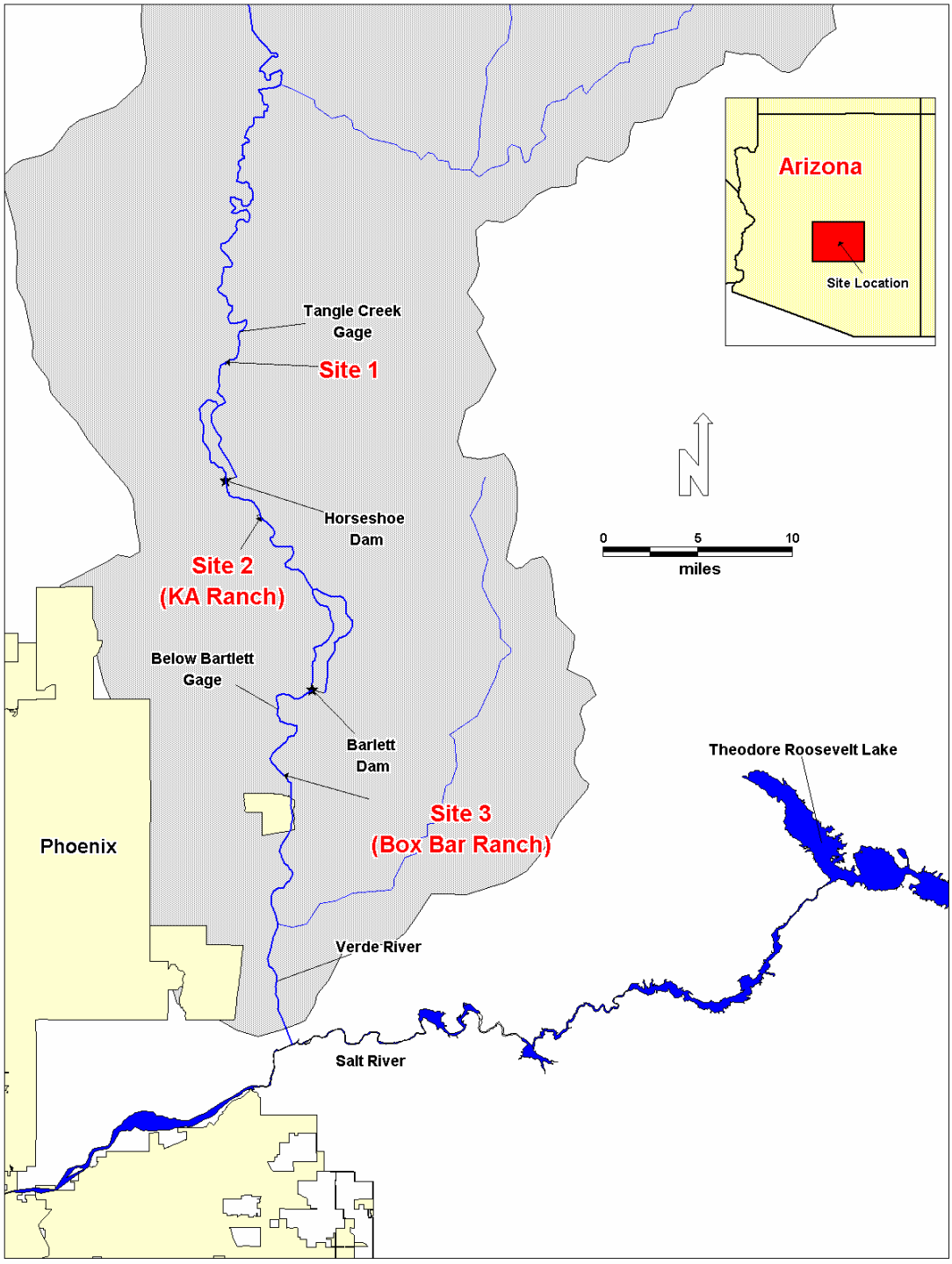

Figure 1.1. Location map.

2. A field visit to each of the three selected study sites was conducted on November 5 through 7, 2002, to lay out cross sections to be surveyed by SRP for use in the hydraulic modeling, to collect sediment samples of the channel bed and the various geomorphic surfaces at each site, and to make other general observations about the physical characteristics of the sites. The cross-section layouts and sediment sampling were performed by Bob Mussetter and Stuart Trabant.

3. Available hydrologic data for the study reach were obtained and reviewed.

4. Recorded hydrographs that could be used to evaluate the effects of operational changes on flood flows at each of the study sites were identified. These hydrographs were provided to SRP, who then used the RiverSim model to develop hydrographs that reflect the effects of the proposed operational changes.

5. One-dimensional (1-D) hydraulic models were developed for each of the study sites using cross-sectional data and aerial mapping that was provided to MEI by SRP, and the models were applied for the range of flows that occur in the observed and routed hydrographs.

6. Results from the hydraulic models were used to evaluate the:

   a. frequency and duration of inundation of various geomorphic surfaces along the river at each site, for each of the hydrographs, and

   b. range of flows necessary to mobilize the sediment that makes up the in-channel bars and channel margins within the riparian zone.

1.3. Authorization and Study Team

This work was performed by MEI under a contract with the Salt River Project Agricultural Improvement and Power District and Salt River Valley Water User's Association (referred to jointly as the SRP). SRP's Authorized Representative responsible for administration of the contract was Mr. Steve Doncaster, Senior Attorney. The Technical Coordinator for SRP was Craig Sommers of ERO. MEI's project manager was Dr. Bob Mussetter, P.E., and the following MEI staff contributed to the work:

- Dr. Mike Harvey, P.G., Principal Geomorphologist
- Mr. Gary Wolff, P.E. (CO), Senior Engineer
- Mr. Stuart Trabant, P.E. (CO), Project Engineer
- Ms. Jesa Lunger, E.I.T, Project Engineer
- Mr. Matt Iman, Graphics and GIS
- Ms. Bonnie Vail, Word Processing

2. PHYSICAL CHARACTERISTICS OF THE STUDY REACH AND STUDY SITES

2.1. General Characteristics of the Verde River

The Verde River heads in, and flows through, the highlands and valleys of central Arizona, and the physiography and geology of the region are transitional between the high elevation, relatively flat Colorado Plateau and the lower elevation Basin and Range province (Pearthree, 1996). Downstream of Big Chino Valley, in the reach of interest to this investigation, the Verde River is entrenched into a relatively narrow, deep canyon from upstream of Horseshoe Reservoir to just downstream of Bartlett Reservoir, where the valley bottom widens, and the river is less confined. The entrenchment of the Verde River through the project reach is due to downcutting through blocked basin outlets that commenced about 2 to 2.5 million years ago and has continued through the Quaternary (Pope and Péwé, 1973; Pope, 1974; Péwé, 1978, Pearthree, 1993; House and Pearthree, 1993).

The long period of downcutting by the Verde River has created a series of terraces that flank the river ranging in age from early-Pleistocene to late Holocene. In general, the older terraces are more erosion-resistant than the younger terraces (Pearthree, 1996). Long-term downcutting and the relative erodibility of pre-Quaternary bedrock and basin-fill units effectively control the extent and character of the Quaternary alluvial deposits and floodplain along the Verde River. Where the lithologies are more erosion-resistant, the river valley is steep and narrow with relatively limited amounts of alluvial storage in the valley bottom. In contrast, where the bounding lithologies are more erodible, the valley width is greater, the slope is flatter, and there is considerably more alluvial storage in the valley bottom (Pearthree, 1996). In common with most canyon-bound rivers, local constrictions and expansions in the valley cause localized accumulations of alluvial sediments (Graf, 1980; Webb et al., 1988; Lisle, 1986; O'Connor et al., 1986; Harvey et al., 1993).

The relative widths of the valley floor determine the geomorphic effectiveness of the large infrequent floods (>10-year recurrence interval) that tend to control channel form in arid regions (Baker, 1977; Wolman and Gerson, 1978; Graf, 1988). In confined reaches of the valley, there is little potential for lateral migration of the river; whereas, the lateral migration potential increases markedly where the valley is wider. In general, where the valleys are narrow and confined the large infrequent flood events tend to disturb most of the valley floor sediments, thereby eliminating, or significantly modifying, any vegetation that may have become established in the interflood period. In contrast, wider reaches tend to be depositional during infrequent flood events, and there is more of a tendency for the channels to relocate, in turn, causing disturbance to established plant communities.

2.2. Characteristics of Detailed Study Sites

During the field reconnaissance, three detailed study sites were selected from an approximately 15-mile long reach of the river that extended from about four miles downstream from Bartlett Dam to about three miles upstream from the head of Horseshoe Reservoir, with one site located upstream from Horseshoe Reservoir, one site between Horseshoe Dam and the head of Bartlett Reservoir, and the third site located downstream from Bartlett Dam (Figure 1.1). The sites were selected in relatively wide segments of the valley where the river is bounded by alluvium on at least one side, because the riparian zone in these areas is more likely to respond to changes in

flow regime than in the more confined reaches. The study sites were selected to have similar geomorphic characteristics, to the extent possible, to provide a basis for evaluating effects of changes in flow regime resulting from the operation of the dams.

The upstream study site (Site 1), is located between the head of Horseshoe Reservoir and the USGS Verde River below Tangle Creek gage (USGS Gage 09508500). The middle site (Site 2), which is also referred to as the KA Ranch site, is located 1.7 miles downstream from Horseshoe Dam and a short just downstream from the mouth of Davenport Wash. The most downstream site (Site 3) is located about 2.3 miles downstream from Bartlett Dam and about 0.6 miles upstream from Box Bar Ranch. Aerial photographs at each site showing model cross sections and sediment sample locations are presented in **Figures 2.1 through 2.3**, respectively. Sites 1 and 2 are located in narrow reaches of the valley, and they have average slopes of 0.0027 (14 feet per mile) and 0.0041 (22 feet per mile), respectively, based on a longitudinal profile of the river that was developed from the USGS 7½" quadrangle maps (**Figure 2.4**). Site 3 is located in a wider reach of the valley and it has a slope of 0.0023 (12 feet per mile).

The following sections provide descriptions of the specific geologic, geomorphic and sedimentologic characteristics of the three sites.

2.2.1. Site 1: Upstream of Horseshoe Reservoir near Tangle Creek Gage

The width of the valley bottom at Site 1 is about 600 feet, and the site is bounded along the left side of the valley by a number of Holocene age terraces. In common with most dryland rivers, there is no defined floodplain between the terraces, and the area between the terraces is occupied by braided channels (Graf, 1988). Several older late- to mid-Pleistocene-age terraces are located father back from the river. The upstream portion of the right side of the valley is composed of pre-Quaternary basin-fill sediments, but the remainder of the right side of the valley is composed of coalesced late- to mid-Pleistocene age terraces and alluvial fans, and late-Holocene-age terraces (Pearthree, 1993). The active channel at this site is about 200 feet wide and flanked by narrow bands of riparian vegetation. In the lower two-thirds of the site, the active channel is flanked along the left bank by a very sparsely vegetated gravel-cobble bar that represents a high-flow chute-channel that is confined on its left margin by a Holocene-age terrace. In the upper third of the site, the chute channel is separated from the main channel by a relatively high-elevation vegetated bar (**Plate 1**). The downstream hydraulic control for the site is created by a constriction caused by the presence of erosion-resistant late- to mid-Pleistocene-age coalesced fans on the right bank, and a late-Holocene-age terrace on the left bank. Plots of the surveyed cross sections that were used in the hydraulic modeling, showing the geometry of the channel are included in **Appendix A**. (The locations of the cross sections are shown in Figure 2.1.)

Pebble counts (Wolman, 1954) were conducted at four locations within the site (Figure 2.1). Riffles in the main channel (WC7, WC9), a low-elevation, bank-attached bar (WC6) within the active channel and a higher-elevation braid bar (WC8) were sampled to characterize the surficial sediments at the site. The median sizes (D_{50}) in the riffles range from 124 to 81 mm, and the D_{84} (size for which 84 percent of the sample is finer) range from 123 to 196 mm (**Figure 2.5**). The low bar sample has a D_{50} of 49 mm, and the D_{50} of the high bar is 73 mm. The corresponding D_{84} values are 83 and 113 mm, respectively. The gradations shown in Figure 2.5 were used to identify the critical discharges (discharges at which the surface sediments are mobilized) for the identified surfaces throughout the site (refer to Chapter 5).

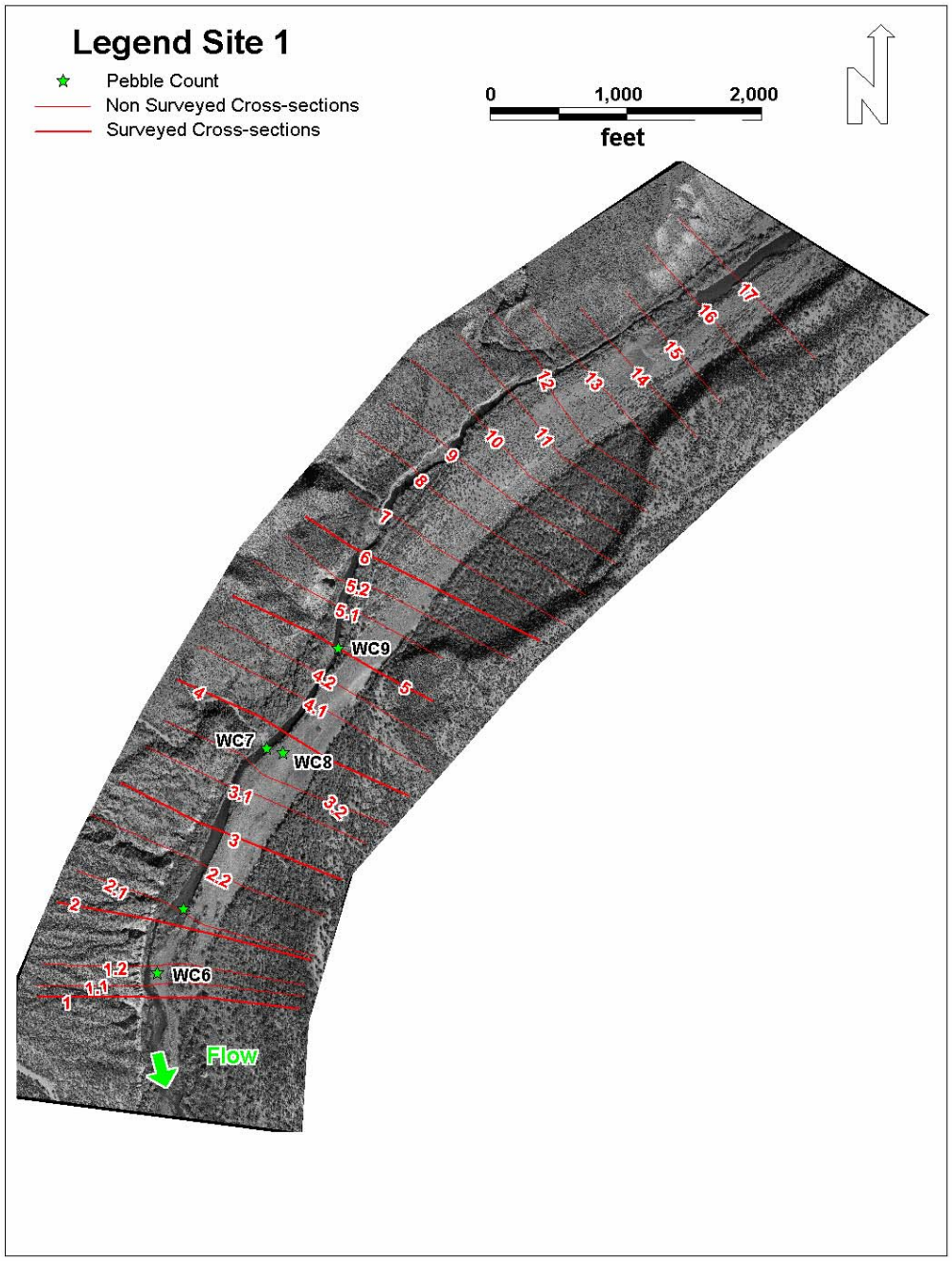

Figure 2.1. Aerial photograph of Site 1 showing the locations of surveyed cross sections and sediment samples.

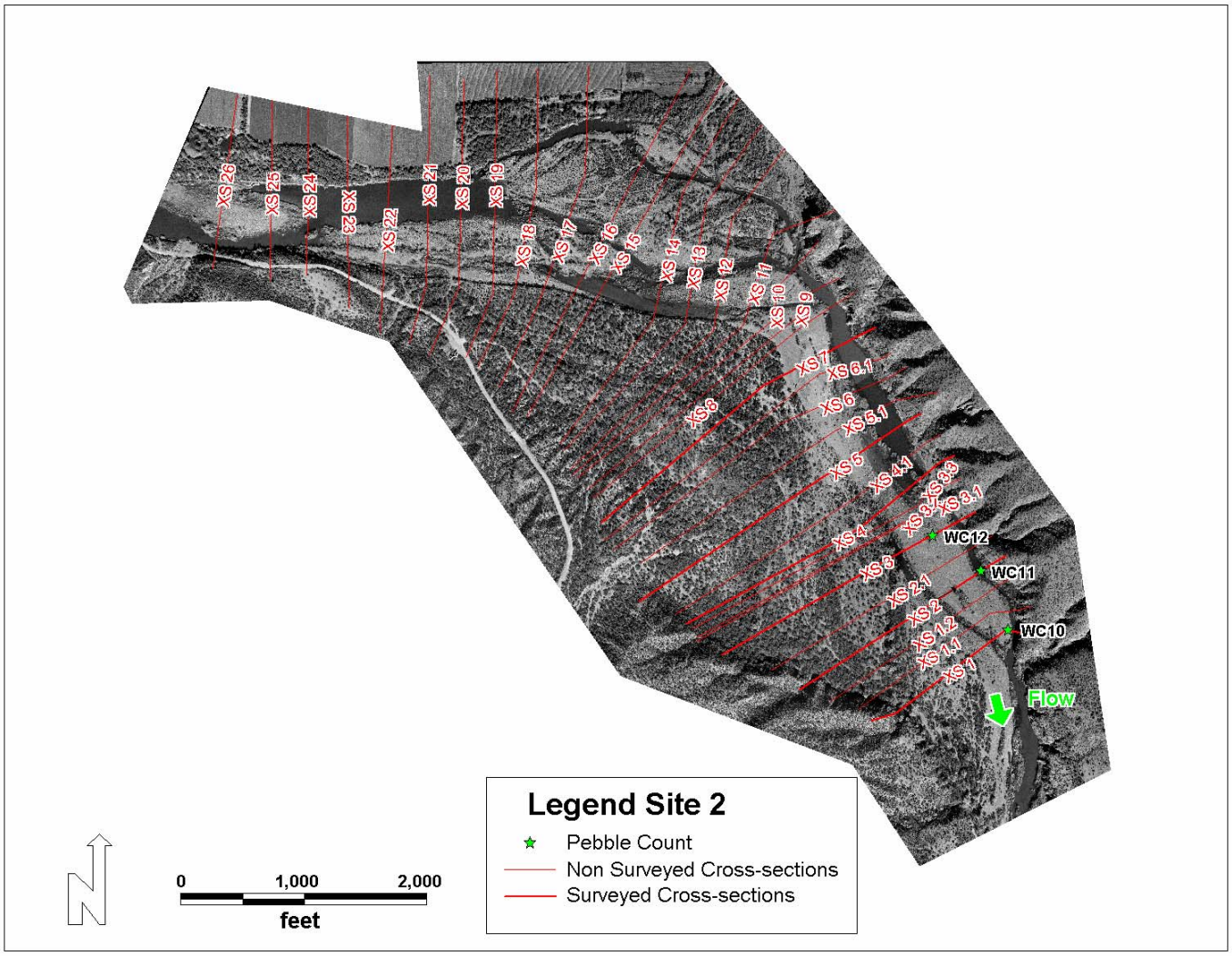

Figure 2.2. Aerial photograph of Site 2 showing the locations of surveyed cross sections and sediment samples.

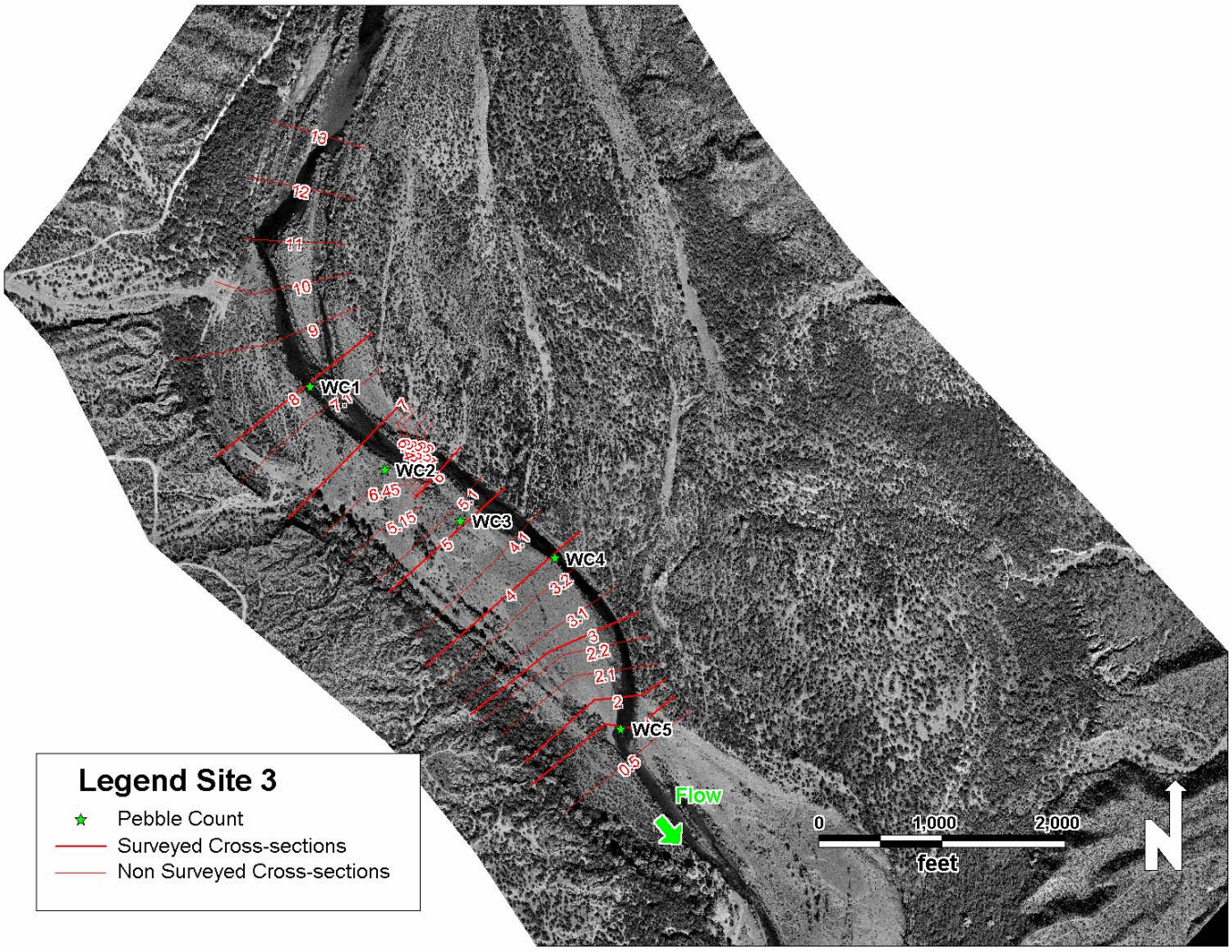

Figure 2.3. Aerial photograph of Site 3 showing the locations of surveyed cross sections and sediment samples.

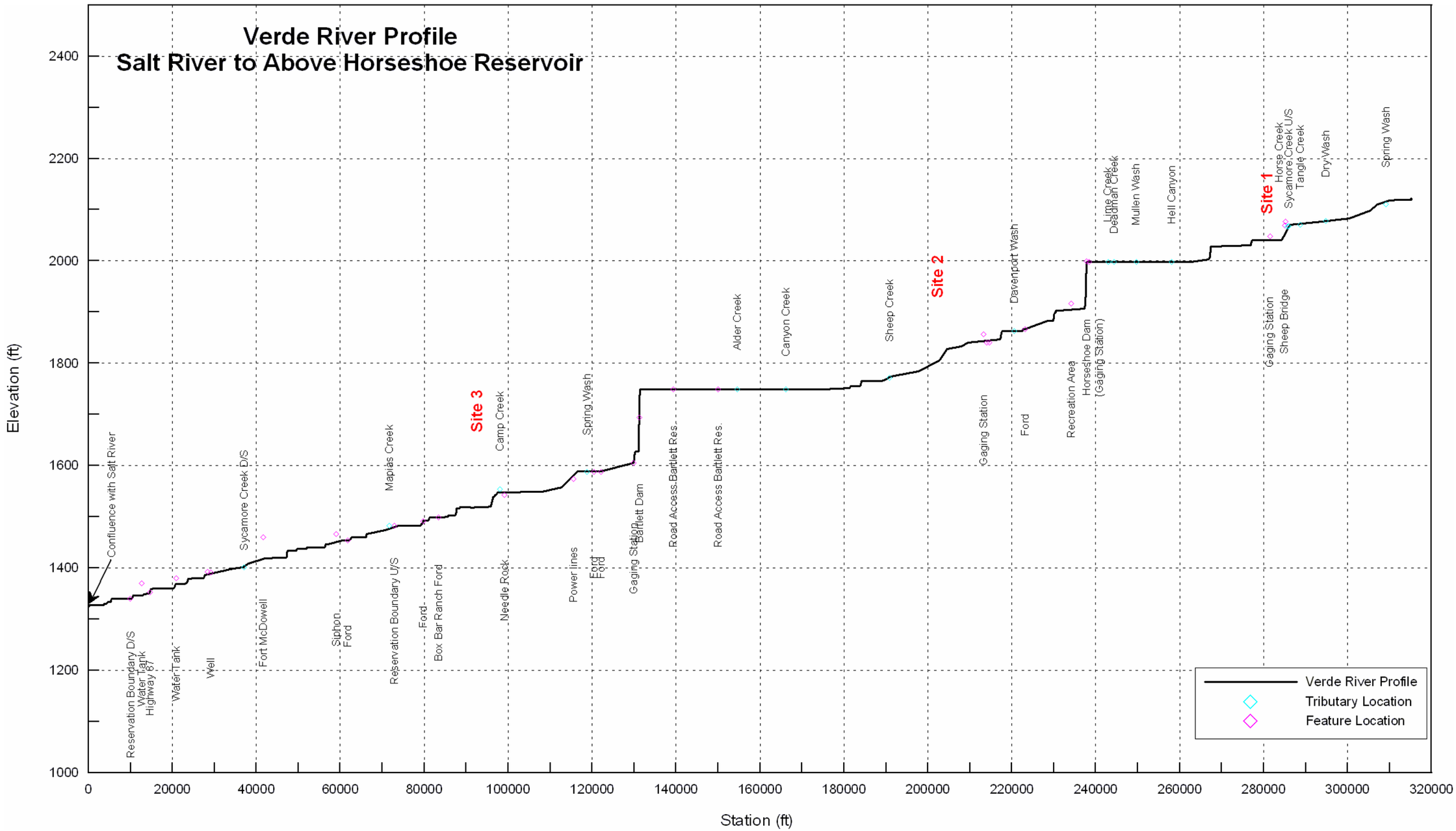

Figure 2.4. Longitudinal profile of Verde River from Salt River confluence to Tangle Creek gage showing the locations of the three studied sites.

Plate 1. View upstream of Site 1 located upstream of Horseshoe Reservoir. The chute channel that extends the length of the site during flood flows is clearly visible, as is the downstream hydraulic control for the site that is formed by old alluvial fans on the right bank and a Holocene terrace on the left bank.

Plate 2. View downstream of Site 2 located downstream of Horseshoe Dam. The left valley wall is composed of basin-fill sediments and the right valley wall is composed of alluvial fan and terraces sediments. The new chute channel, formed in the 1993-1995 floods and that is now flanked by riparian vegetation, can be seen in the lower left portion of the photograph.

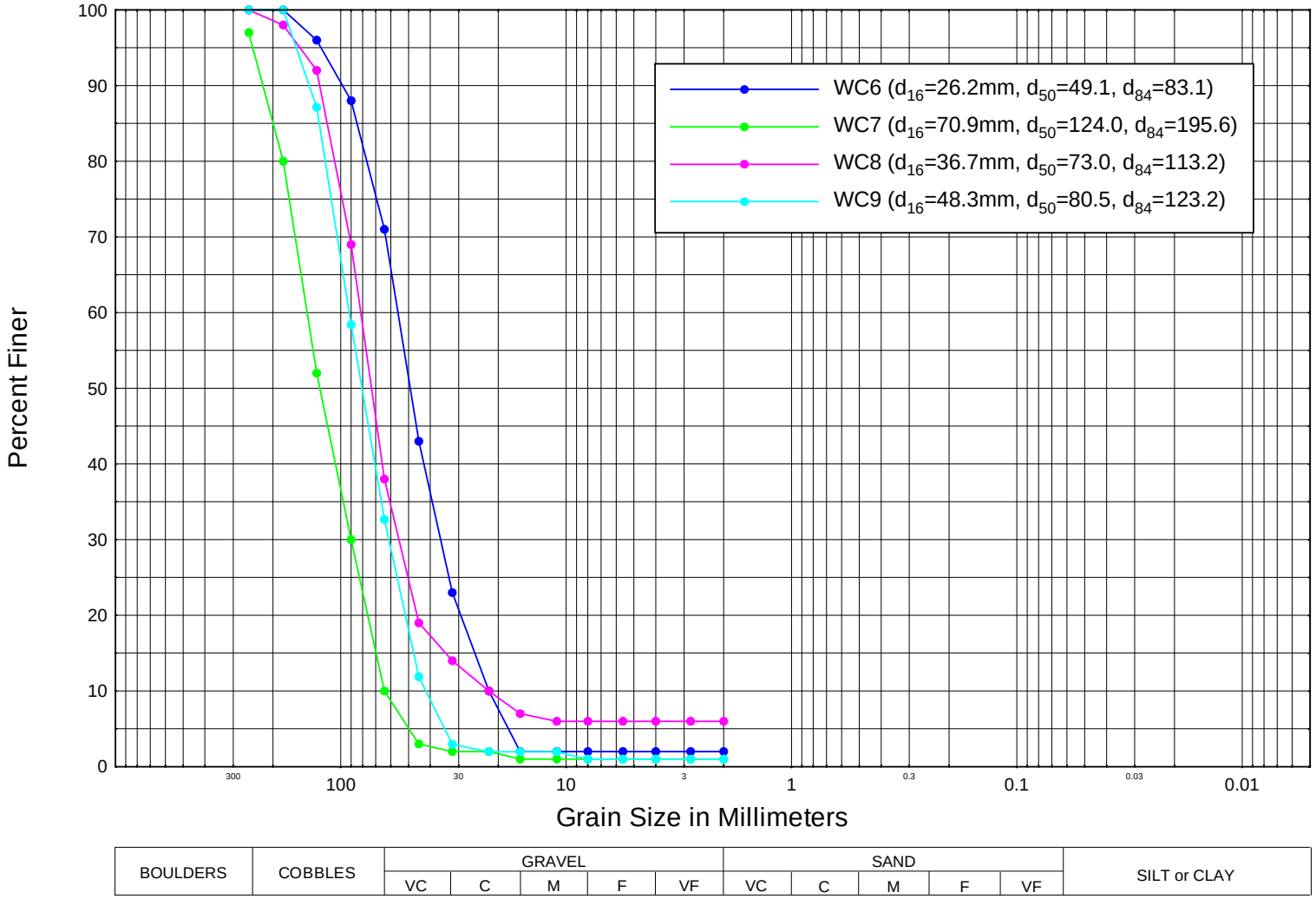

Figure 2.5. Grain-size distribution curves for four pebble counts that were conducted at Site 1.

2.2.2. Site 2: Downstream from Horseshoe Dam near the KA Ranch

Site 2 is located within a section of the Verde River valley that is about 2,000 feet wide (Figure 2.2**, Plate 2**). Within the site, the active channel width is about 450 feet. The site is located in a depositional zone upstream from a valley constriction, located about one mile downstream, that is caused by the presence of more erosion-resistant basin-fill outcrop on the right bank and older alluvial terraces and tributary fan sediments on the left bank. As is common in arid zone rivers, the braided channel occupies the active valley floor between the terraces and the fan, and therefore, there is no floodplain in the classic sense (Graf, 1988). Further enhancing the depositional nature of the site is the presence of two large tributaries that episodically deliver significant quantities of sediment to the river. Davenport Wash is located on the left bank at the upstream end of the site, and an unnamed arroyo is located on the right bank at the site. Sediments delivered by the right bank arroyo have formed a large alluvial fan that has prograded out onto the valley floor. The left valley wall throughout the site is composed of basin-fill sediments that also crop out on the right valley wall immediately downstream of the site. The right valley wall along most of the site is composed of old alluvial and fan sediments into which the present arroyo is inset. Morphologically, the site is characterized by an approximately 200-foot-wide low-flow channel that is fringed by riparian vegetation. A large, sparsely vegetated cobble-gravel bar separates the main channel from a chute channel that is located on the margin of the valley floor and runs along the base of the bounding alluvial fan and terraces for much of the length of the site. The active and chute channels are flanked by thin strands of riparian vegetation. The downstream hydraulic control for the site is created by a constriction caused by the presence of erosion-resistant late- to mid-Pleistocene-age, coalesced fans on the right bank, and an early Holocene-age terrace on the left bank. Plots of the surveyed cross sections that were used in the hydraulic modeling, showing the geometry of the channel are included in Appendix A. (The locations of the cross sections are shown in Figure 2.2.)

Pebble counts (Wolman, 1954) were conducted at three locations within the site (Figure 2.2). A riffle in the main channel (WC11), a low-elevation, bank-attached bar within the active channel (WC10) and a higher-elevation braid bar (WC12) were sampled to characterize the surficial sediments at the site (refer to Figure 5.2 for typical locations of bars). The median (D_{50}) and D_{84} sizes of the riffle sediments were146 and 231 mm, respectively (**Figure 2.6**). The low bar sample had a D_{50} of 73 mm, and the D50 of the high bar was 105 mm. The corresponding D_{84} sizes were 118 and 207 mm, respectively. The sediments that compose the riffle, low bar and high bar surfaces at this site are somewhat coarser than those on the corresponding surfaces at Site 1, but this is probably due to the steeper slope at Site 2, as well as the proximity of the two tributaries that are steeper than the mainstem.

2.2.3. Site 3: Downstream of Bartlett Dam near the Box Bar Ranch

Site 3 is located about 6.5 miles downstream from Bartlett Dam in a section of the Verde River valley that is about 4,000 feet wide (Figure 2.3, **Plate 3**). The active braided channel at the site is about 600 feet wide, and is flanked on the left side by the younger Lehi (Holocene) terrace that was overtopped by the large floods that occurred in the early part of the 20th century. The upper portion of the site is flanked by the older Lehi terrace, but the remainder of the site is flanked by both late- and early-Pleistocene age alluvial sediments that are dissected by a number of relatively small active arroyos. In common with most arid zone rivers, there is no floodplain in the classical sense (Graf, 1988). The older Lehi terrace was not overtopped by the large floods of the early part of the 20th century. The site is located in a depositional zone

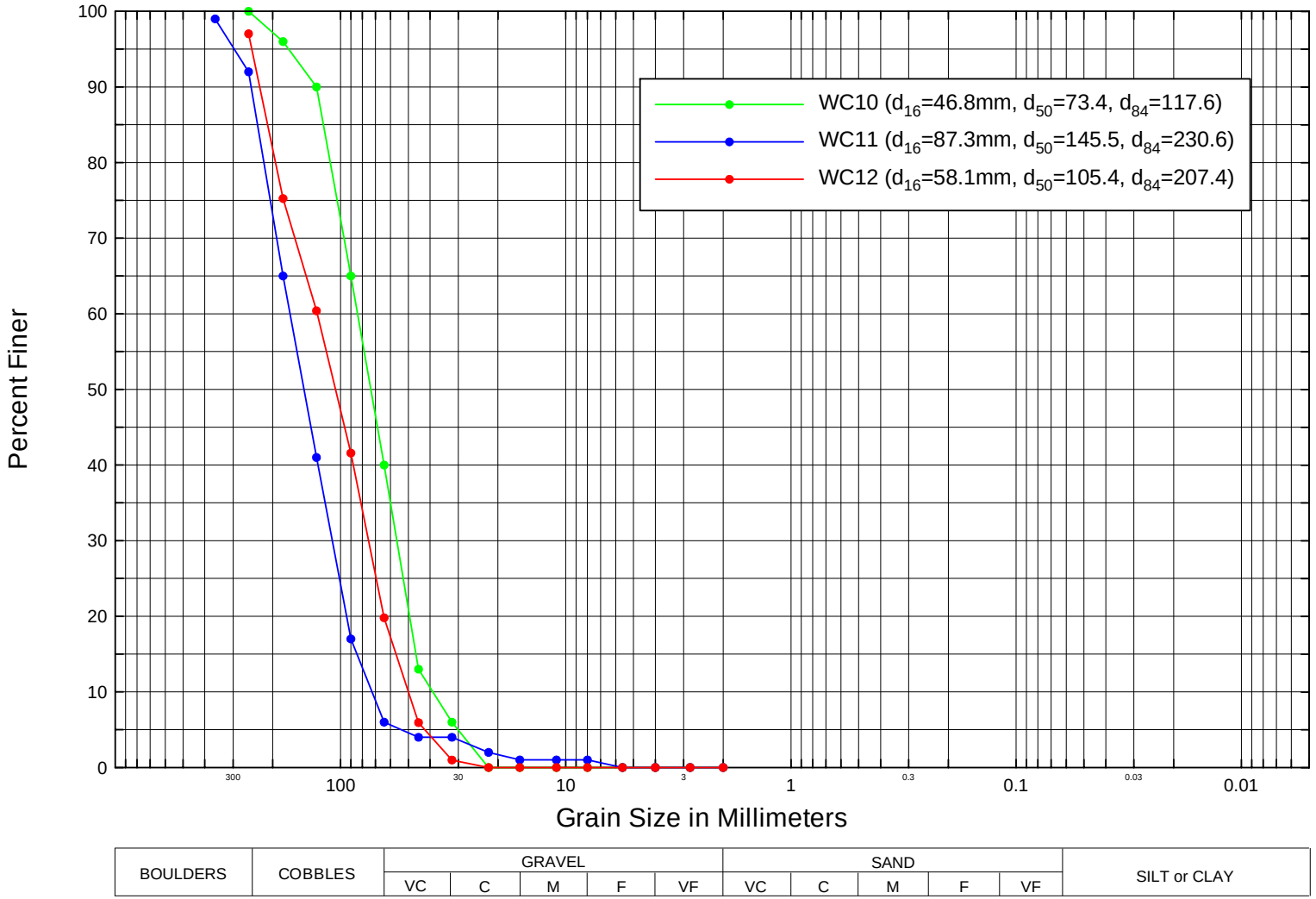

Figure 2.6. Grain-size distribution curves for three pebble counts that were conducted at Site 2.

Plate 3. View upstream of Site 3 in the upper part of the picture. The right valley wall is composed of old alluvial and fan sediments, and the left valley wall is comprised of the older and younger Lehi terraces. The larger cottonwoods are growing on the Lehi terraces. Younger riparian vegetation is located on the margins of the active and chute channels.

upstream of a valley constriction located about one mile downstream that is caused by the presence of more erosion resistant older alluvial deposits on the right bank and outcrop of the Needle Rock Formation on the left bank (Skotnicki, 1996). Morphologically, the site is characterized by an approximately 500-foot-wide active channel that that is separated from a chute channel that runs along the left side of the site for most of its length by a sparsely vegetated gravel-cobble bar. The active and chute channels are flanked by thin strands of riparian vegetation. Plots of the surveyed cross sections that were used in the hydraulic modeling, showing the geometry of the channel are included in Appendix A. (The locations of the cross sections are shown in Figure 2.3.)

Pebble counts (Wolman, 1954) were conducted at five locations within the site (Figure 2.3). Riffles in the main channel (WC1, WC4, WC5), a low-elevation bar (WC3) and a higher-elevation bar (WC2) were sampled to characterize the surficial sediments at the site. The median sizes (D_{50}) of the riffles ranged from 61 to 98 mm, and the D_{84} sizes range from 121 to 164 mm (**Figure 2.7**). The low bar sample has a D_{50} of 54 mm, and the high bar value is 67 mm. The corresponding D_{84} values are 107 and 121 mm, respectively.

2.3. Historical Changes

In arid climates and canyon-bound rivers, most change in river characteristics is driven by relatively infrequent floods (>10-year recurrence interval, Baker, 1977; Wolman and Gerson, 1978). Paleoflood studies of the Verde River (Ely and Baker, 1985; O'Connor et al., 1986) have identified a number of very large floods within the last 1,000 years, the largest of which may have been on the order of 195,000 cfs (House et al., 1995). In more recent times, the largest flood appears to have been that of 1891 (about 150,000 cfs), but the floods of 1993 were comparable in size (House et al., 1995). Other large floods that have occurred on the Verde River include a number in the early part of the 20th century before Bartlett Dam was constructed in 1939 (1906—96,000 cfs, 1920—95,000 cfs, 1927—70,000 cfs, and 1938—100,000 cfs. The next large flood occurred in 1952 (81,600 cfs) after the construction of Horseshoe Dam in 1946, and then there was a period of relatively low flood peaks until 1978 (91,400 cfs), 1979 (94,000 cfs) and 1980 (94,800 cfs). Large floods again occurred in 1993 (145,000 cfs) and 1995 (108,000 cfs). The presence of the dams had relatively little effect on the magnitude of these very large flood flows (refer to Figure 5.3).

Flood-driven changes at the three sites can be evaluated by examining a series of aerial photographs. Photography was available for 1934, 1953, 1967, 1976, 1980, 1988, 1992, 1997, and 2002. A discussion of changes at each of the sites follows.

2.3.1. Site 1: Upstream of Horseshoe Reservoir near Tangle Creek Gage

Although the quality and resolution of the aerial photographs is variable, it appears that the major change that has taken place episodically between 1934 and 2002 has been in the density of the vegetation in the upper portions of the chute channel that extends the length of the site (Figure 2.2 and Plate 1). Following the floods of 1906, 1920 and 1927 [recurrence intervals (RI) ranged from 10 to 18 years]; the 1934 photographs indicate there was very little vegetation growing in the active portion of the channel between the heavily vegetated bounding terraces. By 1953, following the 1952 flood (15-year RI), there appears to have been some vegetation establishment at the downstream end of the high bar surface that separates the main channel from the chute channel (Cross Sections 5 and 6, Appendix A). The 1968 photograph shows a significant increase in vegetation on the bar surfaces, which can probably be attributed to the

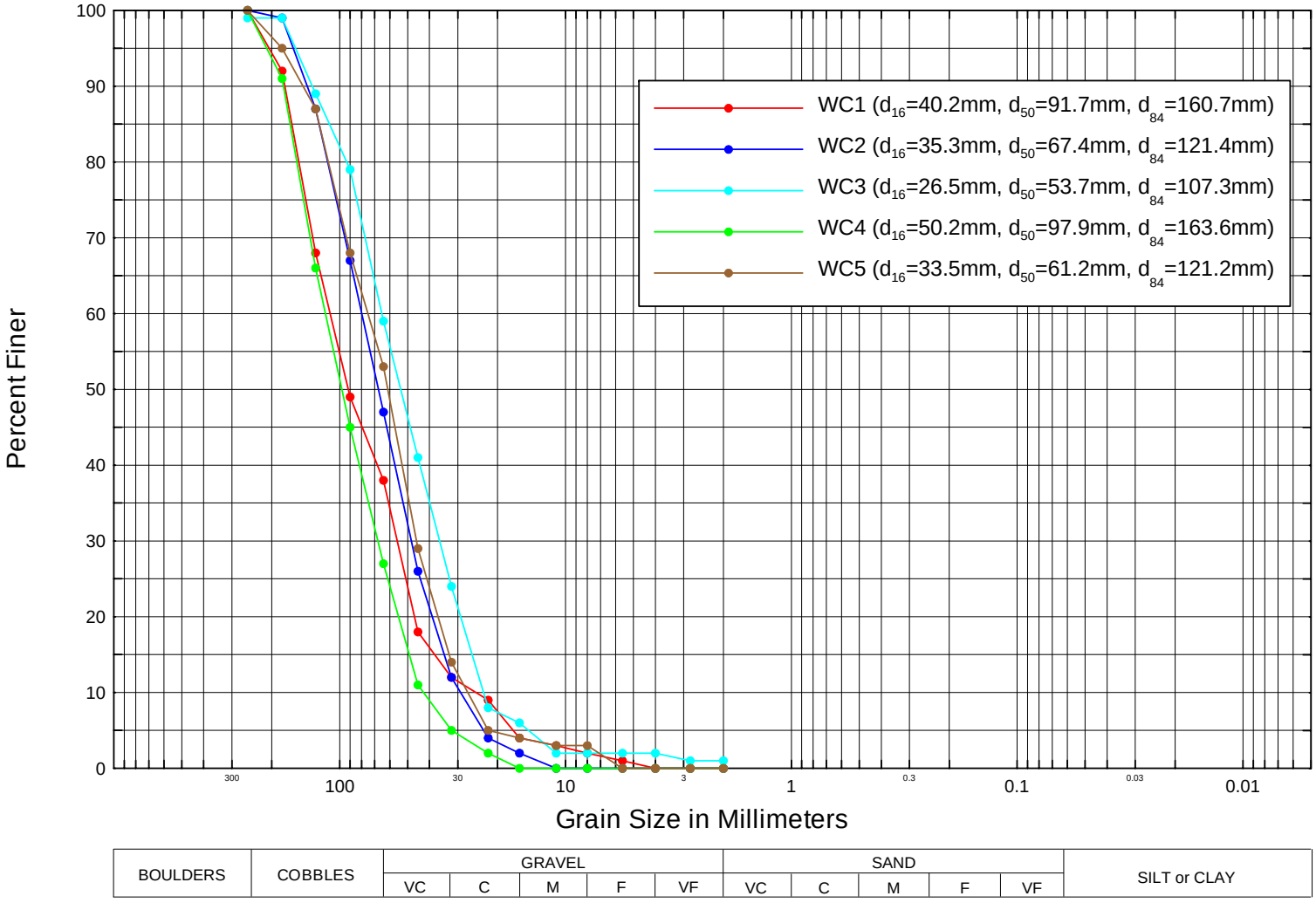

Figure 2.7. Grain-size distribution curves for five pebble counts that were conducted at Site 3.

absence of significant floods since 1952. Following the floods of 1978, 1979 and 1980 (RI 16 through 18 years), the 1980 photograph shows very little vegetation in the active channel. Between 1980 and 1992, there were no significant floods and the amount of vegetation increased. Following the floods of 1993 (>50-year RI) and 1995 (25-year RI), the vegetation in the chute channel and the upstream portion of the bar was stripped, but the vegetation on the high-bar surface separating the main channel and the chute channel persisted, which suggests that even a 50-year flood has little impact on the higher elevation portions of the active channel. The 2002 photographs indicate that the vegetation is returning to the bar surfaces. The general pattern of vegetation encroachment between large flood events and removal during floods is most likely attributable to the relatively confined nature of the site and the resulting high energy during large flood events (Friedman and Auble, 1999).

2.3.2. Site 2: Downstream of Horseshoe Dam near the KA Ranch

The 1934 photographs show sparse vegetation cover within the margins of the active channel. The channel appears to have been modified by the floods of 1906, 1920 and 1927. A large chute channel formed on the right side of the active channel near the middle of the site where a large mid-channel bar formed in the main channel, and this chute channel persisted through the period of record. Some vegetation survived the floods on the margins of the right bank arroyo fan. The 1953 photographs show that there was a general increase in vegetation over the entire site, but the highest density of vegetation was located along the chute channel. By 1967, vegetation cover had further increased across the site, especially in the chute channel. The chute channel is the location of the highest density of large cottonwoods in the 1976 photographs. The sequence of floods in 1978, 1979 and 1980 removed the large, vegetated mid-channel bar at the head of the chute channel, and also removed most of the riparian vegetation along the channel margin, but the heavily vegetated chute channel persisted. The floods of 1993 and 1995 caused a shift in the location of the main channel at the head of the site and created a new chute channel on the right side of the main channel towards the downstream end of the site. The 2002 photography shows that riparian vegetation has become established along the margins of the new chute channel. The abandoned portion of the channel at the mouth of Davenport Wash is a likely site for new vegetation to establish during the post-1993 through 1995 flood period. The general patterns of vegetation encroachment between floods and vegetation removal along the channel margins during the floods is very similar to that observed at the above-Horseshoe Dam site, and probably reflects the relatively minor effect of Horseshoe Reservoir on flood-flow magnitudes.

2.3.3. Site 3: Downstream of Bartlett Dam near the Box Bar Ranch

The 1934 photography shows that there had been significant disturbance of the site, most probably as a result of the large floods in the early part of the 20th century. Areas mapped as the older Lehi terrace (Skotnicki, 1996) do not appear to have been overtopped, but the younger Lehi terrace was overtopped and is devoid of vegetation. Large chute channels were present on the east side of the upper portion of the site, and around the higher Lehi terrace towards the bottom of the site. The main channel was located along the west side of the site. By 1953, vegetation had reestablished on the younger Lehi terrace and in the chute channels around both the younger and older Lehi terraces. The 1967 and 1976 photographs show a progressive increase in vegetation at the site. Following the floods of 1978, 1979 and 1980, the chute channels around the younger Lehi terrace on the east side of the river were reactivated, and the vegetation was stripped from them and on parts of the terrace surface, as well. Although flow entered the chute channel to the east of the higher Lehi terrace, it did not appear to remove any

vegetation, and in fact this old flow path appears to be the location of the most vigorous vegetation growth. The apex of the bend on the west side of the site chute cut-off, and displaced the main channel farther to the east. The 1988 and 1992 photographs show that vegetation density increased throughout the site. The 1997 photographs show that, following the large floods of 1993 and 1995, the chute channels on the east side of the younger Lehi terrace were reactivated in the floods, but very little other change took place within the site. The 2002 photographs show recolonization of the site by vegetation. The cutoff bar apex along the western margin of the site has been vegetated and stabilized.

The vegetation and morphological changes through time at the site may be related to the effects of the upstream dam on the frequency of morphogenetically significant events (**Figure 2. 8**), as well as by the fact that the earlier part of the 20th century was wetter than the latter part. Prior to construction of Bartlett Dam, inundation of portions of the younger Lehi terrace probably occurred with a frequency of about 2.5 to 3 years at a discharge of about 20,000 cfs. In the post-Bartlett period, the same flow has a recurrence interval of about 7 years. Review of the flow records at the Bartlett gage indicates that, between 1942 and 1965, the largest peak flow was less than 10,000 cfs. The aerial photography demonstrates that during this 23-year period, vegetation became well established in areas of the site that were obviously disturbed in the 1934 photographs of the site. In contrast, at the Tangle Creek gage, there were six floods in excess of 20,000 cfs in the same time period. Between 1965 and 1977, there were no flows in excess of 15,000 cfs below Bartlett Dam. Cumulatively, the three floods of 1978, 1979 and 1980 caused significant morphological and vegetation changes at the site, but these flood magnitudes ranged between 75,800 and 101,000 cfs (15- to 50-year RI). Hydraulic modeling of the site indicates that, at a discharge of 100,000 cfs about 20 percent of the total flow is being conveyed in the left overbank and flows in this range are, therefore, capable of effecting change. In contrast, at a discharge of 50,000 cfs, less than 10 percent of the total flow is being conveyed in the left overbank, and hence, there is a much lower potential for change. The large floods of the late 1970s were again followed by a period of 12 years (1981 through 1992) when the maximum flow was less than 17,000 cfs below Bartlett Dam, but 6 events exceeded 20,000 cfs at the upstream gage in the same time period. The 1993 (84,700 cfs) and 1995 (64,100 cfs) floods, with recurrence intervals of 11 and 18 years, respectively, caused very little change at the site, probably because of the extent of the vegetation that has become established since the dam was constructed, due to the infrequent disturbance of the site in the post-dam period.

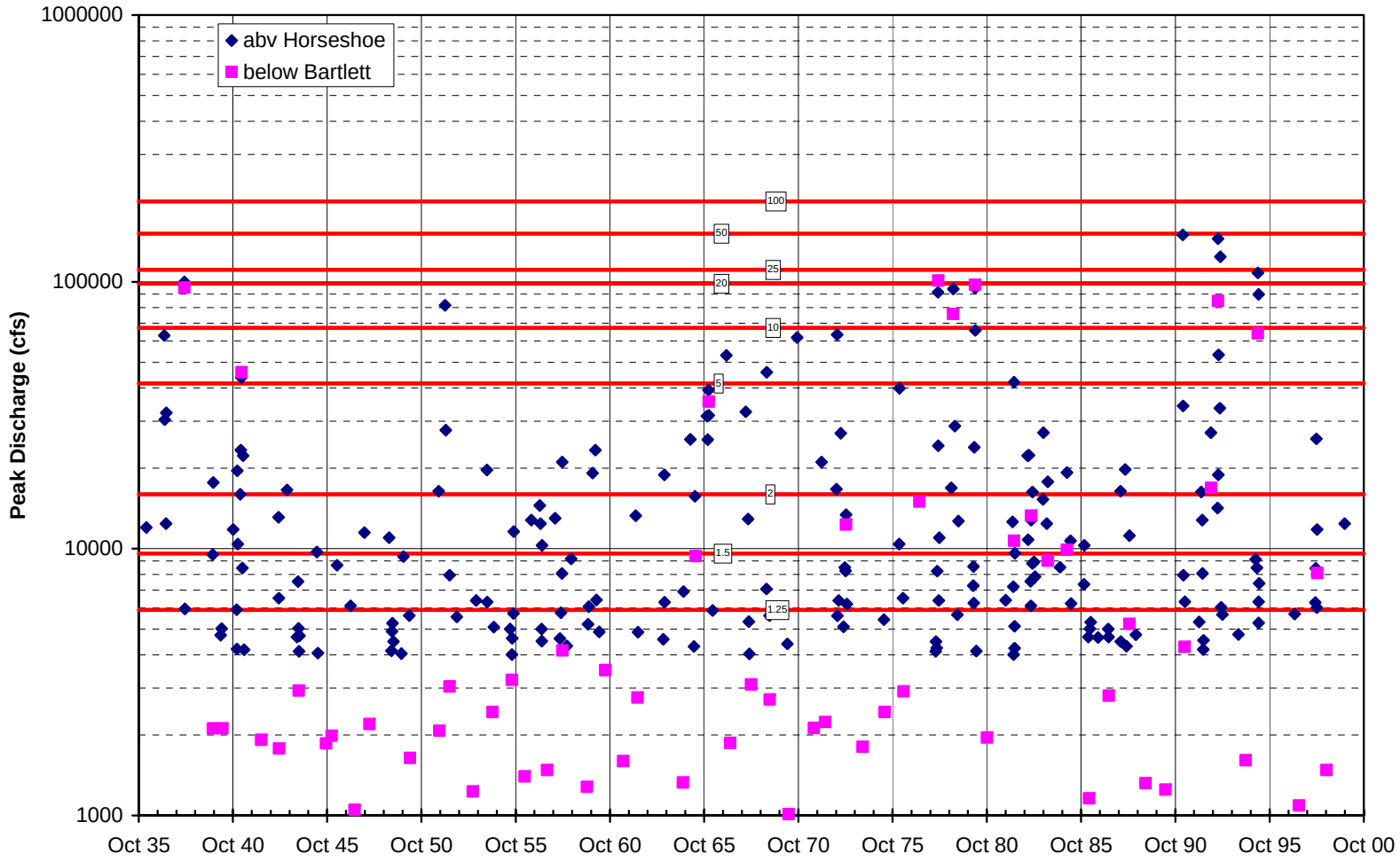

Figure 2.8. Annual flood peaks for above Horseshoe (Gage No. 0908500) and below Bartlett (Gage No. 09510000) gages. Also shown are the above Horseshoe gage flood frequencies.

3. HYDROLOGY

3.1. Descriptive Hydrology

The Verde River is a perennial stream that drains an approximately 6,600-square-mile area of north-central Arizona, joining the Salt River just east of Phoenix (**Figure 3.1**). Elevations within the drainage basin range from over 7,000 feet in the high country near the headwaters to about 1,300 feet at the confluence. Due to its large size, the drainage basin encompasses several different climatic regimes which vary with elevation. The lower portion of the basin, including the study sites, lies in the semi-arid Sonoran Desert. Flows in the river are affected by two periods of moderately heavy precipitation that typically occur during winter and in late summer. Winter precipitation generally results from large-scale cyclonic storms that originate in the Pacific Ocean. Long, steady rains resulting from these storms produce the largest floods on the Verde River because they are sufficiently wide-spread to cover significant portions of the drainage basin, including both low- and high-elevation areas (Graf, 1983). In fact, the largest floods of record (greater than 80,000 cfs) have all occurred in the November through March time-period (**Figure 3.2**). The intense summer thunderstorms are more localized and do not generally result in significant flooding in basins as large as the Verde River (Ely and Baker, 1985).

Flow regulation by Horseshoe and Bartlett Dams alters the flow regime of the lower Verde River. These dams are part of the SRP and are operated to provide water to municipal and agricultural users in the metropolitan Phoenix area. Bartlett Dam began regulating flows in February 1939 and Horseshoe Dam was closed in November 1945. Recent modifications to both dams have been made to address dam-safety issues. The total storage capacity behind Horseshoe Dam is currently about 109,000 ac-ft and the total storage capacity behind Bartlett Dam is currently about 178,000 ac-ft. The combined capacity of the two dams represents about two-thirds of the average annual flow in the Verde River.

3.2. Analysis of Gage Records

Two U.S. Geological Survey (USGS) stream gages are present in the project reach. The Verde River below Tangle Creek above Horseshoe Dam gage (USGS Gage 0908500) is located above both reservoirs, and immediately upstream from Site 1, the most upstream study site (Figure 1.1). Although flows at the this gage are altered somewhat by upstream irrigation and a power plant that is located about 32 miles upstream, the effects are relatively minor, particularly during high flows that are important to channel morphology. The gage, therefore, provides a good representation of natural flow conditions in the project reach. Mean daily flow records for the Tangle Creek gage extend from 1945 to the present, and a record of peak flows is available for 1891, 1906, 1916, 1920, and 1925 to the present.

The Verde River below Bartlett Dam gage (USGS Gage 09510000,) is located about 1.8 miles upstream from Site 3 (Figure 1.1). The mean daily flow record at this gage extends from 1904 to the present, and the peak discharge records include the post Bartlett Dam period (1938-present). The portion of the record after closure of Horseshoe Dam in November 1945, therefore, represents the altered flow regime at the downstream study site resulting from the operation of both dams.

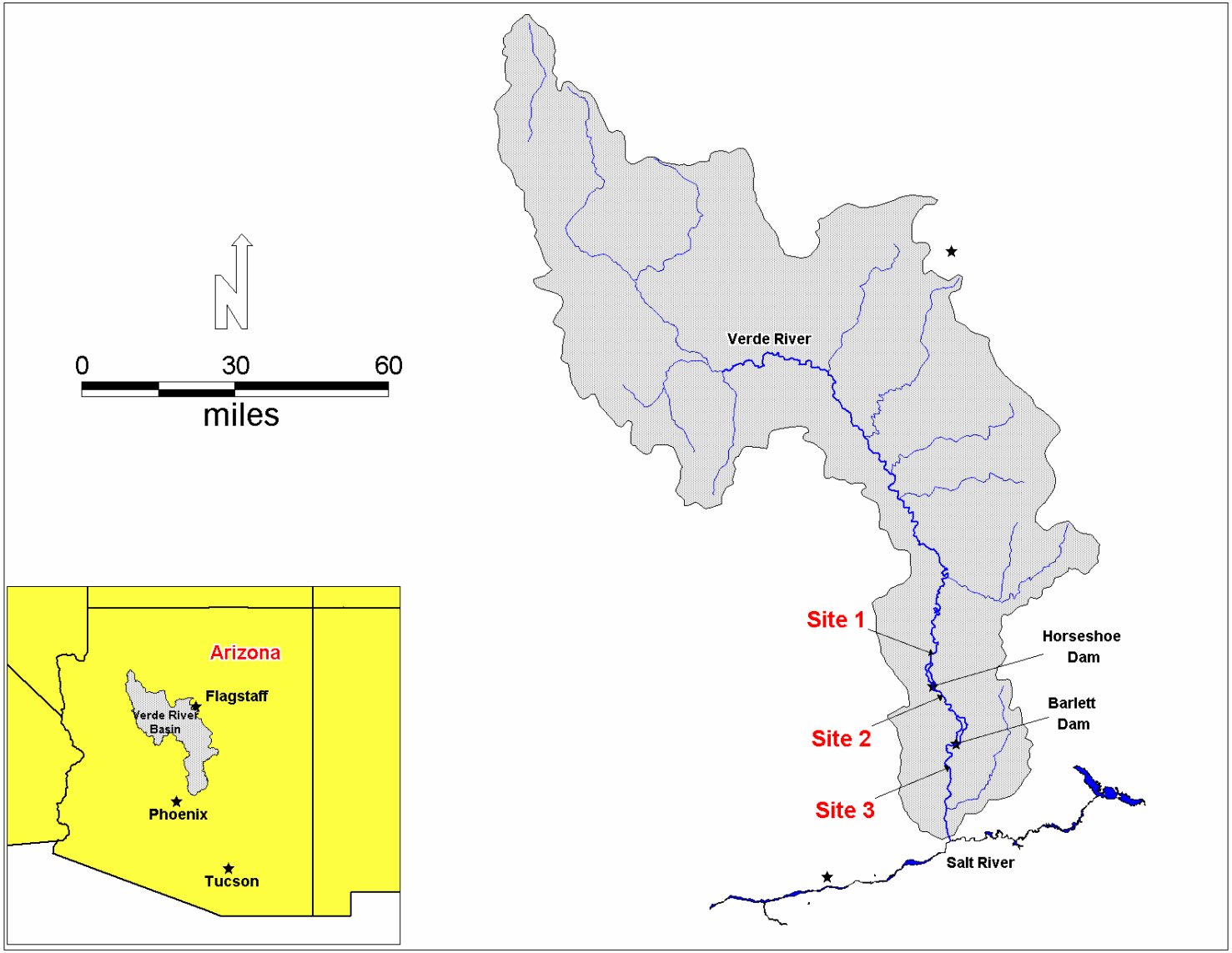

Figure 3.1. Map showing the Verde River drainage basin.

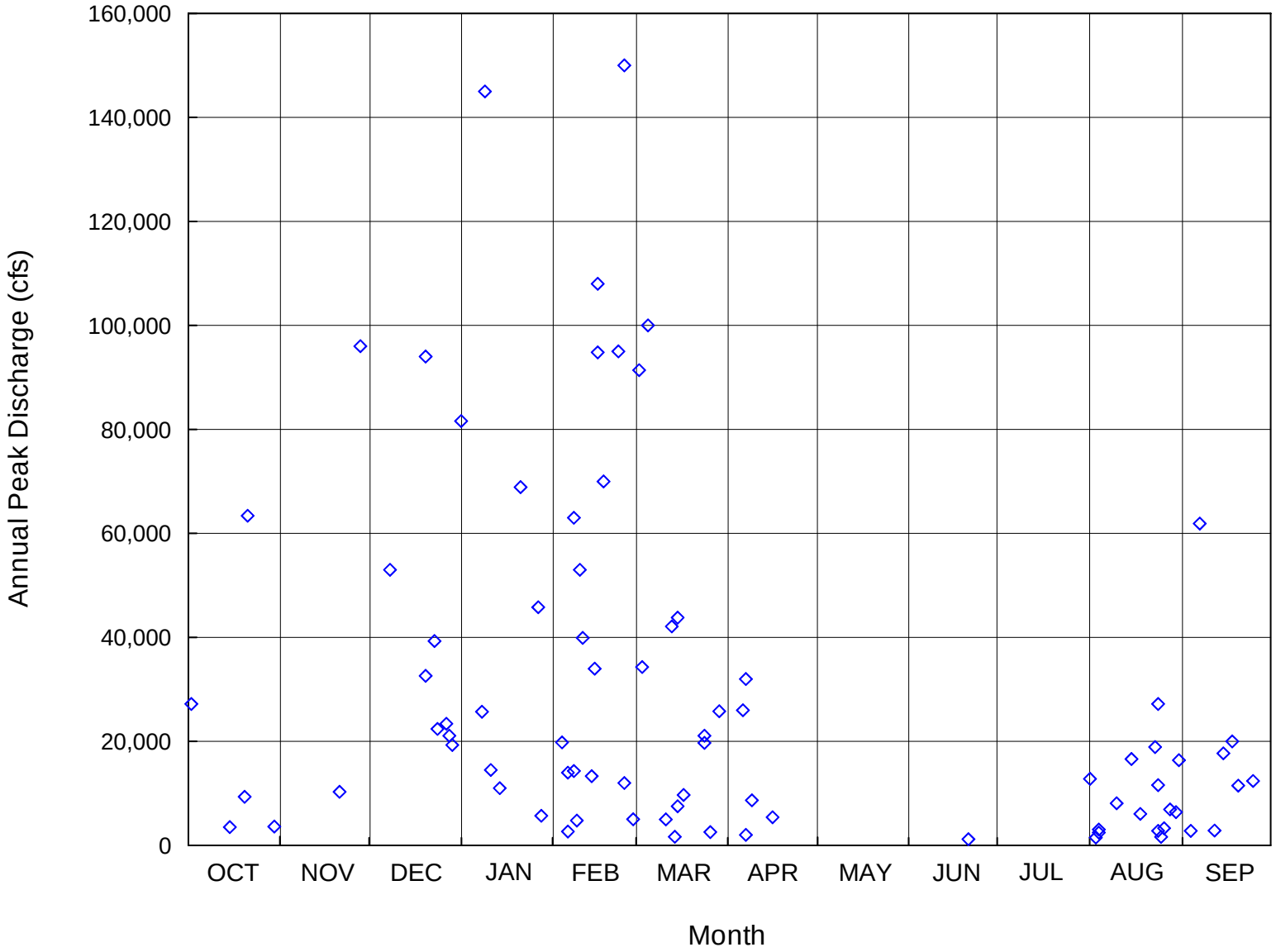

Figure 3.2. Magnitude and day-of-the-year of recorded annual peak flows at the Verde River below Tangle Creek above Horseshoe Dam stream gage (USGS Gage 0908500).

The records at both gages show significant variability in annual peak flows, with peaks ranging from 1,500 cfs (August 1974) to 150,000 cfs (February 1891, estimated value; 145,000 cfs in January 1995 is largest recorded value) at the Tangle Creek gage, and from 905 cfs (December 1995) to 101,000 cfs (March 1978) at the "below Bartlett" gage (**Figure 3.3**). Peak flood-frequency estimates made by the USGS (1998), and confirmed by MEI for this study using the procedures outlined in Water Resource Council (WRC) Bulletin 17B (WRC, 1981) indicate that the 2-, 10- and 100-year peak discharges are about 16,000, 67,300, and 200,300 cfs, respectively (**Figure 3.4**). It should be noted that the data used by both the USGS (1998) and by MEI for this study to confirm the USGS results included estimated historical flood peaks from the paleoflood study of Ely and Baker (1985).

Although the post-dam annual peak flow record (1946 through 2002) at the "below Bartlett" gage does not fit the standard Log-Pearson Type III frequency distribution on which the Tangle Creek frequency curve is based, comparison of the relationships indicated by the relative plotting position of the individual data points shows that the magnitude of the more frequent flood events (i.e., less than about the 10-year flood) has decreased significantly since construction of the dams (**Figure 3.5**). The 2-year flood, for example, decreased from 16,000 cfs to about 2,500 cfs and the 5-year flood decreased from 41,600 cfs to about 11,000 cfs.

Mean daily flow-duration curves were developed for the post-dam period for both gages to assist in evaluating the effects of the dams on the non-flood flow regime at the sites (**Figure 3.6**). These curves indicate that the dams tend to decrease the duration of flows in the range above about 1,400 cfs and below about 210 cfs. Conversely, the duration of flows between 210 and 1,400 cfs is significantly increased. It is interesting to note that the average annual flow volume past these gages during the 57-year period from 1946 through 2002 period was nearly the same (about 410,000 ac-ft at Tangle Creek versus 413,000 ac-ft below Bartlett). On a year-by-year basis, however, the annual flows at the two gages varied significantly with a 56-percent decrease from the Tangle Creek gage to the below Bartlett gage in 1970 to a 76-percent increase between the two gages in 2002. The largest difference, on a percent basis, tends to occur during low-flow years. On a seasonal basis, flows downstream from the dams tend to be lower during winter and early spring (December through April), higher during late-spring and summer (May through August), and about the same during the fall months, compared to the flows upstream from the reservoirs (**Figure 3.7**).

3.3. Operational Scenarios

To assist in evaluating whether or not reservoir operations could be modified in a way that would potentially increase the amount of woody riparian vegetation that provides suitable habitat for the bald eagles, southwestern willow flycatchers, and yellow-billed cuckoos, hydrographs for a range of historic floods were evaluated for three basic reservoir-operational scenarios, as follows:

Alternative 1 - Historical Operation,
Alternative 2 - No Permit alternative, and
Alternative 5 - Mimic Natural Hydrograph alternative.

*The alternative numbers correspond to a numbering system that has been used by SRP and ERO to evaluate a broader range of alternatives than were specifically considered in this analysis.

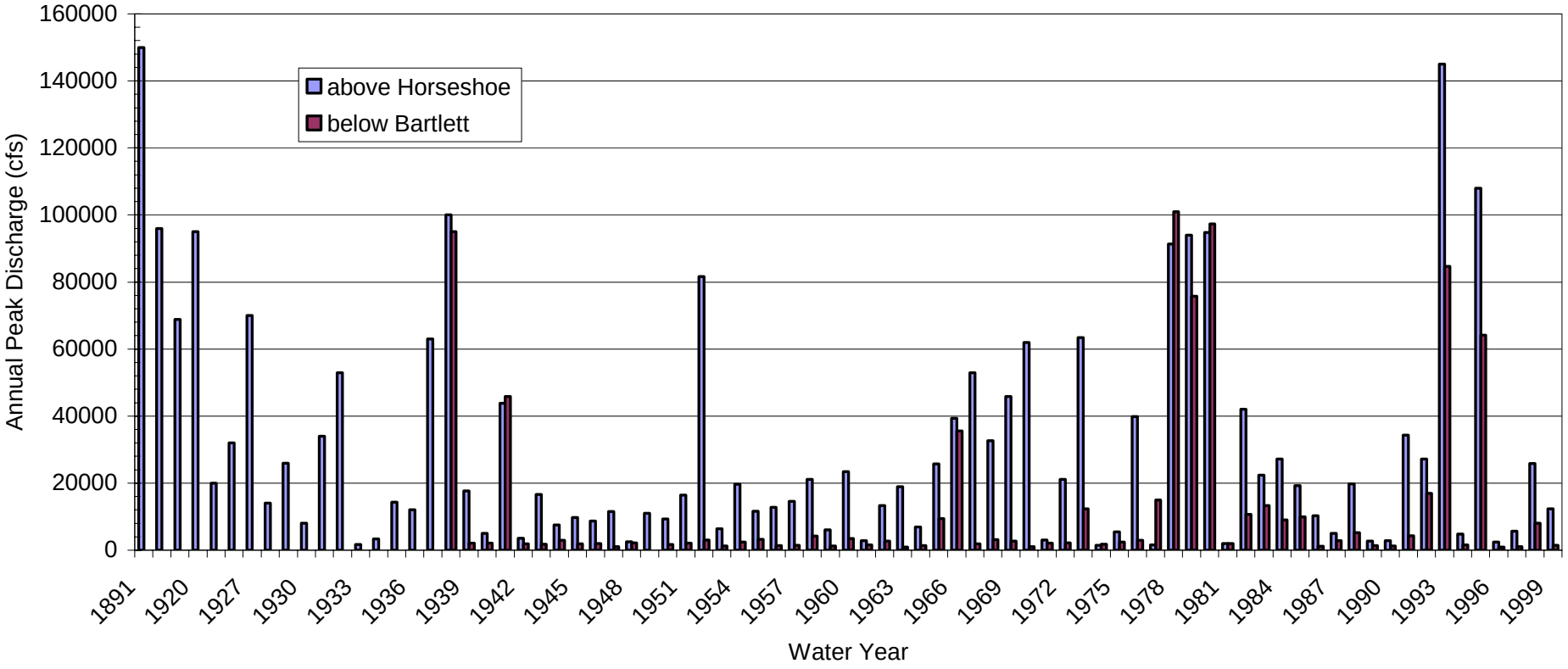

Figure 3.3. Recorded annual peak flows at the Verde River below Tangle Creek above Horseshoe Dam stream gage (USGS Gage 0908500) and the Verde River below Bartlett Dam gage (USGS Gage 09510000). The four historical peaks prior to 1925 at the Tangle Creek gage are estimated values (Ely and Baker, 1985).

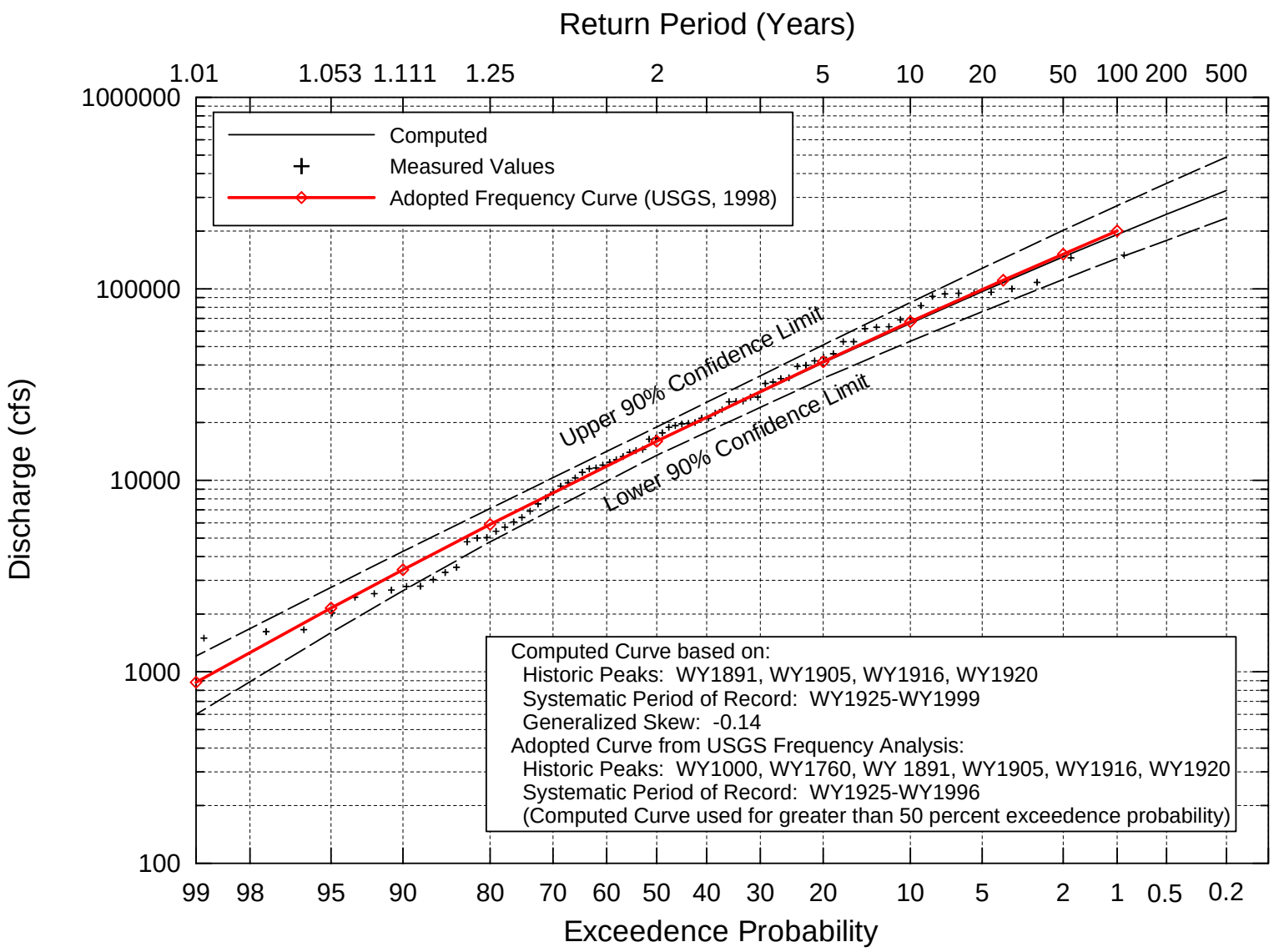

Figure 3.4. Recorded peak flows and estimated flood frequency curves for the period of record at the Verde River below Tangle Creek above Horseshoe Dam stream gage (USGS Gage 0908500).

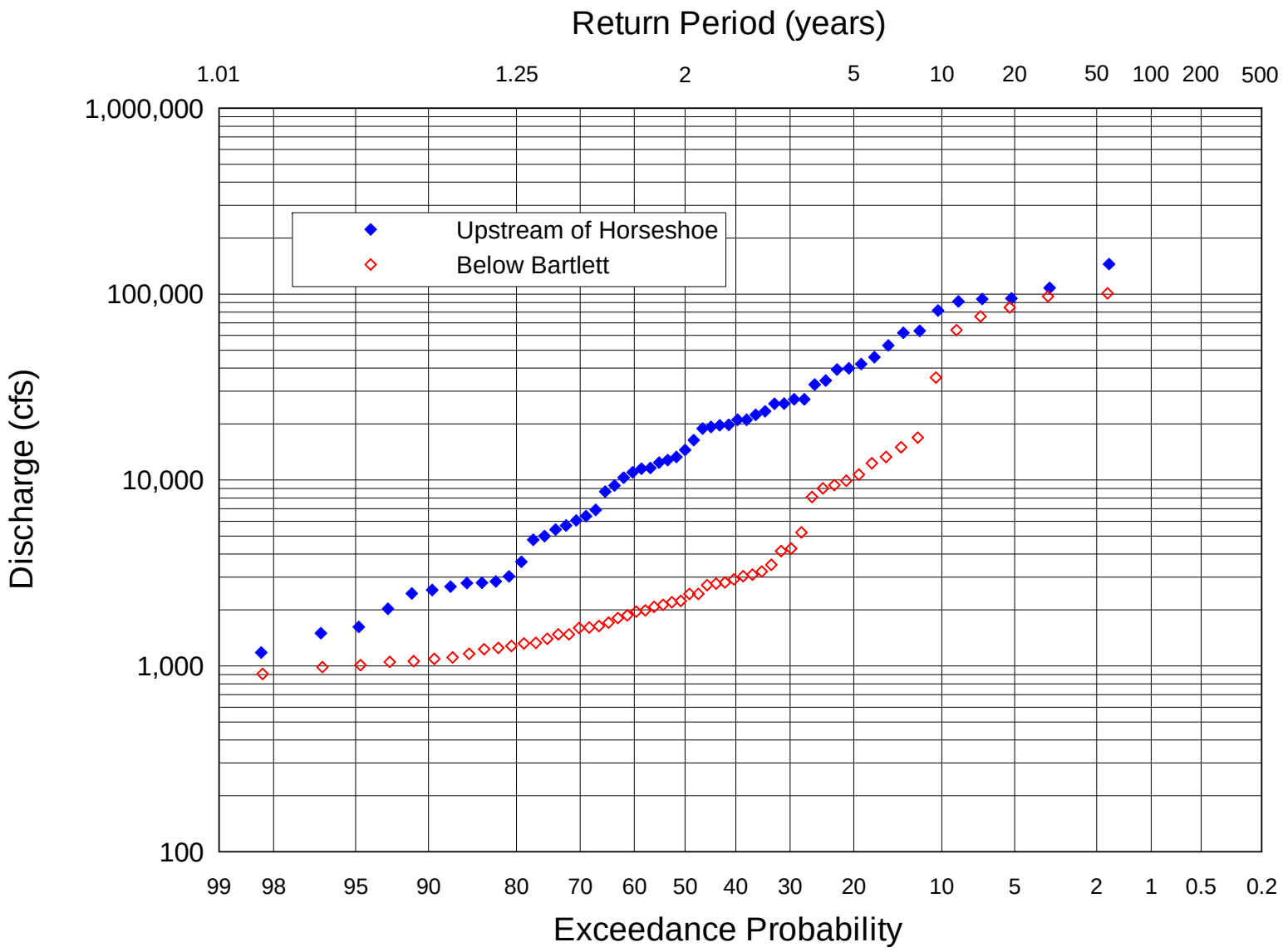

Figure 3.5. Comparison of flood-frequency curves for the Tangle Creek and below Bartlett gages for the post-dam period (1946—2002).

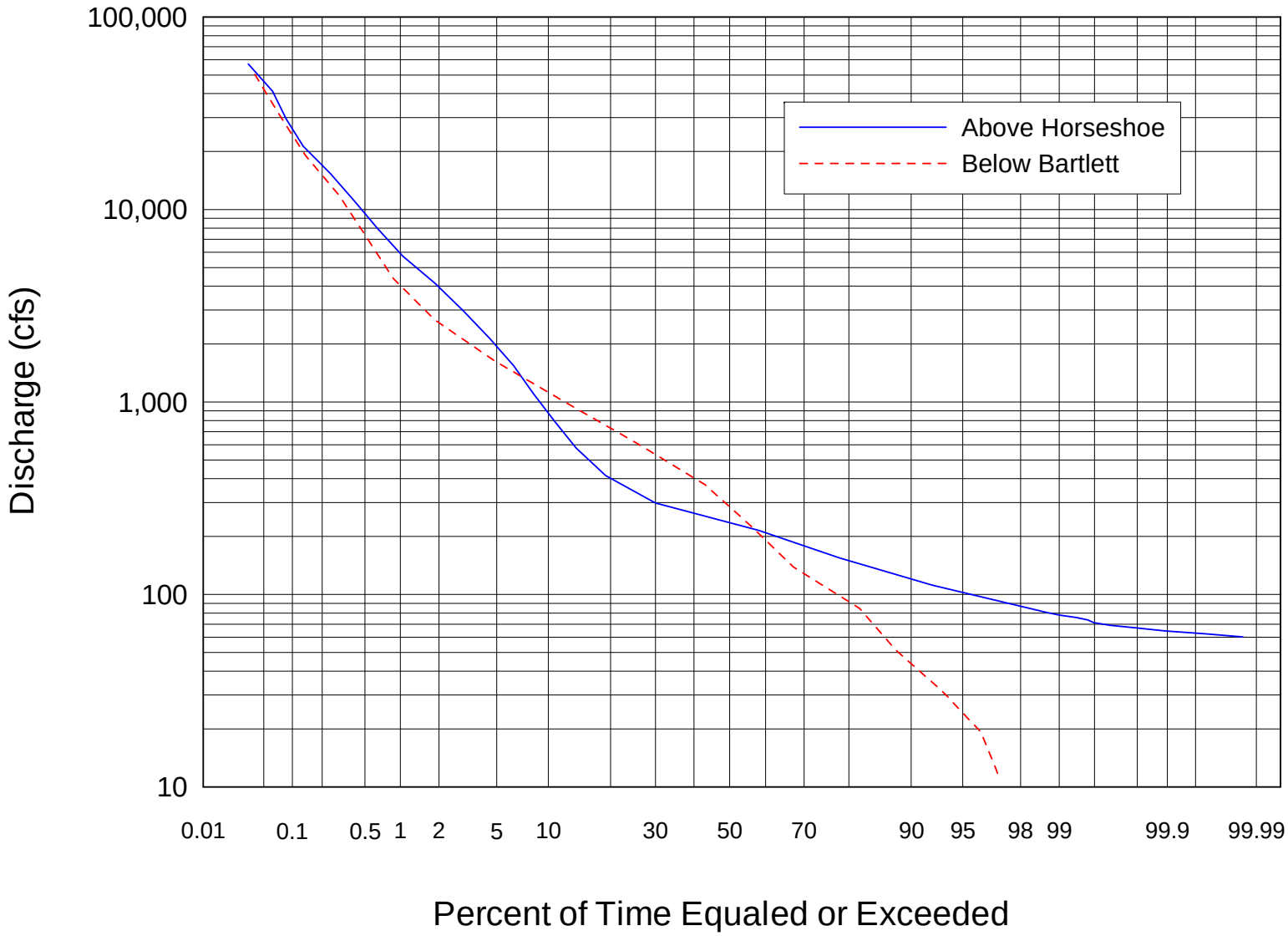

Figure 3.6. Comparison of mean-daily flow duration curves for the above Horseshoe and below Bartlett gages for the post-dam period (1946—2002).

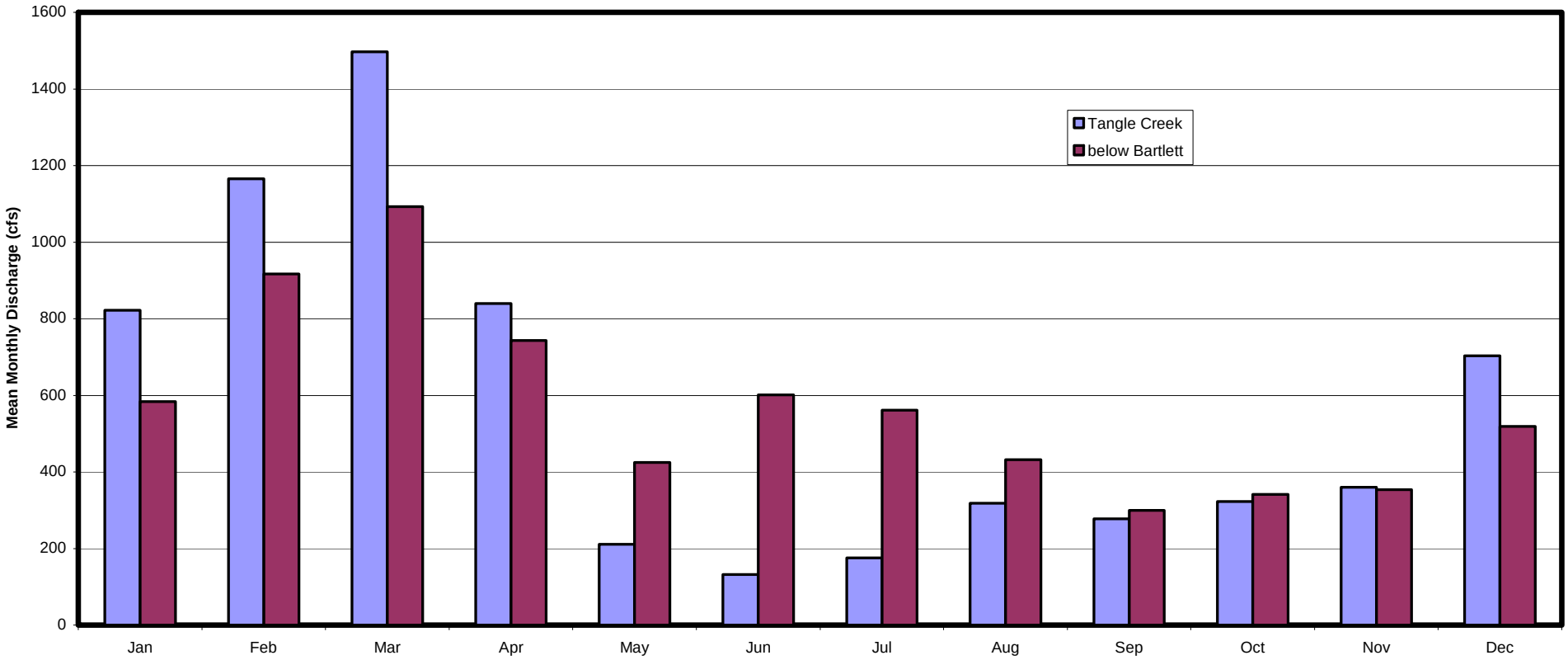

Figure 3.7. Comparison of mean monthly discharges at Tangle Creek and below Bartlett gages for the post-dam period (1946—2002).

The specific hydrographs that were analyzed were selected through joint consultations between MEI, ERO, and SRP. The potential effects of each of the three alternatives on the flood hydrographs at study Sites 2 and 3, which are located between the two dams and downstream from both dams, respectively, were assessed by routing the recorded flows at the Tangle Creek gage through the reservoirs using the RiverSim model, a river-basin model that allows the user to simulate reservoir operations for a given upstream input hydrograph and pre-defined reservoir-operational rules, constraints, and demands (see www.watersteward.com). The RiverSim routings were carried out by SRP, and the results were provided to MEI for use in this analysis. The following paragraphs, taken from information that was provided to MEI by ERO and SRP, describe the basic objectives and constraints that would control operations under each of the three scenarios.

Alternative 1 (Historical Operations) refers to the current and historical operational regime for Horseshoe and Bartlett Reservoirs. This scenario serves as a baseline with which to compare changes that would result from the modified operations associated with Alternatives 2 and 5. Under existing operations, during the winter and spring months (October 1 through April 30), water is typically delivered to meet SRP demands from the Verde River reservoirs to keep storage levels low, thereby maximizing the ability to capture runoff and minimizing the risk of spilling water from Bartlett Dam. These months have the lowest demand and the highest potential to produce the greatest amounts of runoff. Because the storage capacity of the Salt River reservoirs is relatively large in comparison to the Verde River reservoirs, there is usually sufficient space available to store runoff in the Salt River side of the water-supply system during winter and spring, and to provide releases during the summer when water demand is the greatest. In addition, due to the lack of power generation on the Verde River, water is stored during the winter on the Salt River for release during the summer when demand for electricity is the greatest. For these reasons, water releases to meet orders are progressively shifted from the Verde River reservoirs to the Salt River reservoirs in late-April or early-May.

Under **Alternative 2 (No Permit)**, the U.S. Fish & Wildlife Service (USFWS) would not issue an Incidental Take Permit (ITP) to SRP for continued operation of Horseshoe or Bartlett Reservoirs. Without the ITP, SRP would be expected to do everything within its control to avoid take of federally-listed species associated with the continued operation of the reservoirs. To avoid the risk of potential take of SWWFC, it would be necessary to operate Horseshoe Reservoir in a manner that would reduce the water level below the elevation at which SWWFC nested in the previous year (determined to be 1,985 feet in 2002 and 2003). Based on this requirement, the reservoir elevation would be lowered in April to reach a target elevation of 1,985 feet in late-April to early-May to expose the vegetation used for flycatcher nesting (uncontrolled high runoff during late spring could delay meeting the target elevation). Horseshoe Reservoir would be held at or below elevation 1985 feet through August.

Under **Alternative 5 (Mimic Natural Hydrograph),** alternative floods would be passed through Horseshoe and Bartlett Reservoirs from February through May in order to mimic the natural hydrograph, to the extent possible, to benefit downstream riparian areas.

These scenarios were modeled by selecting representative hydrographs from the historical record that cover a range of flood magnitudes. Because the RiverSim simulations are based on a time-step length of one hour, the mean daily flows in the published USGS record could not be used, and a special data request was made to the USGS for detailed flow data with shorter time-steps. The more detailed data were only available for WY1991 and later; thus the six hydrographs that were analyzed were selected from the post-WY1990 time-frame **(Table 3.1).**

Table 3.1. Summary of recorded peak hourly flows for the hydrographs selected for use in the reservoir operation simulations.					
Year	Date of Peak	Above Horseshoe Dam		Below Bartlett Dam	
		Peak Hourly Flow (cfs)	Approximate Recurrence Interval (years)*	Peak Hourly Flow (cfs)	Approximate Recurrence Interval (years)**
1991	27 March	34,180	4.0	4,320	3.2
1993	8 January	135,170	44	114,300	61
1995	15 February	107,720	19	40,620	10
1995 (March)	6 March	87,760	14	40,620	10
1997	27 January	5,660	1.2	1,280	1.2
1998	29 March	25,450	3.0	8,820	3.9

* Based on recorded instantaneous flood peaks and the USGS flood-frequency curve for the above Horseshoe gage (Figure 3.4). The value for the March 1995 flood is based on the peak hourly flow.
**Based on the plotting positions of the individual events (Figure 3.5).

These hydrographs had peak hourly discharges at the Tangle Creek gage ranging from 5,660 to 135,170 cfs (recurrence intervals ranging from about 1.2 to 44 years). Peak hourly flows below Bartlett Dam for the hydrographs ranged from 1,280 to 114,300 cfs (approximate recurrence intervals ranging from about 1.2 to about 61 years).

With the exception of the 1993 and 1997 hydrographs, for which the peak discharge occurred in January, the simulations used a constant hydrograph start-date of February 1. The simulations for 1993 and 1997 used start-dates of January 1 and January 10, respectively. Because the bulk of the runoff for each simulation occurs in one to two months, the effect of the reservoirs on floods primarily occurs before April, the time at which Horseshoe Reservoir would need to be drawn down in order to avoid take of flycatchers under the No Permit Alternative. For the purposes of this analysis, there is, therefore, no difference between Alternatives 1 and 2 (Historical Operation and No Permit). As a result, only two operational scenarios remain for the comparative analysis presented in this report: (1) the Historical Operation/No Permit Alternative, referred to henceforth as the Full Operation scenario, and (2) the Mimic Natural Hydrograph Alternative, referred to henceforth as the Full Release scenario.

The effects of the reservoirs on the downstream hydrographs under either scenario are strongly impacted by the reservoir storage at the beginning of the hydrograph. In addition, the reservoir storage during the winter months when the selected floods occurred can vary significantly from year to year, and cannot be predicted with certainty for future operations. For this reason, the simulations for each of the two scenarios were performed with two different starting reservoir levels to provide a sensitivity analysis on the effects on starting reservoir storage. A statistical analysis of the historic February 1 reservoir storages performed by ERO indicated a bi-modal distribution, with a lower mode at about 50,000 ac-ft and a higher mode at about 290,000 ac-ft (i.e., both reservoirs full). Based on ERO's results, a low initial starting reservoir-storage condition was modeled for each scenario with no storage in Horseshoe Reservoir and 50,000 ac-ft of storage in Bartlett Reservoir. For the Full Operational scenario, a high initial starting reservoir-storage condition, with both reservoirs full (109,217 ac-ft in Horseshoe and 178,186 ac-ft in Bartlett) was modeled. Due to the release criteria under the Full Release scenario, the

high initial reservoir condition was modeled with both reservoirs at the top of the spillways (50,389 ac-ft in Horseshoe and 72,073 ac-ft in Bartlett). Starting with the reservoirs full under this scenario would result in large releases at the beginning of the simulation which would not be in accord with the manner in which the reservoirs would actually be operated.

The assumed average monthly demand on the Verde River reservoirs that was used in the simulations ranged from 277 cfs in January to 1,514 cfs in May (**Table 3.2)**. The simulations also assumed that demand releases from Bartlett would be met as long as sufficient water is available in the reservoir. If sufficient water is not available, releases would be made from Horseshoe Reservoir. Storage-guide curves for the two alternatives considered in the analysis are provided in **Tables 3.3 and 3.4**.

Table 3.2. Demand on Verde River Reservoirs.

Month	Demand	
	Acre-feet	Average Discharge (cfs)
January	17,000	277
February	32,100	578
March	81,100	1,319
April	90,000	1,514
May	49,500	805
June	32,000	538
July	9,000	146
August	8,000	130
September	8,000	134
October	8,000	130
November	27,120	456
December	8,000	130

A summary of computed peak flows for the different simulations is provided in **Figures 3.8 and 3.9** for the reaches below Horseshoe Dam and Bartlett Dam, respectively, and plots of the routed hydrographs are provided in **Appendix B**. Examination of the routing results leads to the following general observations:

- The initial reservoir storage has a more significant effect on downstream flood peaks than changes associated with the proposed operational rules,
- The reservoirs significantly affect downstream floods during the smaller events, but the effect is less significant during the larger events,
- Timing of storms can also be important, as floods with peaks later in the year are less affected by the initial storage because of the effects of water that is stored before the flood occurs, and

Table 3.3. No Permit Alternative reservoir-storage guide.							
Month	Horseshoe Reservoir			Bartlett Reservoir			Verde System
	Maximum Elevation (ft)	Maximum Storage (ac-ft)	Comments	Maximum Elevation (ft)	Maximum Storage (ac-ft)	Comments	Maximum Storage (ac-ft)
October	2,026	109,217		1,798	178,186	No limitations on Bartlett	287,403
November	2,026	109,217		1,798	178,186		287,403
December	2,026	109,217		1,798	178,186		287,403
January	2,026	109,217		1,798	178,186		287,403
February	2,026	109,217		1,798	178,186		287,403
March	2,026	109,217		1,798	178,186		287,403
April	1,985	25,651	Start drawdown for nesting	1,798	178,186		203,837
May	1,985	25,651	Nesting season SWWFC	1,798	178,186		203,837
June	1,985	25,651	Nesting season SWWFC	1,798	178,186		203,837
July	1,985	25,651	Nesting season SWWFC	1,798	178,186		203,837
August	1,985	25,651	Nesting season SWWFC	1,798	178,186		203,837
September	2,026	109,217	Flycatcher leaves for Costa Rica	1,798	178,186		287,403

Table 3.4. Mimic Natural Hydrograph Alternative reservoir-storage guide.							
Month	Horseshoe Reservoir			Bartlett Reservoir			Verde System
	Maximum Elevation (ft)	Maximum Storage (ac-ft)	Comments	Maximum Elevation (ft)	Maximum Storage (ac-ft)	Comments	Maximum Storage (ac-ft)
October	2,026	109,217		1,798	178,186	No limitations on Bartlett	287,403
November	2,026	109,217		1,798	178,186		287,403
December	2,026	109,217		1,798	178,186		287,403
January	2,026	109,217		1,798	178,186		287,403
February	2,000	50,389	Gates fully open	1,748	72,073	Gates fully open	122,462
March	2,000	50,389	Gates fully open	1,748	72,073	Gates fully open	122,462
April	2,000	50,389	Gates fully open	1,748	72,073	Gates fully open	122,462
May	2,000	50,389	Gates fully open	1,798	178,186		228,575
June	1,985	25,651	Nesting season SWWFC	1,798	178,186		203,837
July	1,985	25,651	Nesting season SWWFC	1,798	178,186		203,837
August	1,985	25,651	Nesting season SWWFC	1,798	178,186		203,837
September	2,026	109,217	Flycatcher leaves for Costa Rica	1,798	178,186		287,403

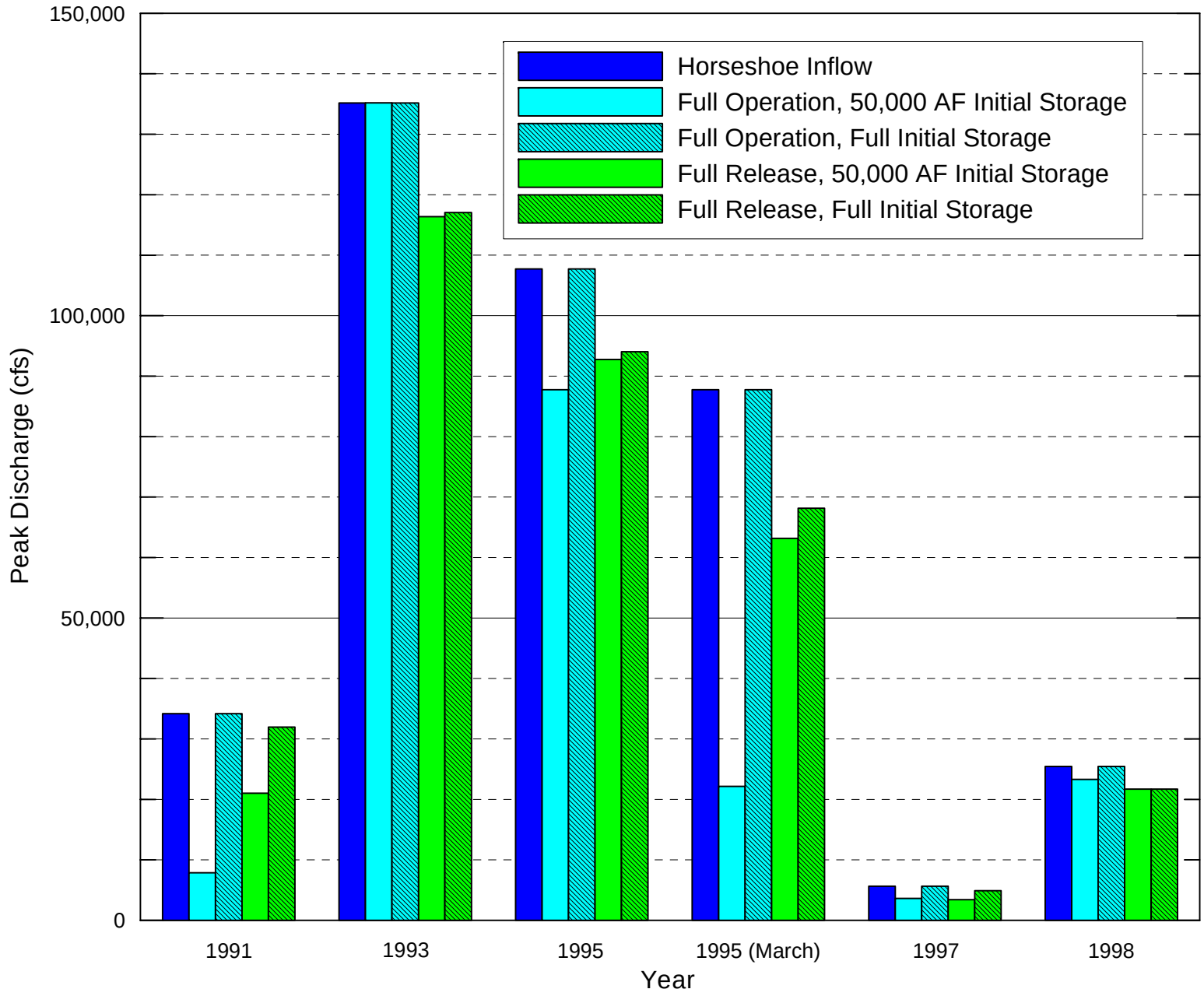

Figure 3.8. Bar graph summarizing computed flood peaks below Horseshoe Dam for the various reservoir operational scenarios.

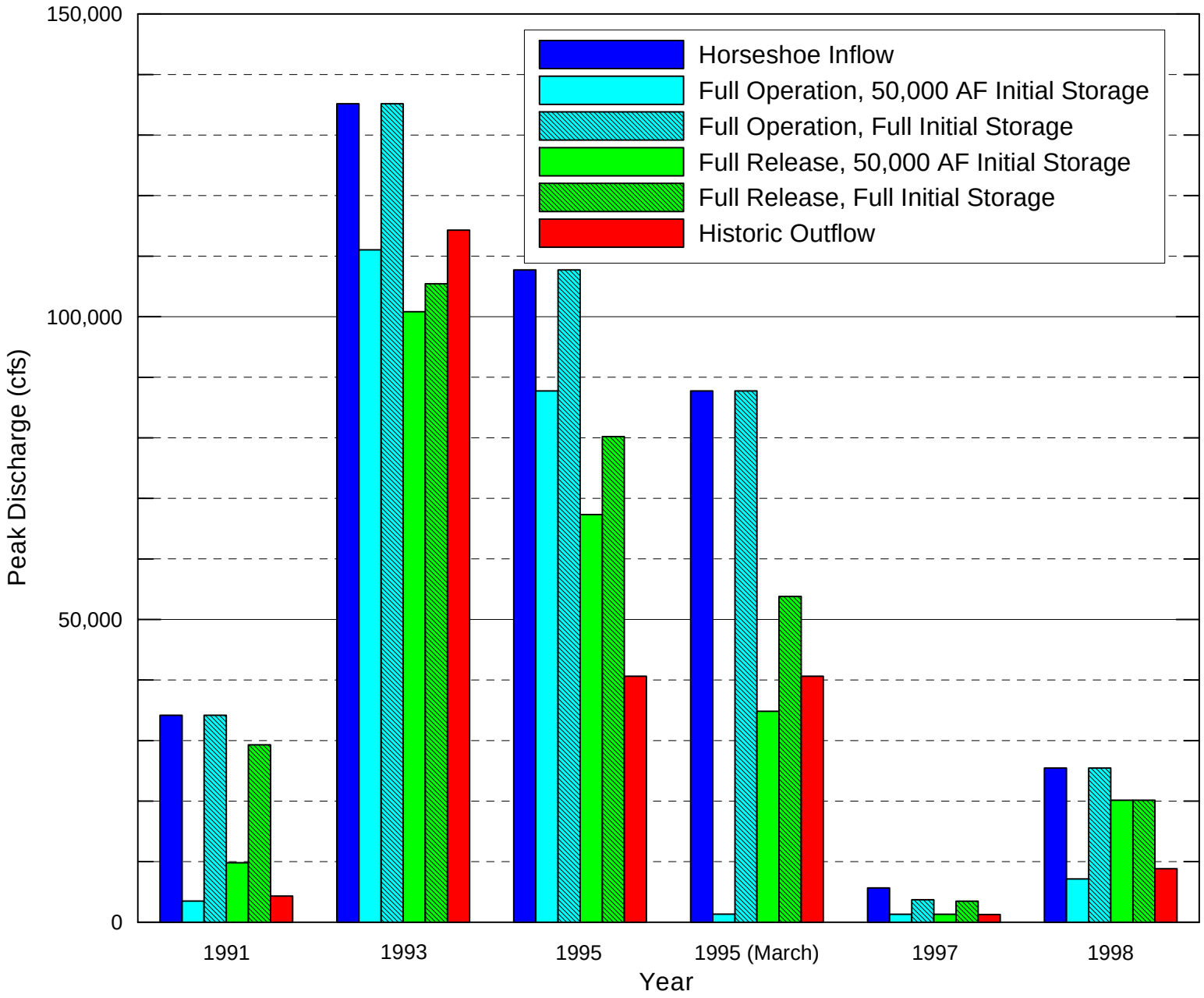

Figure 3.9. Bar graph summarizing computed flood peaks below Bartlett Dam for the various reservoir operational scenarios.

- Because of the above, no general trends with respect to the effects on peak discharges downstream from the dams are evident between the Full Operation and Full Release scenarios.

A detailed examination of the results below Horseshoe Dam (Figure 3.8) illustrates the above points. Under the Full Operation scenario with full initial storage, flood peaks are not attenuated in any of the simulated hydrographs. Because the maximum initial storage under the Full Release scenario is limited to the top of the spillway, there is some storage available, which results in a modest amount of flood-peak attenuation. With no initial storage in Horseshoe Reservoir (simulations with 50,000 ac-ft of system storage), the Full Operation scenario generally results in more flood-peak attenuation than the Full Release scenario. The attenuation is greatest for the 1991 and 1995 (March) events, which had small to moderate-sized flood peaks and small runoff volumes. In 1993, the largest flood examined both in terms of peak-flow and runoff volume, even with no initial storage in Horseshoe, there is no attenuation under the Full Operation scenario, but there is some attenuation under the Full Release scenario. In this case, the reservoir fills under the Full Operation scenario before the flood peak occurs, while earlier releases under the Full Release scenario result in more available storage when the flood peak occurs. In 1998, the peak inflow to Horseshoe occurs late in the simulation, and the results are less affected by the initial storage because the reservoir has time to fill before the flood occurs.

Examination of the results below Bartlett Dam (Figure 3.9) shows trends that are similar to those below Horseshoe Dam. With Bartlett Reservoir full under the Full Operation scenario, there is generally little or no flood-peak attenuation. With the maximum initial storage limited to the top of the spillway under the Full Release scenario, the additional available storage results in a modest amount of flood-peak attenuation. For simulations with only 50,000 ac-ft of initial storage in Bartlett Reservoir, the additional available storage results in more flood-peak attenuation for both scenarios. Under the Full Operation scenario, the additional available storage can result in significant attenuation for floods with small runoff volumes [e.g., 1991 and 1995 (March)].

4. HYDRAULIC ANALYSIS

One-dimensional (1-D) hydraulic models were developed for each of the three study sites to assist in evaluating the amount of inundation and substrate mobilization that would occur over the range of flows encompassed by the routed hydrographs. Model output provides estimates of the water-surface elevation, flow velocities, flow depths and bed shear stresses throughout each of the sites.

4.1. Model Development

The hydraulic analysis was carried out using the Corps of Engineers HEC-RAS computer software (USACOE, 2002). Topographic data for each of the models were developed from surveyed cross-section and aerial mapping that were provided to MEI by SRP. As previously described, the field-surveyed cross sections were laid out by MEI during the November 2002 site visits, and the actual surveys were performed by SRP. Additional topographic information was obtained from 2-foot contour interval mapping of the sites that was developed using aerial photogrammetric mapping techniques by SRP specifically for this project. The mapping was provided to MEI in digital terrain model (DTM) format for use with Bentley Systems InRoads Site, Version 8.04, with MicroStation, Version 8.01. Vertical control for the mapping and hydraulic models is based on the North American Vertical Datum of 1988 (NAVD), and horizontal control is based on the U.S. State Plane Coordinate System of 1983, Arizona Central Zone.

In developing the hydraulic models, the field-surveyed data were used directly in the input files, to the extent possible, because it provides the most accurate data at the survey locations. Where additional topographic data were required to extend cross sections beyond the limits of the field surveys or to add additional cross sections to improve the resolution of the models, this information was taken directly from the DTM using the InRoads and MicroStation software. At the cross sections that were added from the mapping, the below-water profile was estimated based on the typical shape of the surveyed cross sections at geomorphically similar locations. At each of the sites, the mapping and hydraulic models extended sufficiently far upstream from the most upstream surveyed cross section to include flow breakouts that affect the amount of flow that would actually pass through the primary study site over the range of modeled flows. The cross-section layouts for each model are shown in Figures 2.1 through 2.3.

Flow conditions at each of the study sites are very complex, with flow breakouts at high flows, multiple flow paths, and low areas in the overbanks that are not connected to the main channel. To account for this complexity in a manner consistent with the 1-D modeling approach used for this study, each continuous well-defined flow path was analyzed using a separate reach in the hydraulic model. The discharge in each reach was determined automatically using the split-flow routine in HEC-RAS that balances the computed energy grade-line elevation at the upstream end of each branch. Less well-defined flow paths were accounted for using the HEC-RAS ineffective flow-area options to ensure that low areas not connected to the main channel do not flow until the intervening high ground is overtopped, and to ensure reasonable flow continuity in the overbanks from cross section to cross section. Because the nature of the flow paths change with discharge (areas with well-defined separate flow paths at low flows become connected at high flows), different model configurations were used at each site for specific ranges of discharge. The model configurations are illustrated in the georeferenced geometry files included in the HEC-RAS project files set up for each site.

The roughness and energy-loss characteristics of the river channel and overbank areas are accounted for in the HEC-RAS software through the use of Manning's *n* roughness coefficients, and expansion and contraction loss coefficients. Manning's *n*-values for the overbank areas were estimated from aerial photographs and field observations. Horizontal variations in overbank *n*-values were included in the models to account for different zones of vegetation as identified on the aerial photographs. Overbank *n*-values used in the models ranged from 0.035 for bare ground to 0.08 for dense riparian vegetation (**Table 4.1**). A constant main-channel *n*-value of 0.035 was used at each site based on the roughness characteristics of the channel as observed in the field and previous experience with similar rivers, and the selected *n*-values were verified by comparing computed water-surface elevations with field-surveyed water-surface elevations and high-water marks.

Table 4.1. Summary of Manning's *n* roughness values used in the hydraulic models.

Roughness Description	Manning's *n*
Channel bed / bare ground	0.035
Light brush	0.04-0.045
Medium density brush / trees	0.06
Dense brush / trees	0.08

The 1-D hydraulic models require specification of either the water-surface elevation or energy gradient at the downstream cross section. For this project, the water-surface elevation was specified for each modeled flow based on a rating curve that was developed using measured data, where available (i.e., surveyed water-surface elevations at low flows at each site and surveyed high-water marks from recent floods at Sites 1 and 2), and normal depth calculations for flows other than at the measured values. Energy slopes used in the normal depth calculations were estimated so that the computed water-surface elevations would match the measured values as close as possible. At Site 1, the assumed energy slopes ranged from 0.0005 at very low flows to 0.005 at the highest flows. A constant energy slope of 0.004 was used at Site 2 and a constant energy slope of 0.0015 was used at Site 3. At both Sites 2 and 3, the assumed energy slope used in the model is approximately the same as the average bed slope at the respective site.

4.2. Model Verification

The hydraulic models at each site were verified, to the extent possible, using available data. These data included water-surface elevations measured at the time of the cross-section surveys and surveyed high-water marks from recent floods (February and March 2003) at Sites 1 and 2 (data on high-water marks were not available at Site 3). Discharges at the times of the elevation measurements were provided to MEI by SRP (**Table 4.2**).

At Site 1, the computed and measured water-surface elevations are in good agreement at low flows in the 260 to 300 cfs range (**Figures 4.1**). Agreement between the computed water-surface elevations and high-water marks associated with maximum discharges of 7,530 and 13,700 cfs is also very reasonable, although there is more scatter in the surveyed high-water marks than occurs with the measured water-surface profiles (**Figures 4.2 and 4.3**). This is typical because of the difficulty in determining precise flood elevations from debris and other

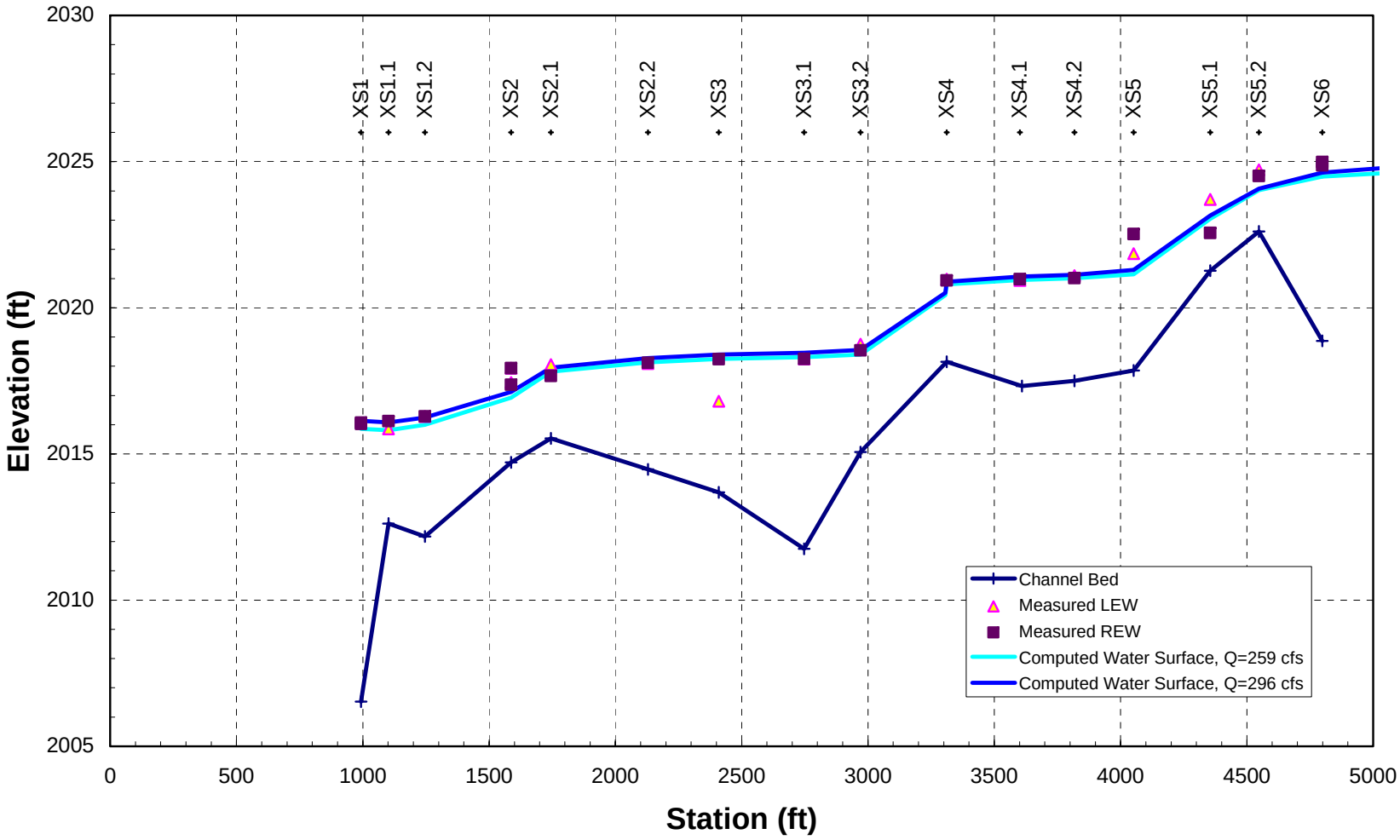

Figure 4.1. Site 1 surveyed water-surface elevations and computed water-surface profiles for the discharges at the time of the survey (259 to 296 cfs).

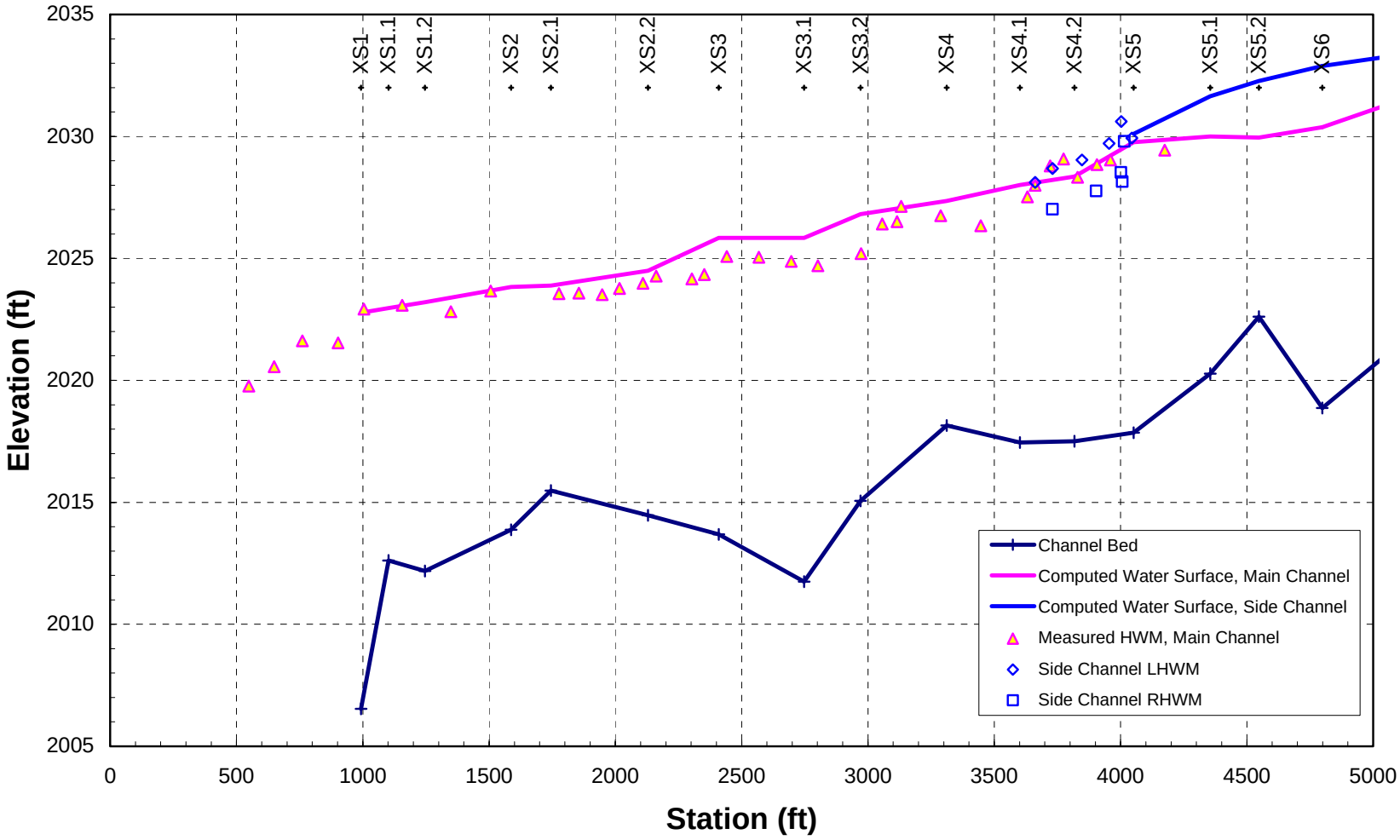

Figure 4.2. Site 1 surveyed high-water marks corresponding to the first 2003 flood peak (February 14) and the computed water-surface profile for the peak discharge (7,530 cfs).

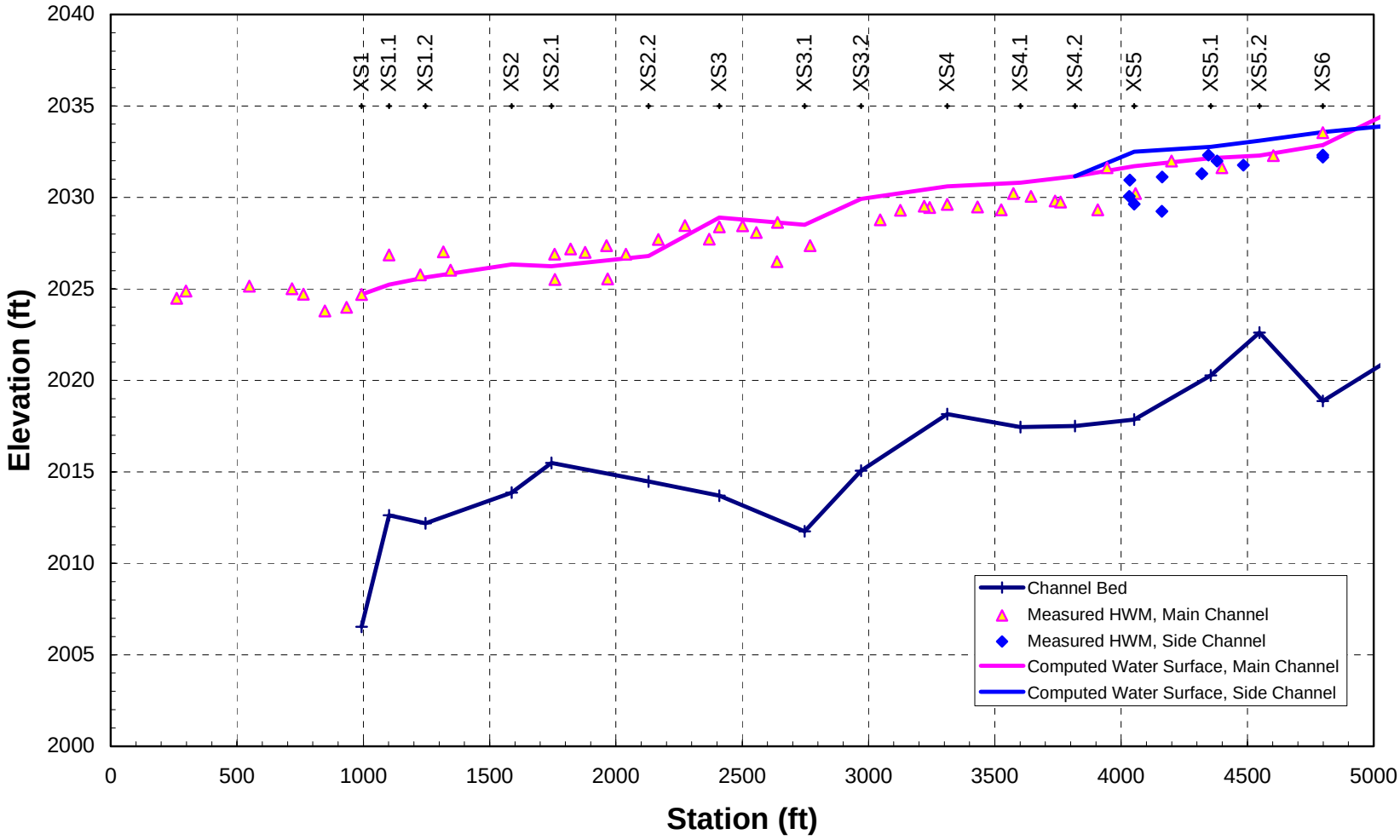

Figure 4.3. Site 1 surveyed high-water marks corresponding to the second 2003 flood peak (March 17) and the computed water-surface profile for the peak discharge (13,700 cfs).

marks left by the flood. In some cases, the surveyed elevations may over-represent flood elevations due to such factors as wind, wave action, and debris piled up on obstructions (representing elevations closer to the energy grade line than the water surface). In other cases, the surveyed elevations may be lower than peak-flood elevations because the actual high-water mark may be obscured and/or the identified mark may be associated with debris lines associated with flows on the recession limb of the hydrograph.

Table 4.2. Summary of data used for model verification.

Location	Description	Discharge (cfs)
Site 1	Surveyed water surface	259—296
	2003 high-water marks, 1st flood peak (February 14)	7,530
	2003 high-water marks, 2nd flood peak (March 17)	13,700
Site 2	Surveyed water surface	225—250
	2003 high-water marks, 1st flood peak (February 28)	1,425
	2003 high-water marks, 2nd flood peak (March 19)	7,100
Site 3	Surveyed water surface	300—500

Similar agreement is obtained at Site 2 for the low-flow water-surface elevations that were measured at discharges ranging from of 225 to 250 cfs (**Figure 4.4**). For the surveyed high-water marks corresponding to a maximum discharge of about 1,425 cfs, the agreement is also very good along the main channel, but the model appears to slightly under-predict water-surface elevations in the overbank area between about XS2 and XS3.1 (**Figure 4.5**). The scatter in the second set of surveyed high-water marks is greater in the downstream portion of the reach, and the modeled water-surface elevation generally passes through the data (**Figure 4.6**).

At Site 3, the agreement between the computed and measured water-surface elevations at discharges of 300 to 500 cfs is also reasonable, although the model slightly under-predicts elevations in the vicinity of the riffles at XS4 and upstream of XS6 (**Figure 4.7**). No surveyed high-water marks were available for this site; however, the model was developed in the same manner as the models at Sites 1 and 2 and should provide similar accuracy.

4.3. Model Results

The hydraulic models for the three sites were run for a range of discharges from very low flows up through the estimated 100-year flood peak (200,300 cfs). HEC-RAS input and output files are included on the CD that accompanies this report. Tables listing the values of important hydraulic variables used in the inundation and incipient-motion analyses are included in **Appendix C**. Water-surface profiles for the main flow path at each site and covering a wide range of flows are shown in **Figures 4.8 through 4.10**.

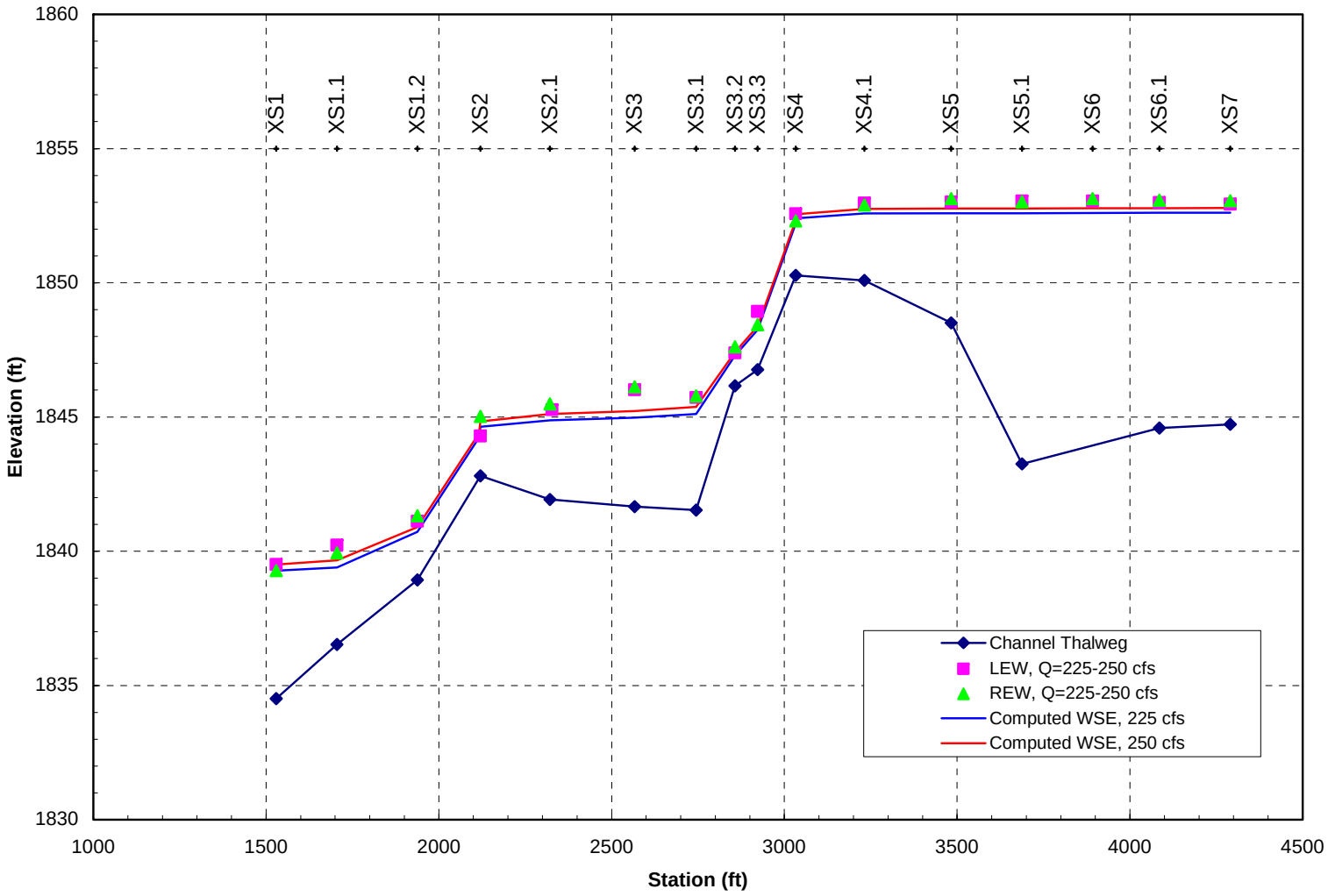

Figure 4.4. Site 2 surveyed water-surface elevations and computed water-surface profiles for the discharges at the time of the survey (225 to 250 cfs).

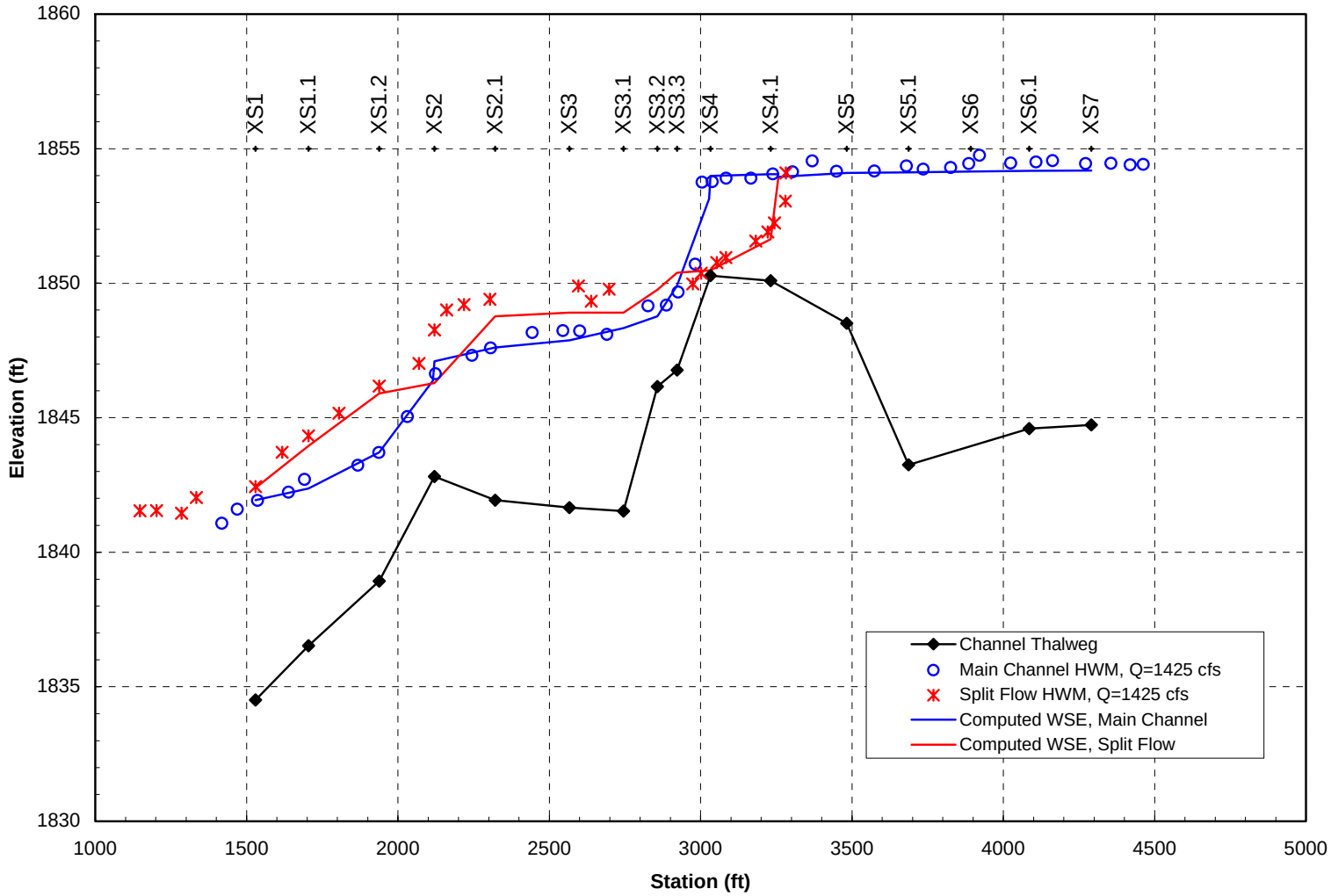

Figure 4.5. Site 2 surveyed high-water marks corresponding to the first 2003 flood peak (February 28) and the computed water-surface profile for the peak discharge (1,425 cfs).

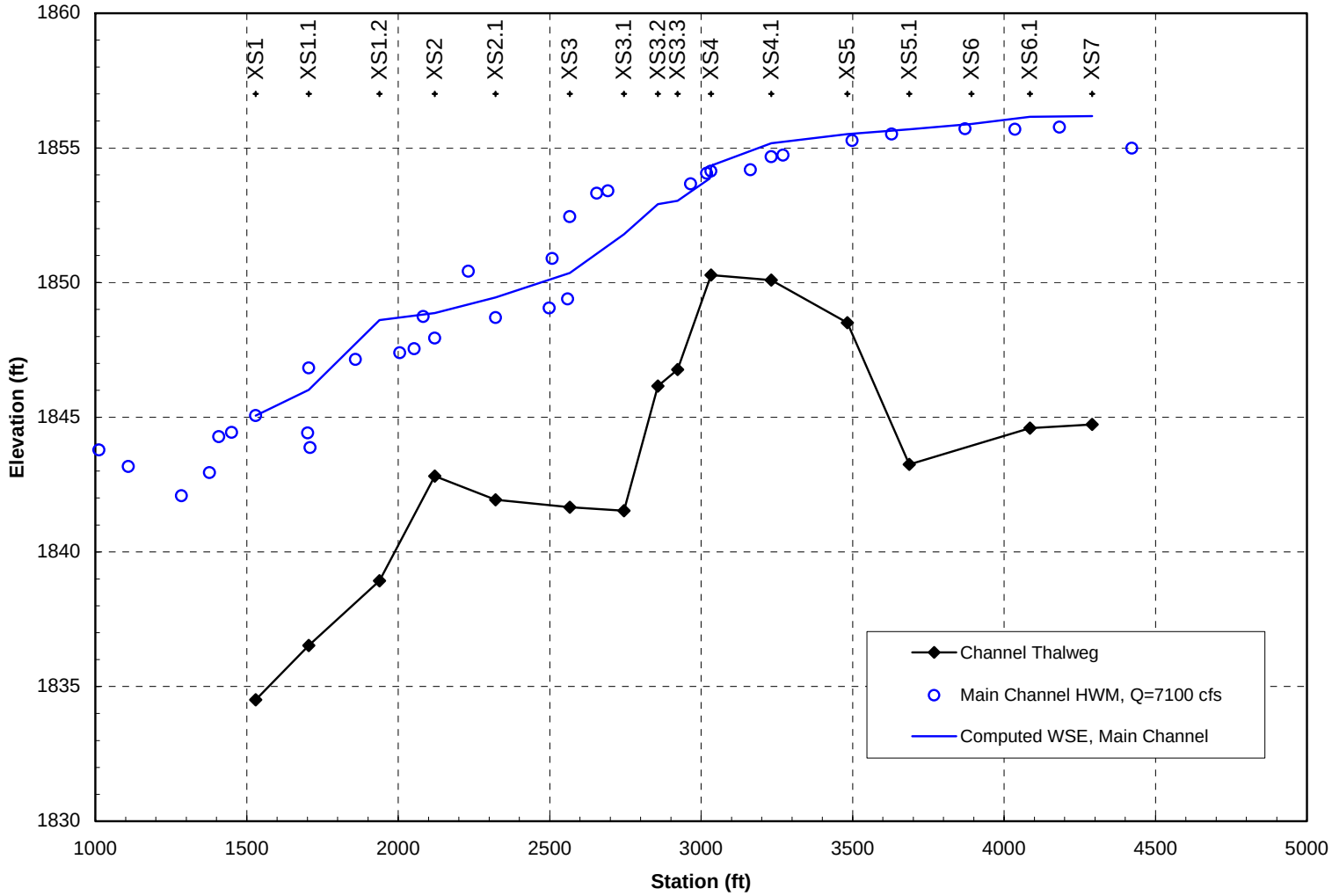

Figure 4.6. Site 2 surveyed high-water marks corresponding to the second 2003 flood peak (March 19) and the computed water-surface profile for the peak discharge (7,100 cfs).

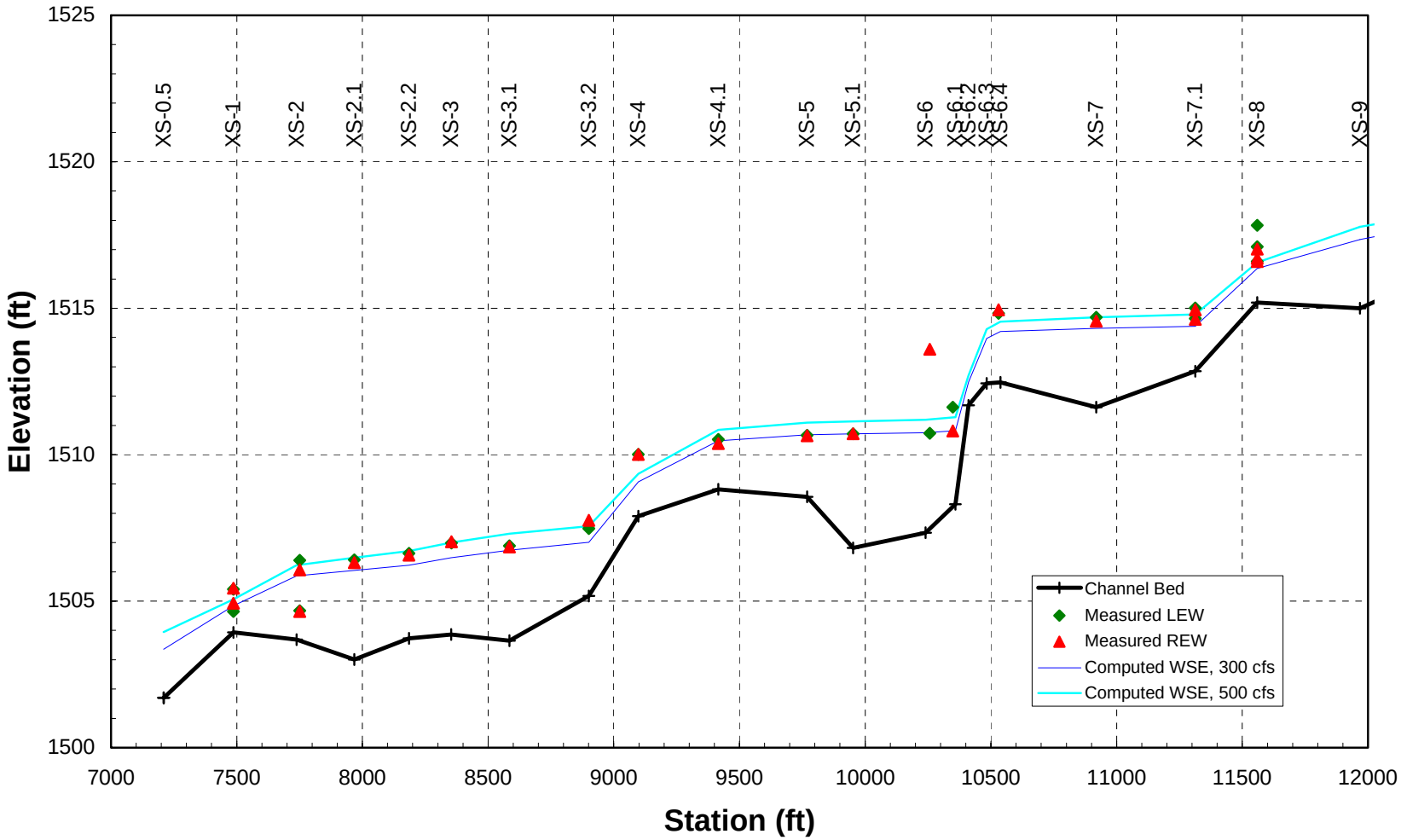

Figure 4.7. Site 3 surveyed water-surface elevations and computed water-surface profiles for the discharges at the time of the survey (300 to 500 cfs).

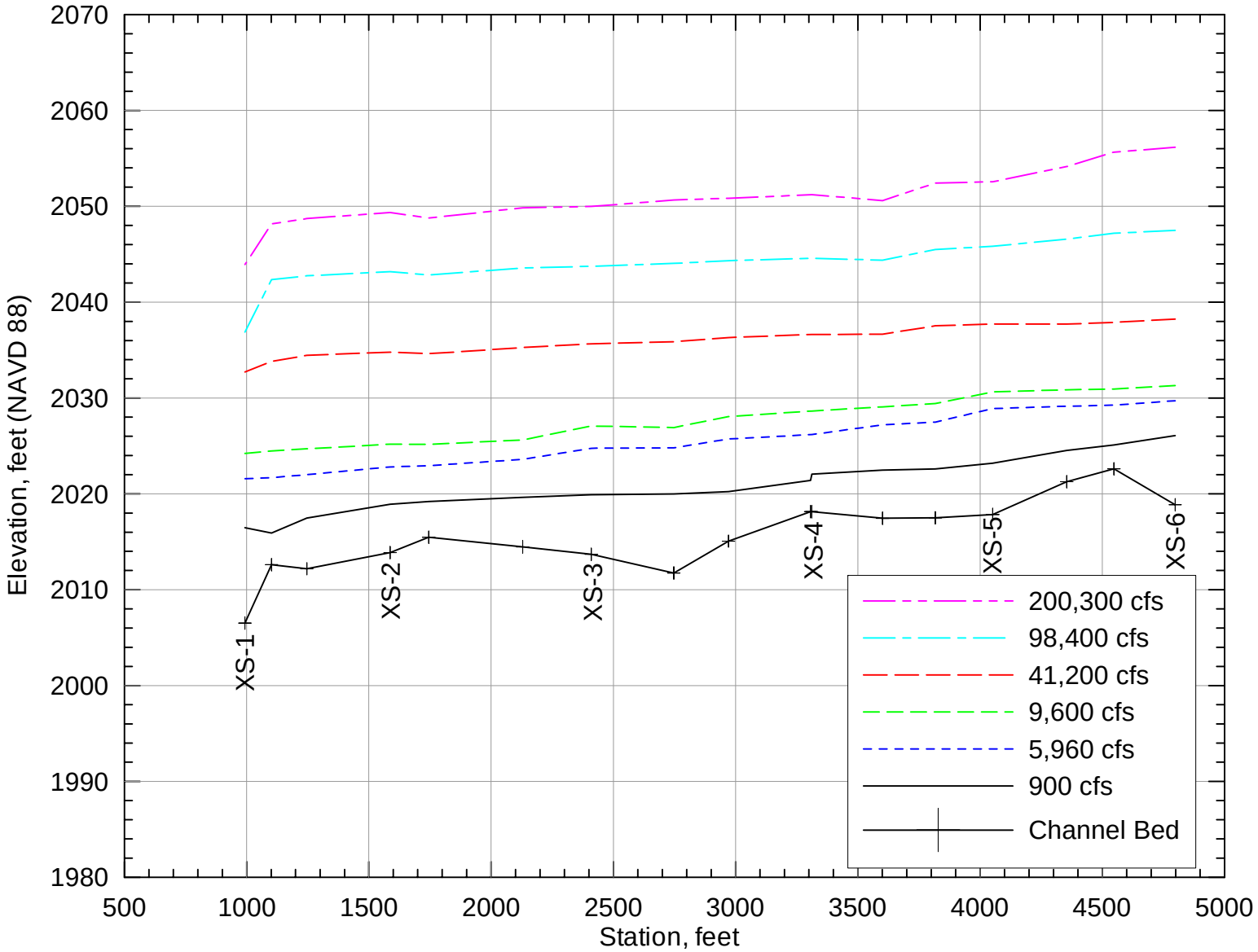

Figure 4.8. Computed water-surface profiles at Site 1 for discharges ranging from 150 to 200,300 cfs.

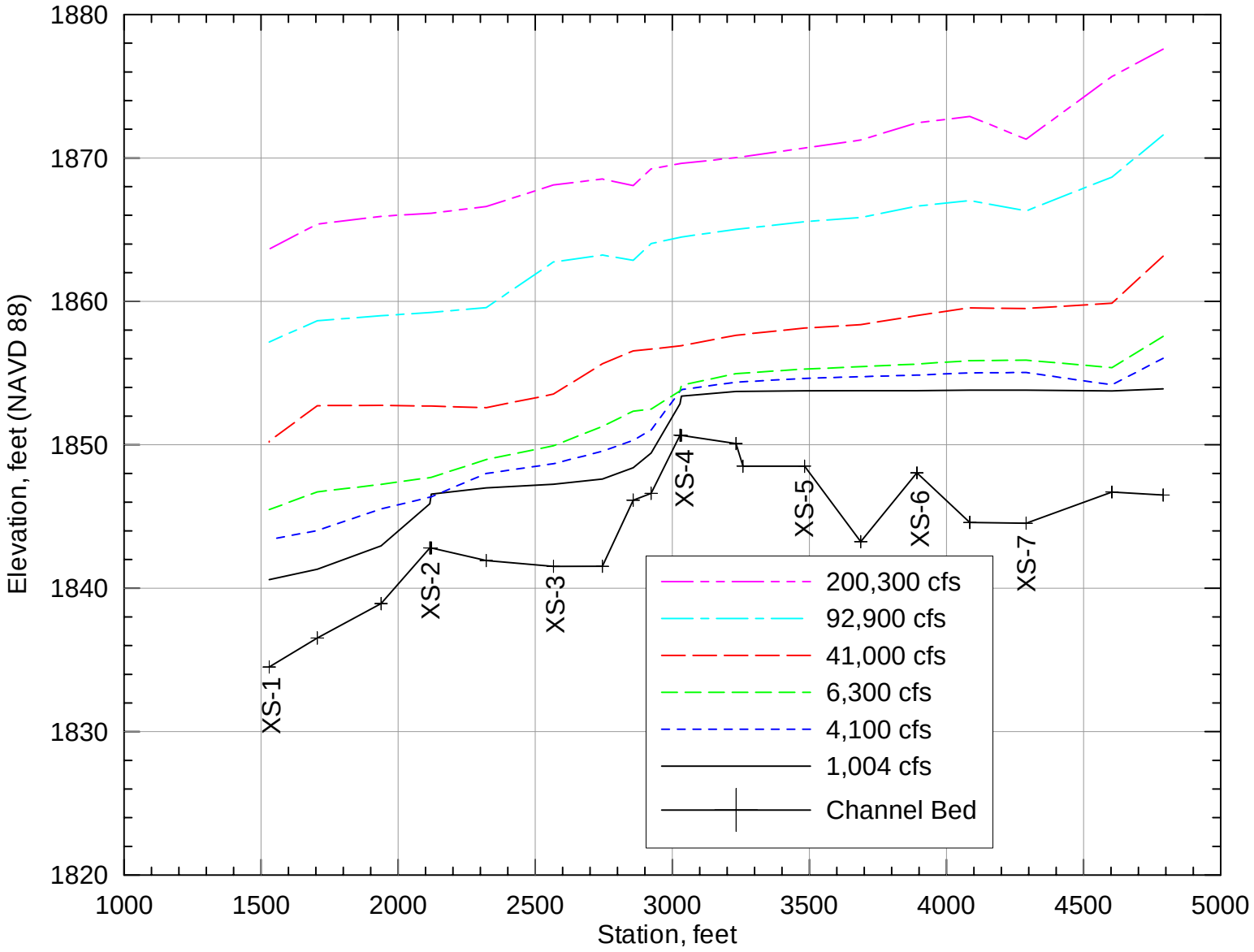

Figure 4.9. Computed water-surface profiles at Site 2 for discharges ranging from 117 to 200,300 cfs.

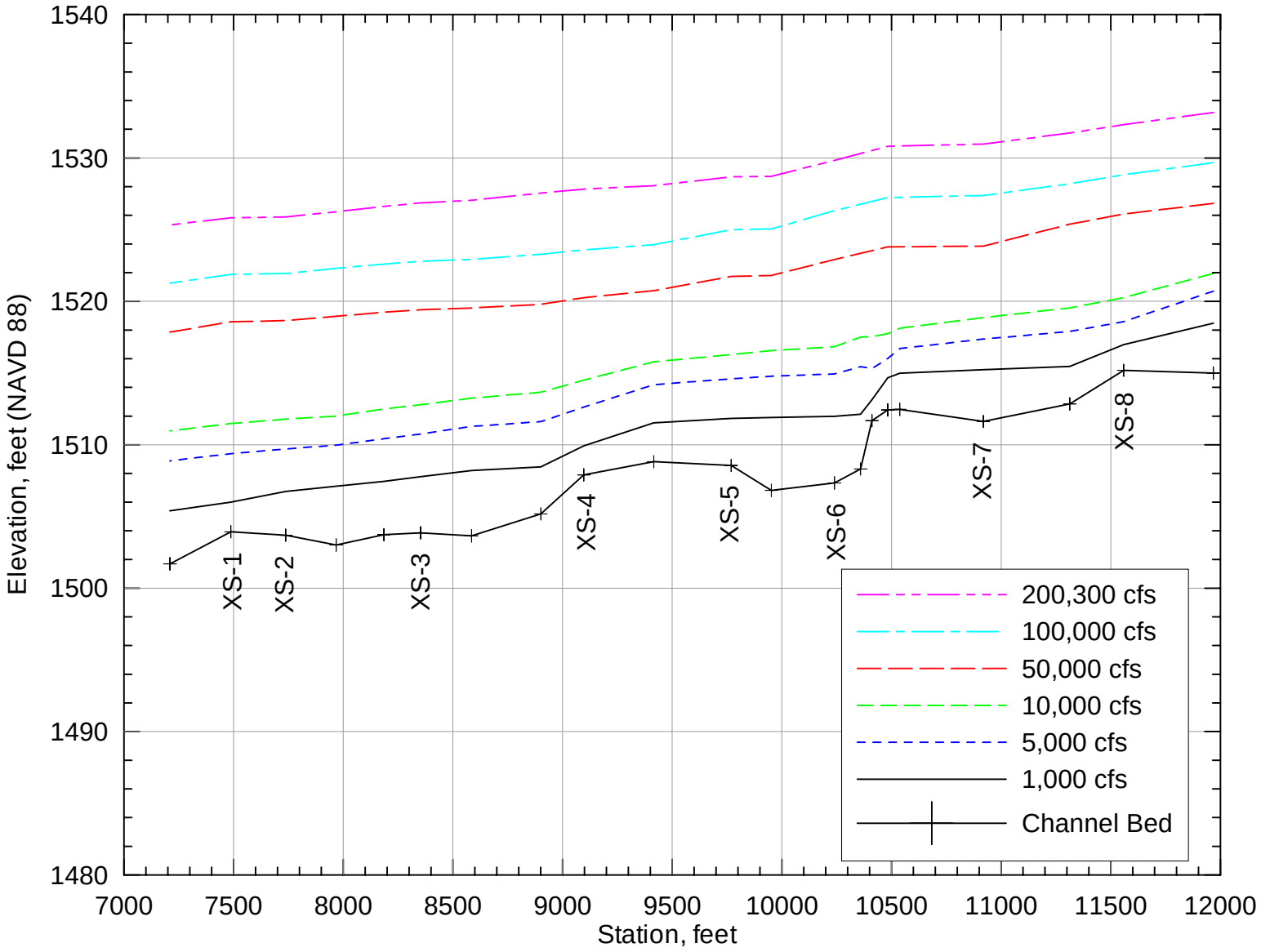

Figure 4.10. Computed water-surface profiles at Site 3 for discharges ranging from 300 to 200,300 cfs.

4.4. Inundation and Incipient-Motion Analyses

The output from the hydraulic modeling was used to conduct incipient-motion and inundation analyses. The inundation analysis quantifies the effects of the different dam operational scenarios on the extent and frequency of inundation of the various geomorphic surfaces along the river at each study site. The incipient-motion analysis determines the flows necessary to mobilize the bed and bar sediments that form the substrate for the riparian vegetation.

For the inundation analysis, the hydraulic models were run for a range of flows from very low flows up through the 100-year event. Results from the models were then used to develop water-surface elevation versus discharge rating curves for each of the surveyed cross sections. Where multiple flow paths exist at a particular cross section (see discussion in Section 4.1), separate rating curves were developed for different portions of the cross section. Modeled water-surface elevations for select discharges covering the range of modeled flows were then plotted on the cross sections to show the extent of inundation that would occur at different flow levels. The cross-section plots are color-coded to show the existing vegetation types on each of the surfaces (Appendix A). Comparison of the water-surface elevations with the color-coded cross-section plots shows the amount and type of vegetation that is inundated for each scenario.

The incipient-motion analysis was carried out by evaluating the effective shear stress on the channel bed in relation to the amount of shear stress that is required to move the sediment sizes that are present. The shear stress required for bed mobilization was estimated using the Shields (1936) relation, given by:

$$\tau_c = \tau_{*c}(\gamma_s - \gamma)D_{50} \qquad (4.1)$$

where τ_c = critical shear stress for particle motion,
τ_{*c} = dimensionless critical shear stress (often referred to as the Shields parameter),
γ_s = unit weight of sediment (~165 lb/ft$_3$),
γ = unit weight of water (62.4 lb/ft$_3$), and
D_{50} = median particle size of the bed material.

In gravel- and cobble-bed streams, when the critical shear stress for the median particle size is exceeded, the bed is mobilized and all sizes up to about five times the median size are capable of being transported by the flow (Parker et al., 1982; Andrews, 1984). Reported values for the Shields parameter range from 0.03 (Neill, 1968; Andrews, 1984) to 0.06 (Shields, 1936). A value of 0.047 is commonly used in engineering practice, based on the point at which the Meyer-Peter, Müller bed-load equation indicates no transport (Meyer-Peter, Müller, 1948). Detailed evaluation of Meyer-Peter and Müller's data and more recent data (Parker et al., 1982, Andrews, 1984) indicates that a value of 0.03 may be more reasonable for true incipient motion in gravel- and cobble-bed streams. In fact, Neill (1968) concluded that a dimensionless shear value of 0.03 corresponds to true incipient motion of the bed-material matrix while 0.047 corresponds to a low, but measurable, transport rate.

In performing the incipient-motion and bed-material transport analysis, the bed shear stress due to grain resistance (τ') is used rather than the total shear stress, because it is a better descriptor of the near-bed hydraulic conditions that are responsible for sediment movement. The grain shear stress is computed from the following relation:

$$\tau' = \lambda Y' S \tag{4.2}$$

where Y' = the portion of the total hydraulic depth associated with grain resistance (Einstein, 1950), and
S = the energy slope.

The value of Y' is computed iteratively by solving the semilogarithmic velocity profile equation:

$$\frac{V}{V_*'} = 5.75 + 6.25 \log\left(\frac{Y'}{k_s}\right) \tag{4.3}$$

where V = mean velocity,
k_s = characteristic grain roughness of the bed, and
V_*' = shear velocity due to grain resistance given by:

$$V_*' = \sqrt{gY'S} \tag{4.4}$$

The characteristic roughness height of the bed (k_s) was assumed to be 3.5 D_{84} (Hey, 1979).

To evaluate the flow necessary to mobilize the sediment on the various surfaces across channel and floodplain it was necessary to estimate the distribution of the grain shear along each cross section. Consistent with the 1-D modeling approach used in this study, the lateral flow distribution was estimated by assuming that the flow varies with the distribution of conveyance across the section. The conveyance for a particular subsection of the cross section is given by:

$$K_i = \frac{1.486}{n_i} A_i R_i^{2/3} \tag{4.5}$$

where K_i = conveyance for subsection i,
n_i = Manning's *n*-value for subsection i,
A_i = area for subsection i, and
R_i = hydraulic radius for subsection i.

The discharge in subsection i is then computed as:

$$Q_i = Q_T \frac{K_i}{K_T} \tag{4.6}$$

where Q_i = discharge in subsection i,
Q_T = total discharge, and
K_T = total conveyance determined by summing the subsection conveyances.

With the flow distribution known, the other hydraulic variables necessary to determine the grain-shear distribution can be computed.

Results from the inundation and incipient-motion analyses are discussed in the next chapter.

5. ANALYSIS OF DAM IMPACTS

Changes in the distribution and composition of riparian vegetation downstream of dams can be due to either changes in the magnitude, frequency or duration of the flows (Rood and Mahoney, 1990; Scott, Wondzell and Auble, 1993; Scott, Auble and Friedman, 1997; Friedman and Auble, 1999: Shafroth et al., 1998); changes in channel morphology or sedimentology (Williams and Wolman, 1984; Harvey and Schumm, 1987; Elliott and Parker, 1997; Elliott and Hammack, 2000); or some combination of hydrologic, morphologic or sedimentologic changes that affect the hydrogeomorphic–botanical relationships (Osterkamp and Hupp, 1984; Hupp and Osterkamp, 1985). To evaluate the hydrogeomorphic relationships, and to identify dam-induced changes in the channel morphology or sedimentology, three evaluations were conducted: (1) an evaluation of the discharges and associated recurrence intervals and durations required to inundate various common geomorphic surfaces identified at the three sites, (2) an evaluation of the discharges and associated recurrence intervals and durations required to initiate motion of the surface sediments comprising the identified geomorphic features at each site, and (3) an evaluation of the discharges and associated recurrence intervals required for significant sediment transport on each of the identified surfaces.

5.1. Inundation, Incipient Motion, and Sediment Transport

At each of the three sites, an analysis of the site morphology was undertaken using the topographic mapping and surveyed cross sections to establish the range of geomorphic surfaces that were present. Based on the analyses, four general geomorphic features were identified: (1) main channel, (2) low bars, (3) high bars, and (4) chute channels. The output from the hydraulic modeling of the sites was used to determine the range of discharges that inundated each of the identified surfaces at each site. The range of discharges that were required to initiate motion of the surface sediments on each of the surfaces, and the range of discharges required to cause significant bed-material transport on each surface were also estimated. Typical cross sections showing the geomorphic surfaces and their associated ranges of discharges for each of the sites are presented in **Figures 5.1 through 5.3.** The distribution of the various vegetation types mapped by ERO across the sections is also shown on the figures. **Table 5.1** provides a description of the vegetation types that are shown on the cross sections. Similar plots of all the surveyed cross sections for the individual sites are presented in Appendix A.

Table 5.1. Description of riparian vegetation stand types (ERO, 2003).	
Type	Definition
Tall Woody Vegetation	
Cottonwood (CW)	More than 80%* cottonwood
Mixed riparian (MR) >15 feet	No single species (cottonwood/willow/tamarisk) comprises more than 80%*, trees generally more than 15 feet in height
Mixed riparian (MR) >15 feet, low density	No single species (cottonwood/willow/tamarisk) comprises more than 80%*, trees generally more than 15 feet in height, but noticeably more open with more spacing between trees
Mixed riparian (MR) <15 feet	No single species (cottonwood/willow/tamarisk) comprises more than 80%*, trees generally less than 15 feet in height
Mixed riparian (MR) <15 feet, low density	No single species (cottonwood/willow/tamarisk) comprises more than 80%*, trees generally less than 15 feet in height, but noticeably more open with more spacing between trees
Other Vegetation	
Mesquite (M)	More than 80%* mesquite
Strand (S)	Areas with dense or sparse vegetation including woody and non-woody plants directly adjacent to stream channels and in gravel bars
Shrub (SH)	Densely vegetated but few woody plants; mostly burro bush less than about 10 feet in height
Sparsely vegetated (SV)	Areas with less than 30%* vegetative cover, including bare sandbars
Tamarisk (T) <15 feet	More than 80%* tamarisk, trees generally less than 15 feet in height

*Relative Cover

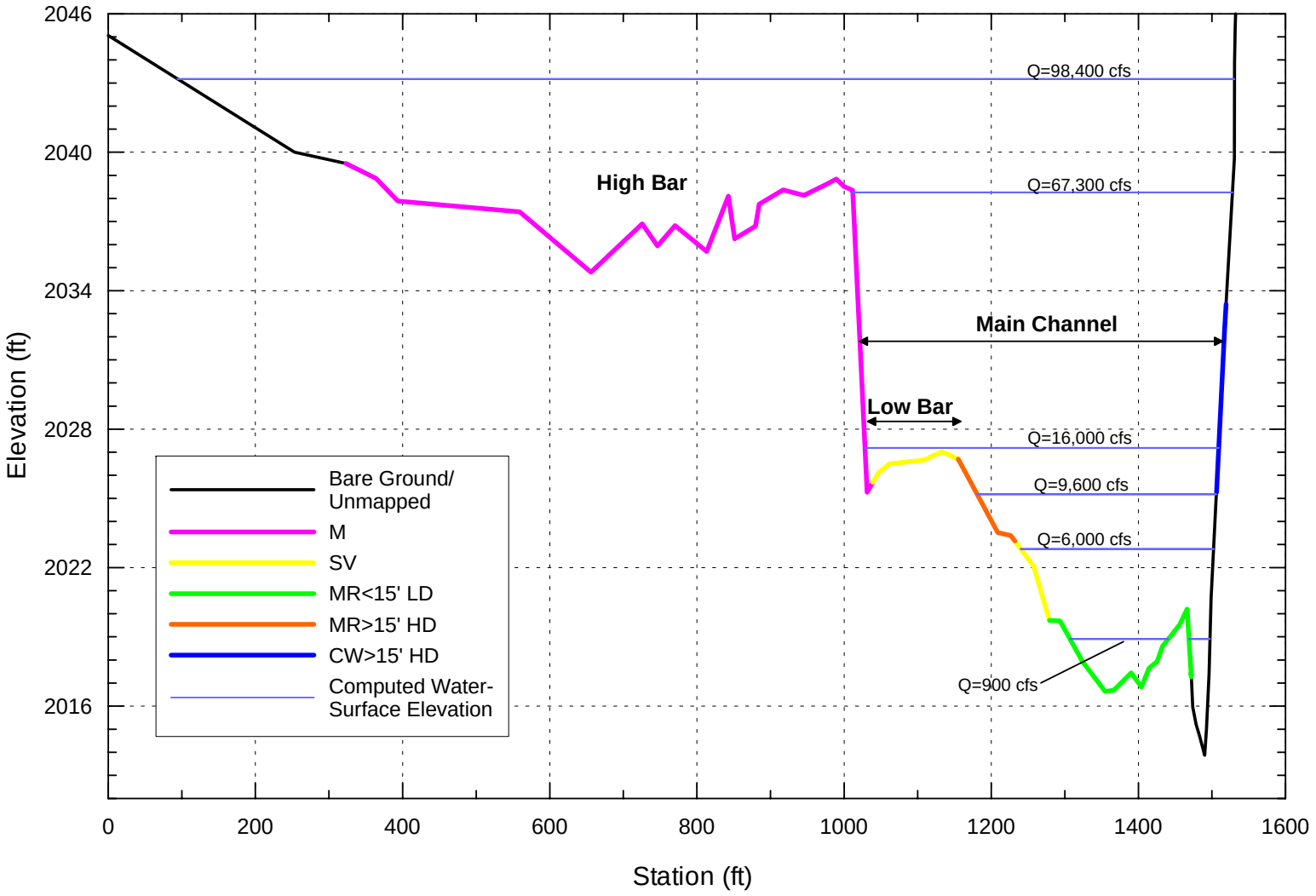

Figure 5.1. Typical cross section at Site 1 (XS2, above Horseshoe Reservoir) showing the geomorphic surfaces and associated inundation discharges.

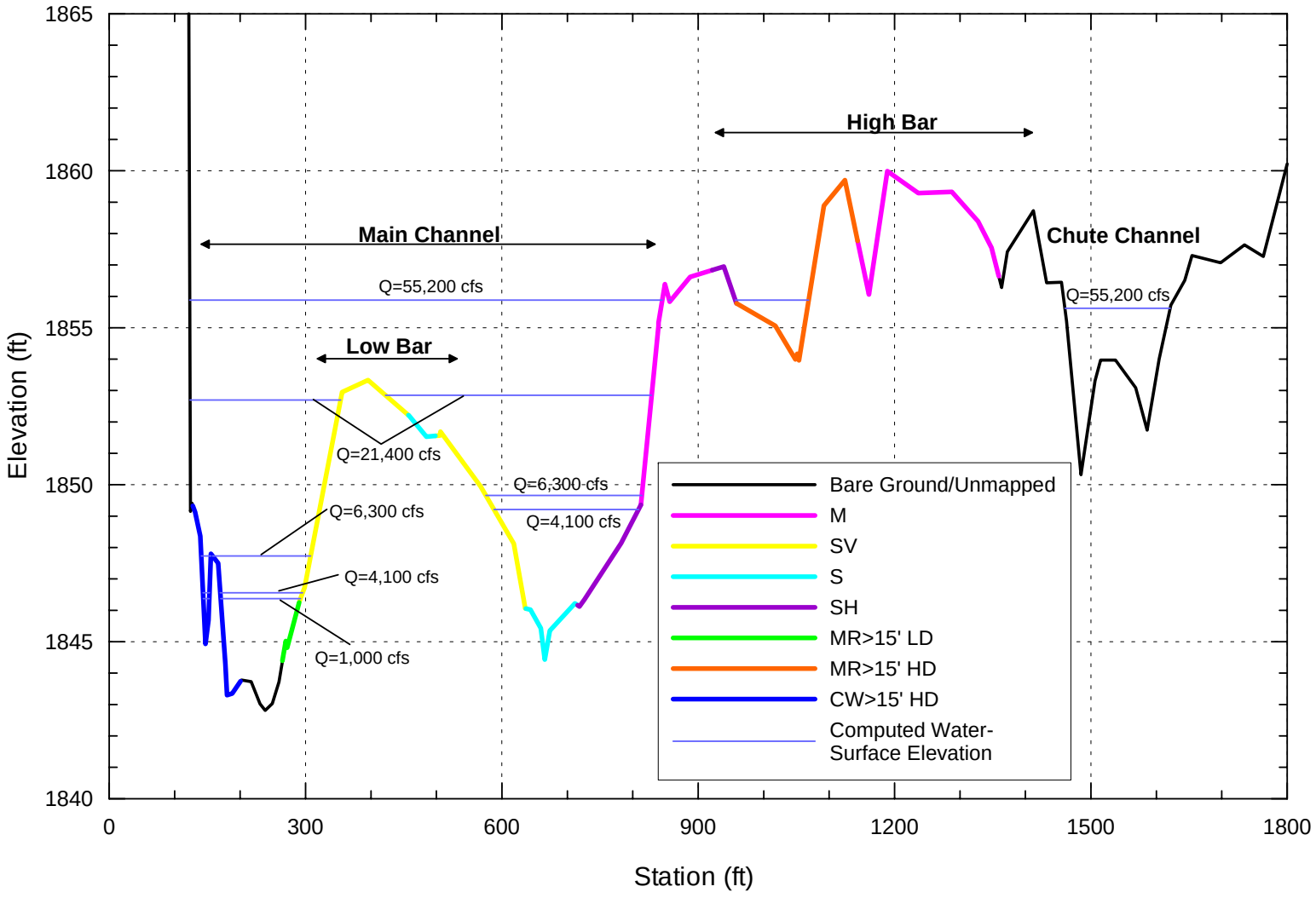

Figure 5.2. Typical cross section at Site 2 (XS2, KA Ranch) showing the geomorphic surfaces and associated inundation discharges.

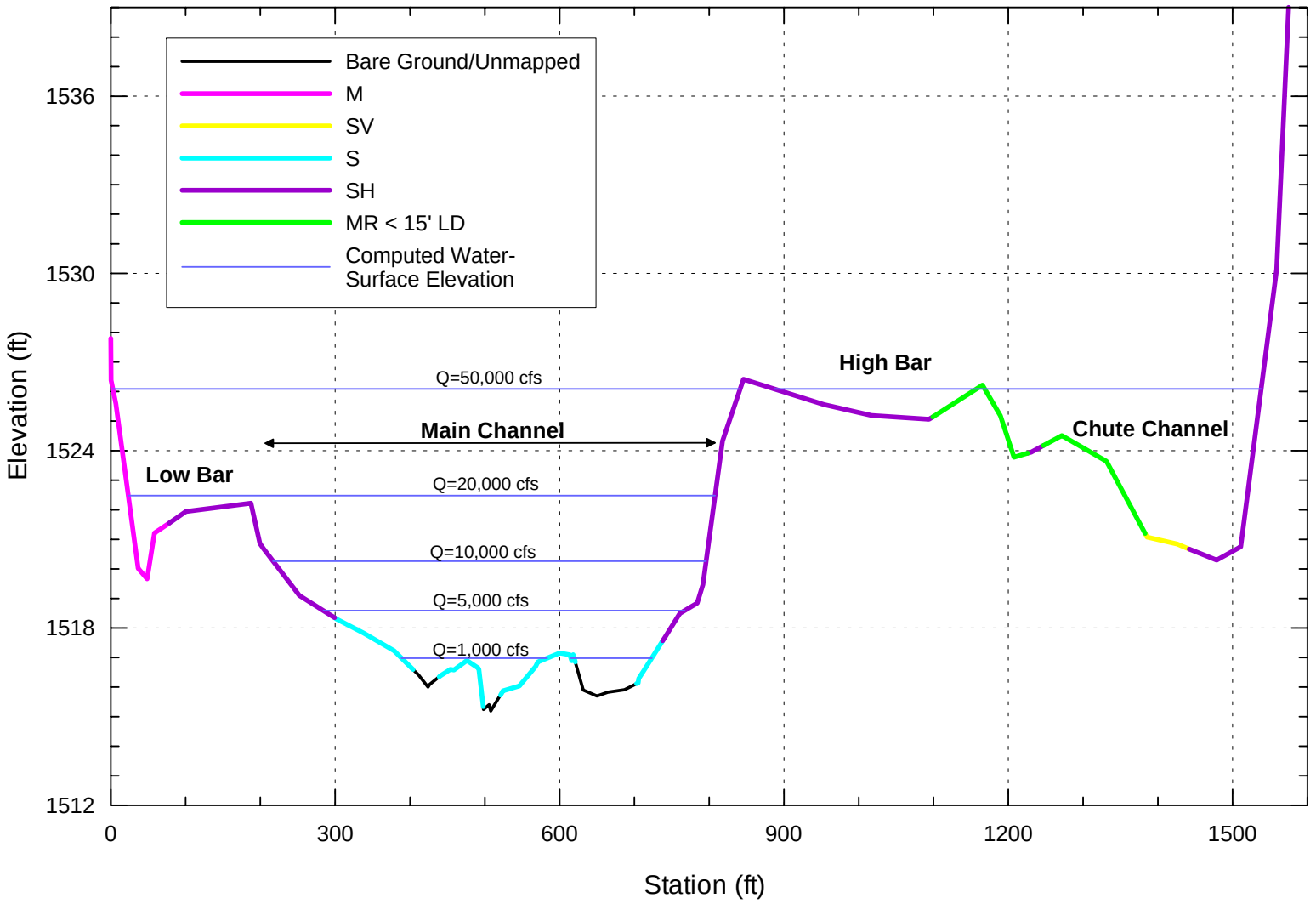

Figure 5.3. Typical cross section at Site 3 (XS8, Box Bar Ranch) showing the geomorphic surfaces and associated inundation discharges.

Table 5.2 provides a summary of the typical main channel characteristics for each of the sites.

Table 5.2. Summary of main channel characteristics for the three sites.

Characteristic	Site 1	Site 2	Site 3
Slope (ft/ft)	0.0027	0.0041	0.0023
Bed Material D_{50} (mm)	80.5	146	95
Main Channel Capacity (cfs)	16,000	20,000	20,000
Recurrence Interval (yrs)*	2.1	4	8.4
Critical Discharge (cfs)	4,600—28,000	2,400—55,000	2,200—16,000
Recurrence Interval (yrs)*	1.3—3.5	1.1—10	1.9—7.7
Discharge for Measurable Sediment Transport (cfs)	10,000—60,000	3,200—120,000	5,000—90,000
Recurrence Interval (yrs)	1.6—7.1	1.3—>57	3.5—>22.6

*Recurrence intervals for Sites 1 and 2 are based on the records at the Tangle Creek and Bartlett gages, respectively, and for Site 3 they are based on a logarithmic interpolation between the upstream and downstream gages.

The bed-material data in Table 5.2 indicate that Site 2 has the steepest slope and coarsest bed material of the three sites. Although the amount of data for each site are somewhat limited, it does not appear that there has been channel armoring below the dams, and this can probably be attributed to the high frequency of tributaries in each of the below-dam reaches that periodically deliver both fine and coarse sediment to the Verde River downstream of the dams. As expected, the main channel capacity increases in the downstream direction (Leopold and Maddock, 1953), however, under existing conditions with the reservoirs in place, the recurrence intervals for the main channel capacity flows increase significantly, clearly indicating the role of the dams in regulating flows in the low to moderate range. If, however, the Tangle Creek frequencies are applied to the channel capacities at Sites 2 and 3, the recurrence intervals for the main channel capacity flow at these sites are 2.5 years, which is very similar to that at Site 1. This suggests that there has been little or no adjustment of the main channel dimensions downstream of the dams. Again, this lack of adjustment is probably related to the tributary sediment supply downstream of the dams, or the flood-driven channel morphology may be relatively insensitive to the sediment supply (Graf, 1988).

Table 5.3 summarizes the reservoir sedimentation data for Horseshoe Reservoir which has an upstream contributing drainage area of about 6,000 square miles.

Table 5.3. Summary of reservoir sedimentation data for Horseshoe Reservoir, 1945-2001.

Survey Years	Volume of Stored Sediment (ac-ft)	Average Annual Sediment Yield (ac-ft/year)	Av. Annual Unit Sediment Yield (ac-ft/sq. mi/yr)	Significant Flood Years (> 5-yr RI)
1945-1950	1,200	240	0.05	None
1950-1963	3,592	276	0.05	1952
1963-1978	7,811	520	0.09	1966, 1967, 1969, 1970, 1973, 1978
1978-2001	22,210	965	0.16	1979, 1980, 1982, 1993, 1995

The unit sediment yield data in Table 5.3 indicate that the sediment yields from the basin upstream of the reservoir are strongly influenced by the occurrence of less frequent flood events, which is typical of rivers in arid and semi-arid regions (Schumm, 1977; Baker, 1977; Graf, 1988). However, regardless of the periods of record being considered these yields are low in comparison with those from other southwestern watersheds (Strand, 1975). Strand's sediment yield—drainage area relationship ($Q_s = 2.4A^{-0.229}$) indicates unit sediment yields on the order of 0.4 ac-ft/ sq. mile/year, which is at least twice as much as the unit yield for the Verde River in the period with the greatest number of large floods, and an order of magnitude higher than the values for periods with less floods. Review of sediment yields to Roosevelt Reservoir on the Salt River indicate that unit sediment yields range from 0.1 to 0.4 ac-ft/mi^2/yr in the 1980 to late 1990 period. The relatively low sediment yield for the Verde River basin may, therefore, explain why there has been little if any morphological adjustment of the channel below the dams.

The wide range of critical discharges within each of the sites reflects the morphological variability of the channel. The recurrence intervals for the range of critical discharges reflect both the hydrologic effects of the dams as well as the grain size. At Site 1, the recurrence interval of the critical discharge ranges from 1.3 to 3.5 years. At Sites 2 and 3, the recurrence intervals range from 1.1 to 10 years under the current hydrologic regime. However, if the Tangle Creek frequency curve, which is representative of the pre-dam hydrology of all three sites, is used, the RI values for Site 2 range from 1.1 to 7 years, and at Site 3 they range from 1.1 to 2.1, which are much closer to the range of values at Site 1.

The discharge range for measurable sediment transport at Site 1 is 10,000 to 60,000 cfs, with corresponding frequencies of 1.6 to 7.1 years (Table 5.2). At Site 2, the discharges range from 3,200 to 120,000 cfs, with corresponding frequencies of 1.3 to more than 57 years, and at Site 3, the discharges range from 5,000 to 90,000 cfs, with corresponding frequencies of 3.5 to 22.6 years. However, if the Tangle Creek frequency curve is used, the frequency values for Site 2 range from 1.1 to 20 years, and at Site 3, they range from 1.2 to 15 years, which are much closer to the range of values at Site 1. The pre-dam (i.e. Tangle Creek) frequencies for incipient motion and substantial transport suggest that the dams have not caused significant morphological or sedimentological changes at Sites 2 and 3.

Table 5.4 summarizes the typical low bar characteristics for each of the sites.

Table 5.4. Summary of low bar characteristics for the three sites.

Characteristic	Site 1	Site 2	Site 3
Bar Material D_{50} (mm)	73	73	61
Inundation (cfs)	10,000—16,000	10,000—20,000	10,000—20,000
Recurrence Interval (yrs)*	1.6—2.1	2.5—4	4.8—8.4
Critical Discharge Range (cfs)	35,000—60,000	32,000—50,000	20,000—100,000
Recurrence Interval (yrs)*	4.2—7.1	6—8	8.4—>50
Discharge Range for Sediment Transport (cfs)	50,000—110,000	42,000—170,000	40,000—190,000
Recurrence Interval (yrs)	6.2—>30	7—>57	9—>57

*Recurrence intervals for Sites 1 and 2 are based on the records at the Tangle Creek and Bartlett gages, respectively, and for Site 3 they are based on a logarithmic interpolation between the upstream and downstream gages.

The data in Table 5.4 indicate that there is little difference between sites in the sizes of the materials that make up the low bank-attached bars. Although the data are somewhat limited, it does not appear that there has been bar armoring below the dams, and this can probably be attributed to the high frequency of tributaries in each of the below-dam reaches that periodically deliver sediment to the Verde River. The magnitude of the flows that inundate the low bars is similar at all of the sites (10,000—20,000 cfs), but because of the reservoirs, the frequencies of inundation decrease in the downstream direction. If the Tangle Creek frequencies are applied to the low bar inundation flows in Sites 2 and 3, the recurrence intervals for the sites are the same as at Site 1. This suggests that there has been little or no adjustment of the low bars within the active channel below the dams, and therefore, any differences in colonization by riparian vegetation are most likely due to the changes in hydrology.

Similar to the main channel, the range of critical discharges for the low bars is also wide within each of the sites, again reflecting the morphological variability of the channel within the individual sites, but the ranges are somewhat similar between sites. The recurrence intervals for the range of critical discharges reflect primarily the hydrologic effects of the dams because the grain sizes are quite similar. At Site 1, the critical discharge has a range of recurrence intervals between 4.2 and 7 years which indicates that the bar materials are mobilized very infrequently. At Sites 2 and 3, the critical discharge recurrence intervals range from 6 to more than 50 years under the current hydrologic regime. However, if the Tangle Creek frequency curve is used, the frequency values for Site 2 range from 4 to 6 years, and at Site 3, they range from 2.5 to 20 years, which are much closer to the range of values at Site 1. Since removal of riparian vegetation by floods is closely tied to mobilization of the substrate (Friedman and Auble, 1999), the persistence of the vegetation downstream of the dams is primarily related to changes in hydrology.

The discharge range for measurable sediment transport on the low bars at Site 1 is 50,000 to 110,000 cfs, with corresponding frequencies of 6.2 to more than 30 years (Table 5.4). At Site 2, the discharges range from 42,000 to 170,000 cfs, with corresponding frequencies of 7 to more than 50 years, and at Site 3, the discharges range from 40,000 to 190,000 cfs with corresponding frequencies of 9 to more than 50 years. However, if the Tangle Creek frequency curve is used, the frequency values for Sites 2 and 3 range from 5 to 50 years, and are much closer to the range of values at Site 1. The data, therefore, indicate that significant transport of sediment and destabilization of the low bars occurs relatively infrequently at all of the sites, but the dams have reduced the frequency at Sites 2 and 3 This suggests that the frequency of vegetation removal from the bars by flood events has been reduced in the post-dam era. Since the ability of flows to remove vegetation is reduced by the increased age of the vegetation (Friedman and Auble, 1999; McBain and Trush, 1997), the net effect of the dams may be to significantly increase the stability of vegetated surfaces.

Table 5.5 provides a summary of the typical high bar characteristics for each of the sites.

The data in Table 5.5 indicate that the high bar surface sediments at Site 2 are much coarser than at Sites 1 and 3, and the magnitude of the flows that inundate the high bars decreases in the downstream direction. At Site 1, high bar inundation occurs throughout the site at a discharge of about 67,000 cfs, whereas at Sites 2 and 3, the high bars are inundated by flows of 55,000 cfs and 50,000 cfs, respectively. Although the discharge required to inundate these surfaces decreases in the downstream direction, the recurrence interval between inundation discharges increases from about 9 years at Site 1 to 12 years at Site 3 due to the influence of the reservoirs (Figure 3.5). If the Tangle Creek frequencies are applied to the high bar inundation flows in Sites 2 and 3, the recurrence intervals for the sites are essentially the same

as at Site 1. This further suggests that there has been little or no adjustment of the high bars within the active channel below the dams, and therefore, any differences in colonization by riparian vegetation on these surfaces are due to the changes in hydrology. Table 5.5 also shows that the critical discharge for the high bar surface at all of the sites exceeds 160,000 cfs (> 50-year RI) and measurable transport of the bar sediments occurs at flows in excess of 200,000 cfs (>100-year RI). Therefore, mobilization of the upper bar surfaces occurs very infrequently at all of the sites, and the dams have had little effect on the dynamics of this surface (Figure 3.5).

Table 5.5. Summary of high bar characteristics for the three sites.

Characteristic	Site 1	Site 2	Site 3
Bar Material D_{50} (mm)	73	105	61
Inundation (cfs)	67,000	55,000	50,000
Recurrence Interval (yrs)*	8.6	10	12
Critical Discharge Range (cfs)	170,000	> 200,000	160,000
Recurrence Interval (yrs)*	>50	—	>50
Discharge Range for Sediment Transport (cfs)	>200,000	>200,000	>200,000
Recurrence Interval (yrs)	—	—	—

*Recurrence intervals for Sites 1 and 2 are based on the records at the Tangle Creek and Bartlett gages, respectively, and for Site 3 they are based on a logarithmic interpolation between the upstream and downstream gages.

Table 5.6 summarizes the typical chute channel characteristics for each of the sites.

Table 5.6. Summary of chute channel characteristics for the three sites.

Characteristic	Site 1	Site 2	Site 3
Bar Material D_{50} (mm)	73	105	61
Inundation (cfs)	16,000	30,000--55,000	10,000--50,000
Recurrence Interval (yrs)*	2.1	6—10	4.8—12
Critical Discharge Range (cfs)	>200,000	120,000—170,000	40,000—180,000
Recurrence Interval (yrs) *	—	>50	9—>50
Discharge Range for Sediment Transport (cfs)	>200,000	>200,000	55,000—150,000
Recurrence Interval (yrs)	—	—-	13—>50

*Recurrence intervals for Sites 1 and 2 are based on the records at the Tangle Creek and Bartlett gages, respectively, and for Site 3 they are based on a logarithmic interpolation between the upstream and downstream gages.

No sediment measurements were made in the chute channels during the field visit, so for the purposes of the sediment mobilization analyses, the high bar surface sediment gradations were assumed to apply (Table 5.6). The magnitude of the flow that inundates the chute channel that occupies a significant part of the upper reaches of Site 1 is about 16,000 cfs, and this has a

frequency of 2.1 years. Because of the high frequency of inundation, there is a general absence of vegetation in the chute channel over time (refer to Chapter 2). Inundation of the chute channel at Site 2 occurs at a range of discharges between 30,000 cfs and 55,000 cfs, and the corresponding frequencies are from 6 to 10 years. At Site 3, inundation of the chute channels occurs at flows between 10,000 cfs and 50,000 cfs, and the corresponding frequencies are 4.8 to 12 years. The critical discharge and sediment transport data for the three sites indicate that sediment mobilization in the chute channels is an infrequent event at all of the sites. The low frequency of sediment mobilization explains why chute channels at all of the sites have persisted over time, and also why riparian vegetation persists at these sites.

5.2. Flow-Duration Analysis

To evaluate whether modification of reservoir operations could be used to increase the amount of woody riparian vegetation and SWWFC habitat, hydrographs for the 1991, 1993, 1995 (2), 1997 and 1998 floods were routed through the reservoirs under the Full Operation and Full Release alternatives for two reservoir storage conditions (low pool and high pool elevations, refer to Chapter 3 for details). Water-surface elevations for each of the sites were determined at each cross section for the individual floods for the various alternatives with the HEC-RAS models. Typical examples of the model output for the three sites are presented in **Figures 5.4 through 5.6**. The bar charts show the elevations of the peak discharges for the various floods for the modeled scenarios next to the plotted cross section that has been color-coded to show the vegetation types at each of the sites (Table 5.1). On Figure 5.4, the only scenario shown is the natural hydrograph since Site 1 is located upstream of the reservoirs. Figures 5.5 and 5.6 show the water-surface elevations for the routed floods for each of the scenarios. Similar plots for all of the cross sections at the three sites are provided in **Appendix D.**

For each of the geomorphic surfaces identified at the three sites (Table 5.2—main channel, Table 5.4—low bar, Table 5.5—high bar; and Table 5.6—chute channel) an analysis of the duration of the discharge(s) that inundated the surfaces, mobilized the sediment and transported the sediment, for each of the scenarios was conducted to determine whether modification of the reservoir operations would to able to cause an increase in the amount of woody riparian habitat. Bar graphs showing the number of days that the discharges were equaled or exceeded for each of the simulated hydrographs generated for the various scenarios are presented in **Appendix E**.

At Site 1, the discharge associated with the main channel capacity (16,000 cfs), low bar inundation (16,000 cfs), high bar inundation (67,000 cfs) and chute channel inundation (16,000 cfs) was equaled or exceeded for about 9.5 days in 1993, but during the other evaluated floods, it was equaled or exceeded for less than 3 days. The critical discharge for the bed material in the main channel was equaled or exceeded for about 10 days in the 1991 flood, for up to 27 days in 1993, for 10 days in the 1995 flood, and for about 11 days in the 1978 flood. With the exception of 1993, where measurable transport of the bed material in the main channel occurred for about 16 days, the remainder of the floods would have transported sediment in the main channel for between 1 and 4 days. From a morphological perspective, the 1993 and 1995 floods were the most effective in the main channel, and would be expected to cause the most change at the site. The critical discharge for the low bar surfaces (35,000—60,000 cfs) would only have been exceeded in the 1993 and 1995 floods, and then only for between 1 and 3.5 days. Sediment transport on the low bar surfaces (50,000 to 110,000 cfs) would have occurred for between 1 and 2 days in 1993 and 1995. Neither incipient motion nor measurable transport would have occurred on the high bar surfaces during any of the floods.

At Sites 2 and 3, the same general patterns were observed for the durations of inundation, exceedence of the critical discharge and measurable sediment transport for each of the routed floods. However, as can be seen in **Figures 5.7 and 5.8** which are typical examples for Sites 2 and 3, respectively, the various operational scenarios have very little, if any, influence on the flow durations for any of the surfaces. Therefore, it is unlikely that they will have significant effect on the amount of woody riparian vegetation at the sites.

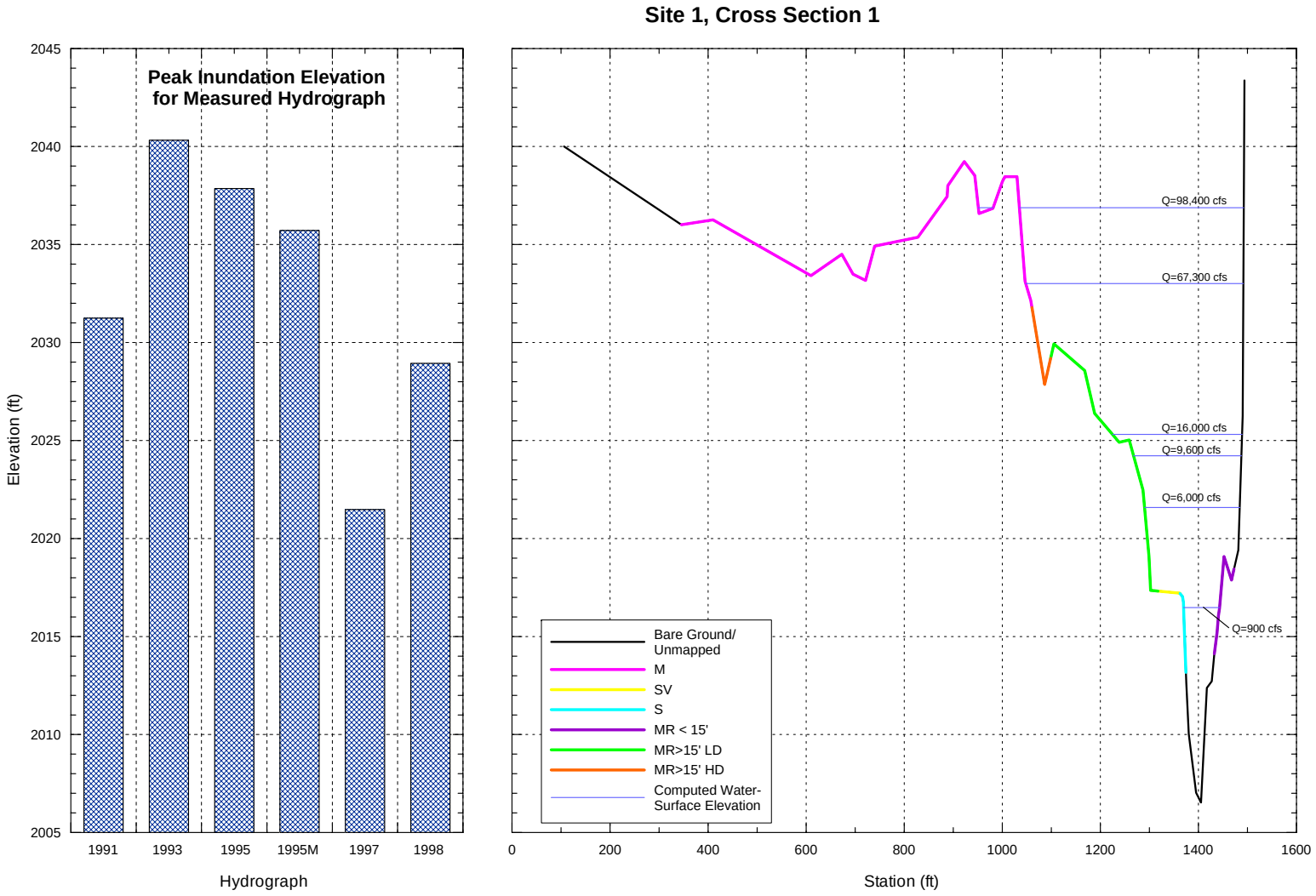

Figure 5.4. Peak discharge elevations for the 1991, 1993, 1995, 1995M, 1997 and 1998 floods plotted with the cross section profile for Cross Section 1 at Site 1. The cross section is color coded to show the distribution of the various types of vegetation at the site (refer to Table 5.1 for full descriptions of the vegetation codes).

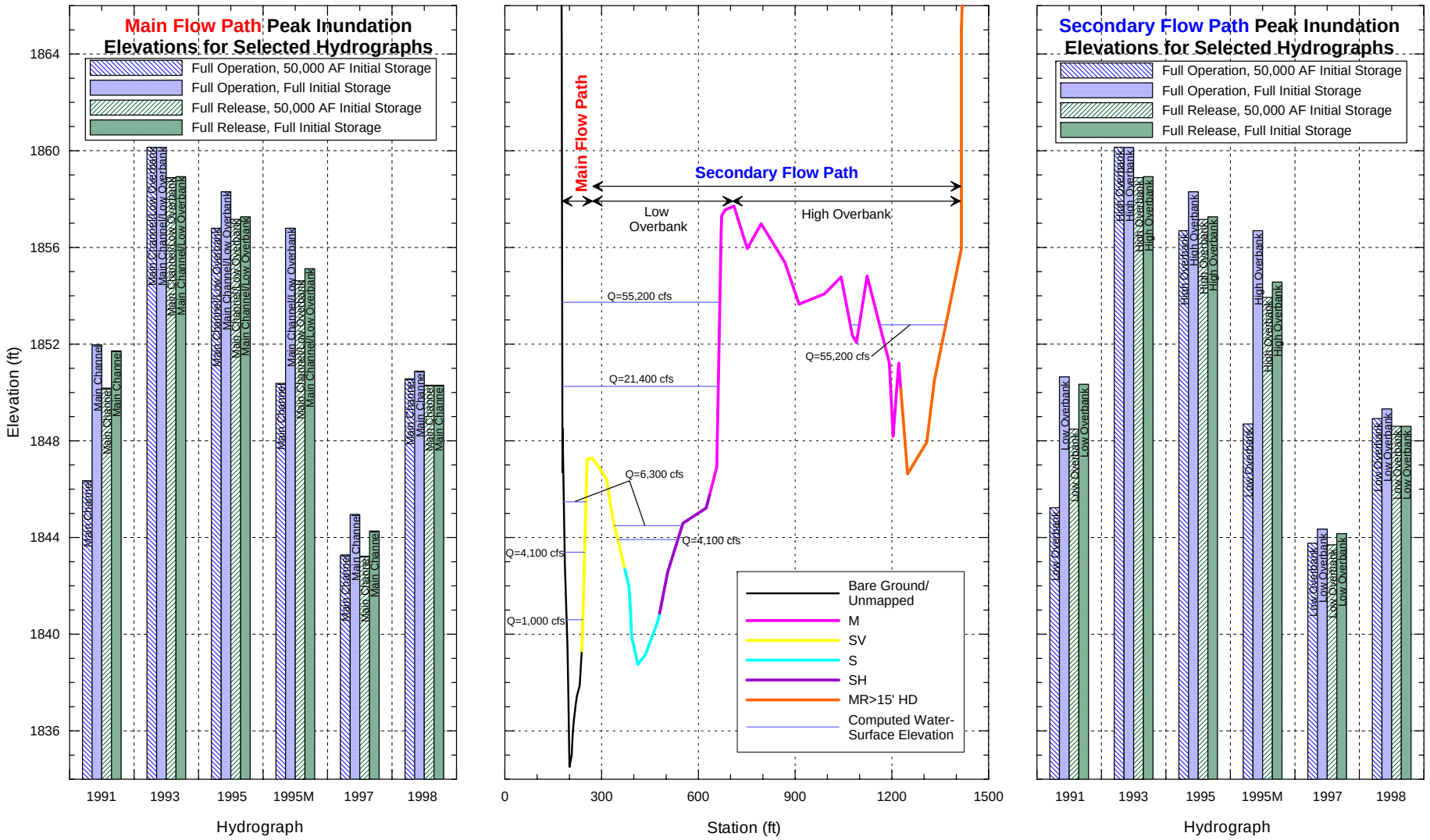

Figure 5.5. Peak discharge elevations for the 1991, 1993, 1995, 1995M, 1997 and 1998 floods for the various scenarios plotted with the cross section profile for Cross Section 1 at Site 2. The cross section is color coded to show the distribution of the various types of vegetation at the site (refer to Table 5.1 for full descriptions of the vegetation codes).

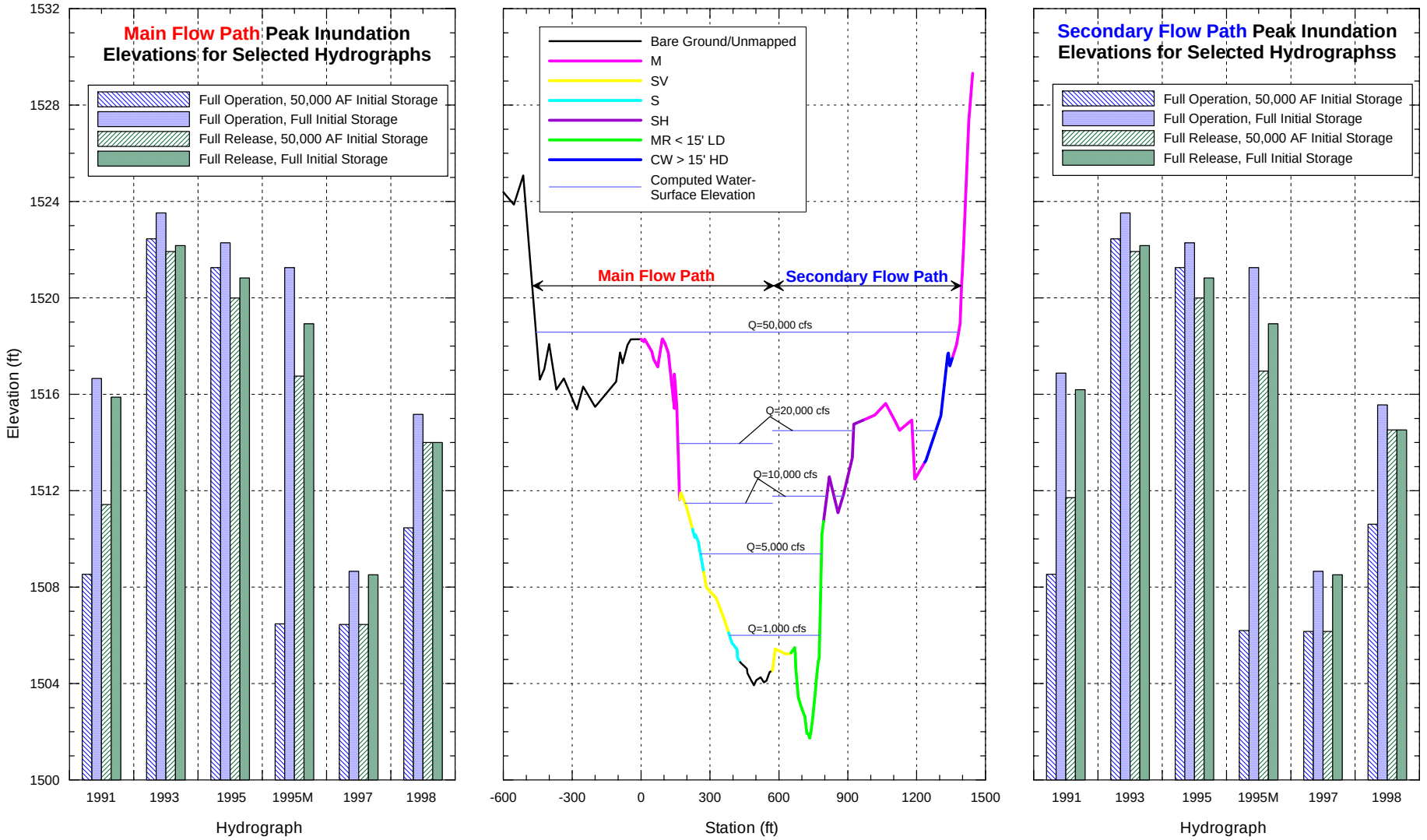

Figure 5.6. Peak discharge elevations for the 1991, 1993, 1995, 1995M, 1997 and 1998 floods for the various scenarios plotted with the cross section profile for Cross Section 1 at Site 1. The cross section is color coded to show the distribution of the various types of vegetation at the site (refer to Table 5.1 for full descriptions of the vegetation codes).

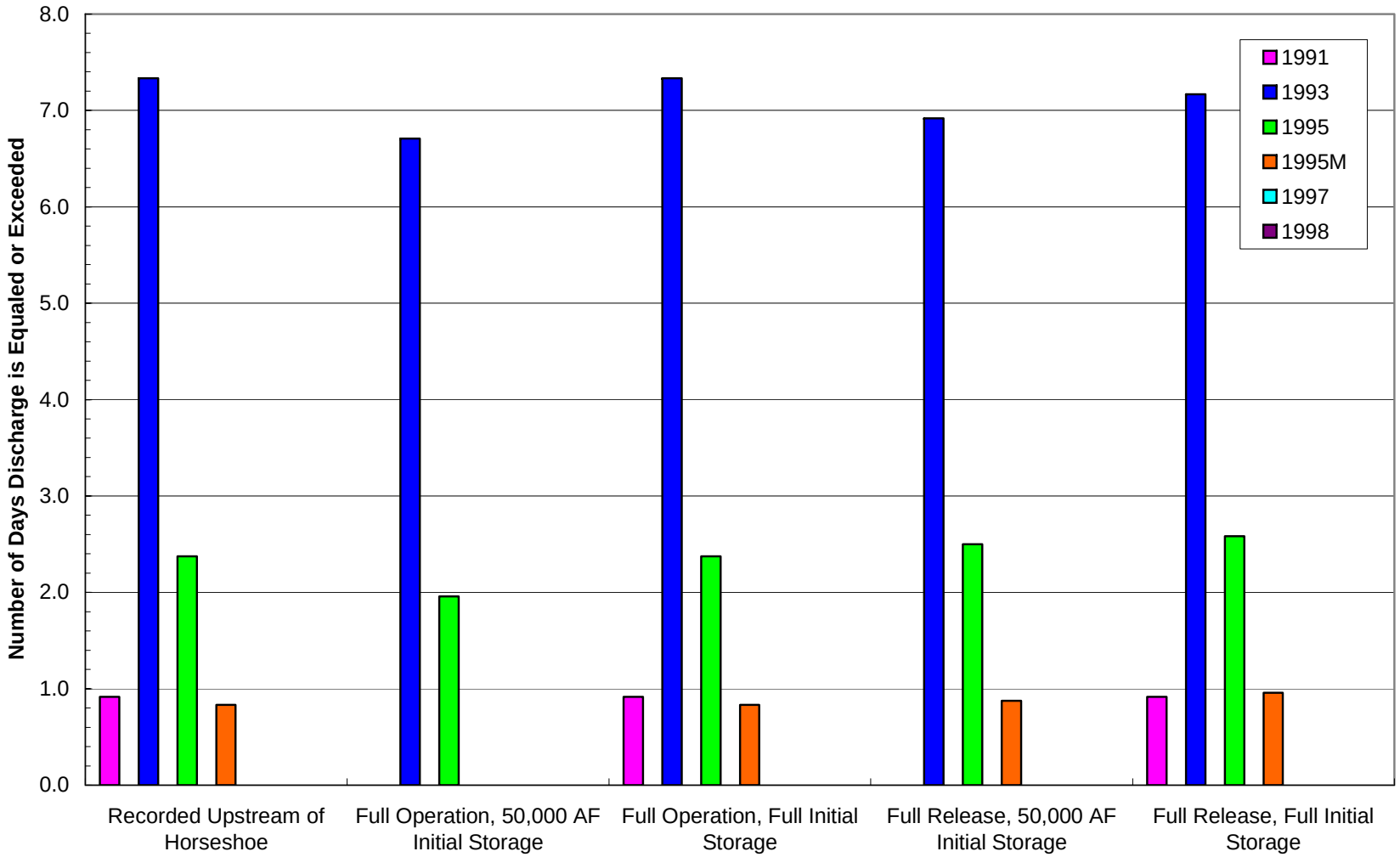

Figure 5.7. Durations that main channel capacity is equaled or exceeded for the various scenarios during the simulated flood hydrographs at Site 2.

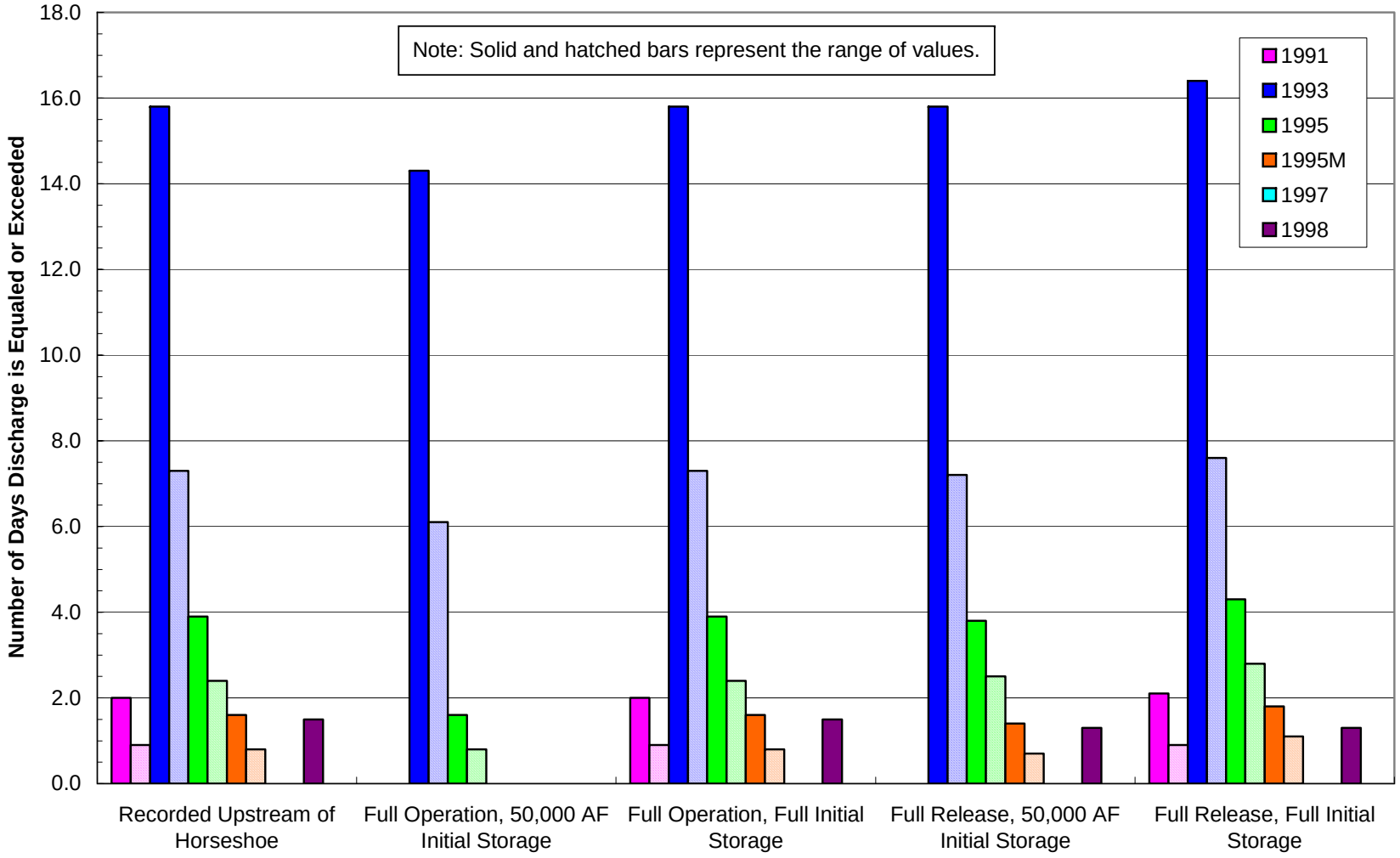

Figure 5.8. Durations of the flows at which the low bars are inundated for the various scenarios during the simulated flood hydrographs at Site 3.

6. SUMMARY AND CONCLUSIONS

In order to evaluate the effects of Horseshoe and Bartlett Dams on the Verde River on the distribution of woody riparian vegetation, it is necessary to quantify the effects of various dam operations on the frequency and duration of inundation of likely areas for the establishment and maintenance of the vegetation, and to determine the flows necessary to mobilize the channel bed and bar sediments that form the substrate for the vegetation. This information can then be used by plant ecologists to evaluate the likely effects of various dam operations on the establishment and maintenance of the vegetation.

Mussetter Engineering, Inc. (MEI) was retained by the Salt River Project (SRP) to assist plant ecologists from ERO Resources Corporation (ERO) to address the issue of whether re-operation of the dams on the Verde River could significantly improve downstream conditions for establishment and maintenance of woody riparian vegetation. MEI assisted ERO in selecting study sites (Figure 1.1) for the analysis; sampled the bed and bar sediments, developed one-dimensional (1-D) hydraulic models, and used the models to evaluate the extent and frequency at which various geomorphic surfaces are inundated and the range of flows that are required to mobilize the sediment that makes up the in-channel bars and channel margins within the riparian zone at each of the sites.

6.1. Summary

The geomorphic surfaces within each of the sites were identified from field inspections and analysis of aerial photographs and topographic maps prepared for each of the sites. Time-sequential aerial photography between 1934 and 2002 was reviewed to identify changes in channel morphology and vegetation cover, particularly as related to the occurrence of large floods. At the Tangle Creek gage, floods with recurrence intervals in excess of five years (40,000 cfs) occurred in 1891, 1906, 1916, 1920, 1927, 1932, 1937, 1938, 1941, 1952, 1967, 1969, 1970, 1973, 1978, 1979, 1980, 1982, 1993 and 1995. Following construction of the dams in 1939 (Bartlett) and 1946 (Horseshoe), floods of a similar magnitude occurred much less frequently at the Bartlett gage (1941, 1978, 1979, 1980, 1993 and 1995). Because of the relatively small capacity of the reservoirs, the effects of the dams on the flood-frequency relationships are most pronounced for events less than about the 10-year event (Figure 3.5). At larger flows, the above- and below-dam frequencies are similar. Analysis of the effects of various operational scenarios for the reservoirs for a range of simulated flood hydrographs that were based on the 1991, 1993, 1995 (2), 1997 and 1998 floods, demonstrated that the durations of inundation of the identified geomorphic surfaces would be very similar for all of the modeled scenarios. Therefore, modification of reservoir operations is unlikely to increase the amount of woody riparian vegetation.

6.1.1. Site 1: Upstream of Horseshoe Reservoir near Tangle Creek Gage

Site 1 is located upstream of Horseshoe Dam and just downstream of the Tangle Creek gage (Figure 1.1). The braided channel of the Verde River at this site is confined between alluvial terraces and Tertiary-age basin-fill sediments in a relatively narrow valley, and there is no well-developed floodplain. Within the site, the following geomorphic surfaces were identified: (1) main channel with a capacity of about 16,000 cfs [2.1–year recurrence interval (RI)], (2) low bar surfaces inundated at about 16,000 cfs, (3) high bar surfaces inundated at about 67,000 cfs

(8.6–year RI), and (4) chute channels that are inundated at about 16,000 cfs. The slope of the river at the site is 0.0027, and the median (D_{50}) sizes of the sediments that comprise the main channel, low bars, high bars, and chute channels are 81, 73, 73, and 73 mm, respectively. The critical discharge (discharge at which sediment begins to be mobilized) in the main channel, the edges of which support a fringe of riparian vegetation, ranges from 4,600 to 28,000 cfs, which has corresponding RI of 1.3 to 3.5 years. Significant bed mobilization occurs at a range of discharges between 10,000 and 60,000 cfs (1.6 to 7-year RI). The critical discharge range for the low bar surfaces that tend to be associated with the riparian vegetation is 35,000 to 60,000 cfs (4 to 7-year RI), and significant sediment mobilization occurs at a range of discharges between 50,000 and 110,000 cfs (6 to >30-year RI). The critical discharge range for the high bar surfaces that tend to be associated with mesquite and other non-riparian vegetation species, is about 170,000 cfs (>50-year RI), and significant sediment mobilization occurs at discharges of >200,000 cfs (>100-year RI). The chute channel that extends for much of the length of the site is inundated at about 16,000 cfs, but because of the presence of very coarse bed material, the critical discharge and significant sediment mobilization occur at flows in excess of 200,000 cfs. Frequent flows within the chute channel remove any fine sediment.

Review of the time-sequential aerial photographs of the site confirms the findings of the hydraulic and sediment-transport analyses. Between large floods, vegetation tends to establish on the lower bar surfaces, but the vegetation is stripped off during large floods. The high bar surfaces tend to remain vegetated even when there have been large floods because the flow depths, and therefore, shear stresses are low.

6.1.2. Site 2: Downstream of Horseshoe Dam Near the KA Ranch

Site 2 is located about two miles downstream of Horseshoe Dam near the KA Ranch (Figure 1.1). The site is located within a wider reach of the Verde River valley that is controlled at the downstream end by a narrower valley constriction. The downstream constriction, and the locally wider reach of the valley that is confined between old alluvial fans to the west and Tertiary-age basin-fill sediments to the east, has created a net depositional reach of the river that has a braided planform. Davenport Wash on the east, and a large unnamed arroyo on the west, episodically deliver sediment to the reach, and this sediment at least partially compensates for the loss of the upstream sediment supply. Sedimentation rates in Horseshoe Reservoir (Table 5.2) suggest that the Verde River transports significantly less sediment than many other rivers in the southwestern US, and this may explain why there have been few reservoir-related morphological changes to the river below the dam.

Within the site, the following geomorphic surfaces were identified: (1) main channel with a capacity of about 20,000 cfs (4-year RI), (2) low bar surfaces inundated at flows between 10,000 and 20,000 cfs (2.5- to 4-year RI), (3) high bar surfaces inundated at about 55,000 cfs (10-year RI), and (4) chute channels that are inundated at flows between 30,000 and 55,000 cfs (6 to 10-year RI). If the Tangle Creek gage flood frequencies, which are representative of the pre-dam hydrology at all three study sites, are applied to the discharges that are associated with the geomorphic surfaces at Site 2, they are very similar to those at Site 1, which indicates that there has been little, if any, morphological adjustment of the Horseshoe and Bartlett Dams. The differences in the associated flow frequencies are due to the changes in hydrology.

The slope of the river at the site is 0.0047, and the median (D_{50}) sizes of the sediments that comprise the main channel, low bars, high bars, and chute channels are 146, 73, 105 and 105 mm, respectively, which are somewhat coarser than those at Site 1, probably because of the steeper slope and local delivery of sediment by both Davenport Wash and the unnamed arroyo.

The critical discharge in the main channel, the edges of which support a fringe of riparian vegetation, ranges from 2,400 to 55,000 cfs which have corresponding RI's of 1.1 to 10 years. Significant bed mobilization occurs at a range of discharges between 3,200 and 120,000 cfs (1.3 to >57-year RI). The critical discharge range for the low bar surfaces that tend to be associated with the riparian vegetation is 32,000 to 50,000 cfs (6- to 8-year RI), and significant sediment mobilization occurs at a range of discharges between 42,000 and 170,000 cfs (7 to >57-year RI). The RI's of the critical discharges and discharges for substantial sediment transport in the main channel and low bars from the Tangle Creek (i.e., pre-dam) flood-frequency curve are similar to those at Site 1, further indicating that there has been little, if any, morphologic adjustment of the channel between Horseshoe and Bartlett Dams. The critical discharge range for the high bar surfaces that tend to be associated with mesquite and other non-riparian vegetation species is above 200,000 cfs. The critical discharges for the chute channels that are located primarily in the downstream portions of the site, are between 120,000 and 170,000 cfs (>50-year RI), and significant sediment transport occurs at flows in excess of 200,000 cfs.

Review of the time-sequential aerial photographs of the site confirms the findings of the hydraulic and sediment-transport analyses. Between large floods, vegetation tends to establish on the lower bar surfaces, but the vegetation is stripped off during large floods. The high bar surfaces tend to remain vegetated even when there have been large floods because the flow depths, and therefore, shear stresses are low. Chute channels are formed during the infrequent large floods and remain stable for long periods of time. They appear to be the preferred sites for cottonwood establishment following the large infrequent floods.

6.1.3. Site 3: Downstream of Bartlett Dam near the Box Bar Ranch

Site 3 is located about 6.5 miles downstream of Bartlett Dam near the Box Bar Ranch (Figure 1.1). The site is located within a much wider reach of the Verde River valley that is located upstream of a narrower valley constriction that makes Site 3 a net depositional area. The braided river is confined between heavily vegetated alluvial terraces to the east and alluvial terraces and old, relatively erosion-resistant, alluvial deposits to the west, and there is no well-developed floodplain. The younger flanking terraces are inundated by large infrequent flows (Skotnicki, 1996).

Within the site, the following geomorphic surfaces were identified: (1) main channel with a capacity of about 20,000 cfs (8.4-year RI), (2) low bar surfaces inundated at flows between 10,000 and 20,000 cfs (4.8 to 8.4-year RI), (3) high bar surfaces inundated at about 50,000 cfs (12-year RI), and 4) chute channels that are inundated at flows between 10,000 and 50,000 cfs (4.8 to 12-year RI). If the Tangle Creek (i.e., pre-dam) flood frequencies are applied to the discharges that are associated with the geomorphic surfaces at Site 3, they are very similar to those at Site 1, which indicates that there has been little, if any, morphological adjustment of the channel downstream of both dams. The differences in the associated flow frequencies are due to the changes in hydrology.

The slope of the river at the site is 0.0023, and the median (D_{50}) sizes of the sediments that comprise the main channel, low bars, high bars, and chute channels are 95, 61, 61 and 61 mm, respectively, which are somewhat finer than those at Site 2, probably because of the flatter slope. The critical discharge in the main channel, the edges of which support a fringe of riparian vegetation, ranges from 2,200 to 16,000 cfs, which have corresponding RI's of 1.9 to 7.7 years. Significant bed mobilization occurs at a range of discharges between 5,000 and 90,000 cfs (3.5 to 22-year RI). The critical discharge range for the low bar surfaces that tend to be associated

with the riparian vegetation is 20,000 to 100,000 cfs (8.4 to >50-year RI), and significant sediment mobilization occurs at a range of discharges between 40,000 and 190,000 cfs (9 to >57-year RI). The RI's of the critical discharge and discharge for substantial sediment transport in the main channel and low bars from the Tangle Creek (i.e., pre-dam) flood-frequency curves are similar to those at Site 1, further indicating that there has been little, if ay, morphologic adjustment of the channel downstream from both dams. The critical discharge range for the high bar surfaces that tend to be associated with mesquite and other non-riparian vegetation species, is about 160,000 cfs, but significant sediment transport does not occur at flows under 200,000 cfs. The critical discharges for the chute channels that are located primarily in the downstream portions of the site, are between 40,000 and 180,000 cfs (9 to >50-year RI), and significant sediment transport occurs at flows between 55,000 and 150,000 cfs (13 to >50-year RI).

The vegetation and morphological changes that were observed on the time-sequential aerial photography may be related to the effects of the upstream dam on the frequency of morphogenetically significant events (Figure 2. 7), as well as by the fact that the earlier part of the 20th century was wetter than the later part. Prior to construction of Bartlett Dam, inundation of portions of the younger Lehi terrace probably occurred with a frequency of about 2.5 to 3 years at a discharge of about 20,000 cfs. In the post-Bartlett period, the same flow has a recurrence interval of about 7 years. Review of the flow records at the Bartlett gage indicates that between 1942 and 1965 the largest peak flow was less than 10,000 cfs. The aerial photography shows that vegetation became well established during this 23-year period in areas of the site that were obviously disturbed in the 1934 photographs. In contrast, at the Tangle Creek gage, there were six floods in excess of 20,000 cfs in the same time period. Between 1965 and 1977, there were no flows in excess of 15,000 cfs below Bartlett Dam. Cumulatively, the three floods of 1978, 1979 and 1980 caused significant morphological and vegetation changes at the site, but these flood magnitudes ranged between 75,800 and 101,000 cfs (15 to 50-year RI). Hydraulic modeling of the site indicates that, at a discharge of 100,000 cfs, about 20 percent of the total flow is being conveyed in the left overbank area and this magnitude of flow is, therefore, capable of effecting change. In contrast, at a discharge of 50,000 cfs, less than 10 percent of the total flow is being conveyed in the left overbank area, and hence there is a much lower potential to effect change. The large floods of the late 1970s were again followed by a period of 12 years (1981 through 1992) when the maximum flow was less than 17,000 cfs below Bartlett Dam, but six events exceeded 20,000 cfs at the upstream gage in the same time period. The 1993 (84,700 cfs) and 1995 (64,100 cfs) floods with RI's of 11 and 18 years, respectively, caused very little change in the left overbank area at the site, probably because of the extent of the vegetation that has become established since the dam was constructed due to the infrequent disturbance of the site in the post-dam period.

6.2. Conclusions

This study was conducted to determine whether re-operation of the dams could significantly improve conditions for establishment and maintenance of woody riparian vegetation. The following general conclusions can be drawn from the results of the investigation:

1. The magnitudes of the discharges that inundate the channels and bars, and that mobilize the sediments that comprise these geomorphic features at all of the sites are similar, which indicates that there has been little, if any, morphological or sedimentological adjustment of the Verde River in response to the dams.

2. The reduced frequencies of inundation of the channels and bars, and mobilization of their constituent sediments downstream of the dams are due to the changes in hydrology imposed by the dams. Because of the smaller capacity of Horseshoe Reservoir, the frequency reductions at Site 2 are less than those at Site 3 that is located below Bartlett Reservoir and has a much larger storage capacity.

3. Reduction in the frequency of morphogenetically significant events below Bartlett Dam has enabled primarily mesquite vegetation to become better established in the left overbank area, and this reduces the erodibility of the low terrace during the less frequent, higher magnitude events that are not significantly affected by the upstream dams.

4. The reservoir re-operation scenarios that were considered in this analysis would have an insignificant effect on the frequency and duration at which geomorphic surfaces along the margins of the Verde River are inundated and mobilized. These processes are part of the disturbance regime that is important for establishing and maintaining riparian vegetation; thus, implementation of the scenarios would also have an insignificant effect on the health of the riparian corridor.

5. Comparison of the below Bartlett Dam flow-duration curve with the Tangle Creek gage flow-duration curve (Figure 3.6) shows that the durations of flows in the 200- to 1,400-cfs range have been increased by the dams, and these increased flows occur during the May through October period (Figure 3.7). The increased flows may well be responsible for supporting the relatively low-elevation channel margin riparian vegetation (Appendix A).

7. REFERENCES

Andrews, E.D., 1984. Bed material entrainment and hydraulic geometry of gravel-bed rivers in Colorado. Geological Society of America Bulletin 95, 371-378, March.

Baker, V.R., 1977. Stream Channel Response to Floods, with Examples from Central Texas. Geologist Society of America Bulletin, v. 86, pp. 1057-1071.

Einstein, H.A., 1950. The bedload function for sediment transportation in open channel flows. U.S. Soil Conservation Service, Tech. Bull. No. 1026.

Elliott, J.G. and Hammack, L.A., 2000. Entrainment of riparian gravel and cobbles in an alluvial reach of a regulated canyon river. Regulated Rivers: Research and Management 16, John Wiley & Sons, Ltd., pp. 37-50.

Elliott, J.G. and Parker, R.S., 1997. Altered streamflow and sediment entrainment in the Gunnison Gorge. Water Resources Bulletin, v. 33, no. 5, October, pp. 1041-1054.

Ely, L.L. and Baker, V.R., 1985. Reconstructing paleoflood hydrology with slackwater deposits: Verde River, Arizona. Physical Geography 5, 2, pp. 103-126.

Friedman, J.M. and Auble, G.T., 1999. Mortality of riparian boxelder from sediment mobilization and extended inundation. Regulated Rivers: Research and Management 15, John Wiley & Sons, Ltd., pp. 463-476.

Graf, W.L., 1988. Fluvial Processes in Dryland Rivers. The Blackburn Press, Caldwell, New Jersey, 346 p.

Graf, W.L., 1983. Flood-related channel changes in an arid region river. Earth Surface Processes and Landforms, Vol. 8, pp. 125-139.

Graf, W.L., 1980. The Effect of Dam Closure on Downstream Rapids. *American Geophysical Union,* Water Resources Research, Vol. 16, No. 1, February, pp. 129-136.

Harvey, M.D. and Schumm, S.A., 1987. Response of Dry Creek, California, to land use change, gravel mining and dam closure. Erosion and Sedimentation in the Pacific Rim. IAHS Publ. No. 165, p. 451-460.

Harvey, M. D., Mussetter, R.A., and Wick, E.J., 1993. A Physical Process - biological Response Model for Spawning Habitat Formation for the Endangered Colorado Squawfish, Rivers, Vol.4, No. 2, pp 114-131.

Hey, R.D., 1979. Flow Resistance in Gravel-Bed Rivers. Journal of the Hydraulics Division, v. 105, no. HY4, p. 365-379.

House, P.K. and Pearthree, P.A., 1993. Surficial geologic maps of the northern Verde Valley, Yavapai County, Arizona. Arizona Geological Survey Open-File Report 93-16, 18 p.

House, P.K., Pearthree, P.A., and Fuller, J.E., 1995. Hydrologic and paleohydrologic assessment of the 1993 floods on the Verde River, Central Arizona. Arizona Geological Survey Open-File Report 95-20, December, 23 p.

Hupp, C.R. and Osterkamp, W.R., 1985. Bottomland vegetation distribution along Passage Creek, Virginia, in relation to fluvial landforms, Ecology, v.66, p. 670-681.

Leopold, L.B and Maddock, T., 1953. The hydraulic geometry of stream channels and some physiographic implications. U.S. Geol. Survey Prof. Paper 252, 57 p.

Lisle, T. E. 1986. Stabilization of a gravel channel by large streamside obstructions and bedrock bends, Jacoby Creek, Northwestern California. *Geological Society of America Bulletin.* 97(8):999-1011.

McBain and Trush, 1997. Trinity River Maintenance Flow Study Final Report. Prepared for Hoopa Valley Tribe Fisheries Department, Hoopa, California, Contract No. 30255, November, 316 p. plus appendices.

Meyer-Peter, E. and Müller, R., 1948. Formulas for bed load transport. In Proceedings of the 2nd Congress of the International Association for Hydraulic Research, Stockholm, 2: Paper No. 2, pp 39-64.

Neill, C.R., 1968. Note on initial movement of coarse uniform bed material. Journal of Hydraulic Research 6(2): 173-176.

O'Connor, J. E., R. H. Webb, and V. R. Baker. 1986. Paleohydrology of pool and riffle pattern development. Boulder Creek, Utah, *Geological Society of America Bulletin.* 97(4):410-420.

Osterkamp, W.R. and Hupp, C.R., 1984. Geomorphic and vegetative characteristics along three northern Virginia streams. Geological Society of America Bulletin, v. 95, September, pp. 1093-1101.

Parker, G., Klingeman, P.C., and McLean, D.G., 1982. Bed load and size distribution in paved gravel-bed streams. Journal of the Hydraulics Divisions, American Society of Civil Engineers, 108(HY4), Proc. Paper 17009: 544-571.

Pearthree, P.A., 1993. Geologic and geomorphic setting of the Verde River from Sullivan Lake to Horseshoe Reservoir. Arizona Geological Survey Open-File Report 93-4, March, 25 p. plus maps.

Pearthree, P.A., 1996. Historical geomorphology of the Verde River. Arizona Geological Survey Open-File 96-13, June, 26 p.

Péwé, T.L., 1978. Terraces of the lower Salt River Valley in relation to the late Cenozoic history of the Phoenix Basin, Arizona. In Burt, D.M. and Péwé, T.L. (eds), Guidebook to the Geology of Central Arizona, Arizona Bureau of Geology and Mineral Technology (Arizona Geological Survey) Special Paper 2, pp. 1-46.

Pope, C.W., 1974. Geology of the lower Verde River Valley, Maricopa County, Arizona. Arizona State University, unpublished M.S. thesis, 104 p.

Pope, C.W. and Péwé, T.L., 1973. Geology of the lower Verde River Valley, Maricopa County, Arizona (abstract). Arizona Academy of Science Proceedings Supplement, v., 42 p.

Rood. S.B. and Mahoney, J.M., 1990. Collapse of riparian poplar forests downstream from dams in western prairies: probable causes and prospects for mitigation. Environmental Management 14, pp. 451-464.

Schumm, S.A., 1977. The Fluvial System. John Wiley and Sons, New York.

Scott, M.L., Auble, G.T., and Friedman, JB., 1997. Flood dependency of cottonwood establishment along the Missouri River, Montana, USA. Ecological Applications 7(2), pp. 677-690.

Scott, M.L., Wondzell, M.A., and Auble, G.T., 1993. Hydrograph characteristics relevant to the establishment and growth of western riparian vegetation. In Morel-Seytoux, H.J. (ed), Proceedings of the Thirteenth Annual American Geophysical Union Hydrology Days, Hydrology Days Publications, Atherton, California, pp. 237-246.

Shafroth, P.B., Auble, G.T., Stromberg, J.C., and Patten, D.T.,1998. Establishment of woody riparian vegetation in relation to annual patterns of streamflow, Bill Williams Reservoir, Arizona. Wetlands, 18(4), pp. 577-590.

Shields, A., 1936. Application of similarity principles and turbulence research to bed load movement. California Institute of Technology, Pasadena; Translation from German Original; Report 167.

Skotnicki, S.J., 1996. Geologic map of the Bartlett Dam quadrangle and southern part of the Horseshoe Dam quadrangle, Maricopa County, Arizona. Arizona Geological Survey Open-File Report 96-22, September, 21 p. plus maps.

Strand, R.I., 1975. Bureau of Reclamation procedures for predicting sediment yield. Agricultural Research Service, ARS-S-40, pp. 10-15.

U.S. Army Corps of Engineers, Hydrologic Engineering Center, 2002. HEC-RAS, River Analysis System, User's Manual. Davis California, Version 3.1, CPD-68.

U.S. Geological Survey, 1998. Statistical Summaries of Streamflow Data and Characteristics of Drainage Basins for Selected Streamflow-Gaging Stations in Arizona Through Water Year 1996. Water-Resources Investigations Report 98-4225.

Water Resources Council, 1981. Guidelines for Determining Flood Flow Frequency. Bulletin No. 17B of the Hydrology Committee.

Webb, R.H., Pringle, P.T., Renneau, S.L., and Rink, G.R., 1988. Monument Creek debris flow: Implications for formation of rapids on the Colorado river in Grand Canyon National Park. Geology 16(1): 50-54.

Williams, G.P. and Wolman, M.G., 1994. Downstream effects of dams on alluvial rivers. USGS Professional Paper 1286.

Wolman, M.G., 1954. A method for sampling coarse river bed material, Transactions of American Geophysical Union, v.35 (6), 951-956.

Wolman, M.G. and Gerson, R., 1978. Relative scale of time and effectiveness. Earth Surface Processes and Landforms, v. 3, p. 189-208.

APPENDIX A

Surveyed Cross Sections for Three Sites Showing the Distribution of Vegetation, Water-Surface Elevations and Incipient Motion, and Measurable Sediment-Transport Thresholds

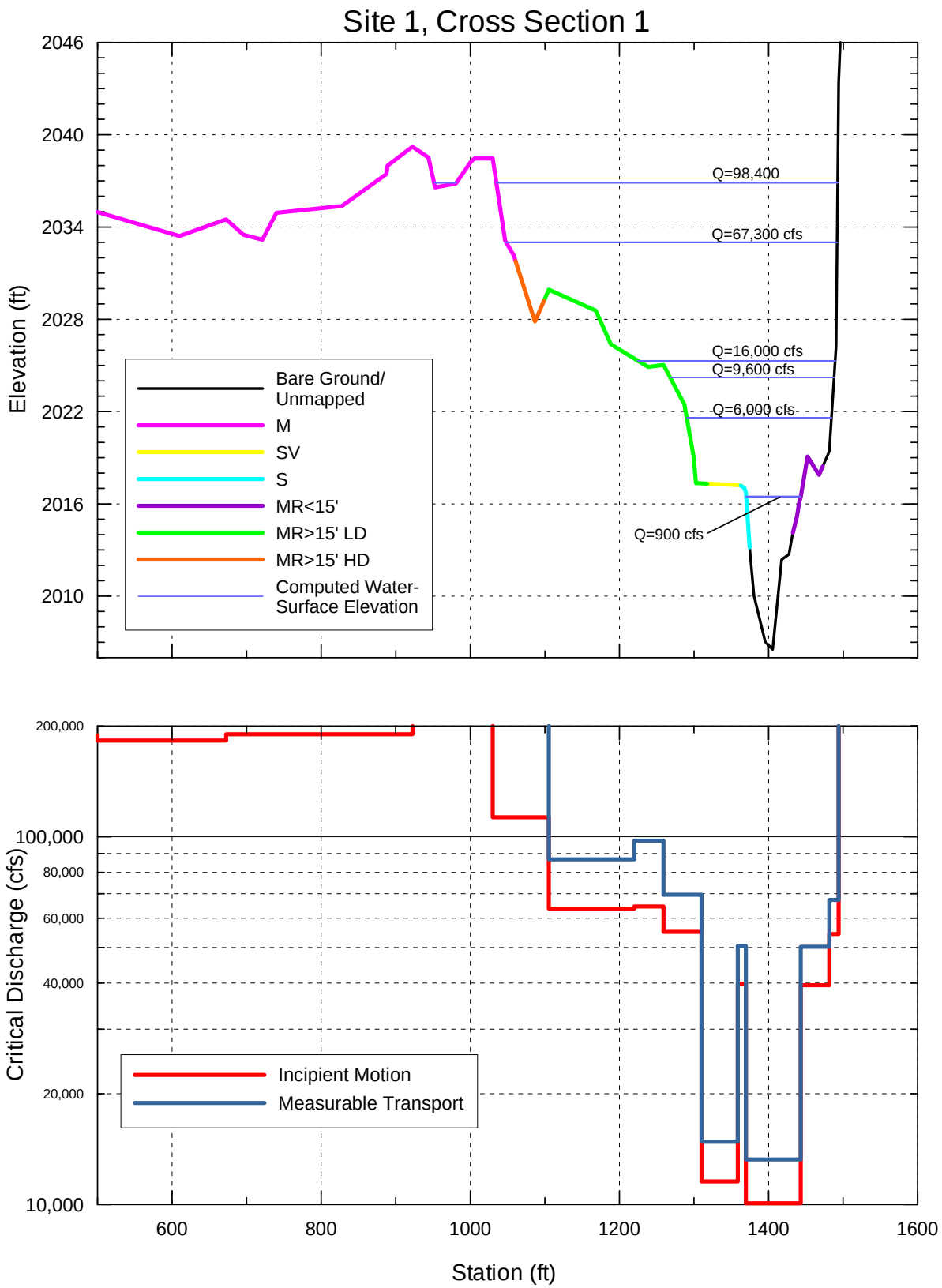
Site 1, Cross Section 1
Elevation (ft)
2046
2040
2034
2028
2022
2016
2010
Q=98,400
Q=67,300 cfs
Q=16,000 cfs
Q=9,600 cfs
Q=6,000 cfs
Q=900 cfs
Bare Ground/ Unmapped
M
SV
S
MR<15'
MR>15' LD
MR>15' HD
Computed Water-Surface Elevation
Critical Discharge (cfs)
200,000
100,000
80,000
60,000
40,000
20,000
10,000
Incipient Motion
Measurable Transport
600
800
1000
1200
1400
1600
Station (ft)

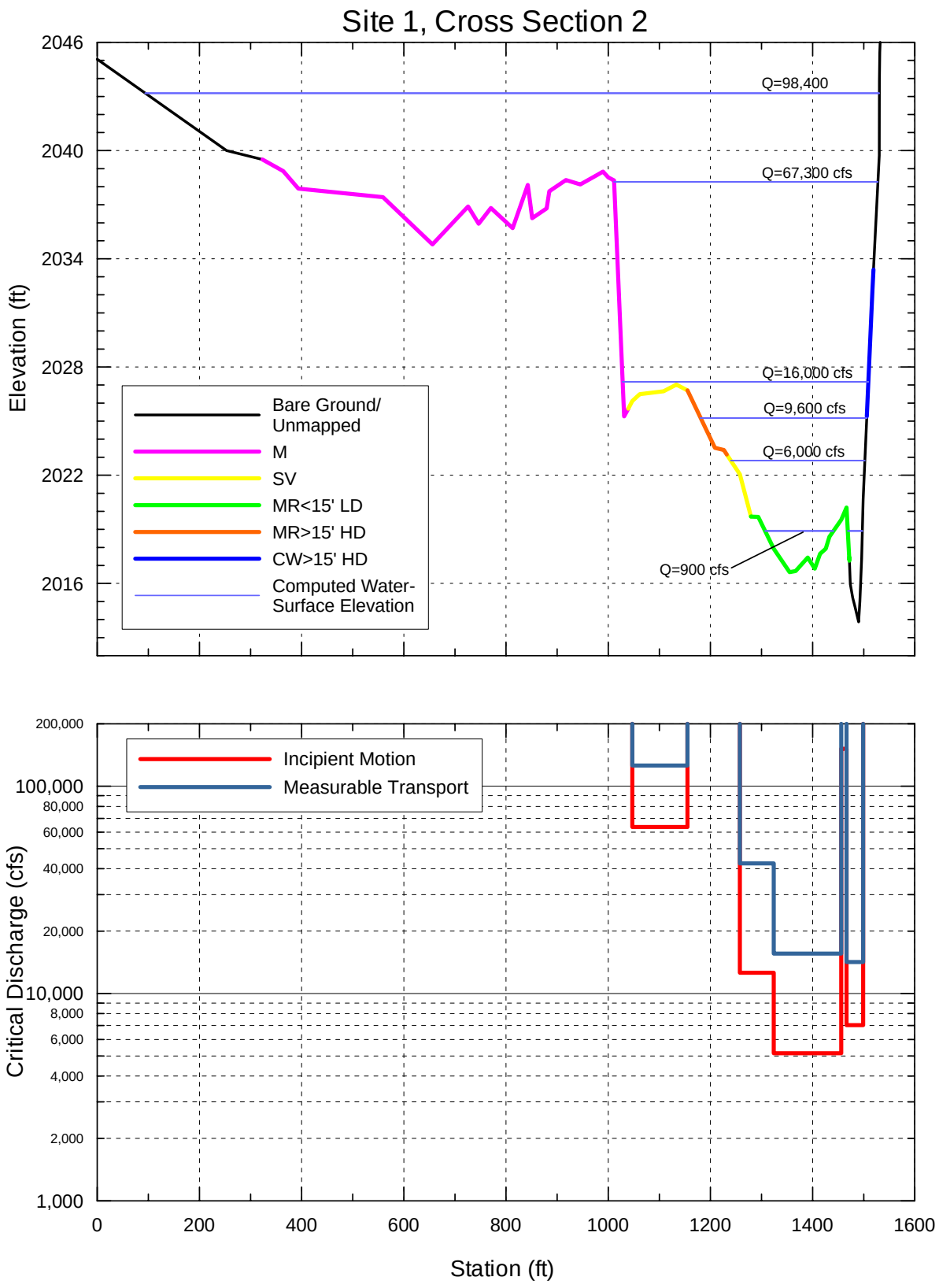
Site 1, Cross Section 2
Elevation (ft)
2046
2040
2034
2028
2022
2016
Q=98,400
Q=67,300 cfs
Q=16,000 cfs
Q=9,600 cfs
Q=6,000 cfs
Q=900 cfs
Bare Ground/ Unmapped
M
SV
MR<15' LD
MR>15' HD
CW>15' HD
Computed Water-Surface Elevation
Critical Discharge (cfs)
200,000
100,000
80,000
60,000
40,000
20,000
10,000
8,000
6,000
4,000
2,000
1,000
Incipient Motion
Measurable Transport
0
200
400
600
800
1000
1200
1400
1600
Station (ft)

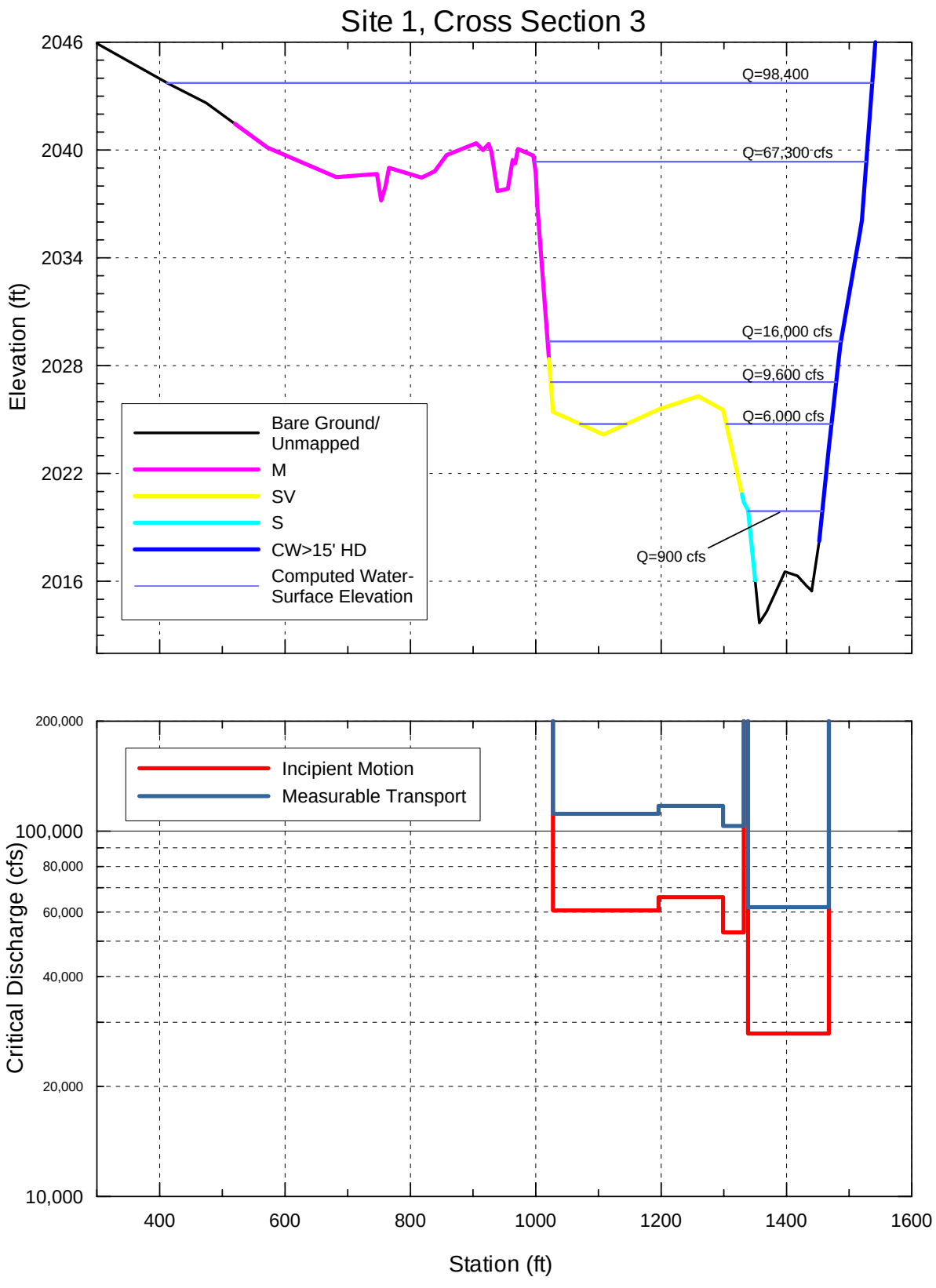
Site 1, Cross Section 3
Elevation (ft)
2046
2040
2034
2028
2022
2016
Q=98,400
Q=67,300 cfs
Q=16,000 cfs
Q=9,600 cfs
Q=6,000 cfs
Q=900 cfs
Bare Ground/ Unmapped
M
SV
S
CW>15' HD
Computed Water-Surface Elevation
Critical Discharge (cfs)
200,000
100,000
80,000
60,000
40,000
20,000
10,000
Incipient Motion
Measurable Transport
400
600
800
1000
1200
1400
1600
Station (ft)

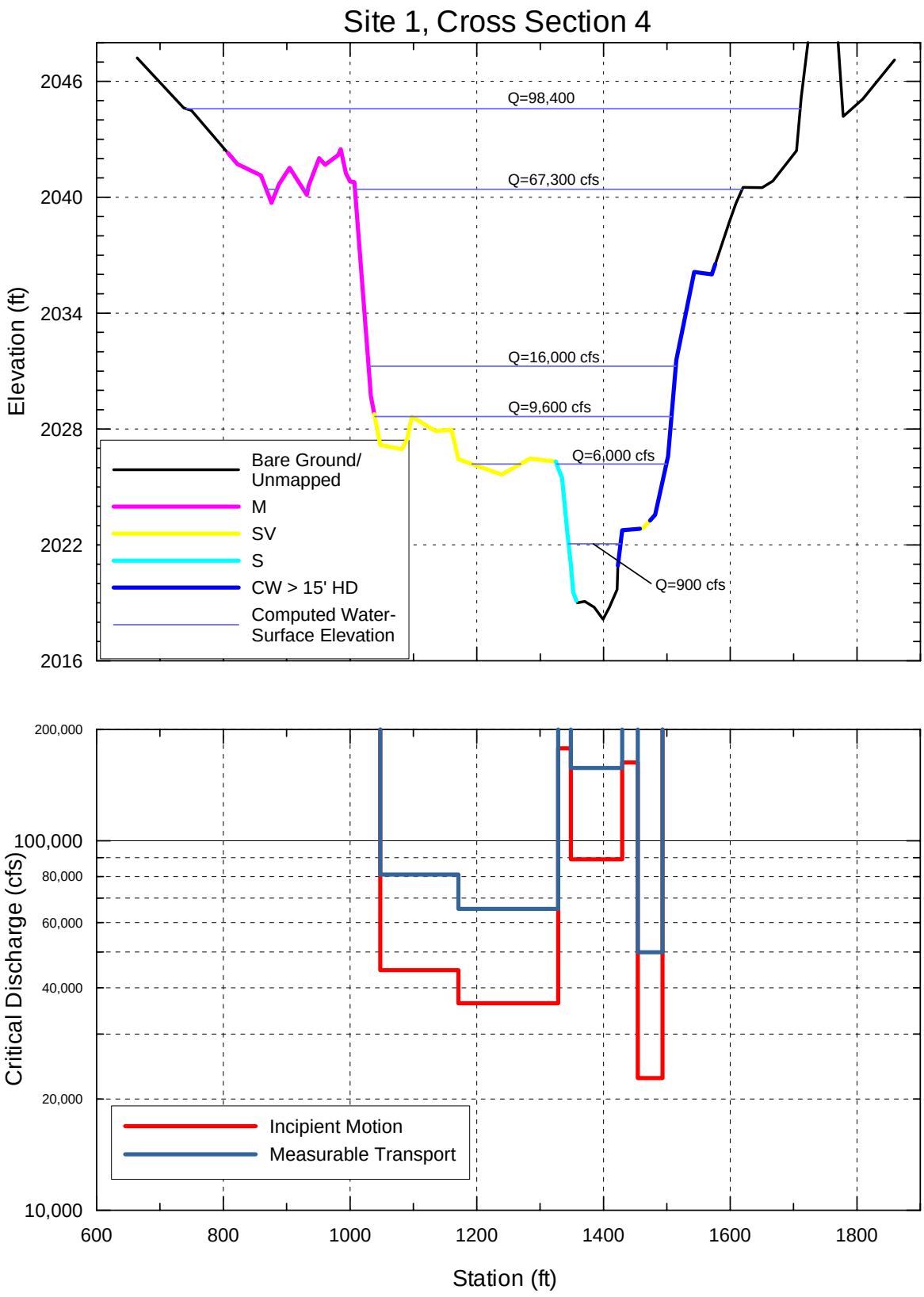
Site 1, Cross Section 4
Elevation (ft)
2046
2040
2034
2028
2022
2016
Q=98,400
Q=67,300 cfs
Q=16,000 cfs
Q=9,600 cfs
Q=6,000 cfs
Q=900 cfs
Bare Ground/ Unmapped
M
SV
S
CW > 15' HD
Computed Water-Surface Elevation
Critical Discharge (cfs)
200,000
100,000
80,000
60,000
40,000
20,000
10,000
600
800
1000
1200
1400
1600
1800
Station (ft)
Incipient Motion
Measurable Transport

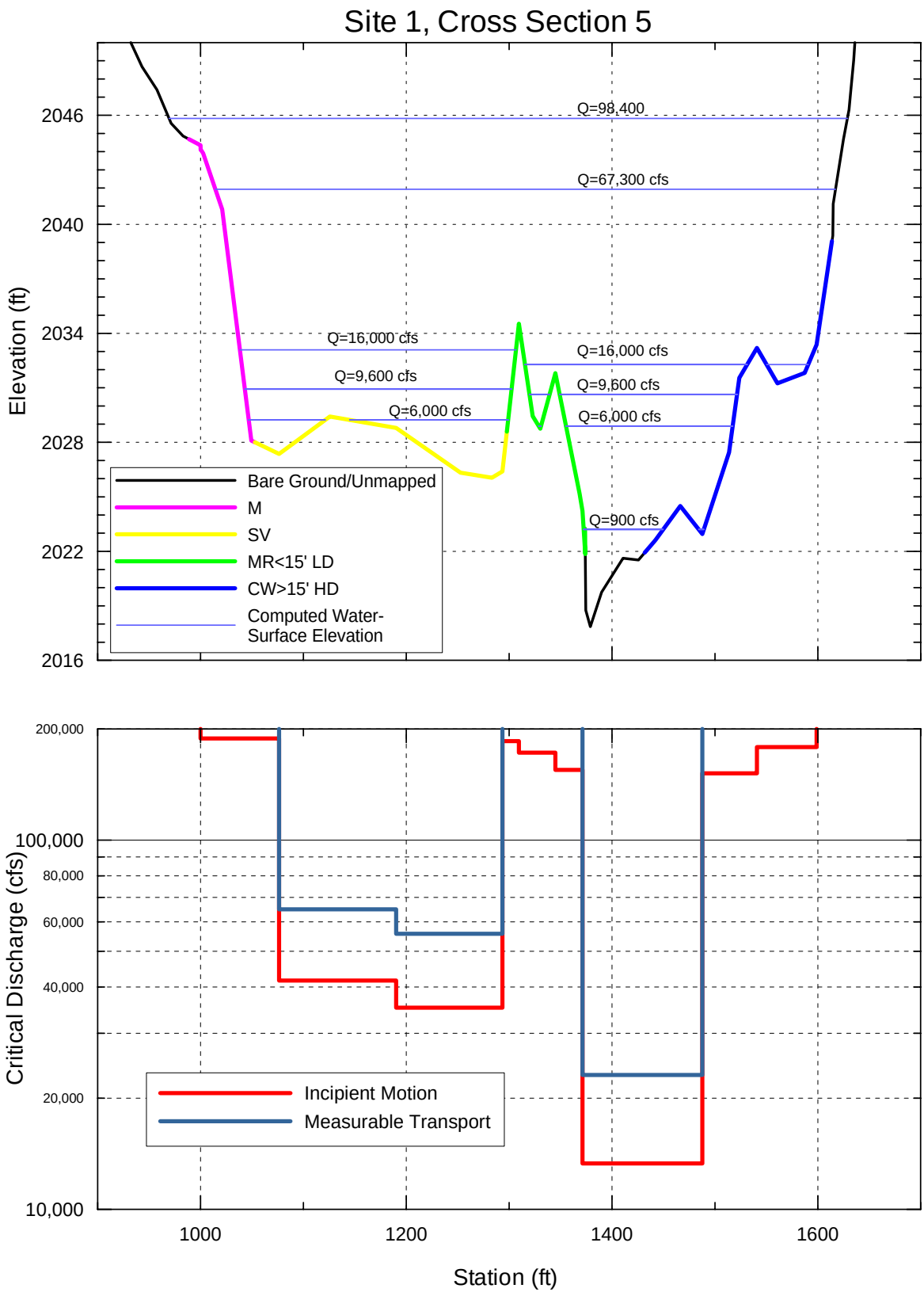
Site 1, Cross Section 5
Elevation (ft)
2046
2040
2034
2028
2022
2016
Q=98,400
Q=67,300 cfs
Q=16,000 cfs
Q=9,600 cfs
Q=6,000 cfs
Q=16,000 cfs
Q=9,600 cfs
Q=6,000 cfs
Q=900 cfs
Bare Ground/Unmapped
M
SV
MR<15' LD
CW>15' HD
Computed Water-Surface Elevation
Critical Discharge (cfs)
200,000
100,000
80,000
60,000
40,000
20,000
10,000
Incipient Motion
Measurable Transport
1000
1200
1400
1600
Station (ft)

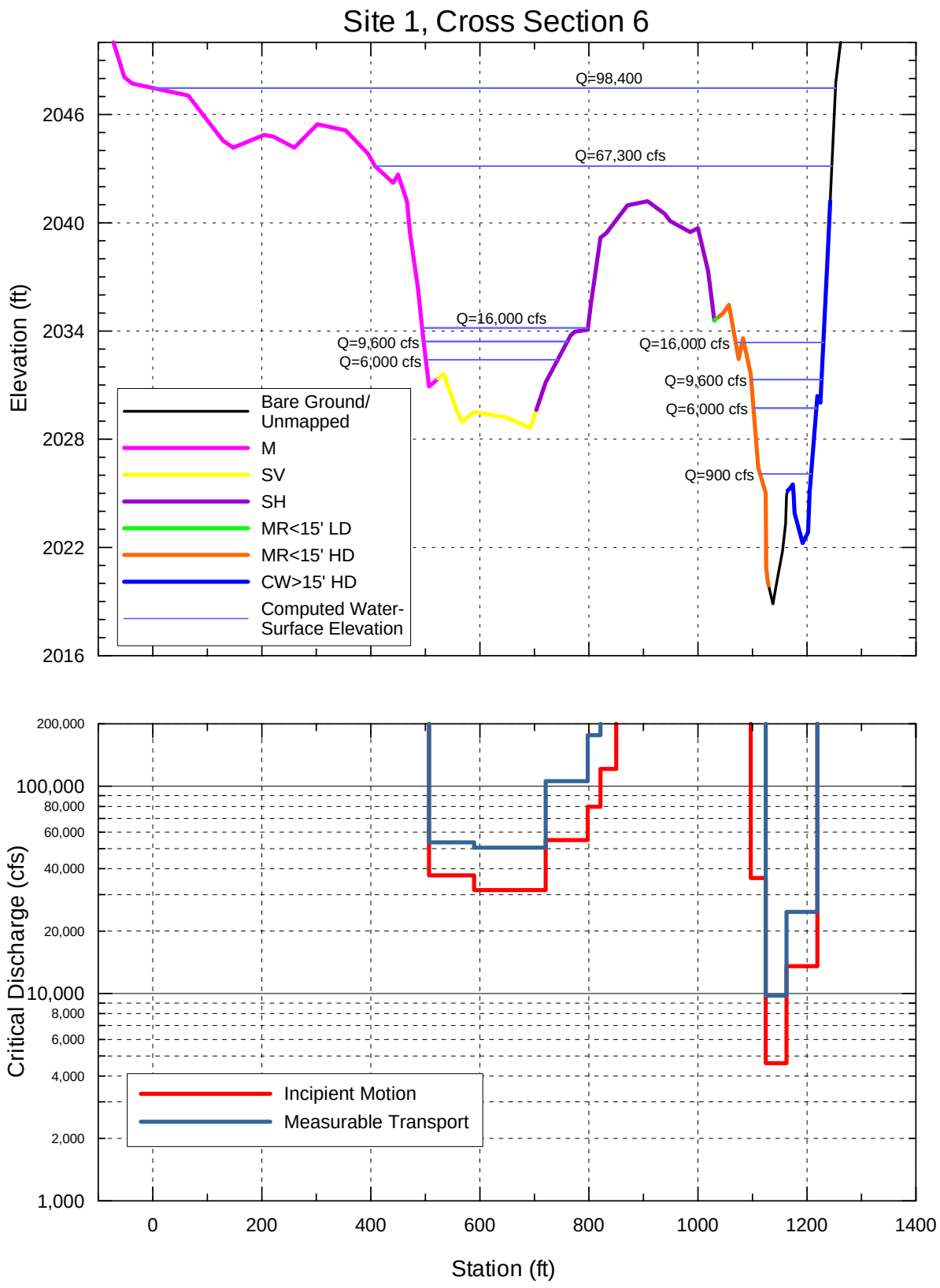
Site 1, Cross Section 6
Elevation (ft)
2046
2040
2034
2028
2022
2016
Q=98,400
Q=67,300 cfs
Q=16,000 cfs
Q=9,600 cfs
Q=6,000 cfs
Q=16,000 cfs
Q=9,600 cfs
Q=6,000 cfs
Q=900 cfs
Bare Ground/ Unmapped
M
SV
SH
MR<15' LD
MR<15' HD
CW>15' HD
Computed Water-Surface Elevation
Critical Discharge (cfs)
200,000
100,000
80,000
60,000
40,000
20,000
10,000
8,000
6,000
4,000
2,000
1,000
Incipient Motion
Measurable Transport
0
200
400
600
800
1000
1200
1400
Station (ft)

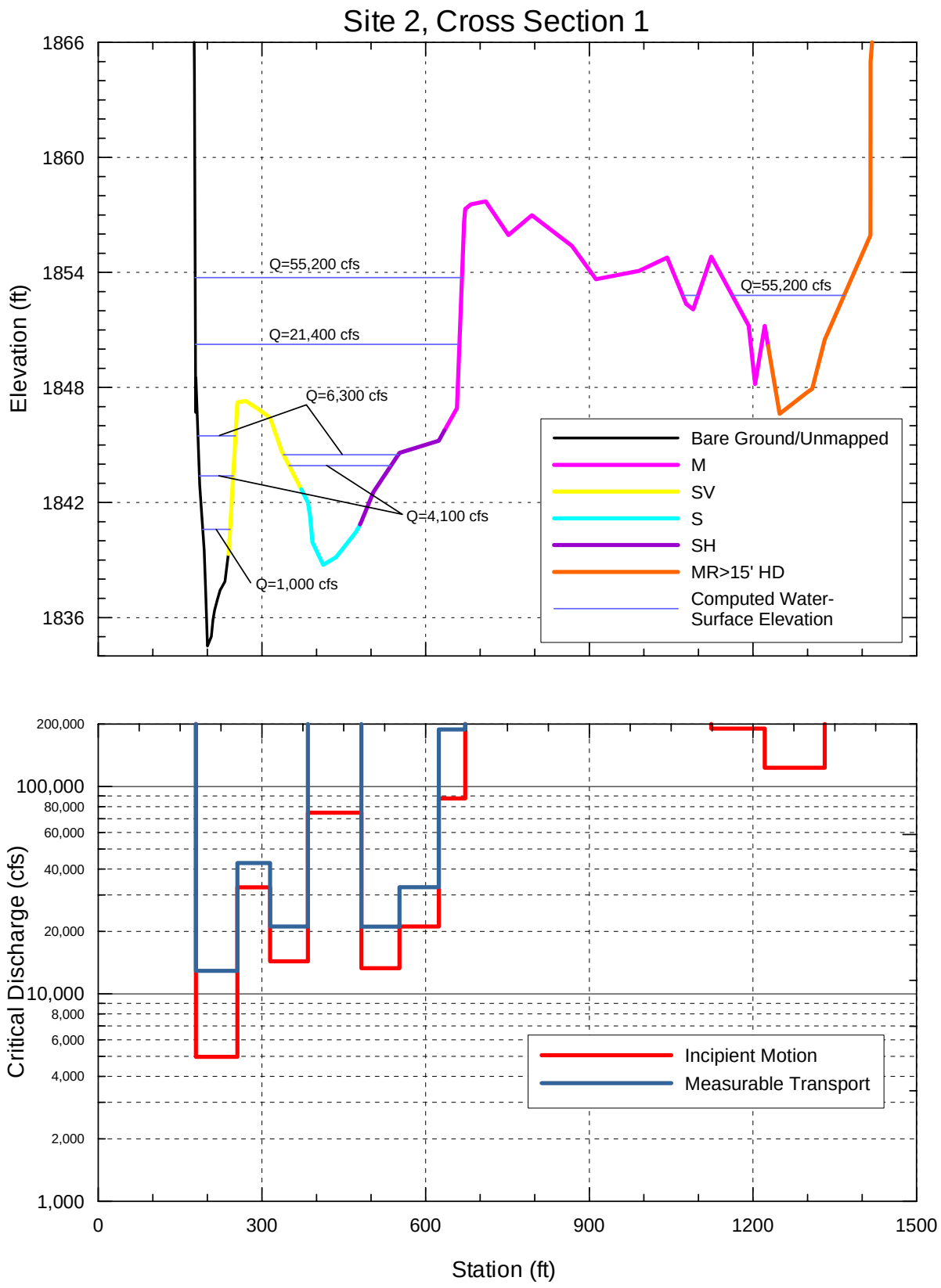
Site 2, Cross Section 1
Elevation (ft)
1866
1860
1854
1848
1842
1836
Q=55,200 cfs
Q=21,400 cfs
Q=6,300 cfs
Q=4,100 cfs
Q=1,000 cfs
Q=55,200 cfs
Bare Ground/Unmapped
M
SV
S
SH
MR>15' HD
Computed Water-Surface Elevation
Critical Discharge (cfs)
200,000
100,000
80,000
60,000
40,000
20,000
10,000
8,000
6,000
4,000
2,000
1,000
0
300
600
900
1200
1500
Station (ft)
Incipient Motion
Measurable Transport

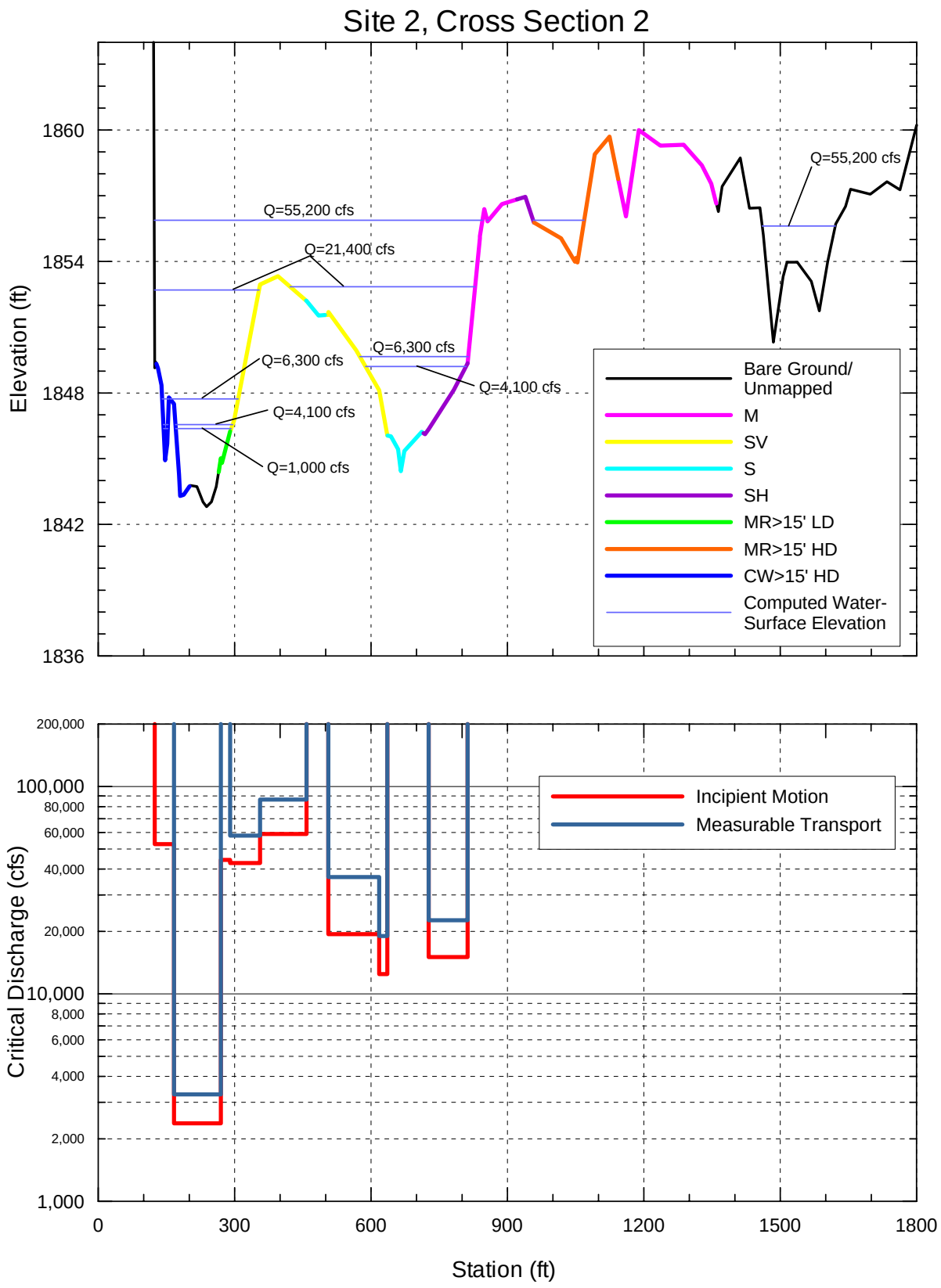
Site 2, Cross Section 2
Elevation (ft)
1860
1854
1848
1842
1836
Q=55,200 cfs
Q=21,400 cfs
Q=6,300 cfs
Q=6,300 cfs
Q=4,100 cfs
Q=4,100 cfs
Q=1,000 cfs
Q=55,200 cfs
Bare Ground/ Unmapped
M
SV
S
SH
MR>15' LD
MR>15' HD
CW>15' HD
Computed Water-Surface Elevation
Critical Discharge (cfs)
200,000
100,000
80,000
60,000
40,000
20,000
10,000
8,000
6,000
4,000
2,000
1,000
Incipient Motion
Measurable Transport
0
300
600
900
1200
1500
1800
Station (ft)

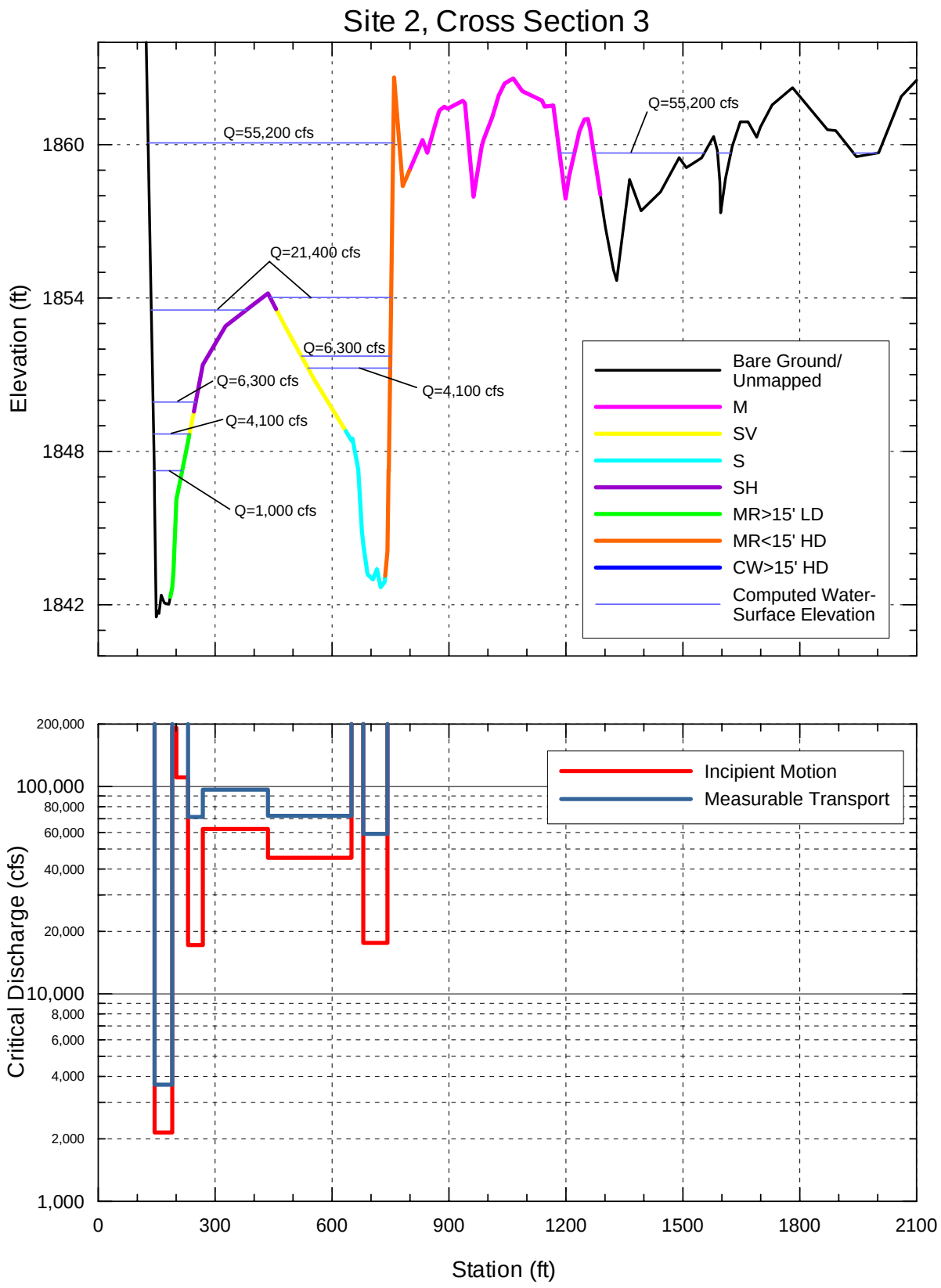
Site 2, Cross Section 3
Elevation (ft)
1860
1854
1848
1842
Q=55,200 cfs
Q=55,200 cfs
Q=21,400 cfs
Q=6,300 cfs
Q=6,300 cfs
Q=4,100 cfs
Q=4,100 cfs
Q=1,000 cfs
Bare Ground/ Unmapped
M
SV
S
SH
MR>15' LD
MR<15' HD
CW>15' HD
Computed Water-Surface Elevation
Critical Discharge (cfs)
200,000
100,000
80,000
60,000
40,000
20,000
10,000
8,000
6,000
4,000
2,000
1,000
Incipient Motion
Measurable Transport
0
300
600
900
1200
1500
1800
2100
Station (ft)

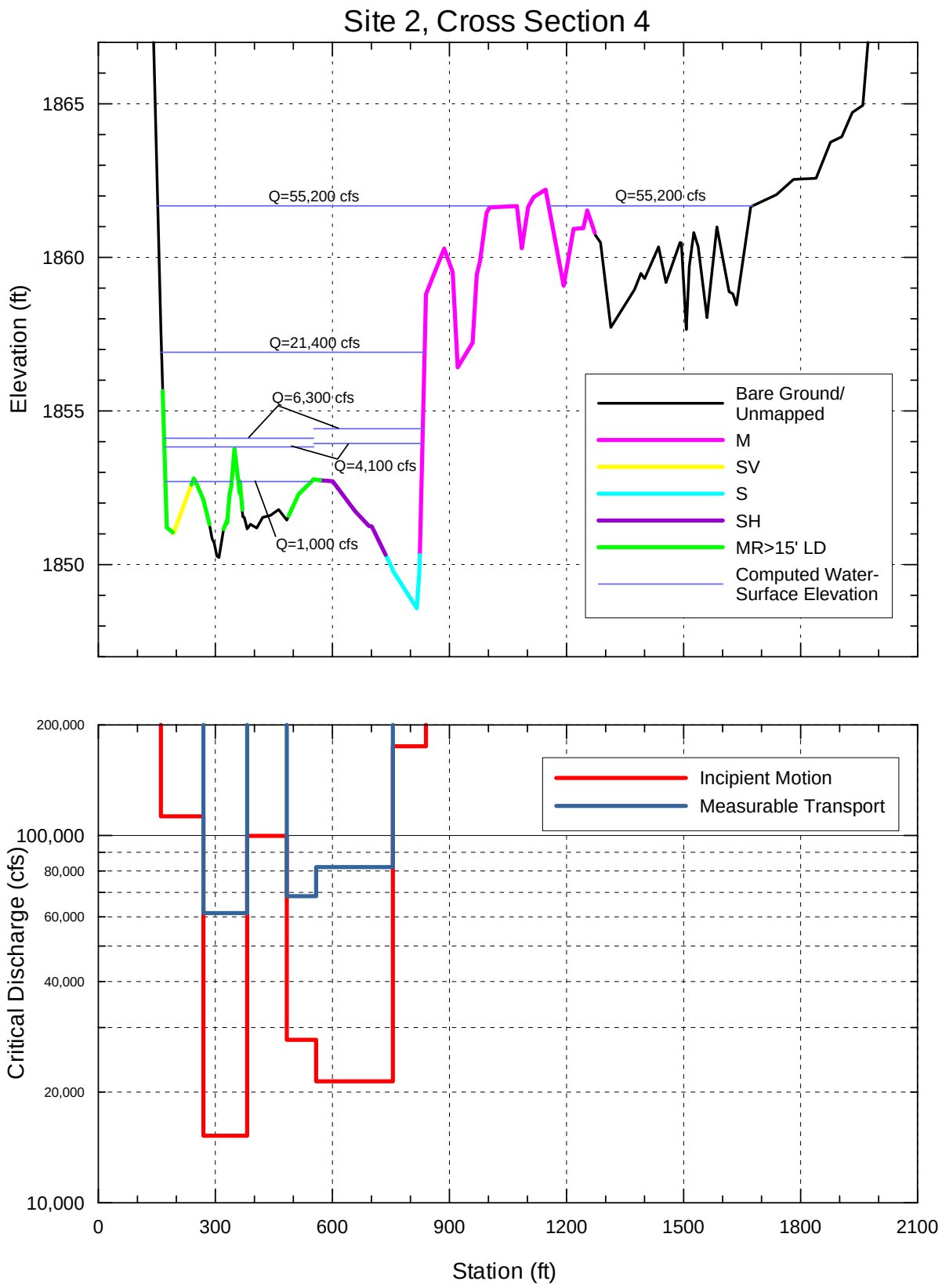
Site 2, Cross Section 4
Elevation (ft)
1865
1860
1855
1850
Q=55,200 cfs
Q=55,200 cfs
Q=21,400 cfs
Q=6,300 cfs
Q=4,100 cfs
Q=1,000 cfs
Bare Ground/ Unmapped
M
SV
S
SH
MR>15' LD
Computed Water-Surface Elevation
Critical Discharge (cfs)
200,000
100,000
80,000
60,000
40,000
20,000
10,000
Incipient Motion
Measurable Transport
0
300
600
900
1200
1500
1800
2100
Station (ft)

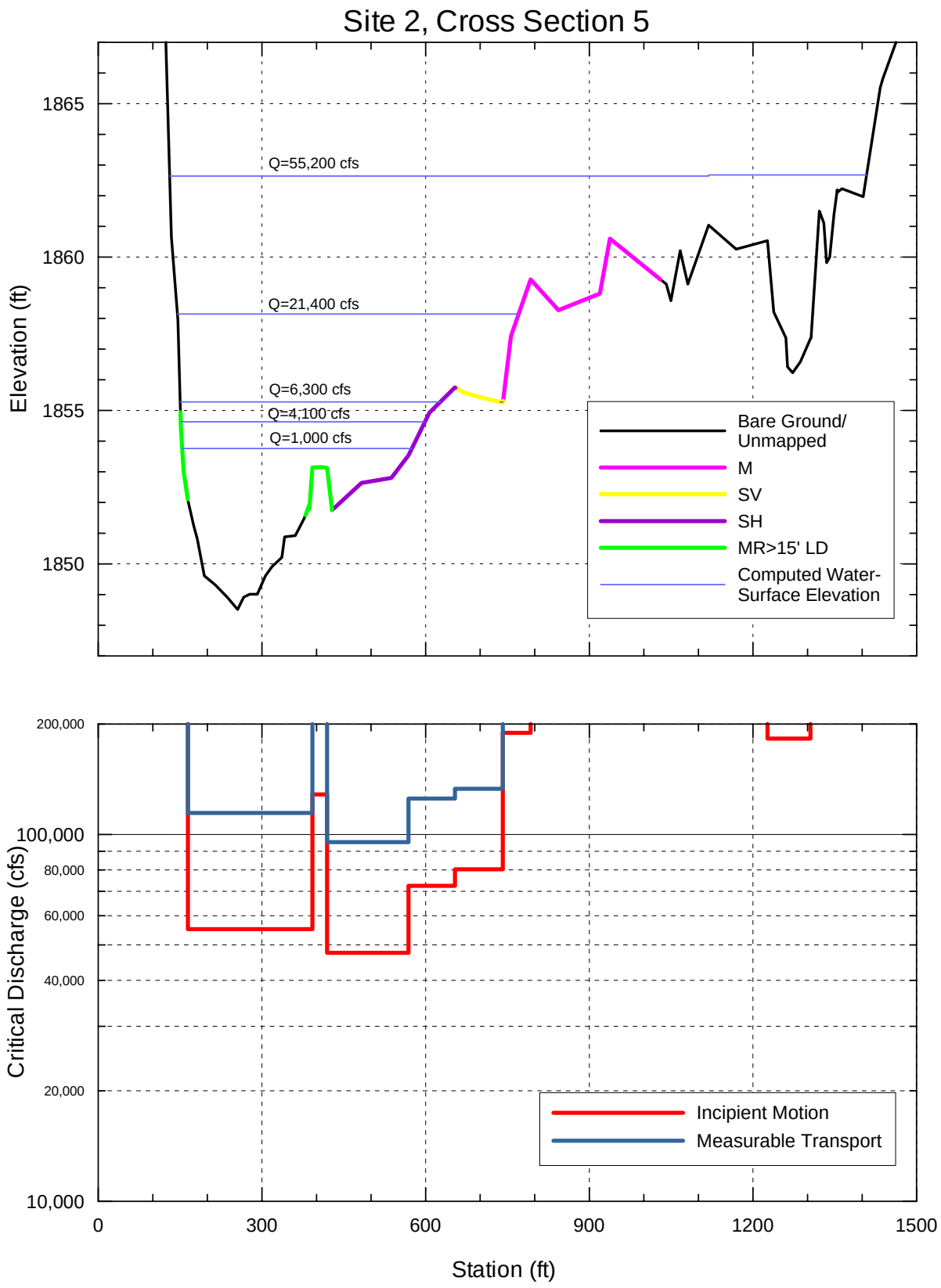
Site 2, Cross Section 5
Elevation (ft)
1865
1860
1855
1850
Q=55,200 cfs
Q=21,400 cfs
Q=6,300 cfs
Q=4,100 cfs
Q=1,000 cfs
Bare Ground/ Unmapped
M
SV
SH
MR>15' LD
Computed Water-Surface Elevation
Critical Discharge (cfs)
200,000
100,000
80,000
60,000
40,000
20,000
10,000
Incipient Motion
Measurable Transport
0
300
600
900
1200
1500
Station (ft)

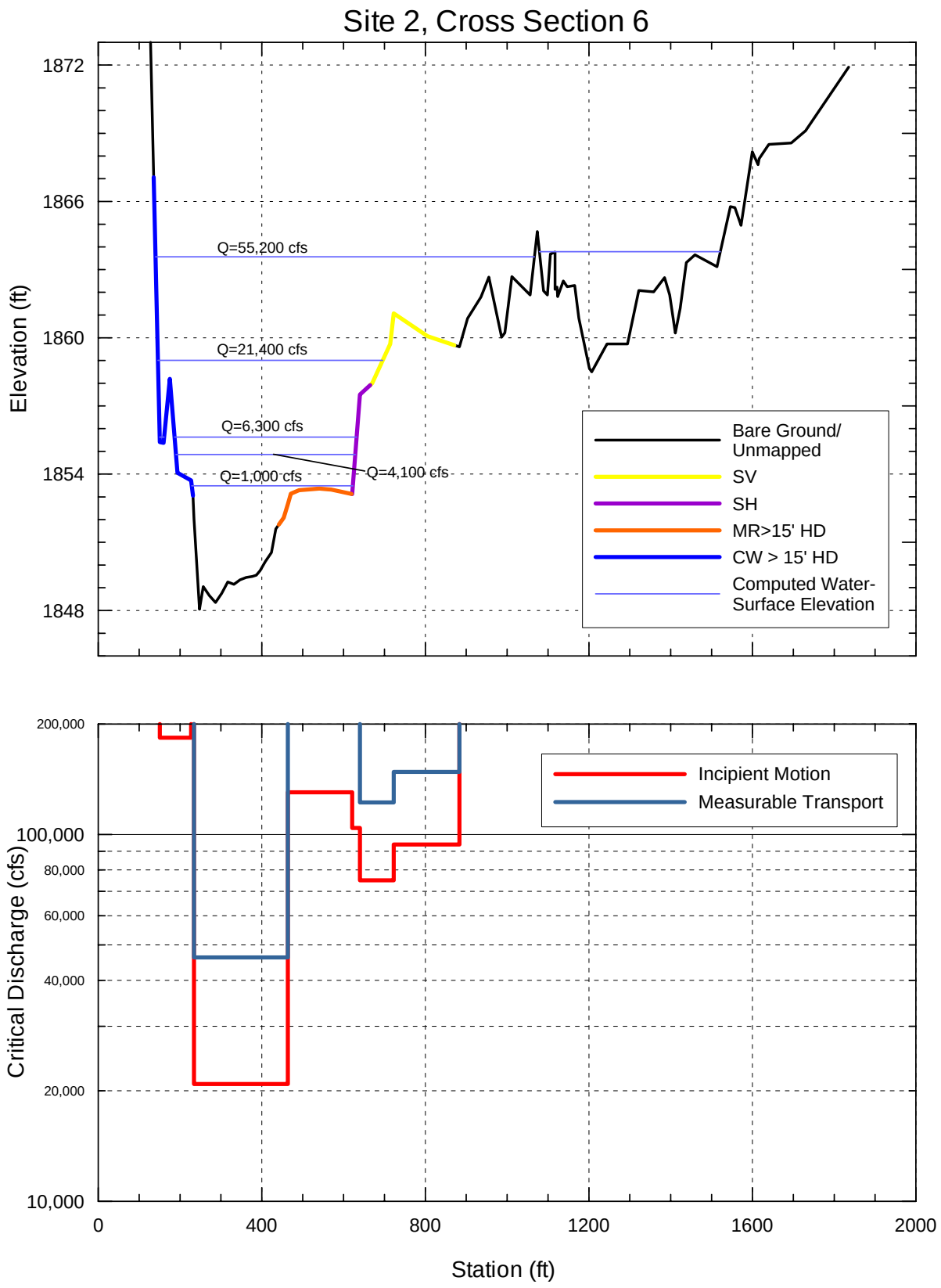
Site 2, Cross Section 6
Elevation (ft)
1872
1866
1860
1854
1848
Q=55,200 cfs
Q=21,400 cfs
Q=6,300 cfs
Q=1,000 cfs
Q=4,100 cfs
Bare Ground/ Unmapped
SV
SH
MR>15' HD
CW > 15' HD
Computed Water-Surface Elevation
Critical Discharge (cfs)
200,000
100,000
80,000
60,000
40,000
20,000
10,000
0
400
800
1200
1600
2000
Station (ft)
Incipient Motion
Measurable Transport

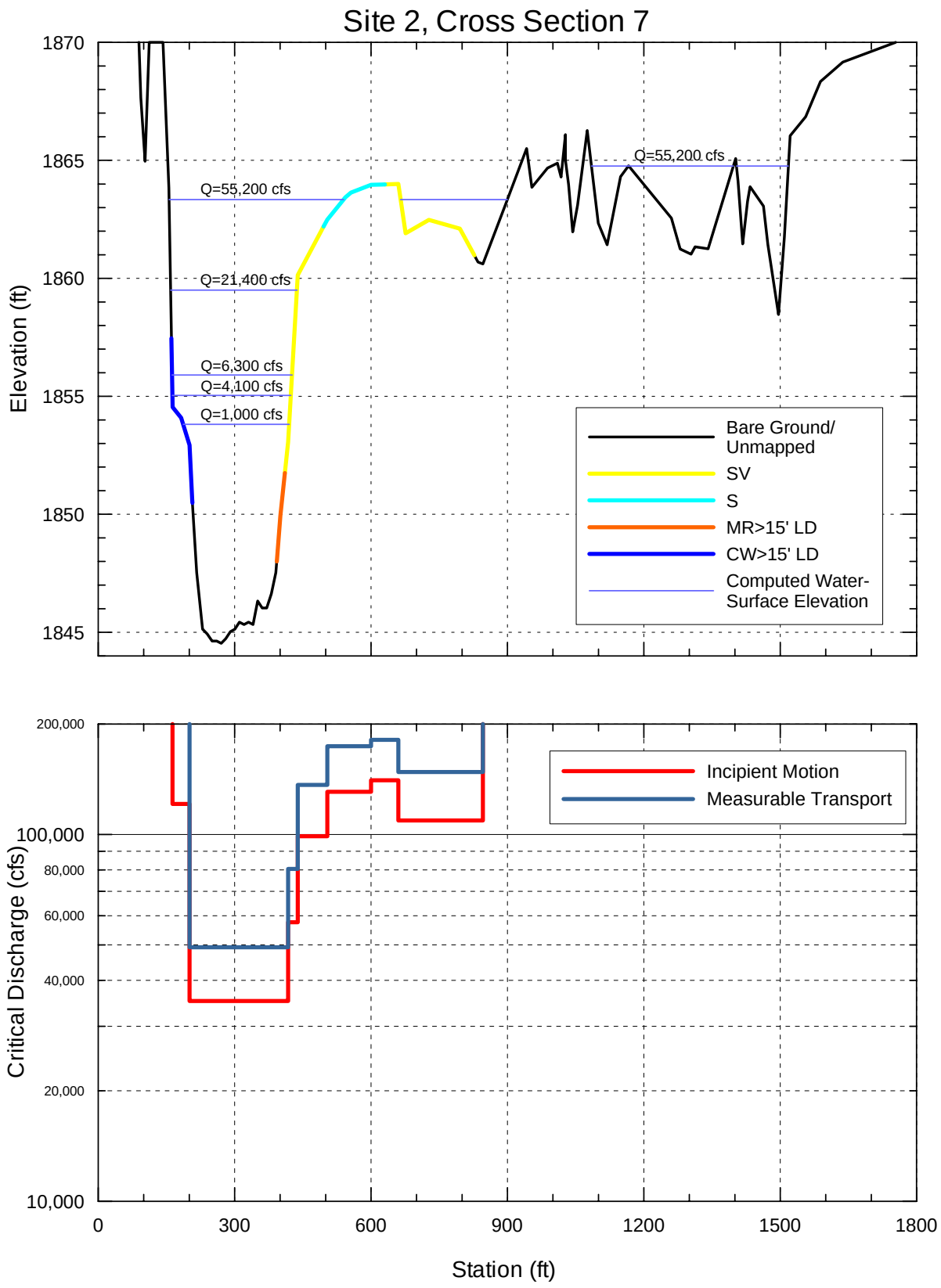
Site 2, Cross Section 7
Elevation (ft)
1870
1865
1860
1855
1850
1845
Q=55,200 cfs
Q=55,200 cfs
Q=21,400 cfs
Q=6,300 cfs
Q=4,100 cfs
Q=1,000 cfs
Bare Ground/ Unmapped
SV
S
MR>15' LD
CW>15' LD
Computed Water-Surface Elevation
Critical Discharge (cfs)
200,000
100,000
80,000
60,000
40,000
20,000
10,000
Incipient Motion
Measurable Transport
0
300
600
900
1200
1500
1800
Station (ft)

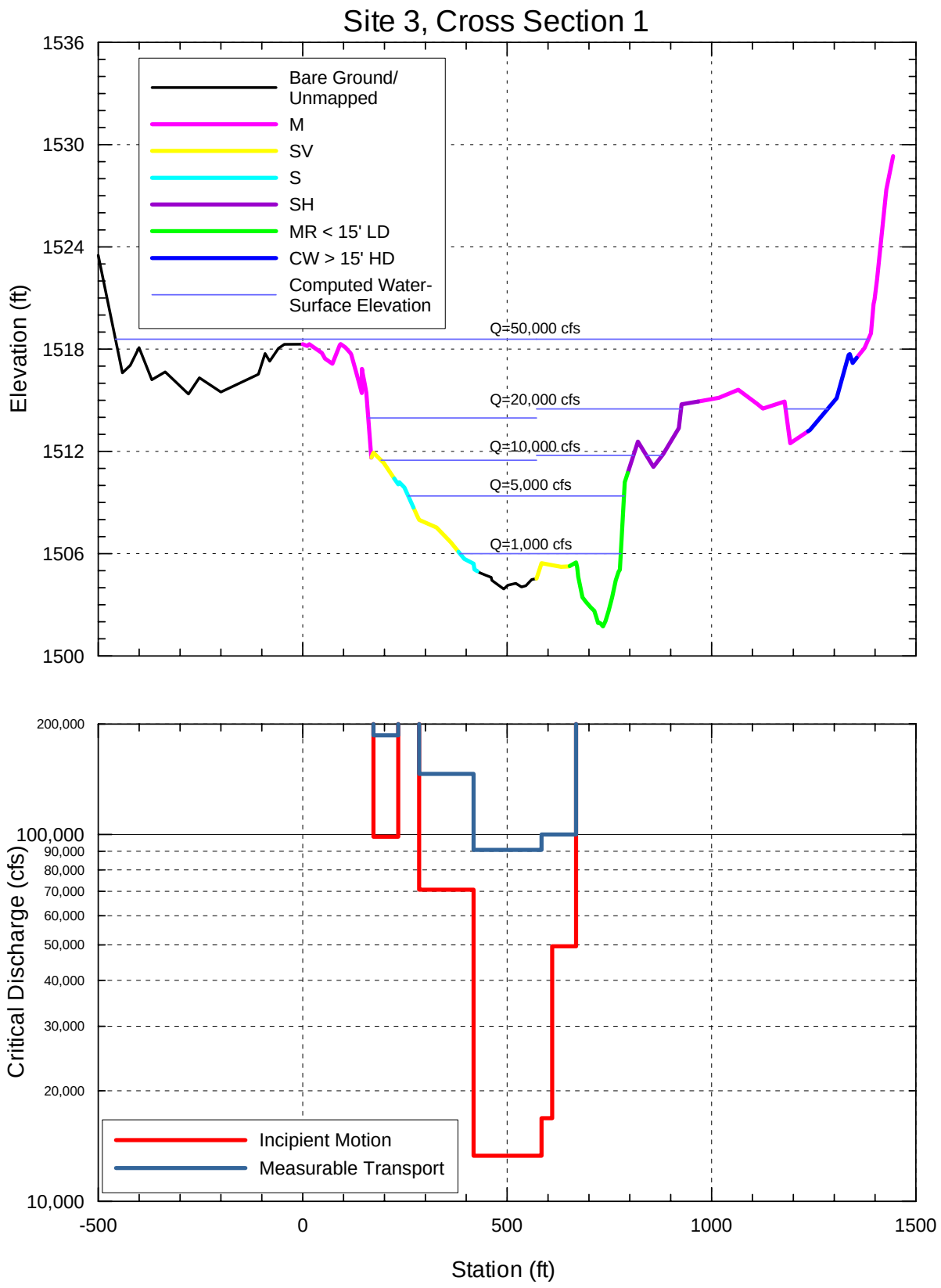
Site 3, Cross Section 1
Elevation (ft)
1536
1530
1524
1518
1512
1506
1500
Bare Ground/ Unmapped
M
SV
S
SH
MR < 15' LD
CW > 15' HD
Computed Water-Surface Elevation
Q=50,000 cfs
Q=20,000 cfs
Q=10,000 cfs
Q=5,000 cfs
Q=1,000 cfs
Critical Discharge (cfs)
200,000
100,000
90,000
80,000
70,000
60,000
50,000
40,000
30,000
20,000
10,000
Incipient Motion
Measurable Transport
-500
0
500
1000
1500
Station (ft)

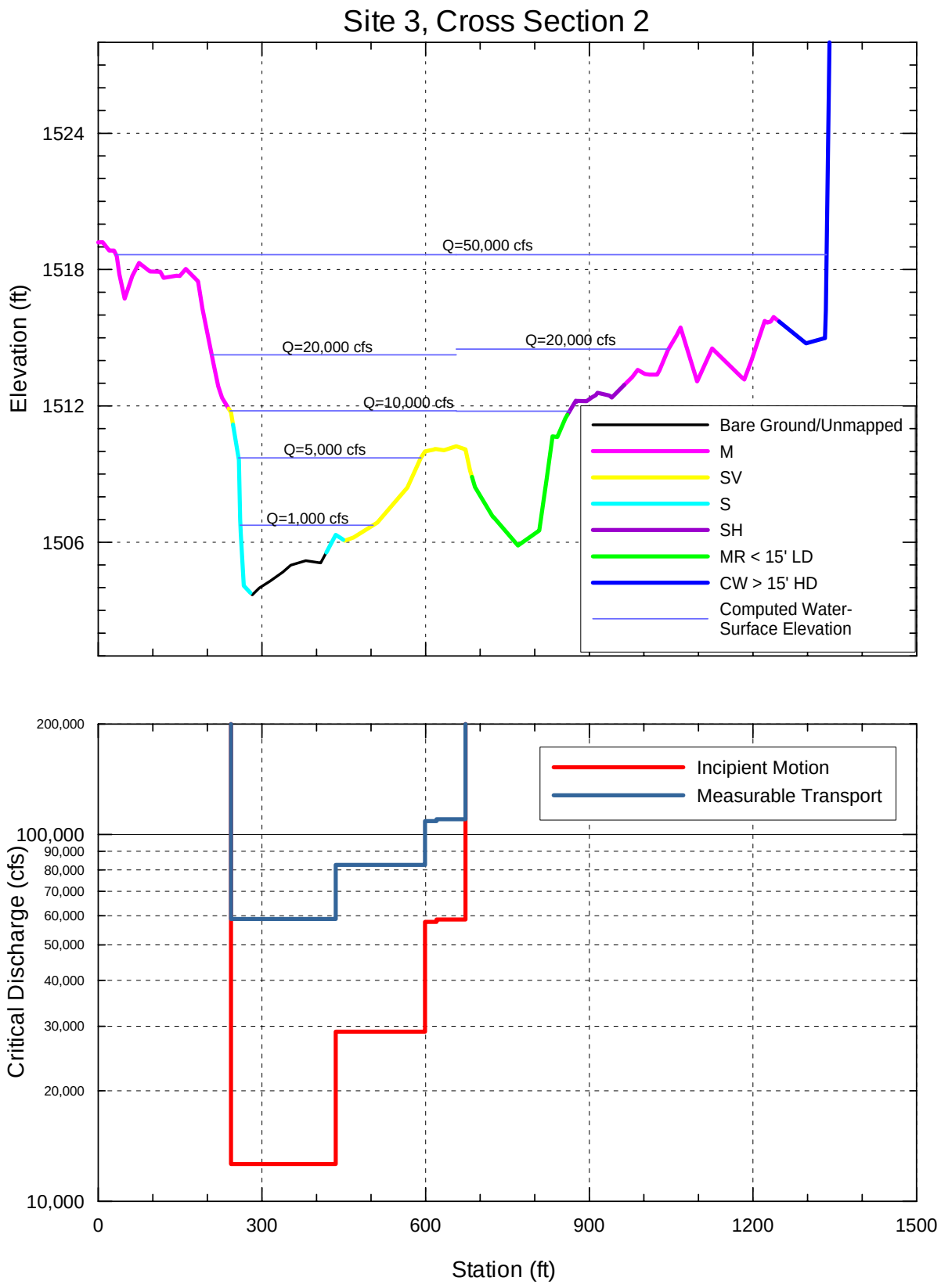
Site 3, Cross Section 2
Elevation (ft)
1524
1518
1512
1506
Q=50,000 cfs
Q=20,000 cfs
Q=20,000 cfs
Q=10,000 cfs
Q=5,000 cfs
Q=1,000 cfs
Bare Ground/Unmapped
M
SV
S
SH
MR < 15' LD
CW > 15' HD
Computed Water-Surface Elevation
Critical Discharge (cfs)
200,000
100,000
90,000
80,000
70,000
60,000
50,000
40,000
30,000
20,000
10,000
Incipient Motion
Measurable Transport
0
300
600
900
1200
1500
Station (ft)

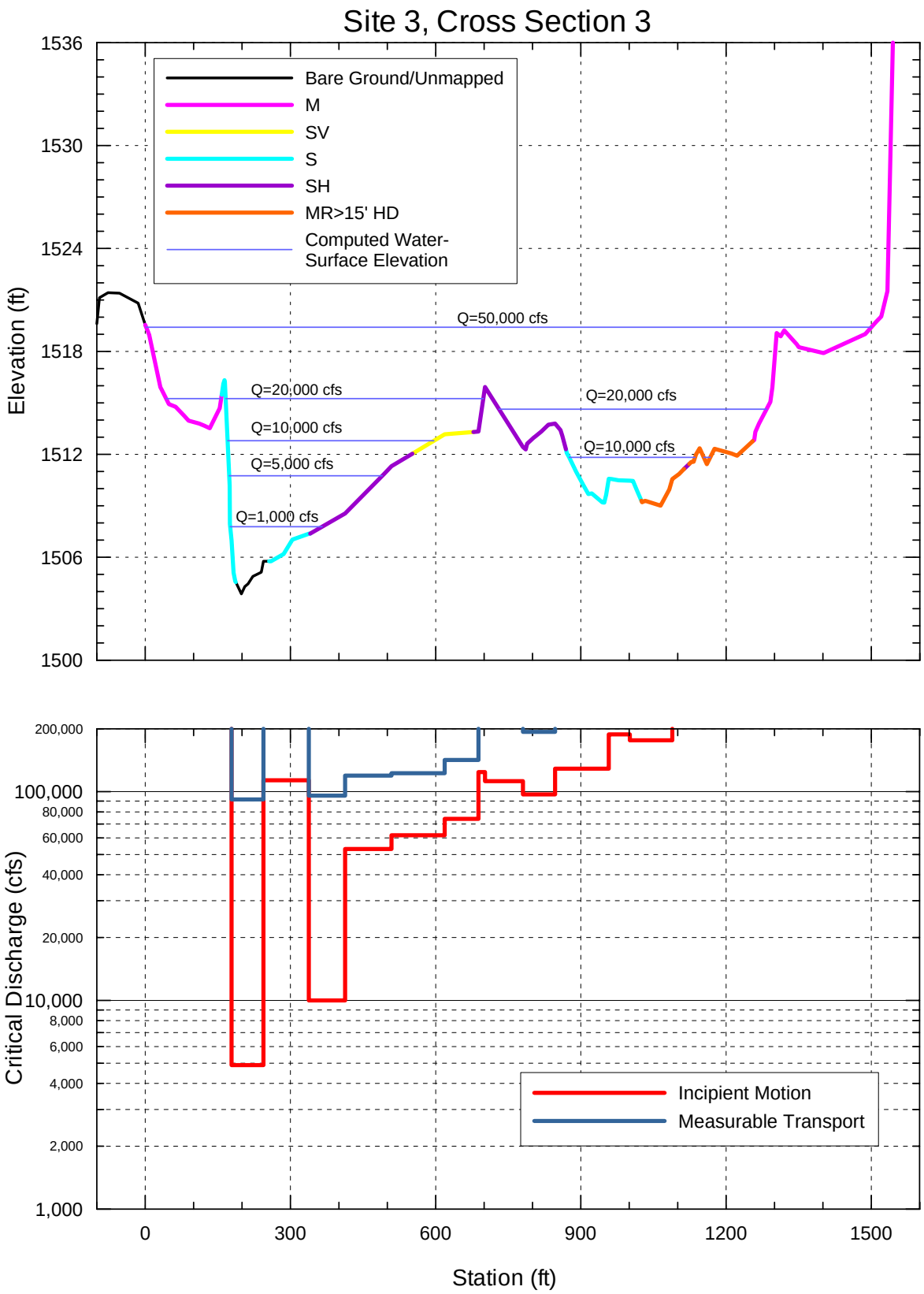
Site 3, Cross Section 3
Bare Ground/Unmapped
M
SV
S
SH
MR>15' HD
Computed Water-Surface Elevation
Q=50,000 cfs
Q=20,000 cfs
Q=10,000 cfs
Q=5,000 cfs
Q=1,000 cfs
Q=20,000 cfs
Q=10,000 cfs
Elevation (ft)
1536
1530
1524
1518
1512
1506
1500
Critical Discharge (cfs)
200,000
100,000
80,000
60,000
40,000
20,000
10,000
8,000
6,000
4,000
2,000
1,000
Incipient Motion
Measurable Transport
0
300
600
900
1200
1500
Station (ft)

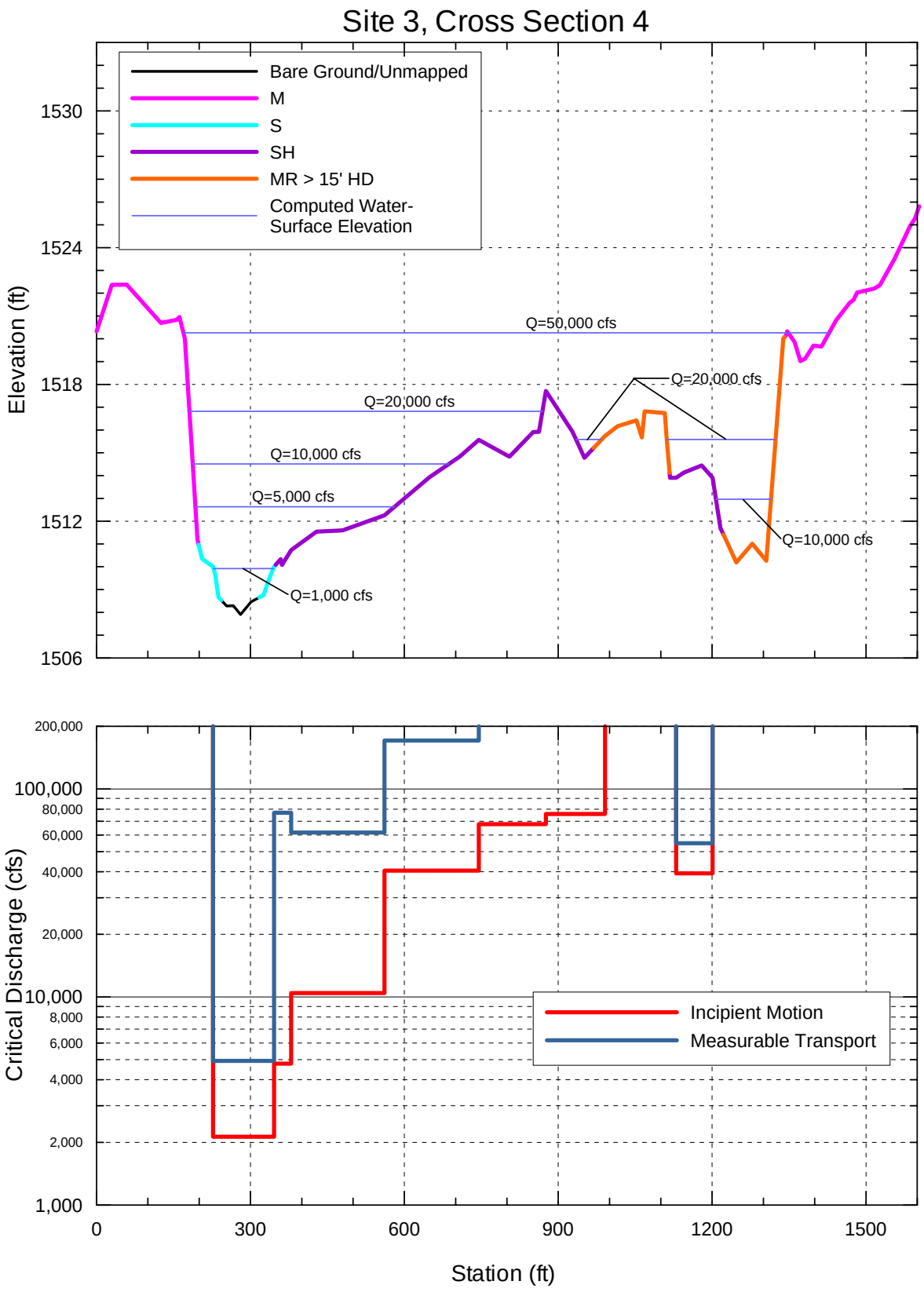
Site 3, Cross Section 4
Bare Ground/Unmapped
M
S
SH
MR > 15' HD
Computed Water-Surface Elevation
Elevation (ft)
1530
1524
1518
1512
1506
Q=50,000 cfs
Q=20,000 cfs
Q=20,000 cfs
Q=10,000 cfs
Q=5,000 cfs
Q=1,000 cfs
Q=10,000 cfs
Critical Discharge (cfs)
200,000
100,000
80,000
60,000
40,000
20,000
10,000
8,000
6,000
4,000
2,000
1,000
Incipient Motion
Measurable Transport
0
300
600
900
1200
1500
Station (ft)

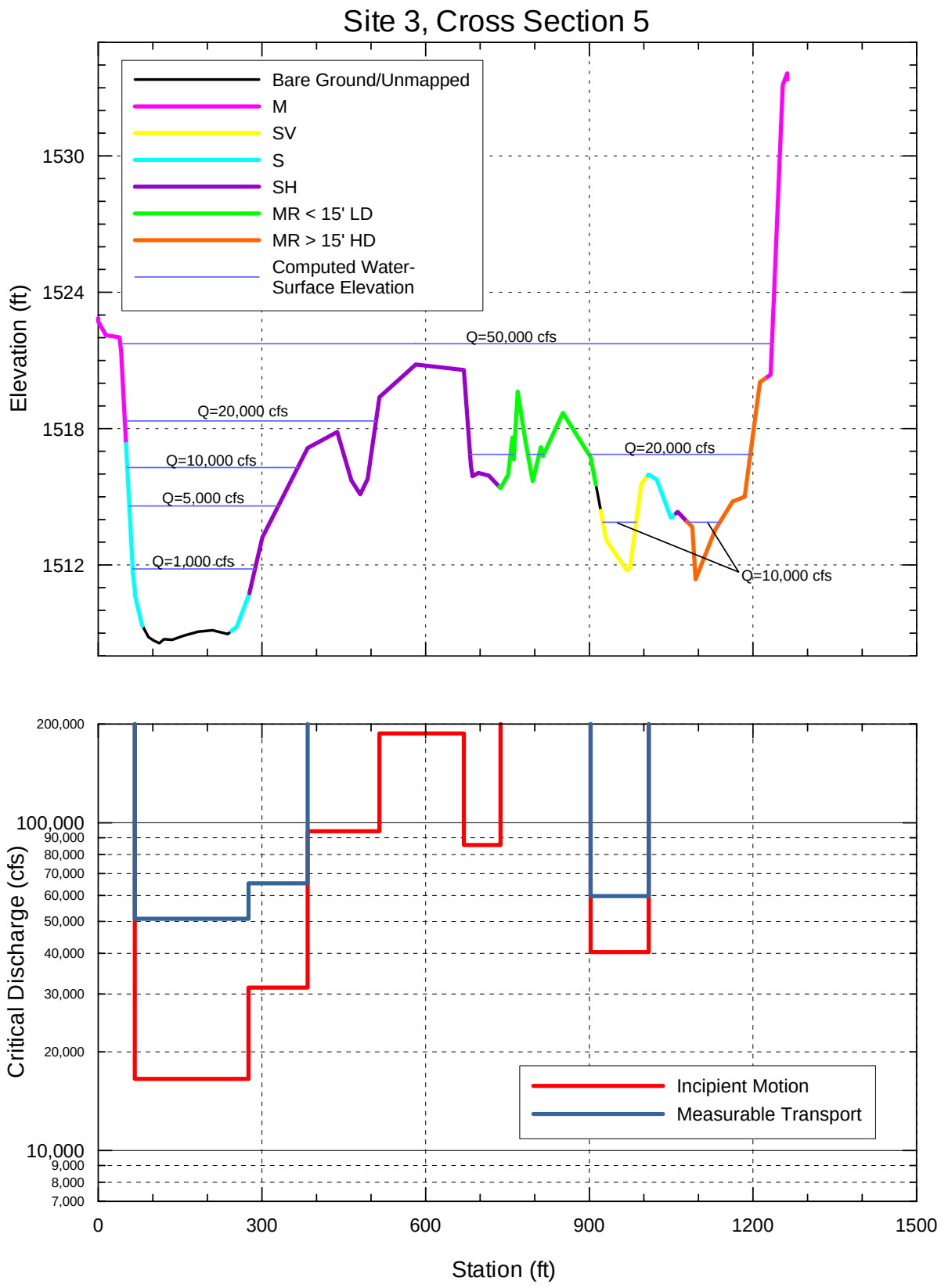
Site 3, Cross Section 5
Bare Ground/Unmapped
M
SV
S
SH
MR < 15' LD
MR > 15' HD
Computed Water-Surface Elevation
Elevation (ft)
1530
1524
1518
1512
Q=50,000 cfs
Q=20,000 cfs
Q=10,000 cfs
Q=5,000 cfs
Q=1,000 cfs
Q=20,000 cfs
Q=10,000 cfs
Critical Discharge (cfs)
200,000
100,000
90,000
80,000
70,000
60,000
50,000
40,000
30,000
20,000
10,000
9,000
8,000
7,000
Incipient Motion
Measurable Transport
0
300
600
900
1200
1500
Station (ft)

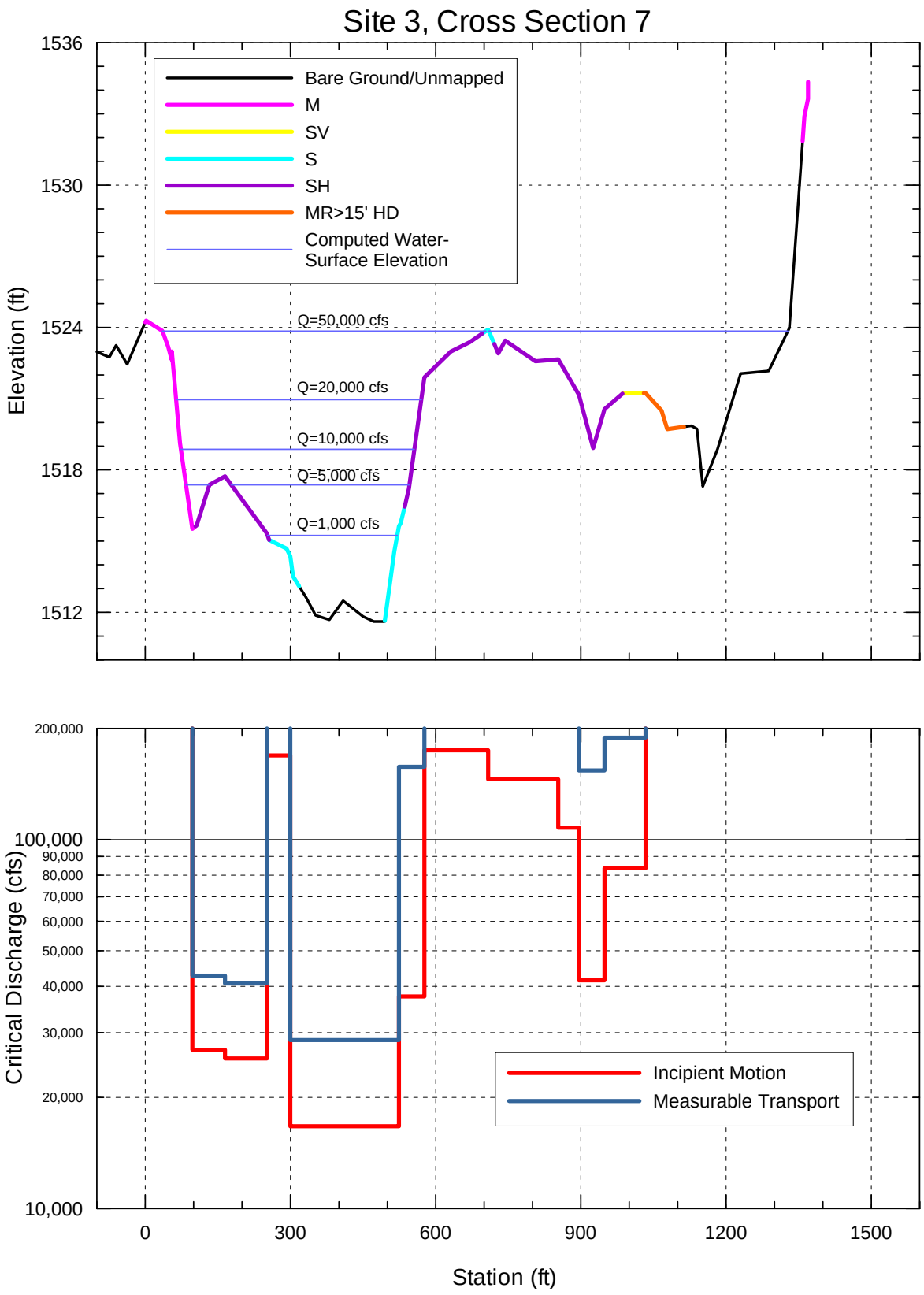
Site 3, Cross Section 7
Elevation (ft)
1536
1530
1524
1518
1512
Bare Ground/Unmapped
M
SV
S
SH
MR>15' HD
Computed Water-Surface Elevation
Q=50,000 cfs
Q=20,000 cfs
Q=10,000 cfs
Q=5,000 cfs
Q=1,000 cfs
Critical Discharge (cfs)
200,000
100,000
90,000
80,000
70,000
60,000
50,000
40,000
30,000
20,000
10,000
Incipient Motion
Measurable Transport
0
300
600
900
1200
1500
Station (ft)

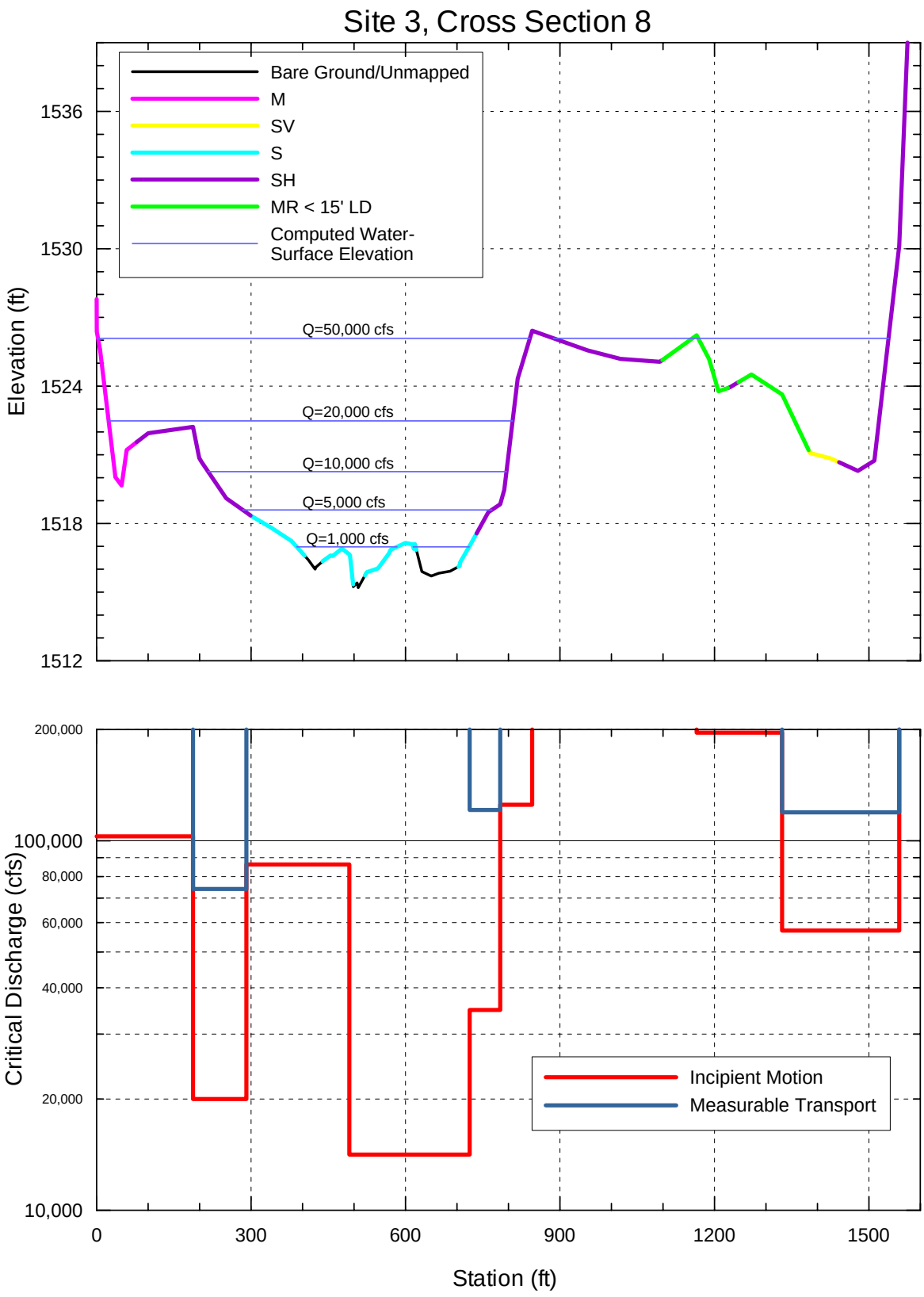
Site 3, Cross Section 8
Bare Ground/Unmapped
M
SV
S
SH
MR < 15' LD
Computed Water-Surface Elevation
Q=50,000 cfs
Q=20,000 cfs
Q=10,000 cfs
Q=5,000 cfs
Q=1,000 cfs
Elevation (ft)
1536
1530
1524
1518
1512
Critical Discharge (cfs)
200,000
100,000
80,000
60,000
40,000
20,000
10,000
Incipient Motion
Measurable Transport
0
300
600
900
1200
1500
Station (ft)

APPENDIX B

Plots of the Hydrographs from the Reservoir Routings Carried Out for the Different Operational Scenarios

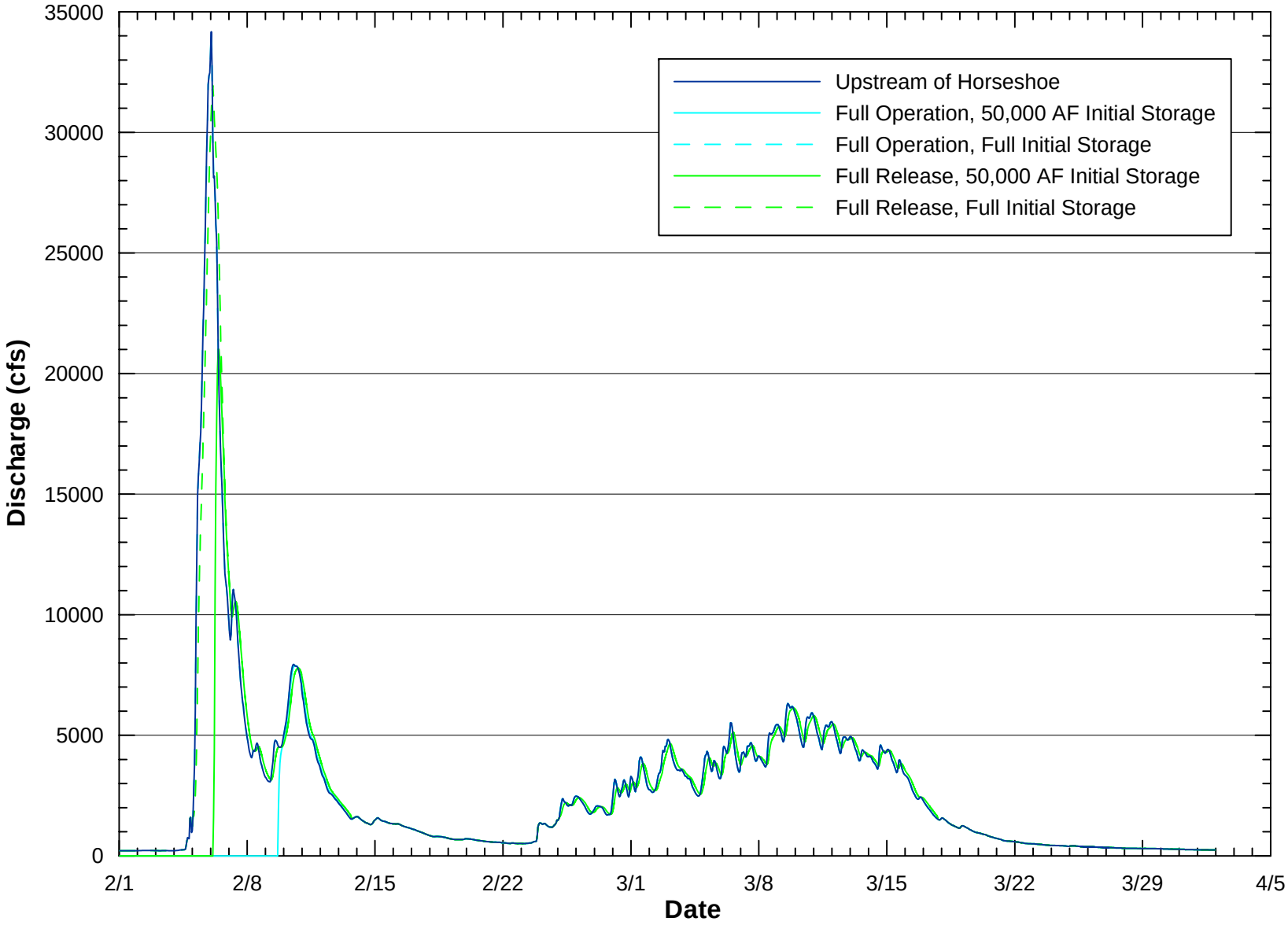

Figure B.1. Simulated hydrographs downstream of Horseshoe Reservoir for the 1991 event.

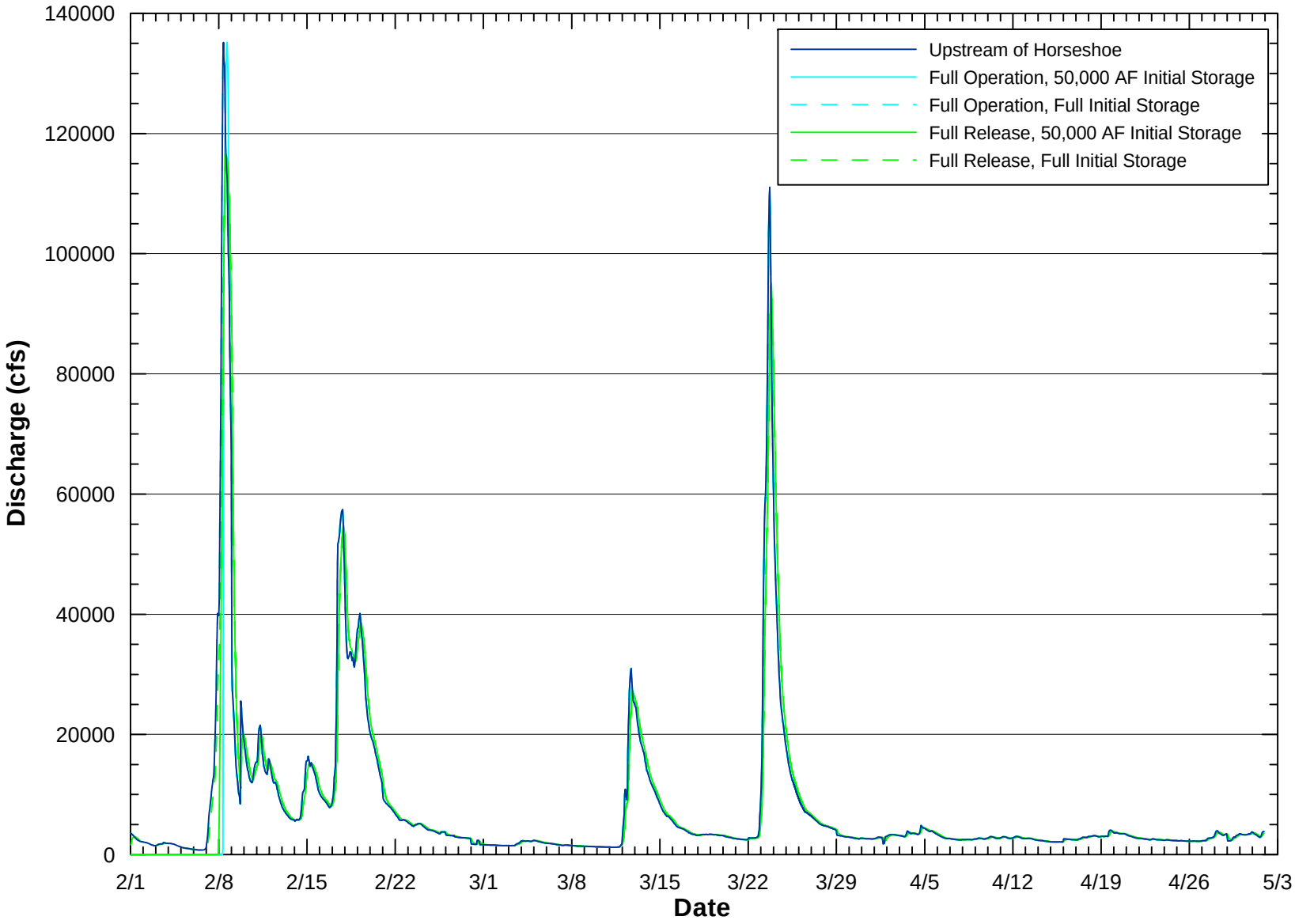

Figure B.2. Simulated hydrographs downstream of Horseshoe Reservoir for the 1993 event.

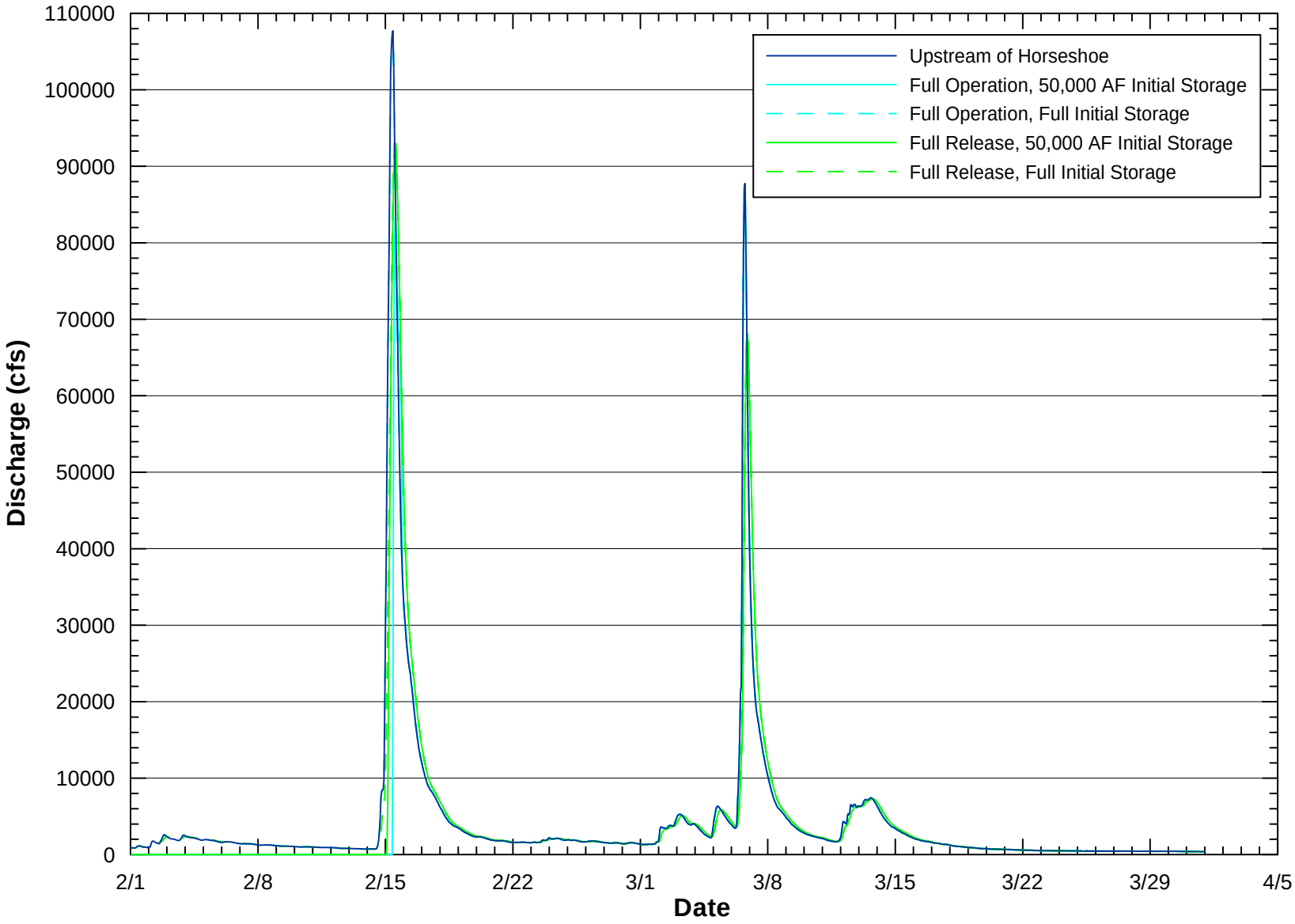

Figure B.3. Simulated hydrographs downstream of Horseshoe Reservoir for the 1995 event.

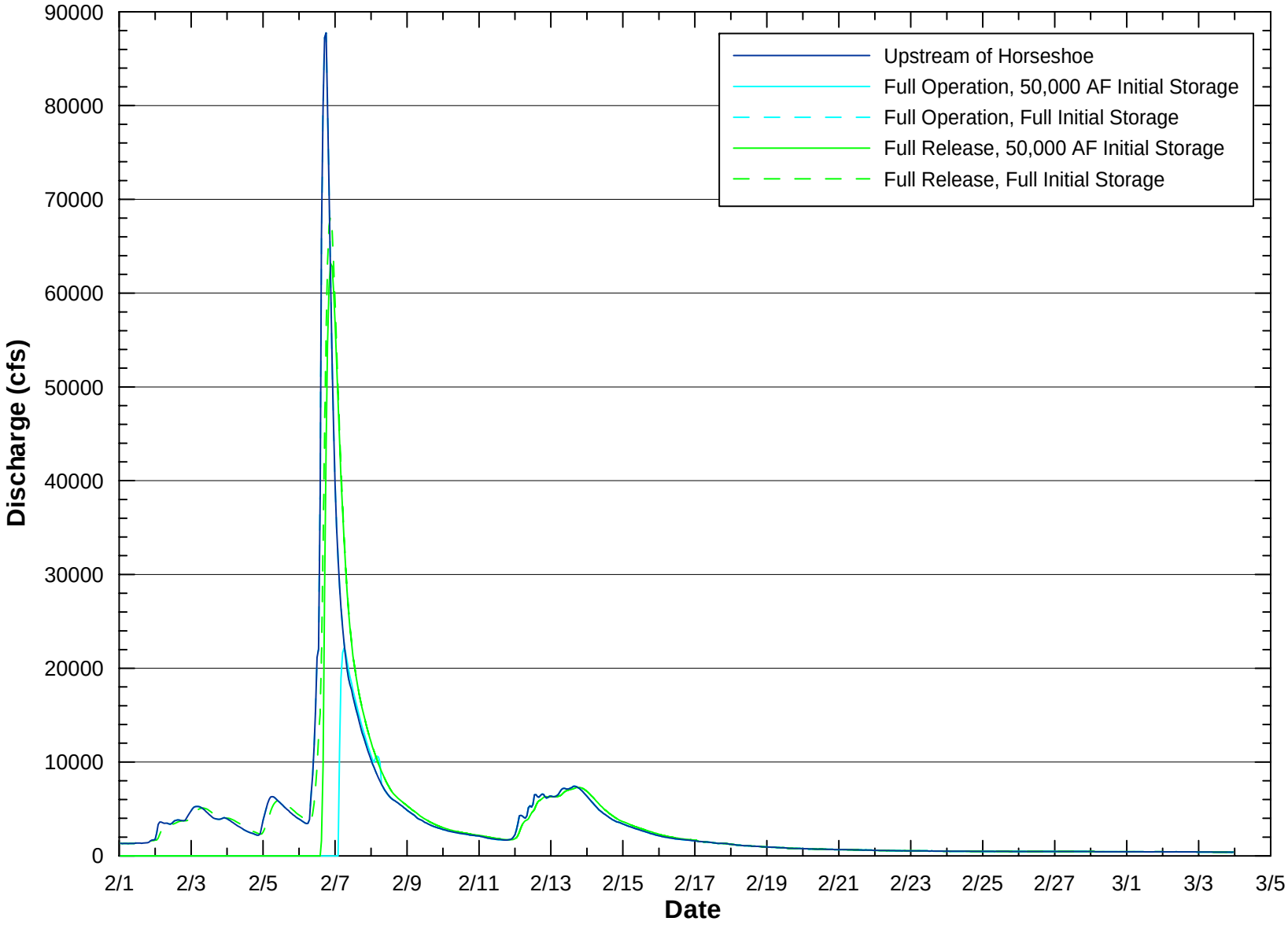

Figure B.4. Simulated hydrographs downstream of Horseshoe Reservoir for the 1995 (March) event.

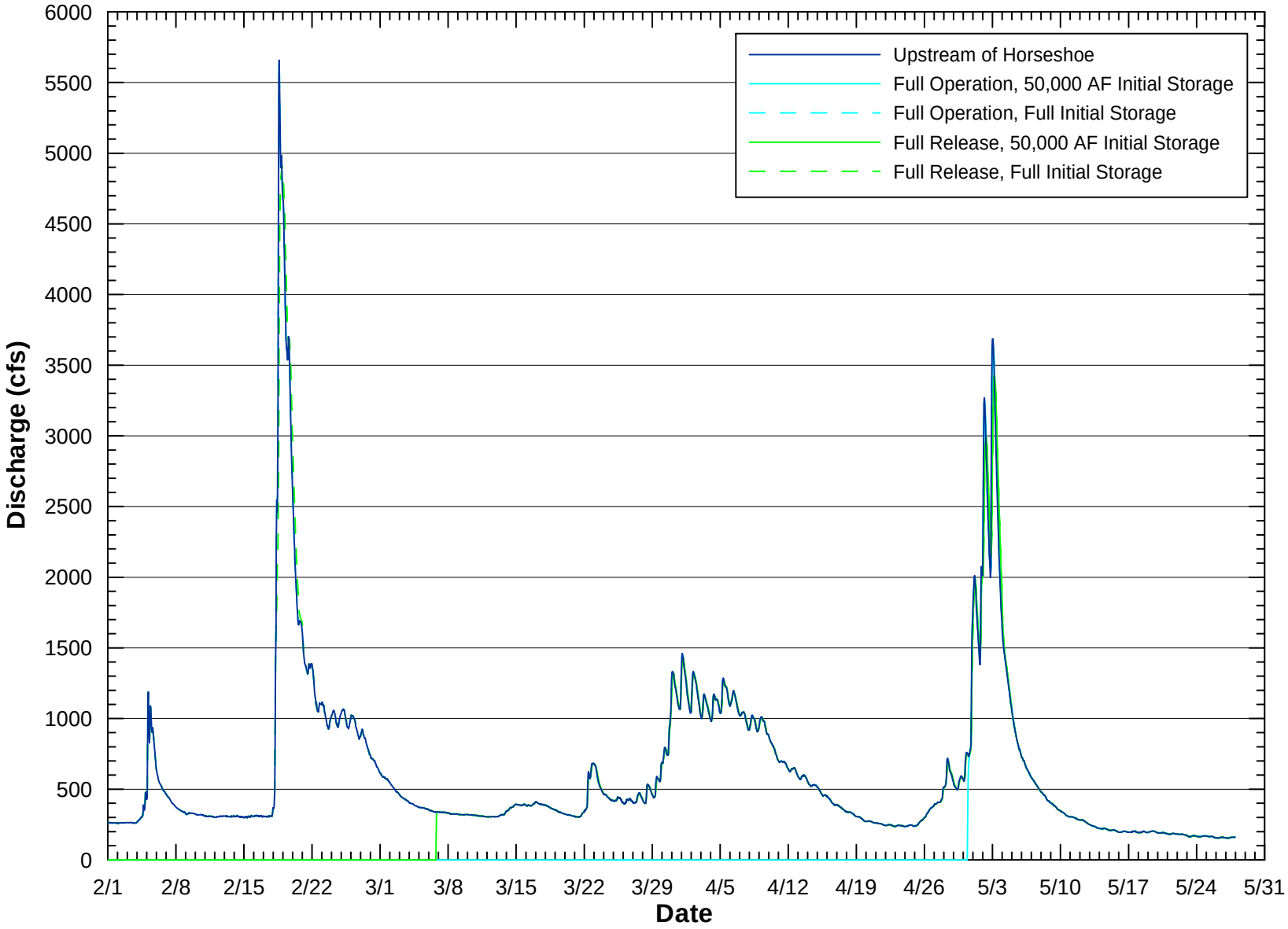

Figure B.5. Simulated hydrographs downstream of Horseshoe Reservoir for the 1997 event.

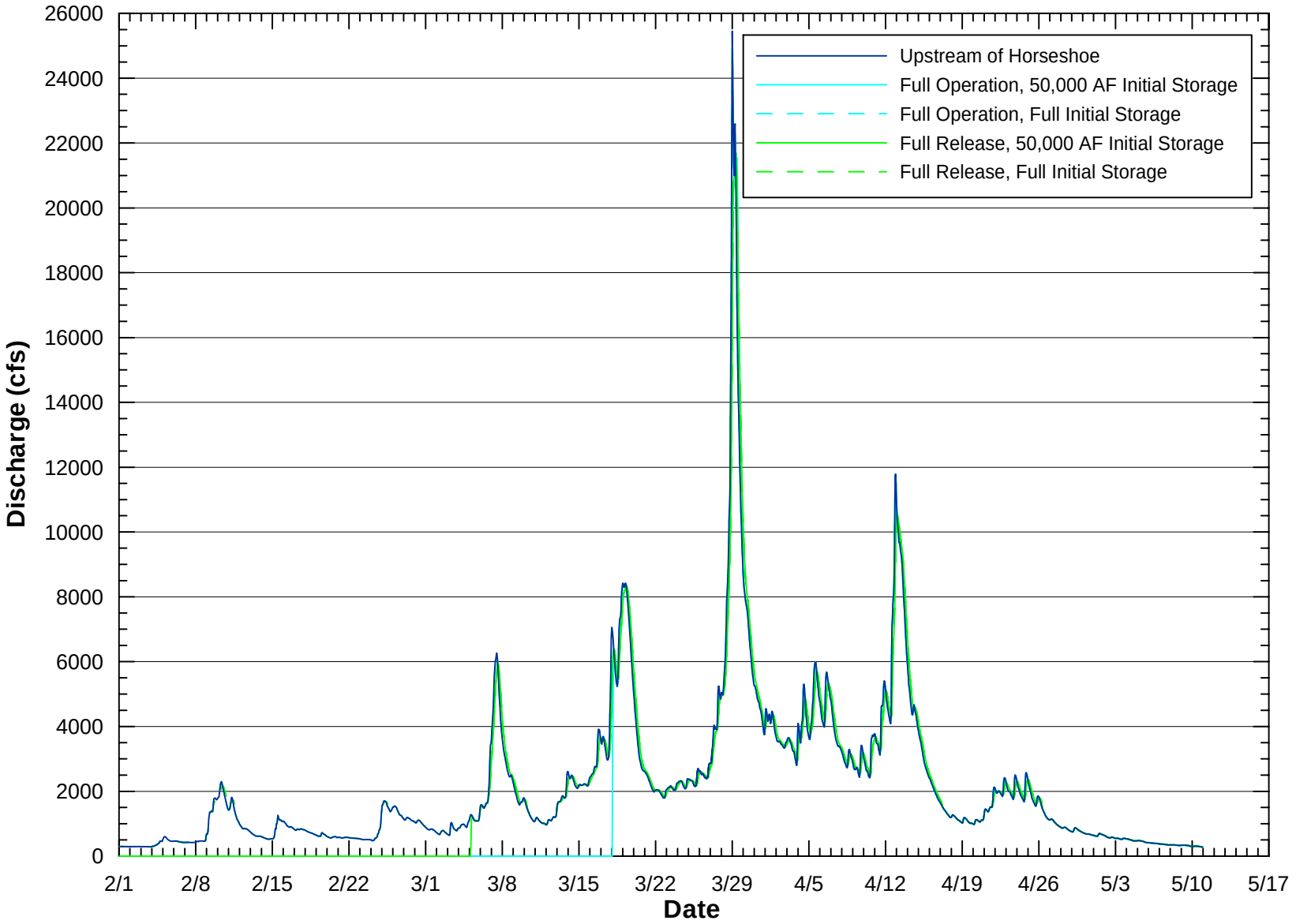

Figure B.6. Simulated hydrographs downstream of Horseshoe Reservoir for the 1998 event.

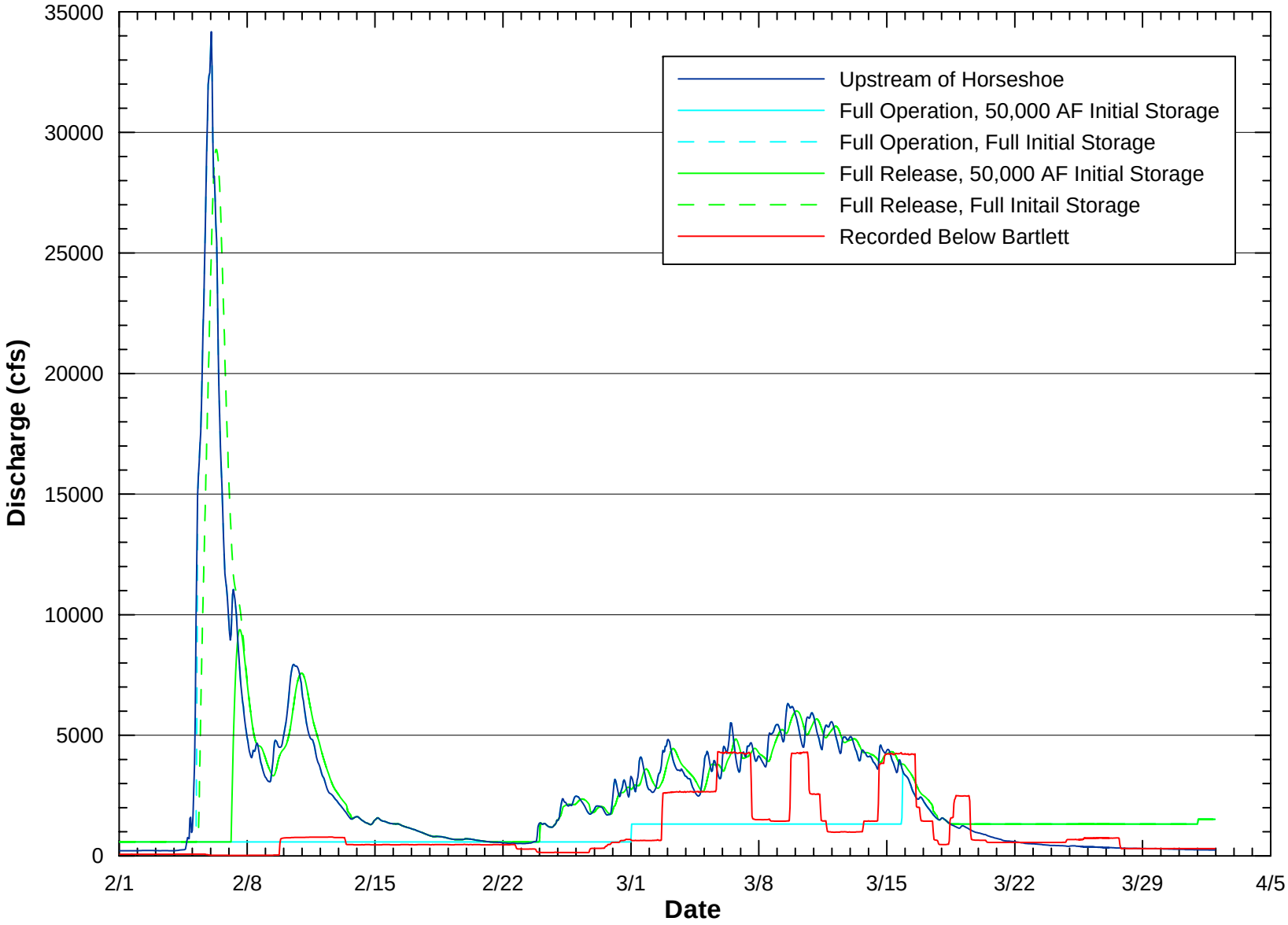

Figure B.7. Simulated hydrographs downstream of Bartlett Reservoir for the 1991 event.

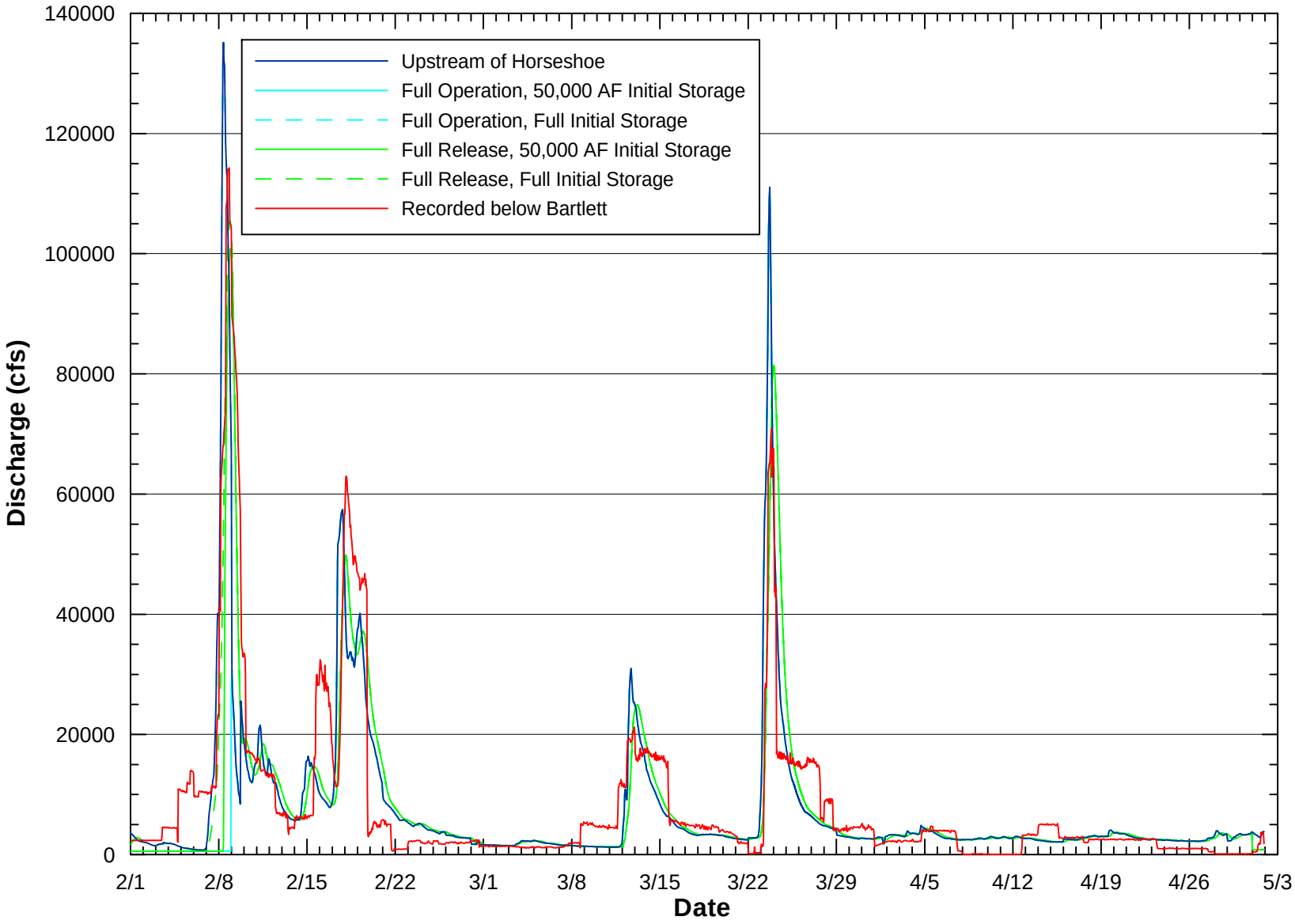

Figure B.8. Simulated hydrographs downstream of Bartlett Reservoir for the 1993 event.

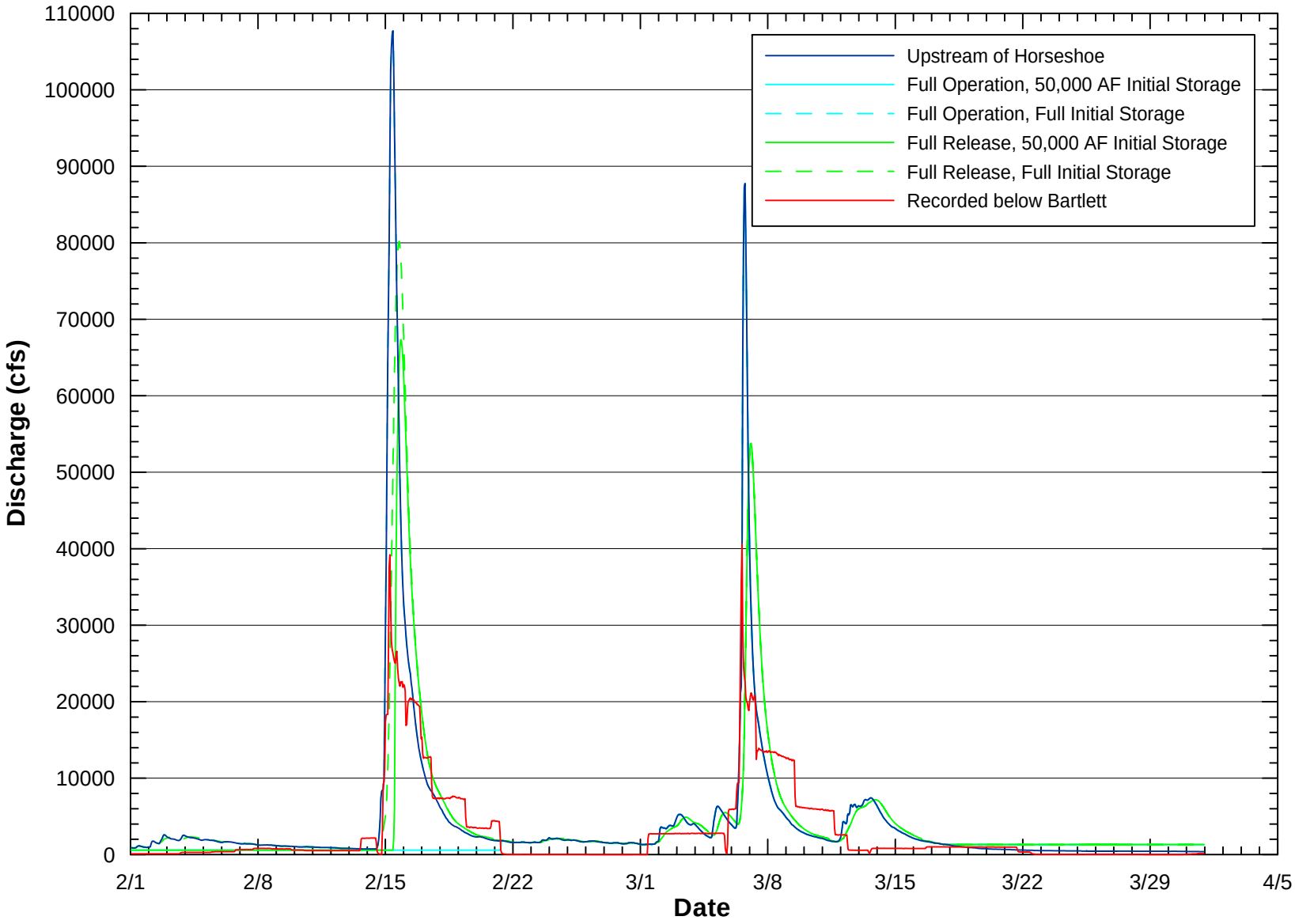

Figure B.9. Simulated hydrographs downstream of Bartlett Reservoir for the 1995 event.

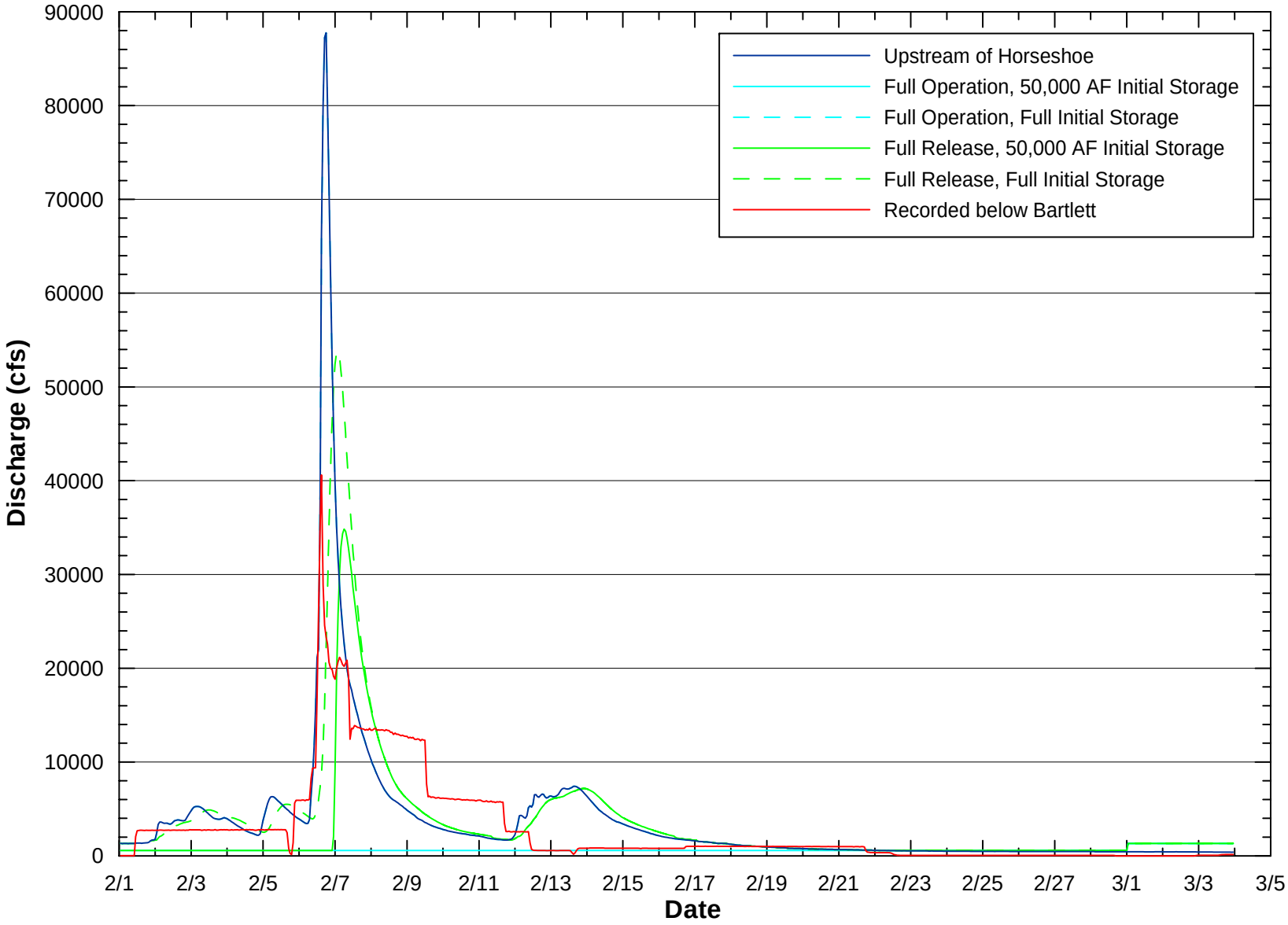

Figure B.10. Simulated hydrographs downstream of Bartlett Reservoir for the 1995 (March) event.

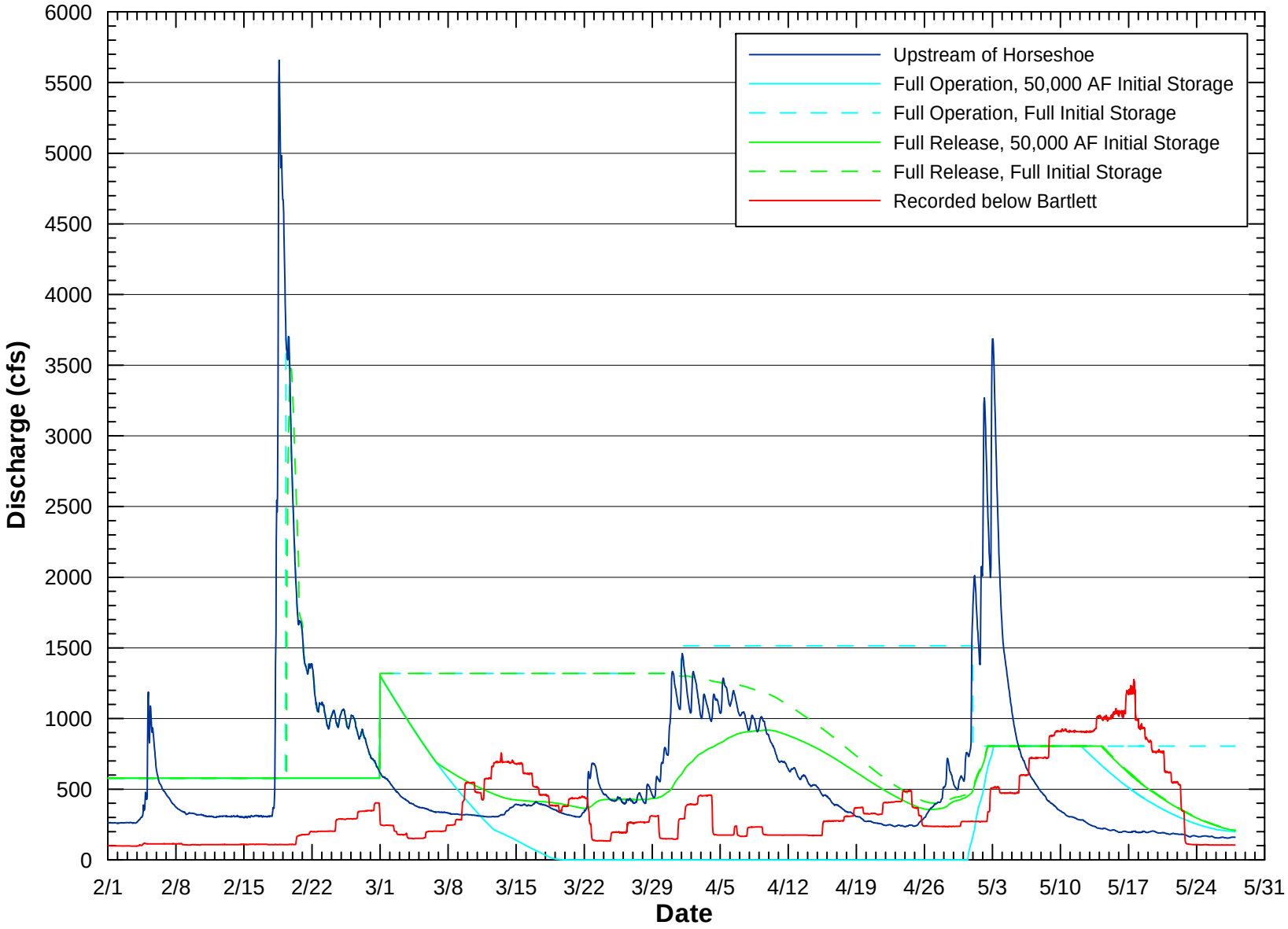

Figure B.11. Simulated hydrographs downstream of Bartlett Reservoir for the 1997 event.

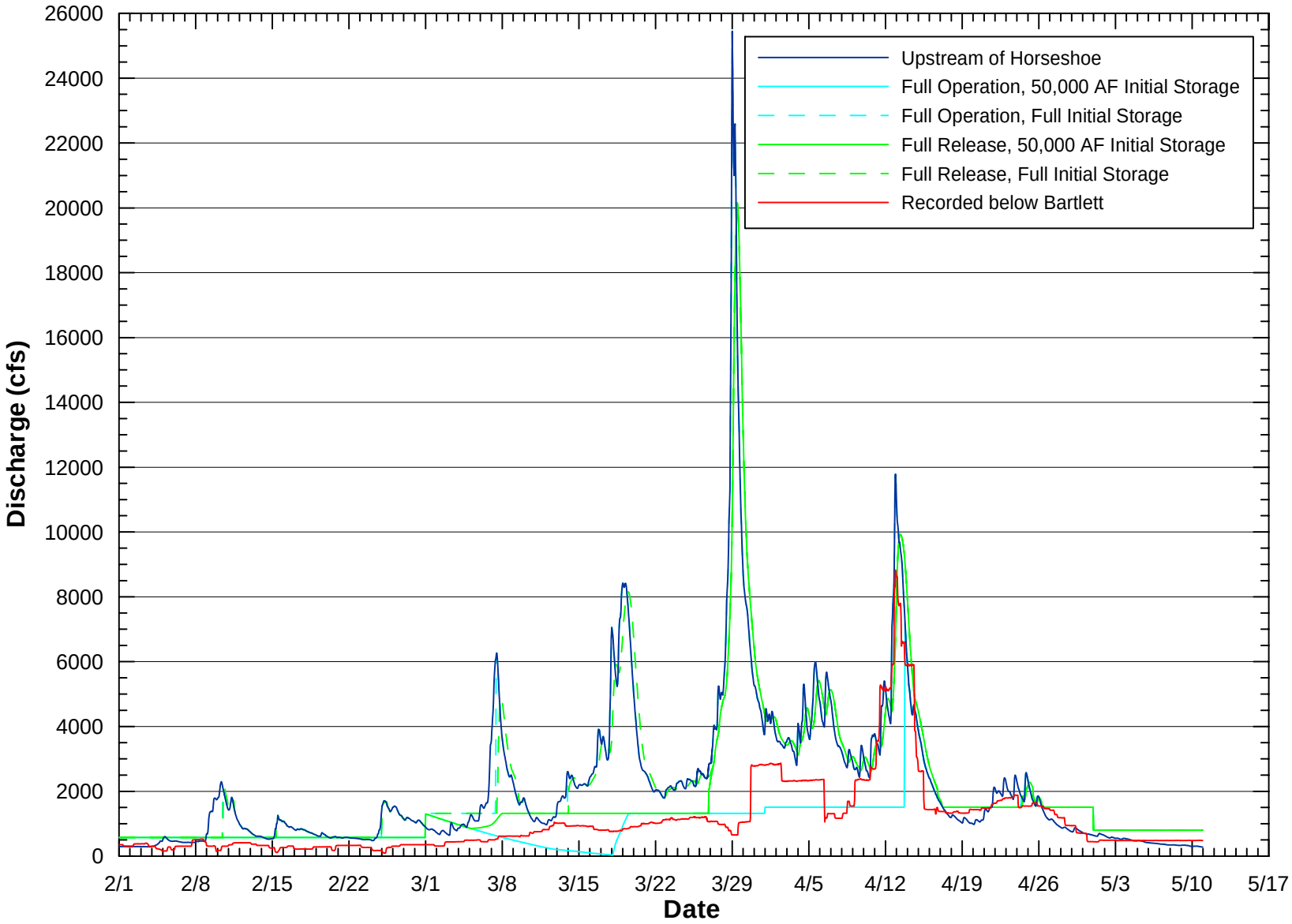

Figure B.12. Simulated hydrographs downstream of Bartlett Reservoir for the 1998 event.

APPENDIX C
Summary of Important Hydraulic Variables Used in the Analysis

Table C.1. Summary of important hydraulic variables for Site 1.							
Cross Section	Discharge (cfs)	Main Flow Path				Secondary Flow Path	
		Water-surface Elevation (ft, NAVD88)	Main-channel Velocity (ft/s)	Hydraulic Depth Channel (ft)	Energy Slope	Water-surface Elevation (ft, NAVD88)	Energy Slope
1	150	2013.50	0.71	3.78	0.000050	n/a	n/a
	240	2014.93	0.81	4.61	0.000050	n/a	n/a
	410	2013.80	1.79	3.98	0.000300	n/a	n/a
	900	2016.48	2.22	5.53	0.000300	n/a	n/a
	1,990	2019.41	2.94	8.44	0.000300	n/a	n/a
	5,960	2021.58	6.25	10.61	0.001001	n/a	n/a
	9,600	2024.22	7.25	13.25	0.001001	n/a	n/a
	16,000	2025.31	10.82	14.34	0.002003	n/a	n/a
	41,200	2032.71	14.27	21.74	0.002002	n/a	n/a
	67,300	2033.01	22.77	22.04	0.005004	n/a	n/a
	98,400	2036.88	25.37	25.91	0.005006	n/a	n/a
	145,000	2041.09	26.02	30.12	0.004305	n/a	n/a
	151,700	2041.44	26.46	30.47	0.004386	n/a	n/a
	200,300	2043.93	28.63	32.96	0.004625	n/a	n/a
2	150	2016.31	5.05	1.41	0.009486	n/a	n/a
	240	2016.90	5.49	1.88	0.007786	n/a	n/a
	410	2017.62	5.24	2.39	0.005249	n/a	n/a
	900	2018.91	4.31	3.30	0.002364	n/a	n/a
	1,990	2020.39	4.42	4.32	0.001779	n/a	n/a
	5,960	2022.81	6.12	6.71	0.001911	n/a	n/a
	9,600	2025.18	6.13	9.07	0.001281	n/a	n/a
	16,000	2027.19	7.56	11.08	0.001493	n/a	n/a
	41,200	2034.79	8.38	18.69	0.000914	n/a	n/a
	67,300	2038.26	10.64	22.15	0.001174	n/a	n/a
	198,400	2043.18	10.77	27.08	0.000920	n/a	n/a
	145,000	2046.18	12.97	30.07	0.001161	n/a	n/a
	51,700	2046.61	13.20	30.51	0.001179	n/a	n/a
	200,300	2049.35	14.76	33.24	0.001315	n/a	n/a
3	150	2017.75	0.70	2.04	0.000106	n/a	n/a
	240	2018.18	0.92	2.41	0.000148	n/a	n/a
	410	2018.77	1.26	2.91	0.000215	n/a	n/a
	900	2019.91	1.97	3.86	0.000364	n/a	n/a
	1,990	2021.53	3.04	5.29	0.000569	n/a	n/a
	5,960	2024.76	5.42	8.24	0.001001	n/a	n/a
	9,600	2027.08	6.01	10.57	0.000886	n/a	n/a
	16,000	2029.35	6.85	12.83	0.000887	n/a	n/a
	41,200	2035.66	8.58	19.15	0.000817	n/a	n/a
	67,300	2039.34	10.56	22.83	0.000978	n/a	n/a
	98,400	2043.74	11.48	27.22	0.000914	n/a	n/a
	145,000	2046.81	13.95	30.30	0.001172	n/a	n/a
	151,700	2047.24	14.23	30.73	0.001196	n/a	n/a
	200,300	2049.98	16.09	33.46	0.001364	n/a	n/a

Table C.1. Summary of important hydraulic variables for Site 1.							
Cross Section	Discharge (cfs)	Main Flow Path				Secondary Flow Path	
		Water-surface Elevation (ft, NAVD88)	Main-Channel Velocity (ft/s)	Hydraulic Depth Channel (ft)	Energy Slope	Water-surface Elevation (ft, NAVD88)	Energy Slope
4	150	2020.47	1.34	1.55	0.000561	n/a	n/a
	240	2020.74	1.82	1.80	0.000853	n/a	n/a
	410	2021.16	2.52	2.17	0.001277	n/a	n/a
	900	2022.06	3.88	2.96	0.002004	n/a	n/a
	1,990	2023.50	5.62	4.29	0.002559	n/a	n/a
	5,960	2026.19	9.08	6.98	0.003488	n/a	n/a
	9,600	2028.64	8.36	9.43	0.001983	n/a	n/a
	16,000	2031.25	8.06	12.04	0.001330	n/a	n/a
	41,200	2036.63	10.23	17.42	0.001309	n/a	n/a
	67,300	2040.41	11.96	21.20	0.001377	n/a	n/a
	98,400	2044.58	13.02	25.37	0.001285	n/a	n/a
	145,000	2047.85	15.61	28.64	0.001571	n/a	n/a
	151,700	2048.29	15.92	29.09	0.001600	n/a	n/a
	200,300	2051.21	17.87	32.01	0.001776	n/a	n/a
5	150	2020.66	4.18	1.39	0.006917	n/a	n/a
	240	2021.07	5.05	1.56	0.008669	n/a	n/a
	410	2021.81	5.30	1.38	0.010892	n/a	n/a
	900	2023.20	5.27	2.12	0.006008	n/a	n/a
	1,990	2025.17	5.22	3.24	0.003311	n/a	n/a
	5,960	2028.90	4.59	6.97	0.000918	2029.23	0.015978
	9,600	2030.64	5.30	8.71	0.000912	2030.93	0.004058
	16,000	2032.28	8.45	10.35	0.001841	2033.09	0.000868
	41,200	2037.71	10.45	15.77	0.001603	2038.31	0.001236
	67,300	2041.93	11.95	19.99	0.001529	2041.93	0.001529
	98,400	2045.83	13.58	23.89	0.001557	2045.83	0.001557
	145,000	2049.25	16.57	27.31	0.001940	2049.25	0.001940
	151,700	2049.69	16.95	27.76	0.001986	2049.69	0.001986
	200,300	2052.56	19.54	30.63	0.002314	2052.56	0.002314
6	150	2024.09	1.16	3.47	0.000160	n/a	n/a
	240	2024.43	1.69	3.77	0.000308	n/a	n/a
	410	2024.98	2.52	4.25	0.000589	n/a	n/a
	900	2026.08	4.29	5.35	0.001258	n/a	n/a
	1,990	2027.55	6.77	6.81	0.002266	n/a	n/a
	5,960	2029.72	8.85	8.99	0.002677	2032.88	0.001860
	9,600	2031.30	10.36	10.56	0.002958	2033.99	0.002190
	16,000	2033.37	15.47	12.63	0.005201	2034.68	0.001940
	41,200	2038.23	19.65	17.49	0.005433	2039.64	0.001570
	67,300	2043.14	14.89	22.41	0.002243	2043.14	0.002243
	98,400	2047.48	14.55	26.74	0.001691	2047.48	0.001691
	145,000	2051.83	15.23	31.10	0.001515	2051.83	0.001515
	151,700	2052.40	15.30	31.67	0.001493	2052.40	0.001493
	200,300	2056.16	15.90	35.42	0.001390	2056.16	0.001390

Table C.2. Summary of important hydraulic variables for Site 2.							
Cross Section	Discharge (cfs)	Main Flow Path				Secondary Flow Path	
		Water-surface Elevation (ft, NAVD88)	Main-channel Velocity (ft/s)	Hydraulic Depth Channel (ft)	Energy Slope	Water-surface Elevation (ft, NAVD88)	Energy Slope
1	117	1837.31	3.28	1.42	0.004001	n/a	n/a
	262	1838.30	3.84	1.78	0.004007	n/a	n/a
	548	1839.39	4.84	2.54	0.004002	n/a	n/a
	1,004	1840.60	5.87	3.41	0.004007	n/a	n/a
	1,425	1841.93	5.81	4.31	0.002882	1842.39	0.000005
	1,790	1842.62	6.10	4.76	0.002794	1842.87	0.000031
	4,100	1843.39	7.82	5.29	0.004003	1843.92	0.004005
	6,300	1845.48	9.14	6.75	0.004001	1844.49	0.004001
	21,400	1850.25	12.37	10.74	0.004002	1848.54	0.004001
	55,200	1853.73	14.91	14.23	0.004000	1852.80	0.004001
	92,900	1857.17	17.23	17.67	0.004001	1857.17	0.004001
	101,100	1857.83	17.66	18.32	0.004007	1857.83	0.004007
	123,200	1859.31	18.59	19.81	0.004002	1859.31	0.004002
	200,300	1863.65	21.22	24.15	0.004003	1863.65	0.004003
2	117	1844.24	2.13	0.98	0.002692	n/a	n/a
	262	1844.89	2.79	1.43	0.002758	n/a	n/a
	548	1845.73	3.44	1.81	0.002794	n/a	n/a
	1,004	1846.56	4.20	2.25	0.003295	n/a	n/a
	1,425	1847.10	4.68	2.57	0.003647	1846.28	0.001227
	1,790	1847.45	5.03	2.79	0.003932	1846.68	0.002168
	4,100	1846.37	8.58	2.28	0.012392	1849.21	0.004893
	6,300	1847.73	8.53	3.02	0.008454	1849.66	0.004803
	21,400	1852.70	6.88	6.56	0.002403	1852.85	0.006889
	55,200	1855.88	12.67	9.67	0.005387	1855.62	0.018876
	92,900	1859.23	13.64	13.02	0.004400	1859.23	0.004400
	101,100	1859.90	13.74	13.69	0.004197	1859.90	0.004197
	123,200	1861.47	13.90	15.26	0.003754	1861.47	0.003754
	200,300	1866.15	14.60	19.94	0.002960	1866.15	0.002960
3	117	1844.50	1.06	2.20	0.000324	n/a	n/a
	262	1845.28	1.74	2.84	0.000677	n/a	n/a
	548	1846.26	2.69	3.65	0.001249	n/a	n/a
	1,004	1847.25	3.86	4.64	0.001874	n/a	n/a
	1,425	1847.88	4.70	5.27	0.002343	1848.90	0.000000
	1,790	1848.30	5.29	5.69	0.002687	1849.14	0.000002
	4,100	1848.68	7.35	6.07	0.004749	1851.26	0.000291
	6,300	1849.93	9.69	7.33	0.006423	1851.73	0.000398
	21,400	1853.53	13.49	10.92	0.007319	1854.02	0.003389
	55,200	1860.07	10.22	17.46	0.002244	1859.67	0.016526
	92,900	1862.75	12.61	20.14	0.002824	1862.75	0.002824
	101,100	1863.27	12.86	20.66	0.002841	1863.27	0.002841
	123,200	1864.23	13.95	21.62	0.003147	1864.23	0.003147
	200,300	1868.12	15.20	25.51	0.002995	1868.12	0.002995

Table C.2. Summary of important hydraulic variables for Site 2.							
Cross Section	Discharge (cfs)	Main Flow Path				Secondary Flow Path	
		Water-surface Elevation (ft, NAVD88)	Main-Channel Velocity (ft/s)	Hydraulic Depth Channel (ft)	Energy Slope	Water-surface Elevation (ft, NAVD88)	Energy Slope
4	117	1852.09	1.94	0.93	0.002982	n/a	n/a
	262	1852.59	2.67	1.12	0.006164	n/a	n/a
	548	1853.34	1.90	1.69	0.002412	n/a	n/a
	1,004	1853.39	3.38	1.74	0.007314	n/a	n/a
	1,425	1853.99	0.76	2.32	0.001233	1850.53	0.000171
	1,790	1854.30	0.83	2.62	0.001196	1851.00	0.000422
	4,100	1853.83	3.24	2.16	0.005060	1853.94	0.001152
	6,300	1854.11	4.69	2.43	0.009125	1854.42	0.001211
	21,400	1856.91	5.95	5.33	0.004577	n/a	n/a
	55,200	1861.68	7.70	10.05	0.003321	1861.95	0.002482
	92,900	1864.49	9.29	12.86	0.003487	1864.49	0.003487
	101,100	1864.94	9.64	13.32	0.003580	1864.94	0.003580
	123,200	1866.03	10.46	14.40	0.003799	1866.03	0.003799
	200,300	1869.62	12.30	17.99	0.003903	1869.62	0.003903
5	117	1852.23	0.23	2.30	0.000009	n/a	n/a
	262	1852.81	0.40	2.80	0.000022	n/a	n/a
	548	1853.48	0.63	3.41	0.000043	n/a	n/a
	1,004	1853.76	1.05	3.68	0.000105	n/a	n/a
	1,425	1854.09	1.32	3.99	0.000142	n/a	n/a
	1,790	1854.41	1.50	4.29	0.000167	n/a	n/a
	4,100	1854.63	3.22	4.51	0.000760	n/a	n/a
	6,300	1855.28	4.12	5.16	0.001052	n/a	n/a
	21,400	1858.14	6.78	6.93	0.001951	n/a	n/a
	55,200	1862.64	9.05	11.43	0.001860	1862.68	0.000703
	92,900	1865.56	10.70	14.35	0.001940	1865.56	0.001940
	101,100	1866.03	11.11	14.83	0.002005	1866.03	0.002005
	123,200	1867.17	12.17	15.97	0.002187	1867.17	0.002187
	200,300	1870.69	14.97	19.49	0.002552	1870.69	0.002552
6	117	1852.23	0.20	2.58	0.000007	n/a	n/a
	262	1852.81	0.37	3.03	0.000018	n/a	n/a
	548	1853.49	0.61	2.29	0.000120	n/a	n/a
	1,004	1853.78	0.99	2.58	0.000273	n/a	n/a
	1,425	1854.14	1.23	2.93	0.000358	n/a	n/a
	1,790	1854.46	1.39	3.26	0.000396	n/a	n/a
	4,100	1854.86	2.83	3.65	0.001410	n/a	n/a
	6,300	1855.63	3.56	4.43	0.001728	n/a	n/a
	21,400	1859.01	6.63	7.81	0.002812	n/a	n/a
	55,200	1863.56	9.17	12.36	0.002921	1863.79	0.003341
	92,900	1866.64	10.72	15.44	0.002963	1866.64	0.002963
	101,100	1867.19	11.00	15.99	0.002982	1867.19	0.002982
	123,200	1868.50	11.81	17.30	0.003093	1868.50	0.003093
	200,300	1872.45	13.90	21.25	0.003253	1872.45	0.003253

Table C.2. Summary of important hydraulic variables for Site 2.							
Cross Section	Discharge (cfs)	Main Flow Path				Secondary Flow Path	
		Water-surface Elevation (ft, NAVD88)	Main-Channel Velocity (ft/s)	Hydraulic Depth Channel (ft)	Energy Slope	Water-surface Elevation (ft, NAVD88)	Energy Slope
7	117	1852.23	0.09	5.98	0.000000	n/a	n/a
	262	1852.82	0.19	6.43	0.000002	n/a	n/a
	548	1853.50	0.36	7.06	0.000005	n/a	n/a
	1,004	1853.81	0.63	7.38	0.000015	n/a	n/a
	1,425	1854.18	0.85	7.74	0.000026	n/a	n/a
	1,790	1854.51	1.02	8.07	0.000035	n/a	n/a
	4,100	1855.04	2.19	8.61	0.000152	n/a	n/a
	6,300	1855.90	3.05	9.46	0.000260	n/a	n/a
	21,400	1859.50	7.36	13.07	0.000986	n/a	n/a
	55,200	1863.34	13.66	16.91	0.002410	1864.76	0.003819
	92,900	1866.31	17.36	19.87	0.003140	1866.31	0.003140
	101,100	1866.90	17.73	20.46	0.003152	1866.90	0.003152
	123,200	1868.22	18.81	21.79	0.003262	1868.22	0.003262
	200,300	1871.31	23.09	24.88	0.004119	1871.31	0.004119

Table C.3. Summary of important hydraulic variables for Site 3.							
Cross Section	Discharge (cfs)	Main Flow Path				Secondary Flow Path	
		Water-surface Elevation (ft, NAVD88)	Main-channel Velocity (ft/s)	Hydraulic Depth Channel (ft)	Energy Slope	Water-surface Elevation (ft, NAVD88)	Energy Slope
1	300	1504.84	4.12	0.52	0.022432	n/a	n/a
	500	1505.06	4.71	0.67	0.020959	n/a	n/a
	1,000	1506.00	3.68	1.57	0.004107	n/a	n/a
	2,000	1507.19	3.83	2.76	0.002101	n/a	n/a
	5,000	1509.38	4.54	4.95	0.001353	n/a	n/a
	10,000	1511.48	5.54	7.05	0.001260	1511.77	0.000004
	20,000	1513.96	6.90	9.53	0.001309	1514.49	0.000057
	50,000	1518.58	7.13	14.15	0.000824	1518.58	0.000824
	100,000	1521.88	8.92	17.45	0.000975	1521.88	0.000975
	150,000	1524.10	10.18	19.68	0.001083	1524.10	0.001083
	200,300	1525.83	11.15	21.40	0.001163	1525.83	0.001163
2	300	1505.86	1.59	1.16	0.001156	n/a	n/a
	500	1506.23	1.99	1.46	0.001330	n/a	n/a
	1,000	1506.75	2.85	1.95	0.001858	n/a	n/a
	2,000	1507.69	3.57	2.87	0.001747	n/a	n/a
	5,000	1509.71	4.55	4.84	0.001421	n/a	n/a
	10,000	1511.79	5.45	6.51	0.001377	1511.77	0.000027
	20,000	1514.25	6.82	8.96	0.001403	1514.50	0.000169
	50,000	1518.66	7.86	13.38	0.001095	1518.66	0.001095
	100,000	1521.94	9.81	16.65	0.001272	1521.94	0.001272
	150,000	1524.15	11.17	18.87	0.001398	1524.15	0.001398
	200,300	1525.88	12.13	20.60	0.001465	1525.88	0.001465
3	300	1506.48	2.46	1.79	0.001559	n/a	n/a
	500	1507.00	3.01	2.27	0.001706	n/a	n/a
	1,000	1507.78	4.16	3.05	0.002191	n/a	n/a
	2,000	1508.80	5.35	4.07	0.002474	n/a	n/a
	5,000	1510.75	7.10	6.02	0.002581	n/a	n/a
	10,000	1512.79	8.25	8.06	0.002364	1511.82	0.000226
	20,000	1515.25	9.19	10.52	0.002056	1514.63	0.000330
	50,000	1519.41	9.01	14.68	0.001268	1519.41	0.001268
	100,000	1522.79	10.65	18.06	0.001344	1522.79	0.001344
	150,000	1525.09	11.89	20.36	0.001427	1525.09	0.001427
	200,300	1526.86	12.76	22.13	0.001469	1526.86	0.001469

Table C.3. Summary of important hydraulic variables for Site 3.							
Cross Section	Discharge (cfs)	Main Flow Path				Secondary Flow Path	
		Water-surface Elevation (ft, NAVD88)	Main-Channel Velocity (ft/s)	Hydraulic Depth Channel (ft)	Energy Slope	Water-surface Elevation (ft, NAVD88)	Energy Slope
4	300	1509.07	4.68	0.67	0.020597	n/a	n/a
	500	1509.35	5.46	0.90	0.018909	n/a	n/a
	1,000	1509.92	6.54	1.32	0.016482	n/a	n/a
	2,000	1510.75	7.76	2.12	0.012311	n/a	n/a
	5,000	1512.63	8.55	4.00	0.006409	n/a	n/a
	10,000	1514.51	9.06	5.88	0.004298	1512.96	0.001251
	20,000	1516.82	9.70	8.19	0.003168	1515.58	0.002587
	50,000	1520.26	10.73	11.63	0.002428	1520.26	0.002428
	100,000	1523.59	12.37	14.95	0.002310	1523.59	0.002310
	150,000	1525.98	12.25	17.35	0.001857	1525.98	0.001857
	200,300	1527.83	12.60	19.20	0.001715	1527.83	0.001715
7	300	1514.31	0.68	2.08	0.000097	n/a	n/a
	500	1514.69	0.96	2.42	0.000157	n/a	n/a
	1,000	1515.24	1.55	2.91	0.000320	n/a	n/a
	2,000	1515.99	2.42	3.61	0.000590	n/a	n/a
	5,000	1517.37	4.17	4.99	0.001136	n/a	n/a
	10,000	1518.87	5.91	6.49	0.001601	n/a	n/a
	20,000	1520.96	8.08	8.58	0.002065	n/a	n/a
	50,000	1523.85	11.90	11.47	0.003043	1523.85	0.003043
	100,000	1527.38	11.89	15.00	0.002125	1527.38	0.002125
	150,000	1529.38	12.48	17.01	0.001980	1529.38	0.001980
	200,300	1530.97	13.26	18.59	0.001986	1530.97	0.001986
8	300	1516.36	4.01	0.51	0.021802	n/a	n/a
	500	1516.56	4.63	0.66	0.020847	n/a	n/a
	1,000	1516.98	5.25	0.90	0.017645	n/a	n/a
	2,000	1517.45	6.31	1.22	0.016976	n/a	n/a
	5,000	1518.59	7.67	2.36	0.010388	n/a	n/a
	10,000	1520.26	8.04	4.03	0.005605	n/a	n/a
	20,000	1522.48	9.24	6.25	0.004120	n/a	n/a
	50,000	1526.09	10.17	9.86	0.002716	1526.09	0.002716
	100,000	1528.83	12.79	12.60	0.003098	1528.83	0.003098
	150,000	1530.73	13.56	14.50	0.002890	1530.73	0.002890
	200,300	1532.32	14.10	16.09	0.002721	1532.32	0.002721

APPENDIX D

Cross-Section Profiles and Water-Surface Elevations for Natural and Routed Flood Peaks for each of the Three Sites

Site 1, Cross Section 1

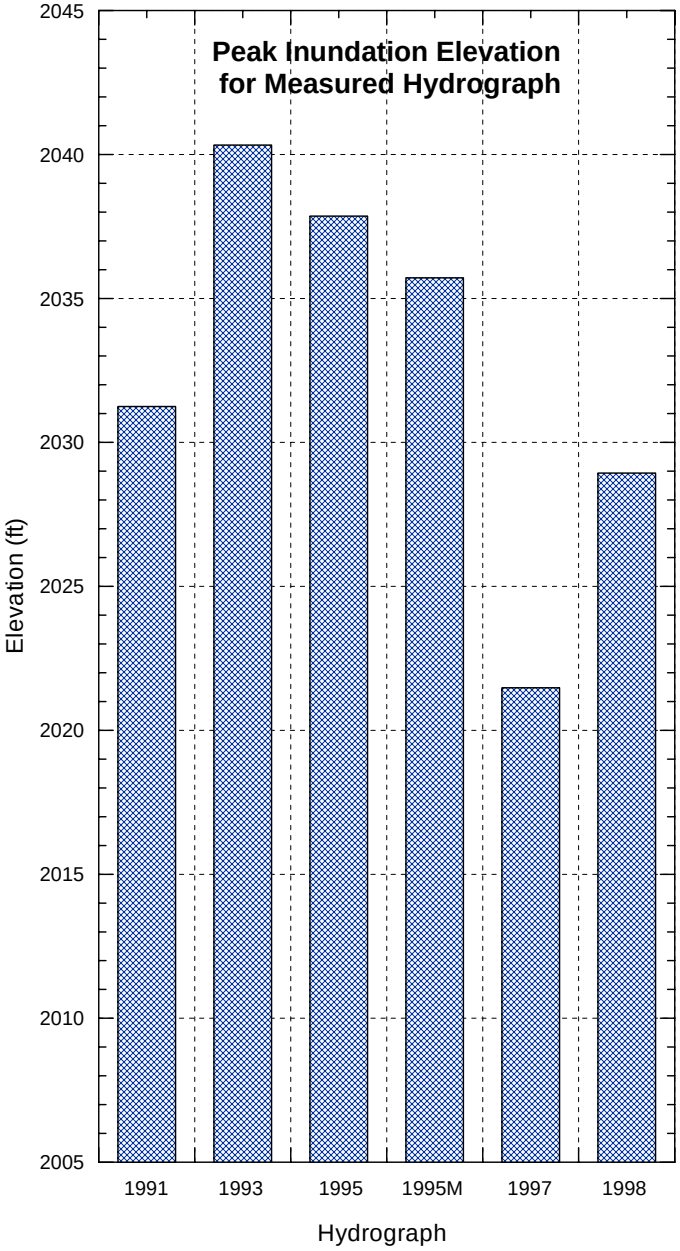

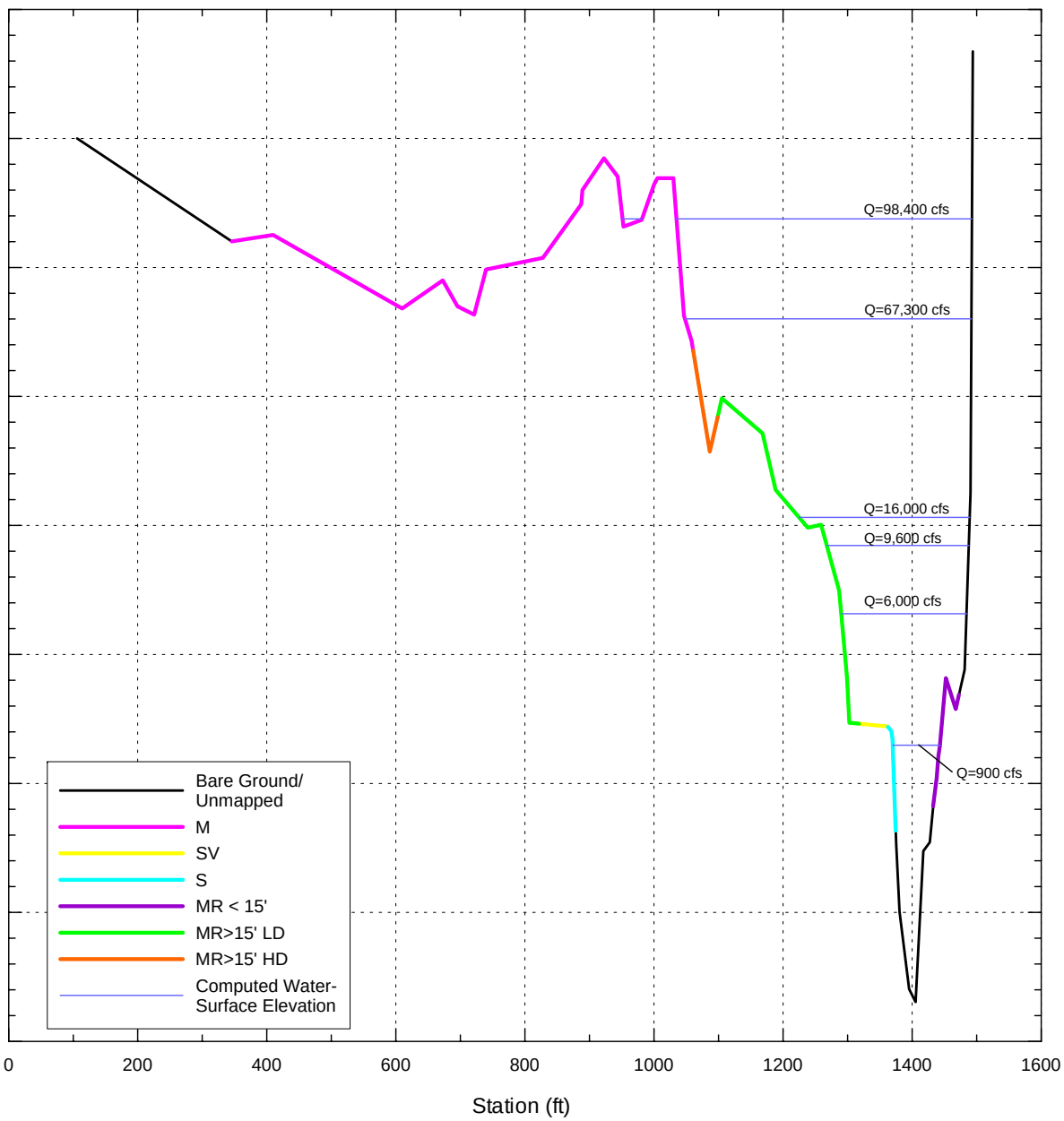

Site 1, Cross Section 2

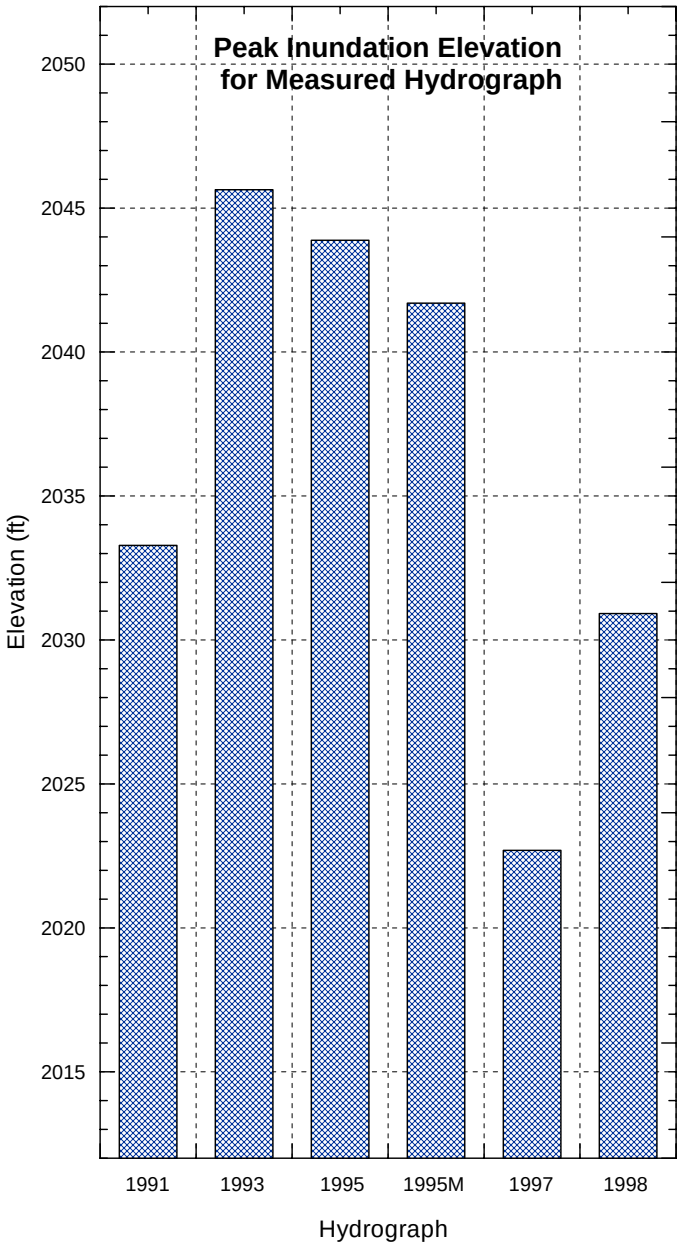

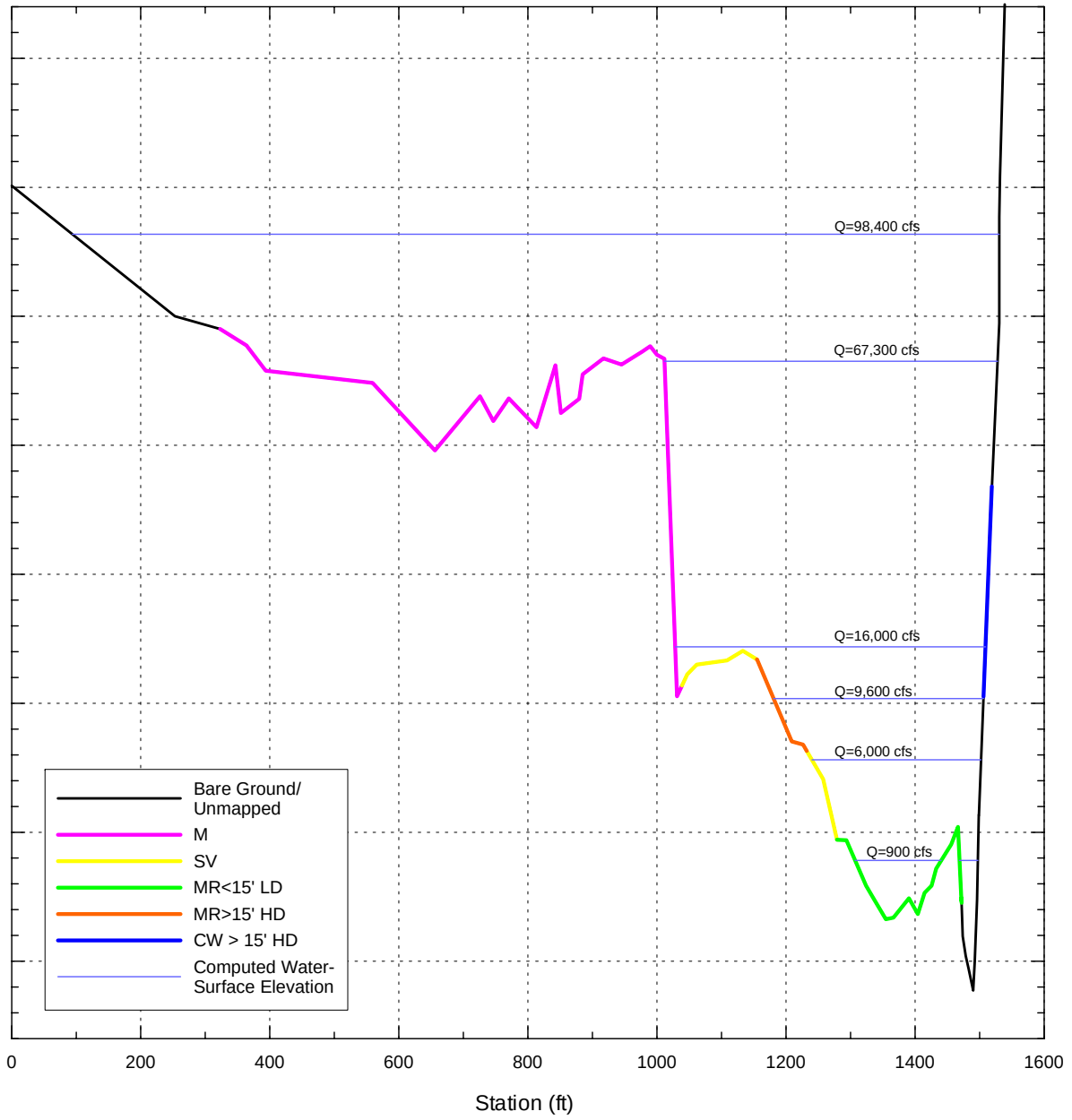

Site 1, Cross Section 3

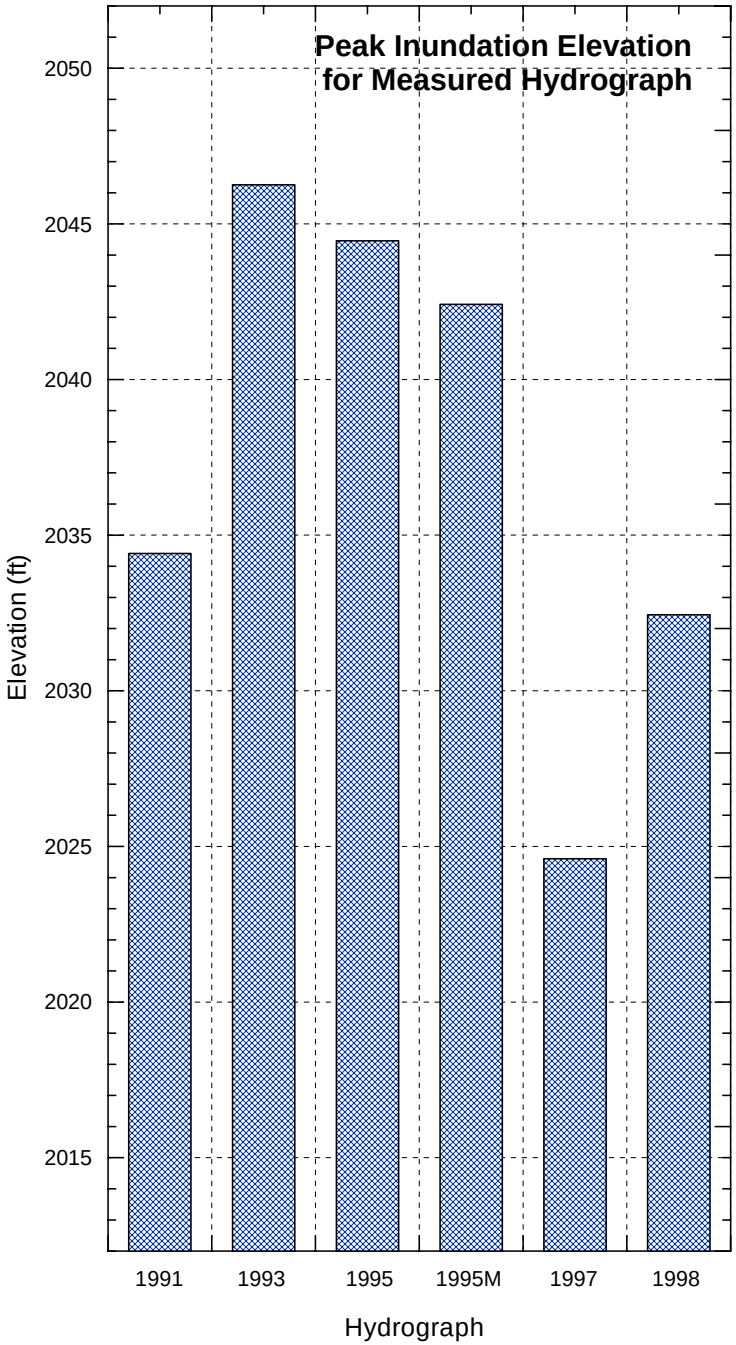

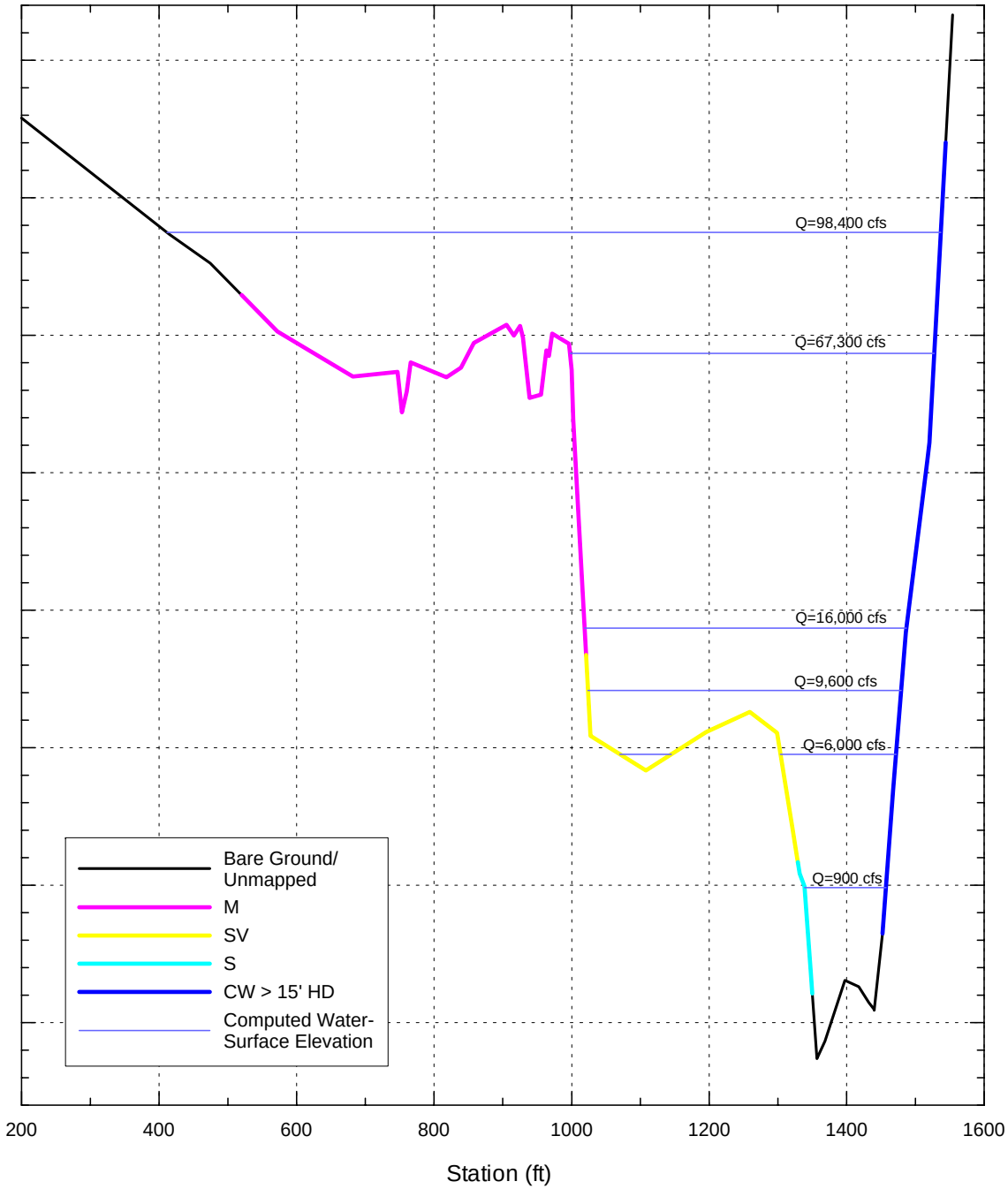

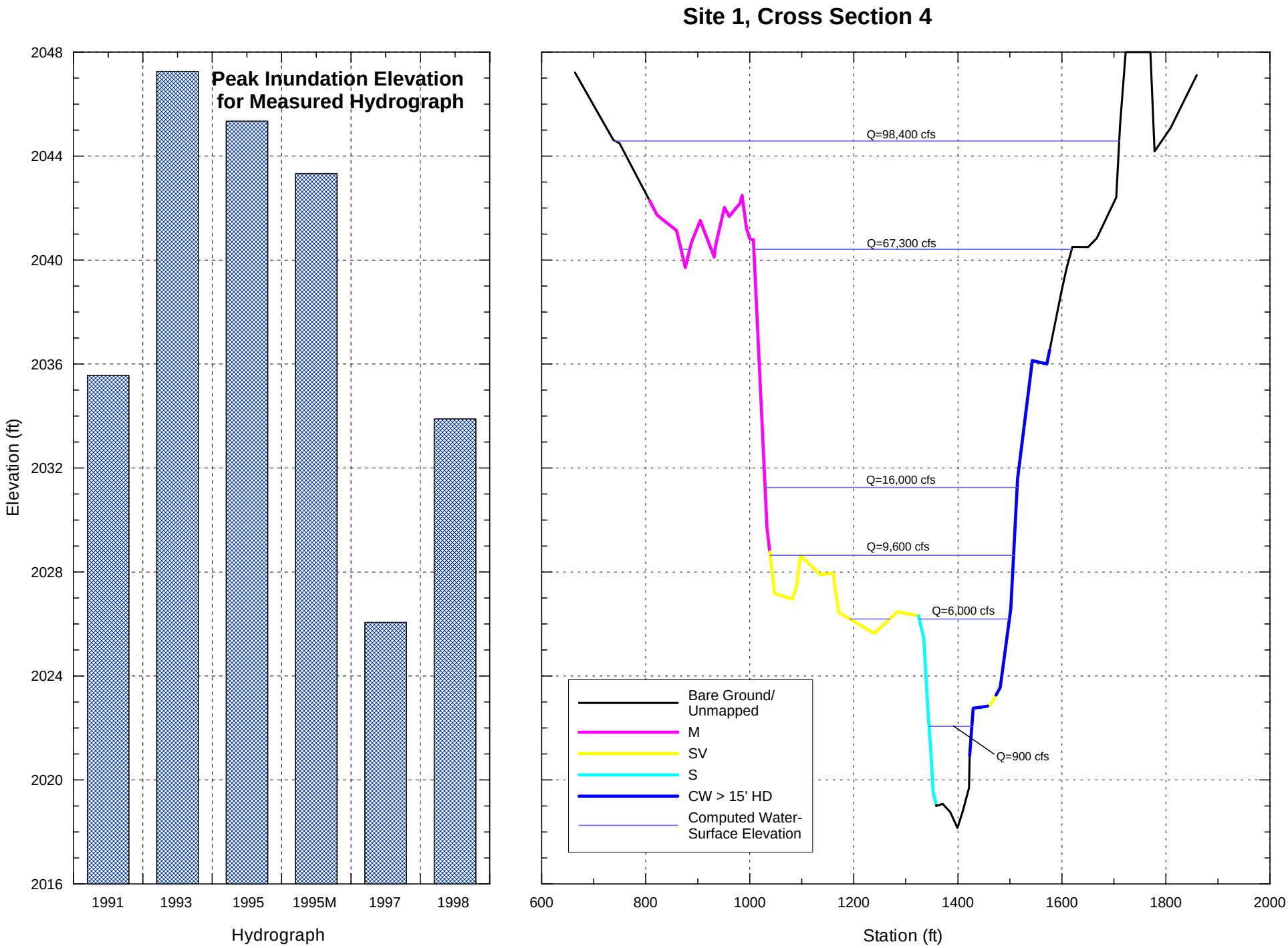
Site 1, Cross Section 4
Peak Inundation Elevation for Measured Hydrograph
Elevation (ft)
2048
2044
2040
2036
2032
2028
2024
2020
2016
1991
1993
1995
1995M
1997
1998
Hydrograph
Q=98,400 cfs
Q=67,300 cfs
Q=16,000 cfs
Q=9,600 cfs
Q=6,000 cfs
Q=900 cfs
Bare Ground/ Unmapped
M
SV
S
CW > 15' HD
Computed Water-Surface Elevation
600
800
1000
1200
1400
1600
1800
2000
Station (ft)

Site 1, Cross Section 5

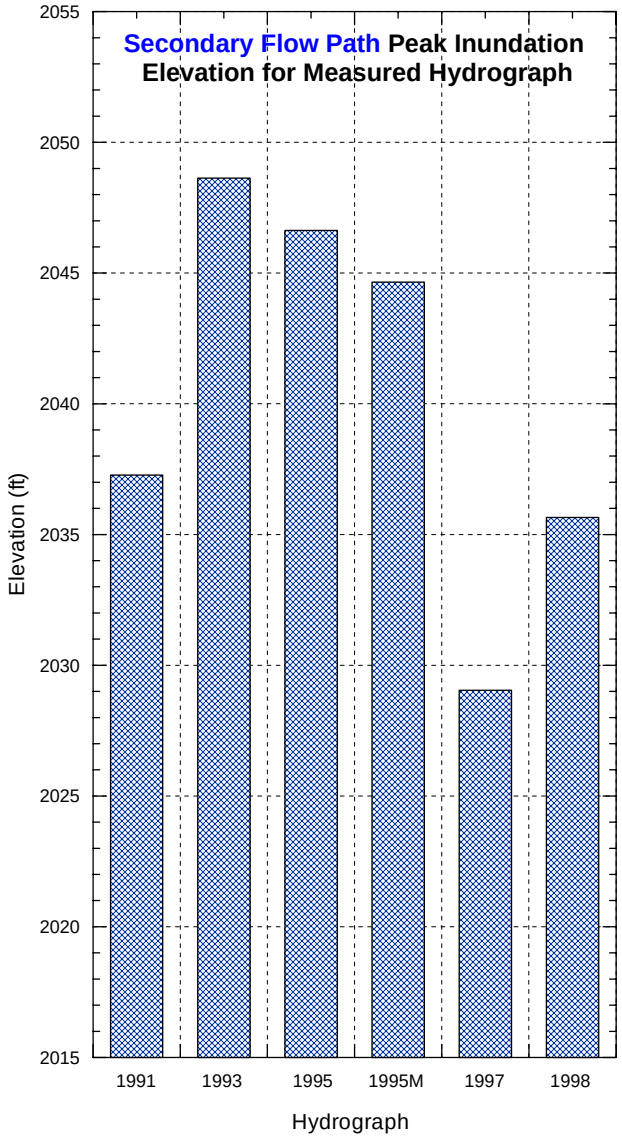

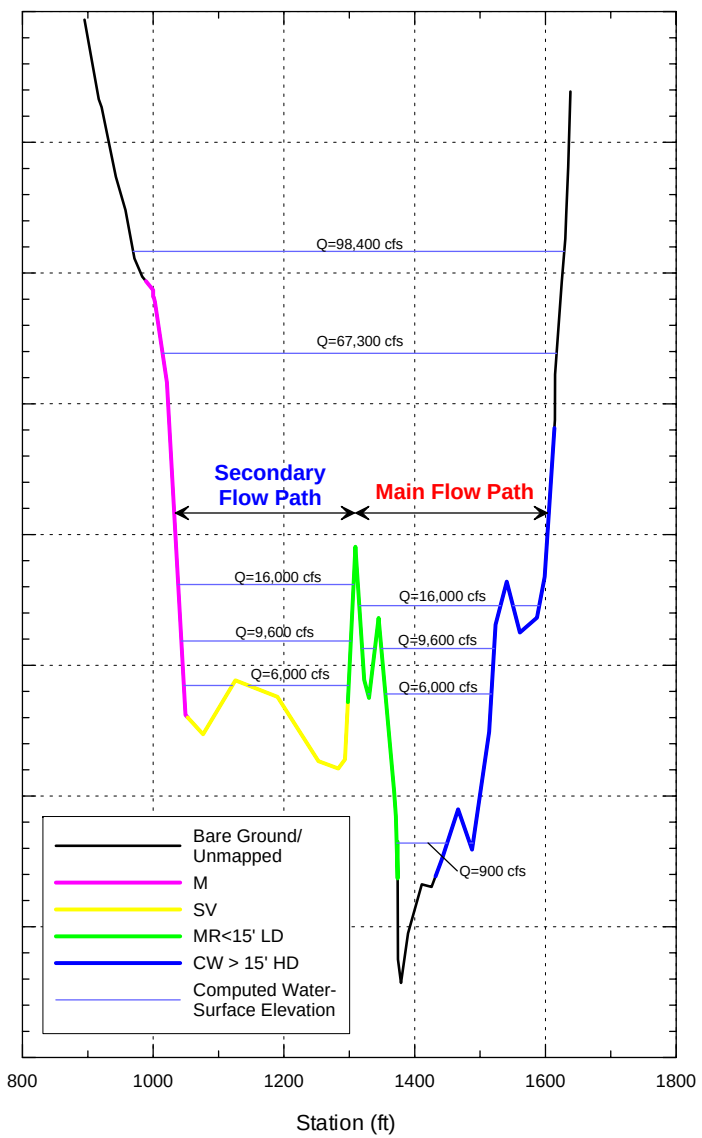

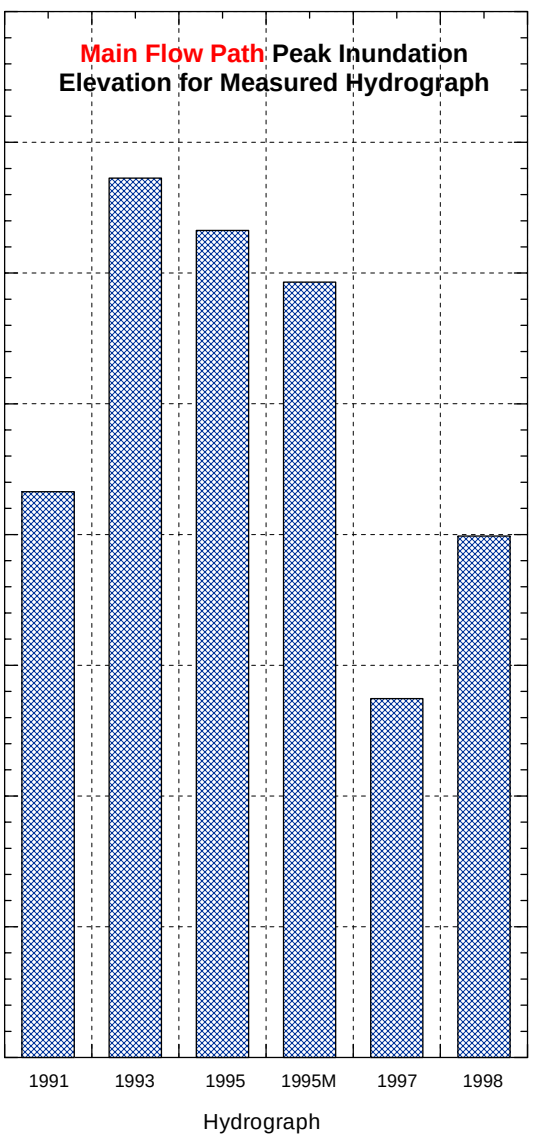

Site 1, Cross Section 6

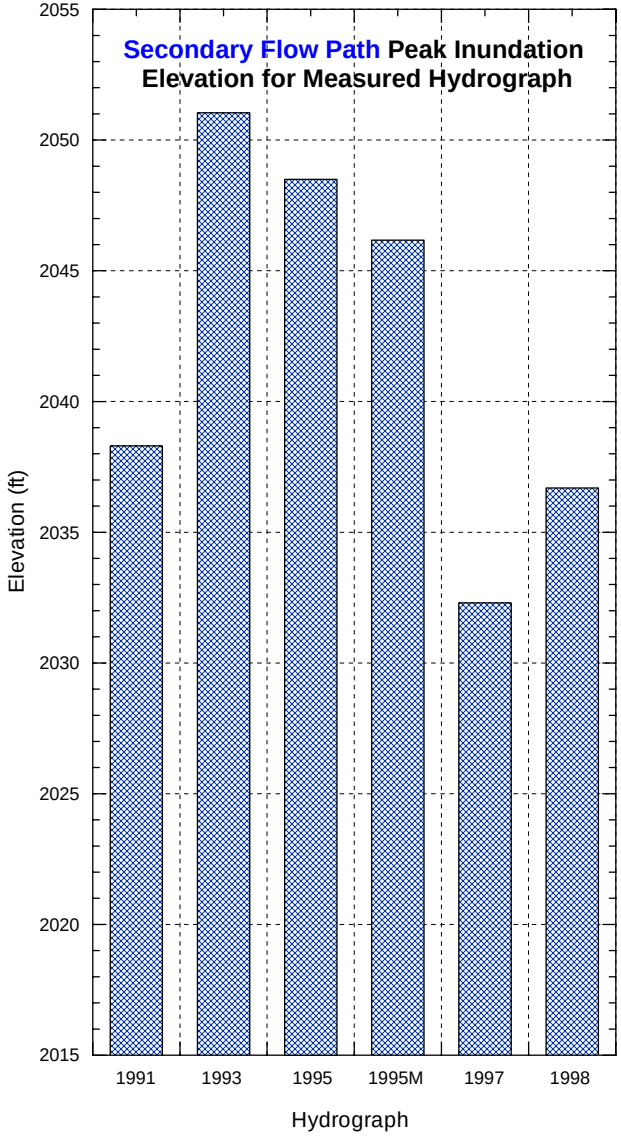

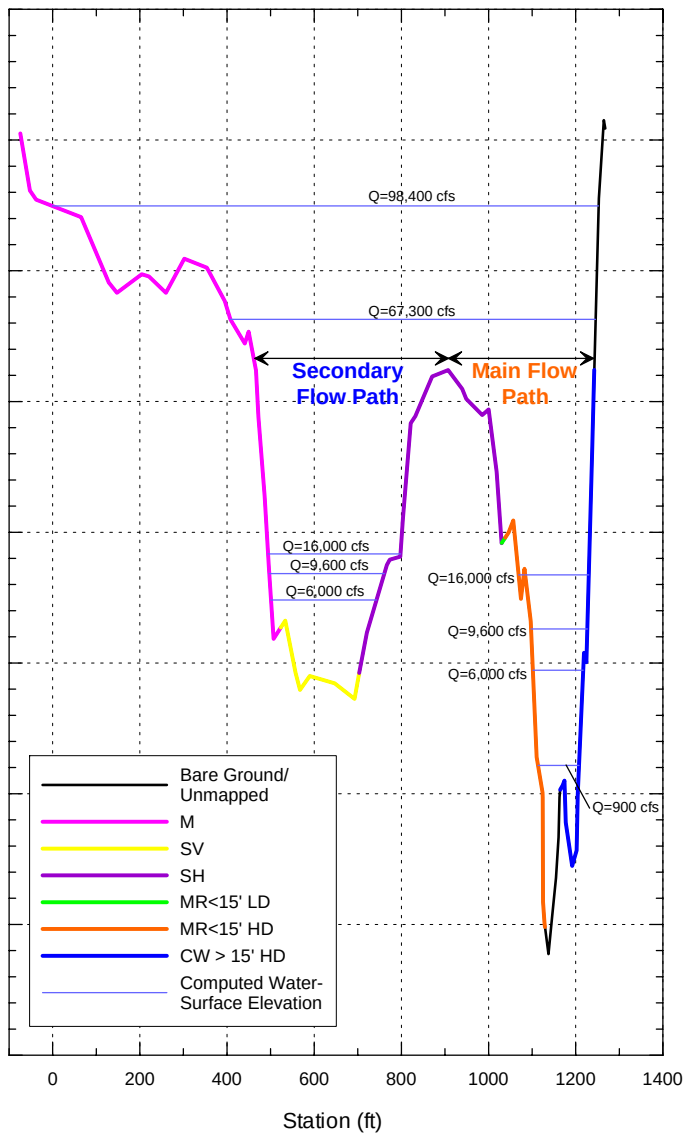

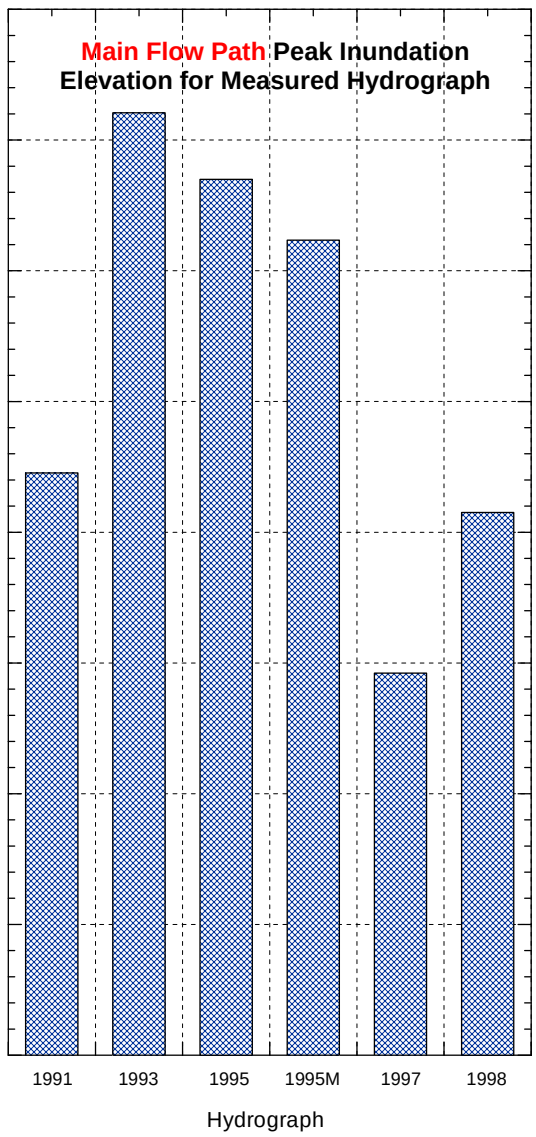

Site 2, Cross Section 1

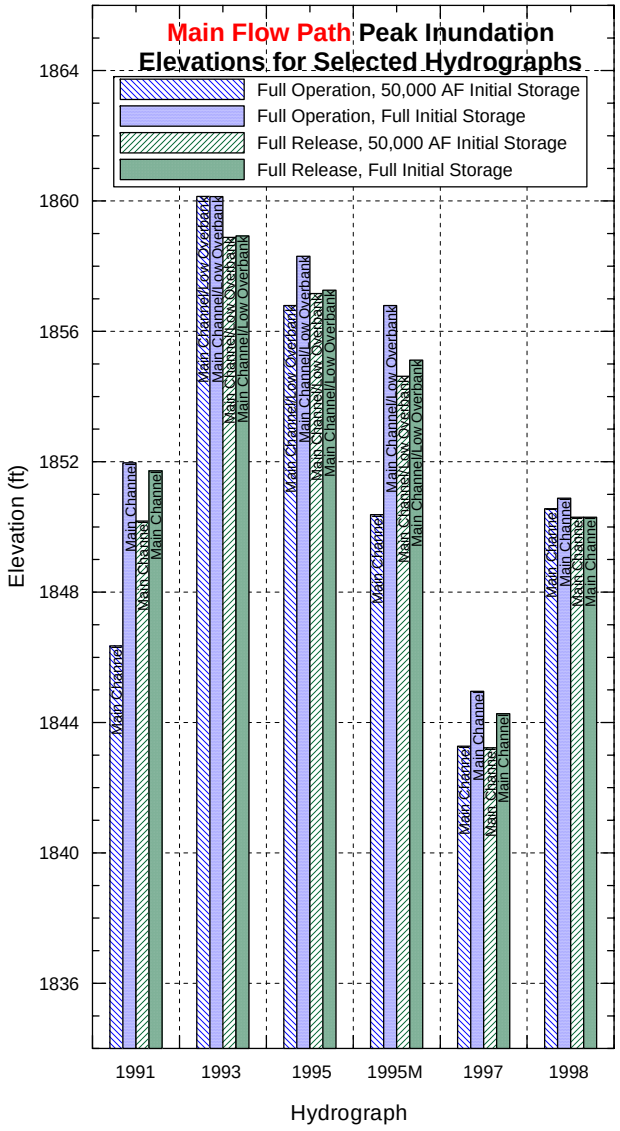

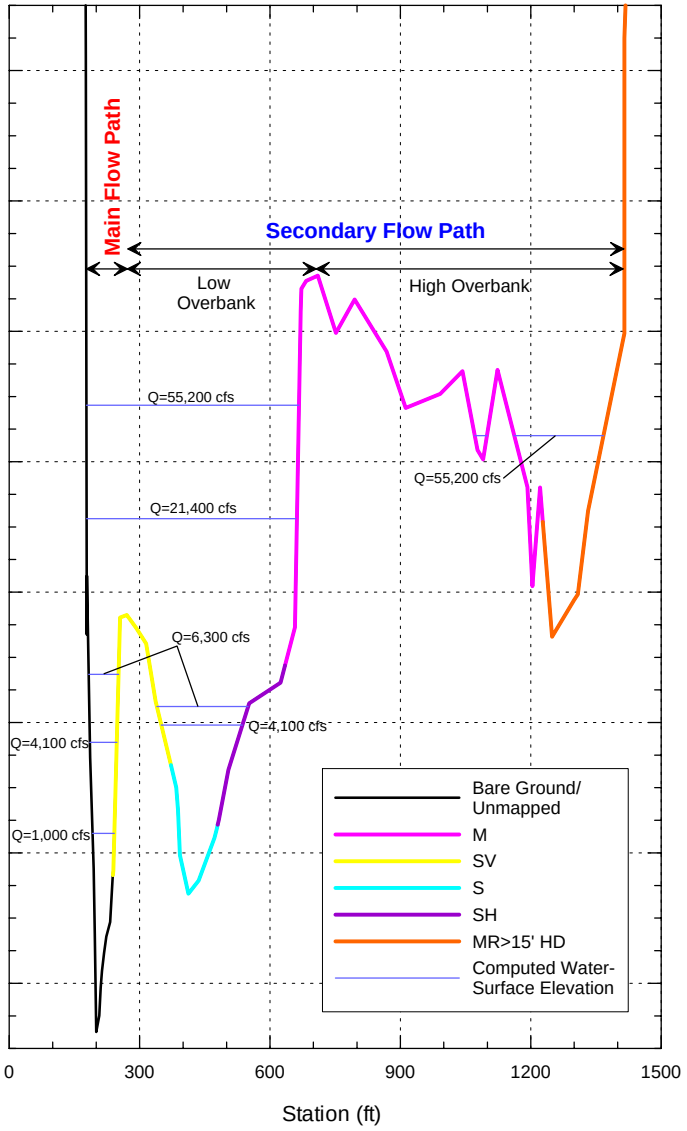

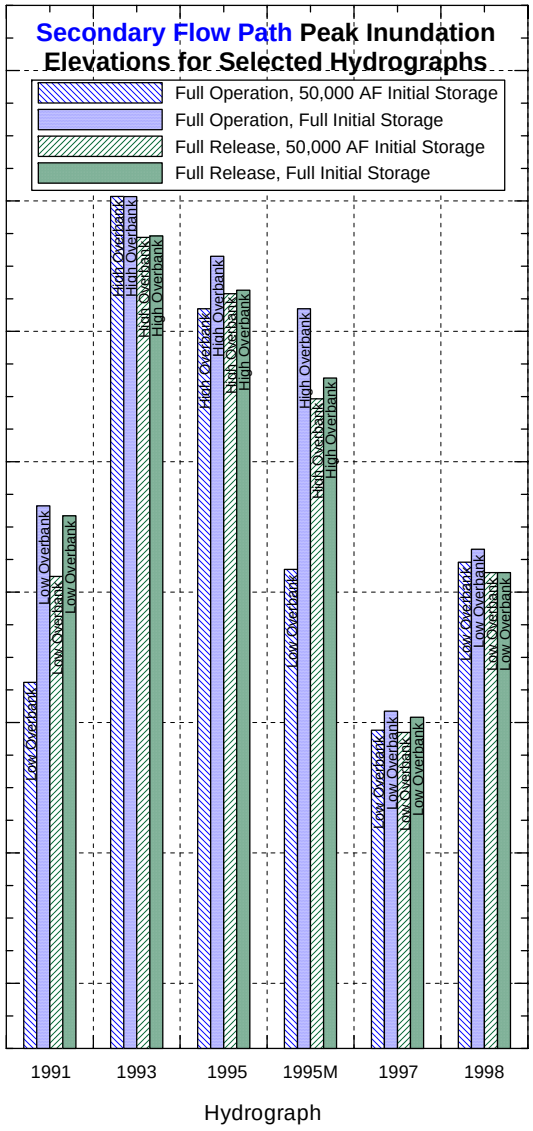

Site 2, Cross Section 2

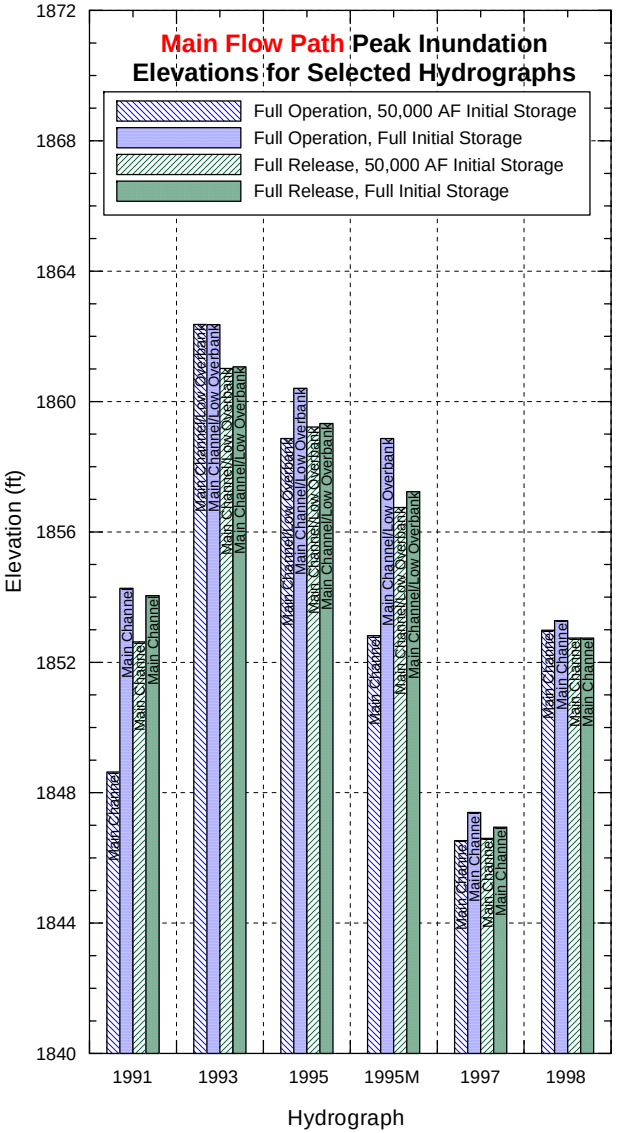

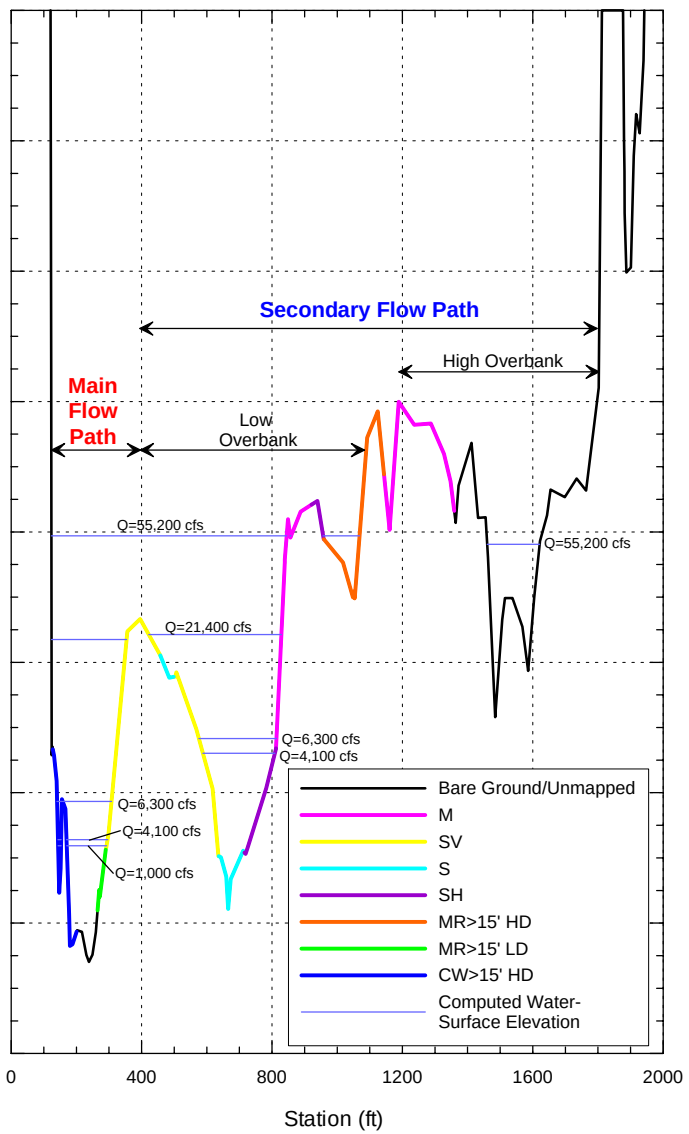

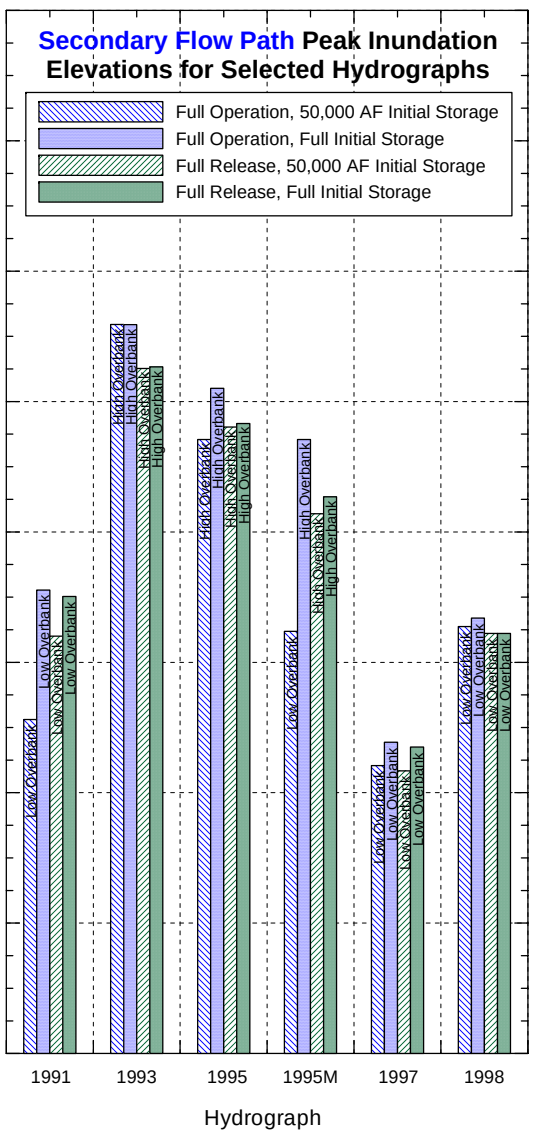

Site 2, Cross Section 3

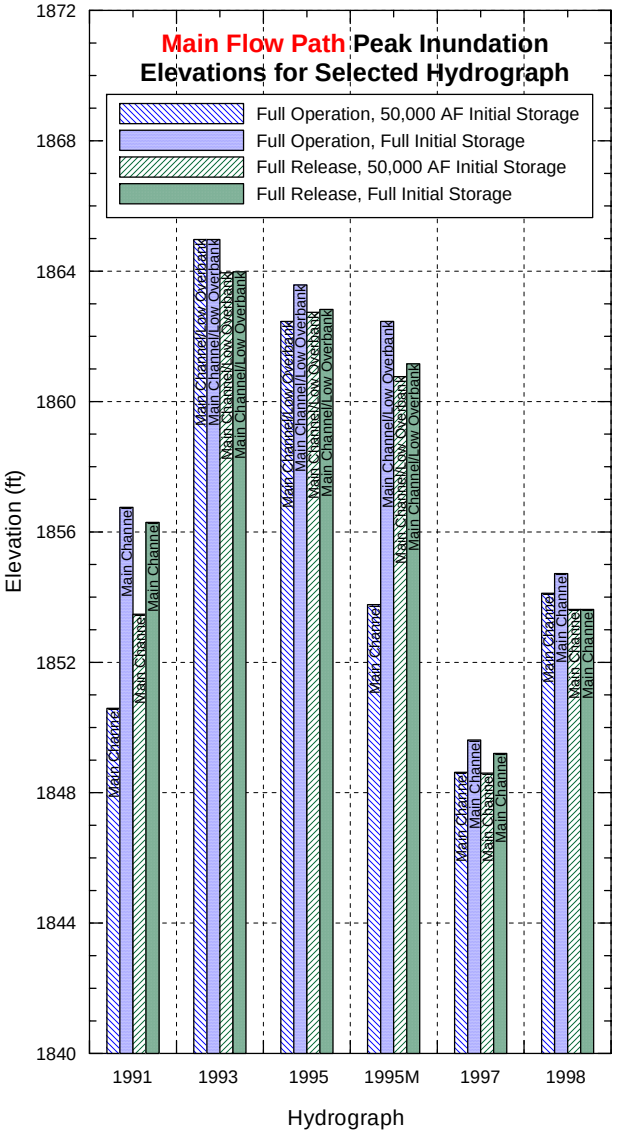

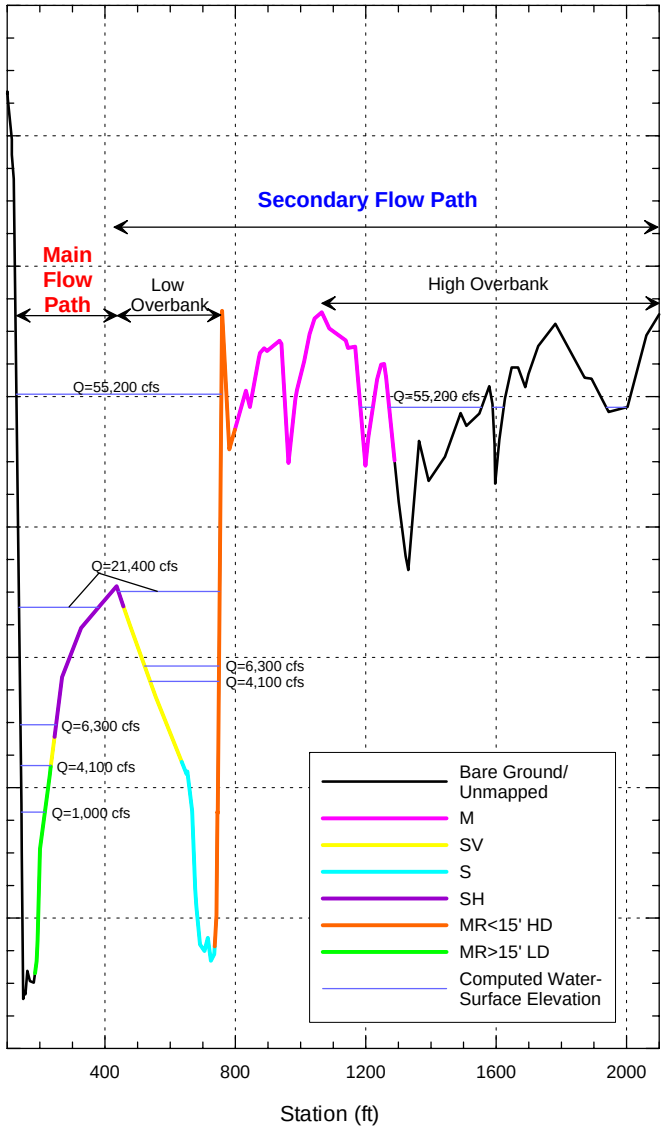

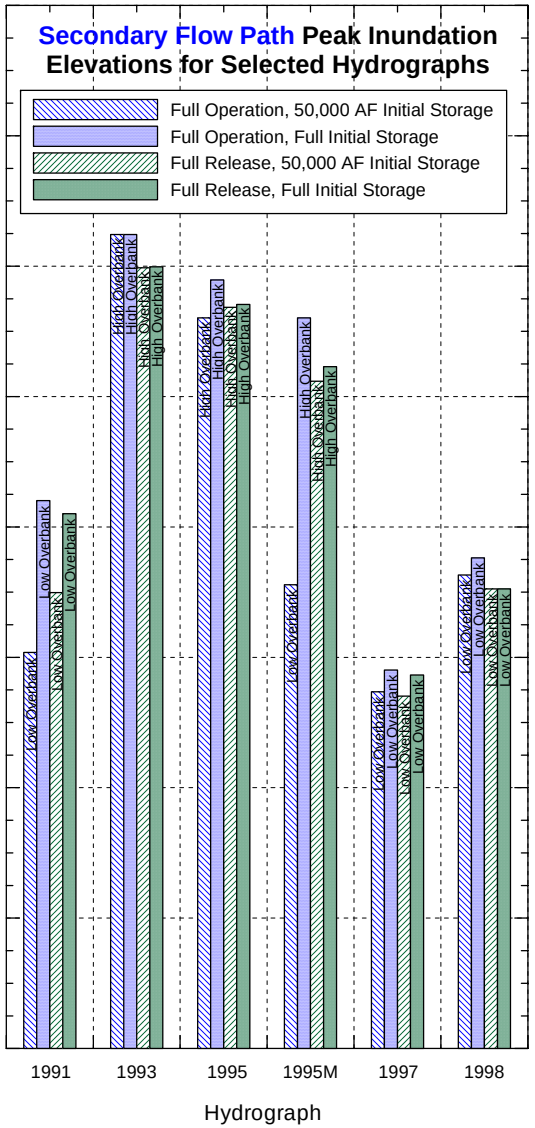

Site 2, Cross Section 4

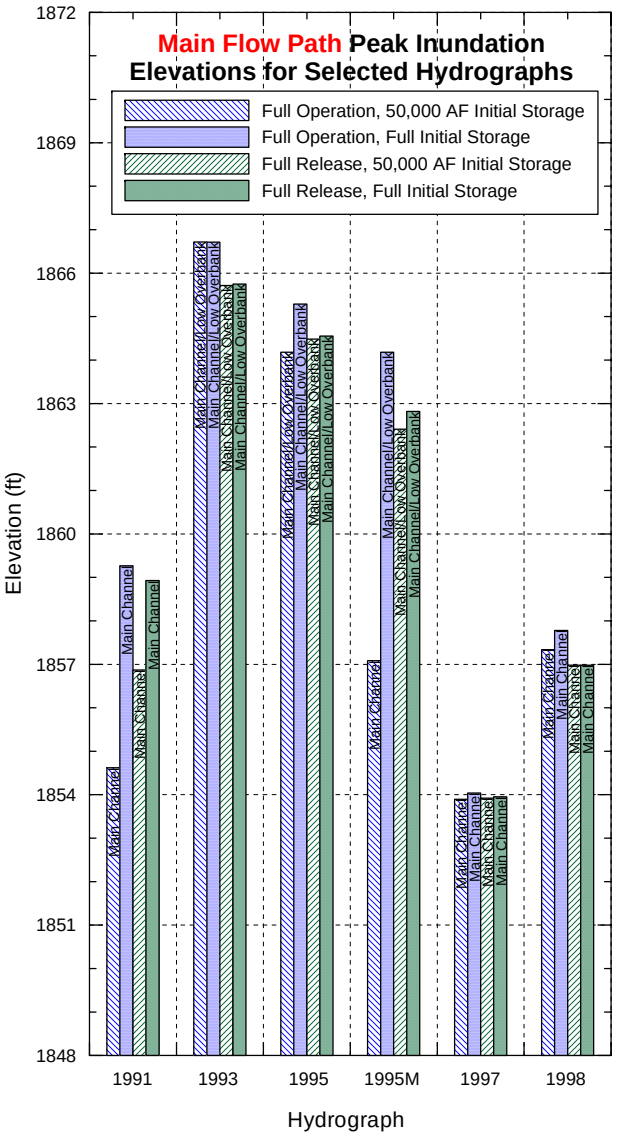

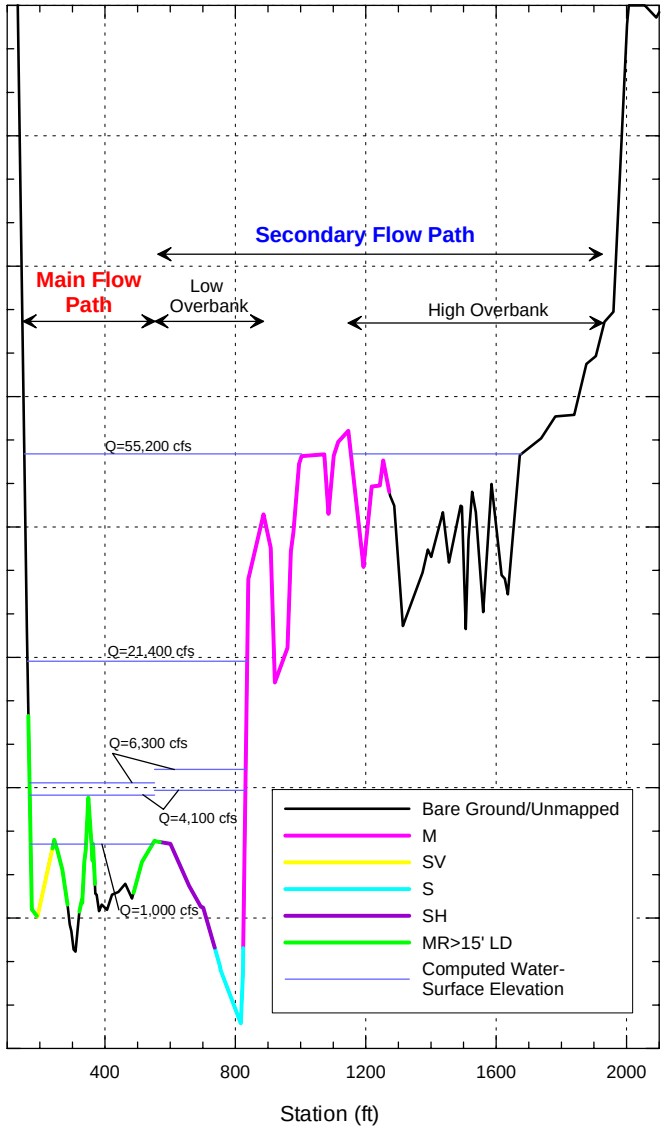

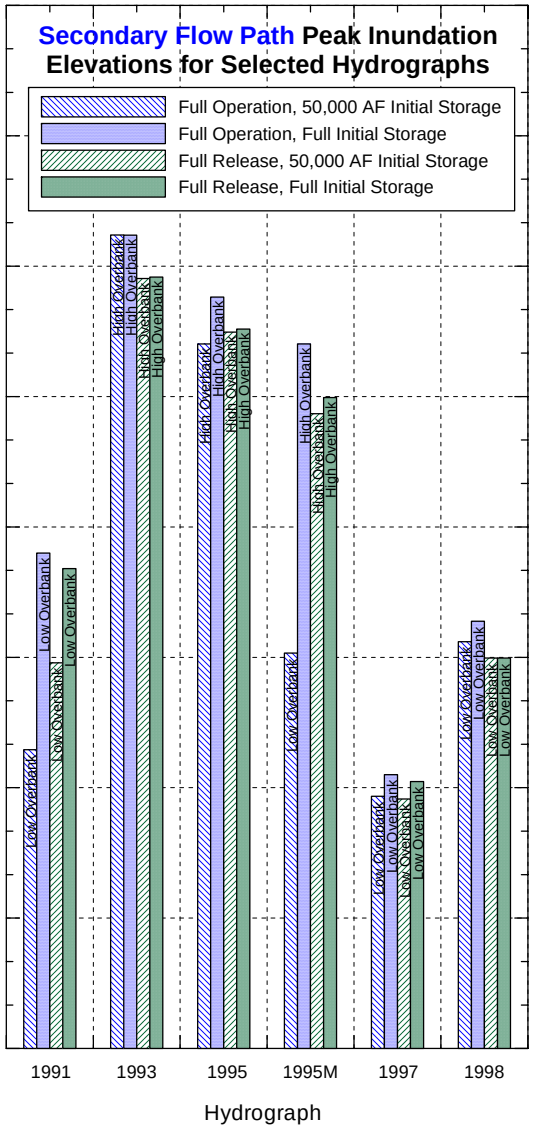

Site 2, Cross Section 5

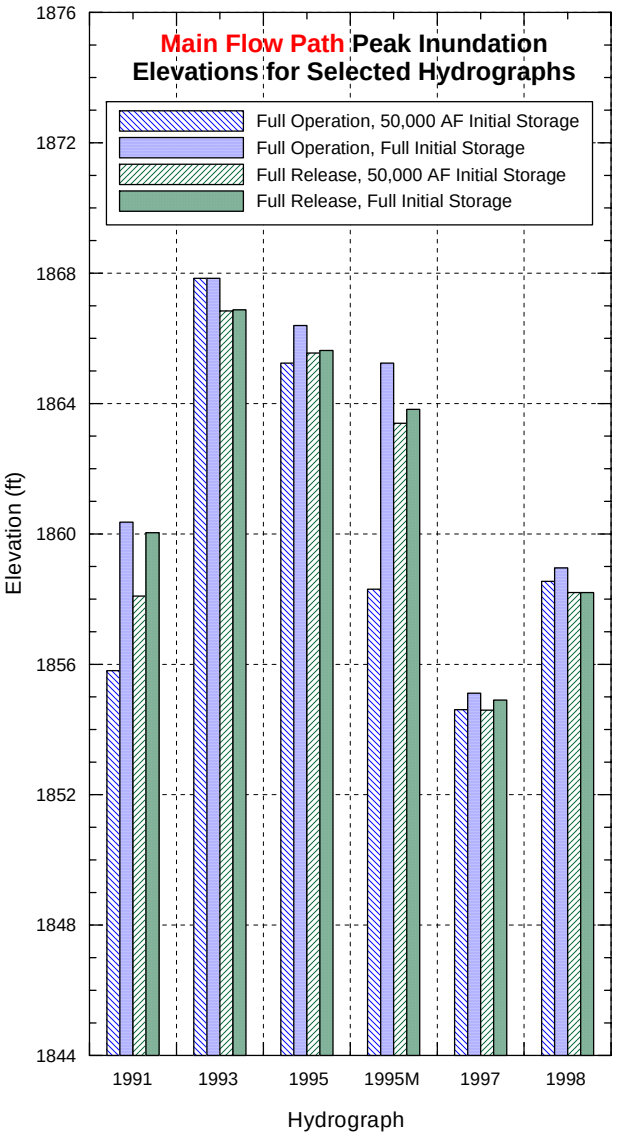

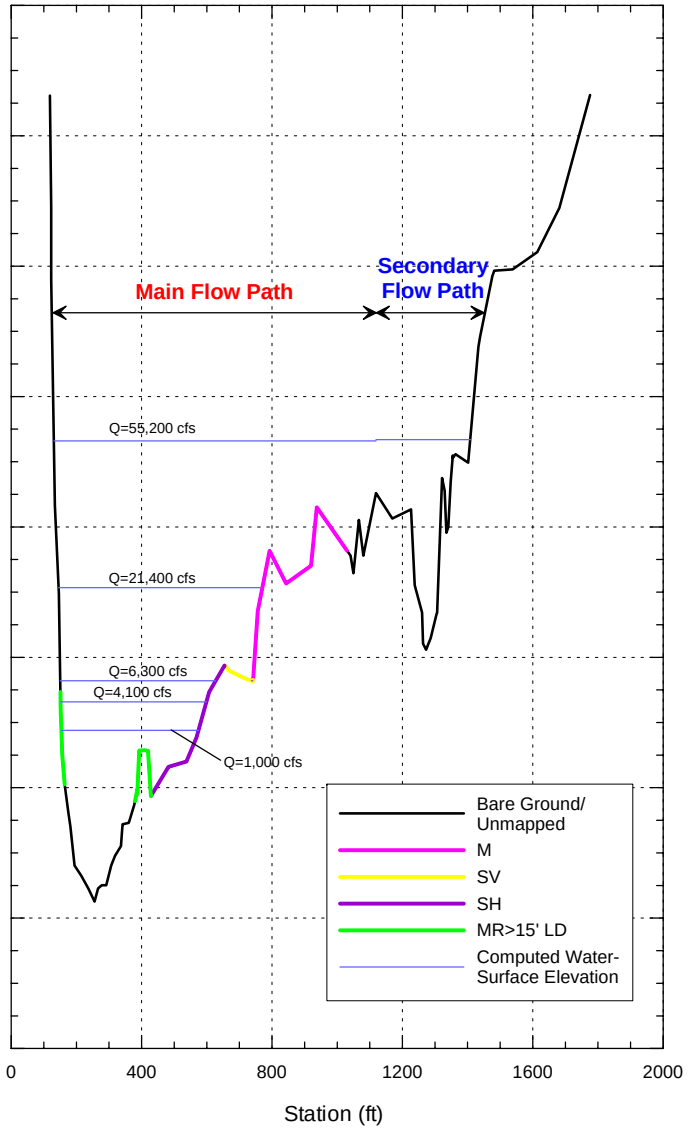

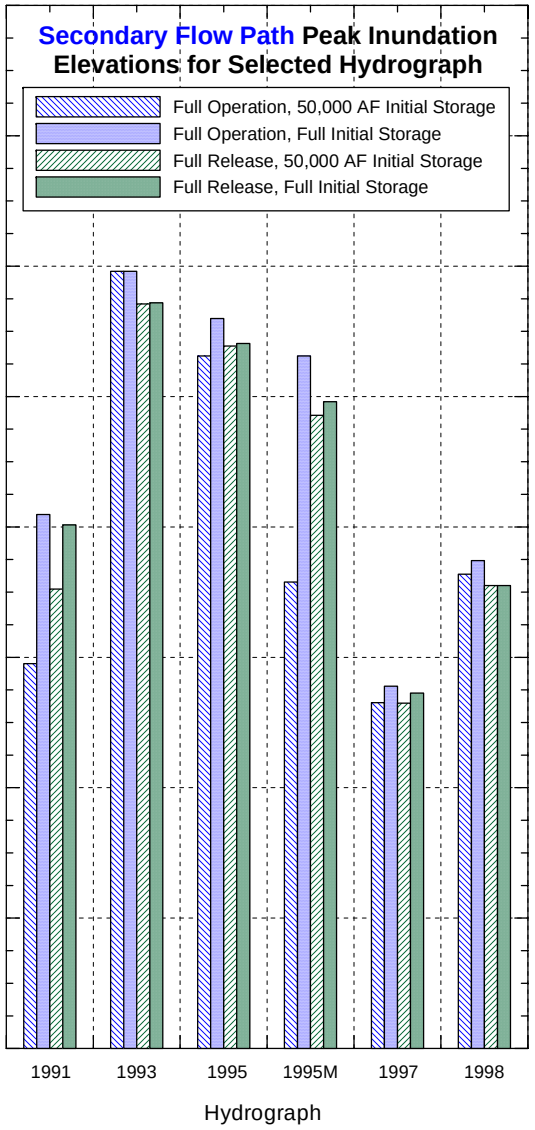

Site 2, Cross Section 6

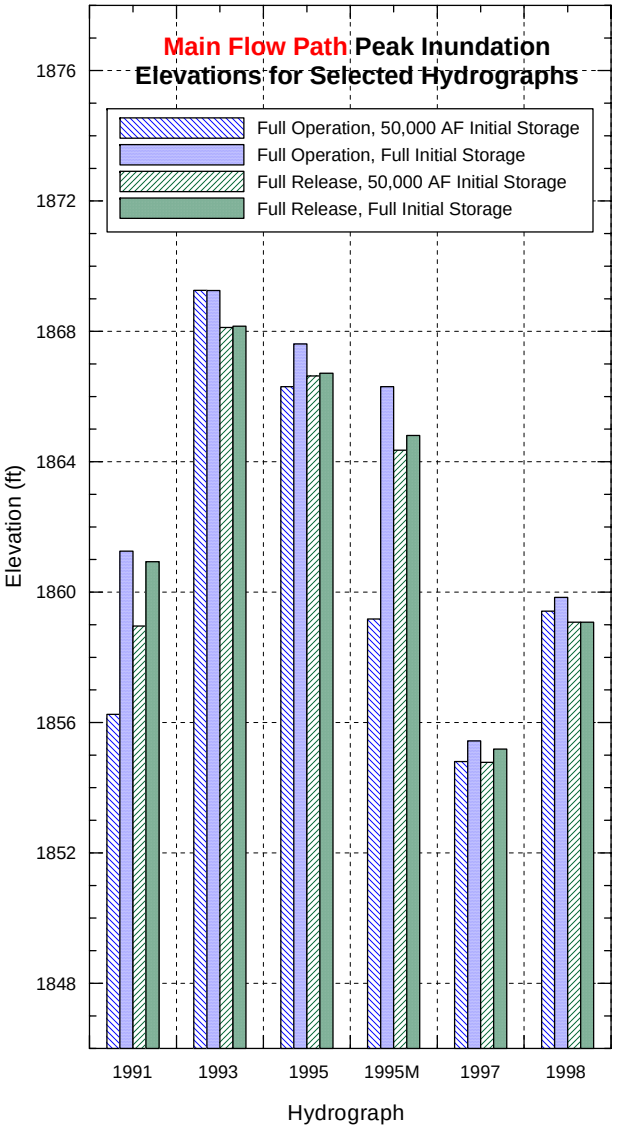

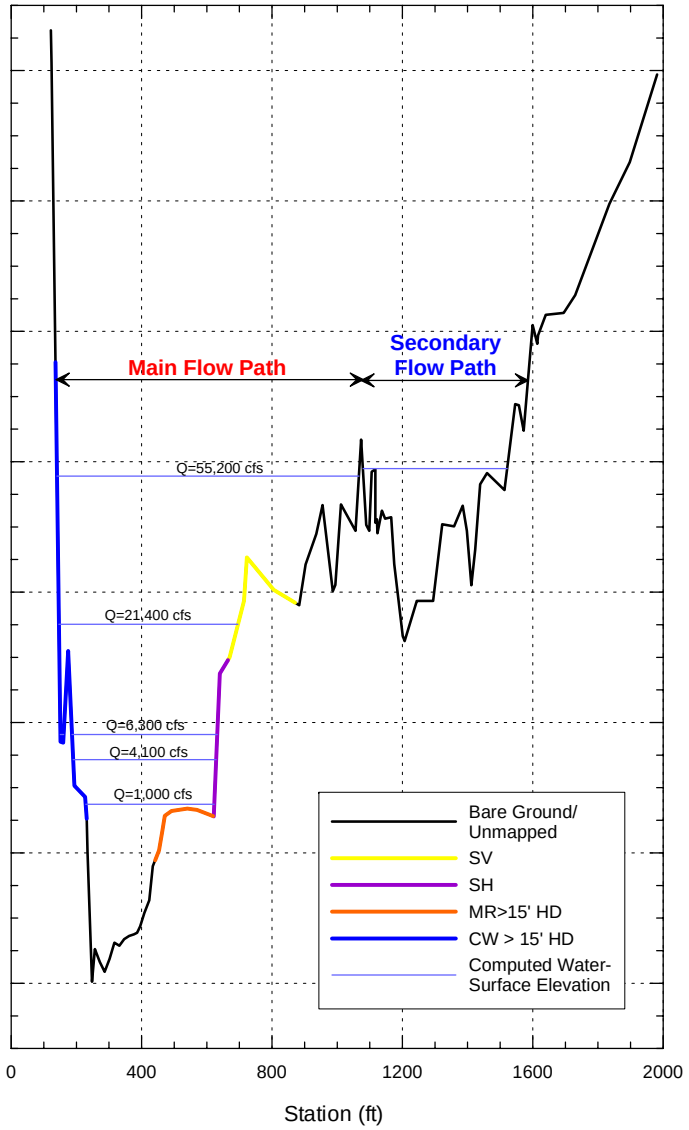

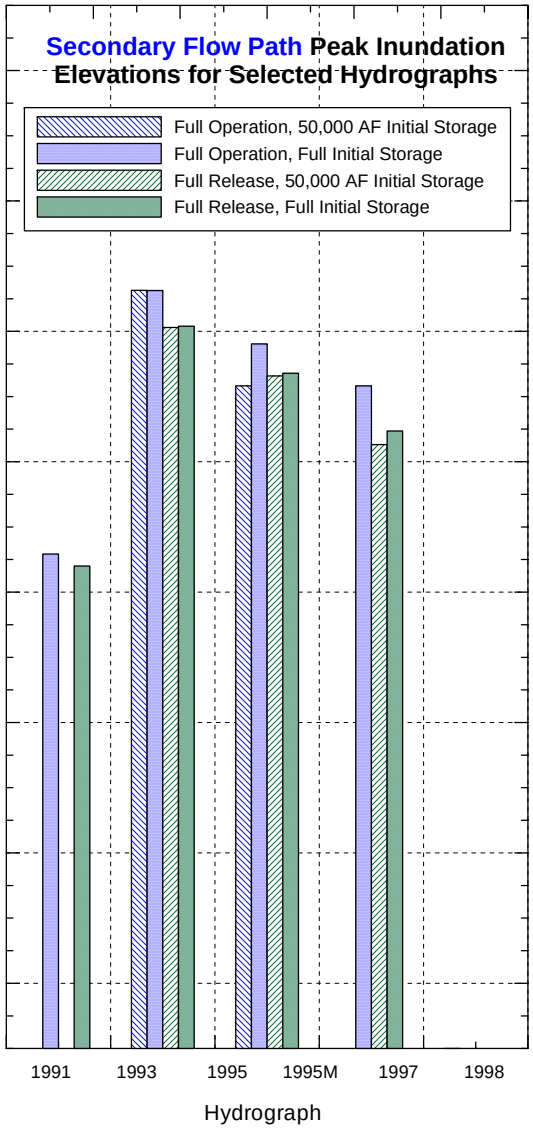

Site 2, Cross Section 7

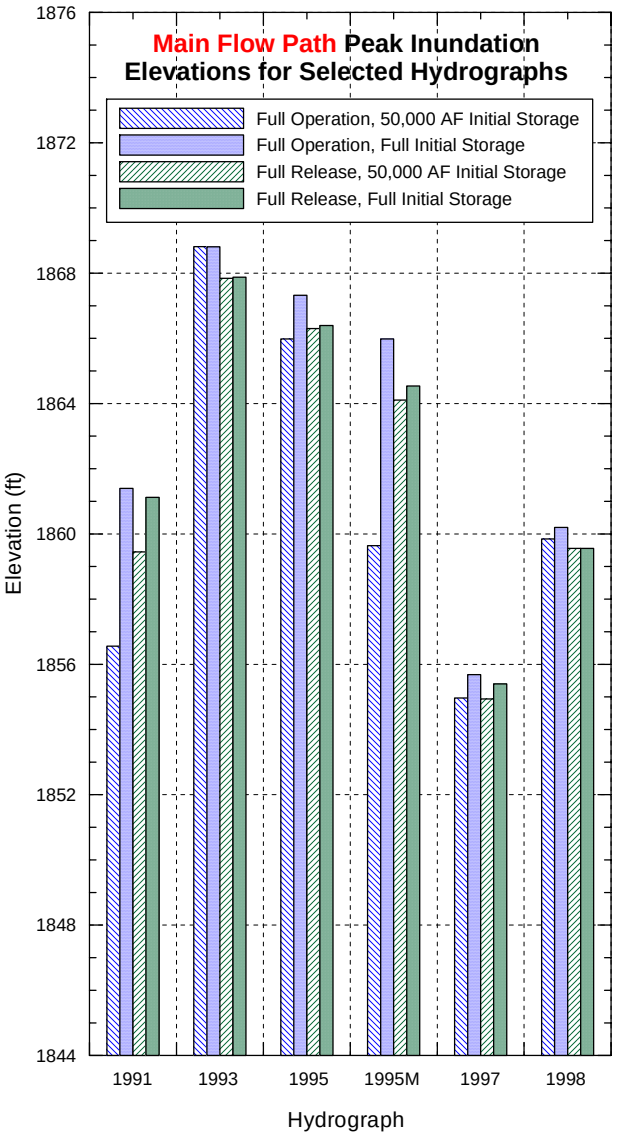

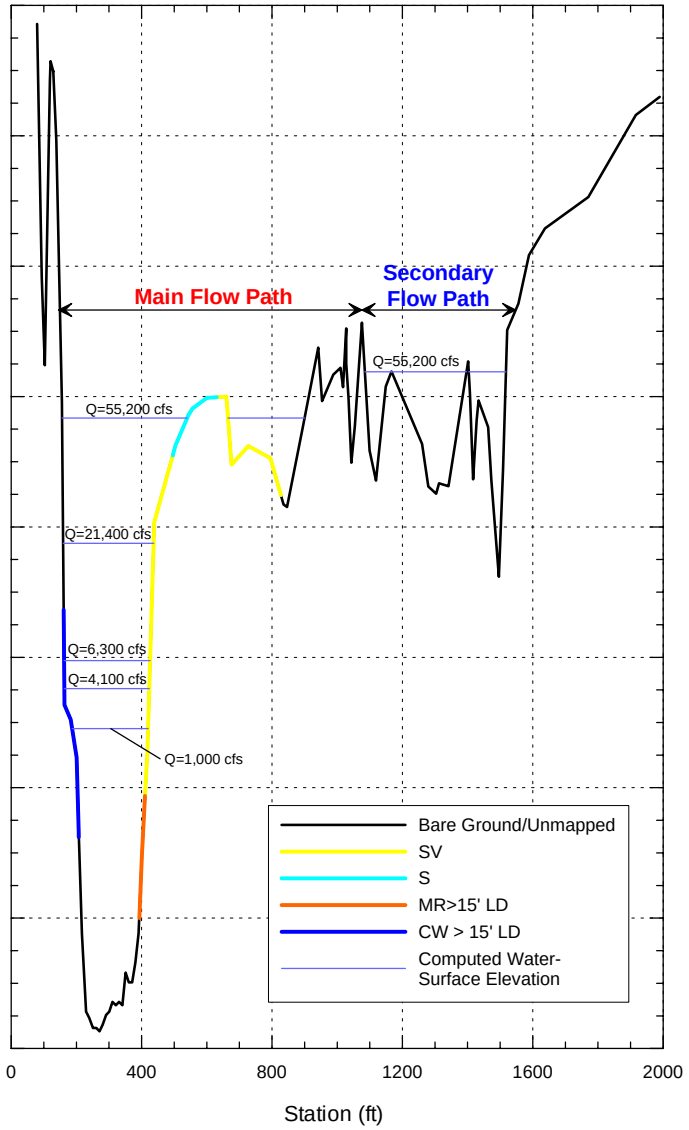

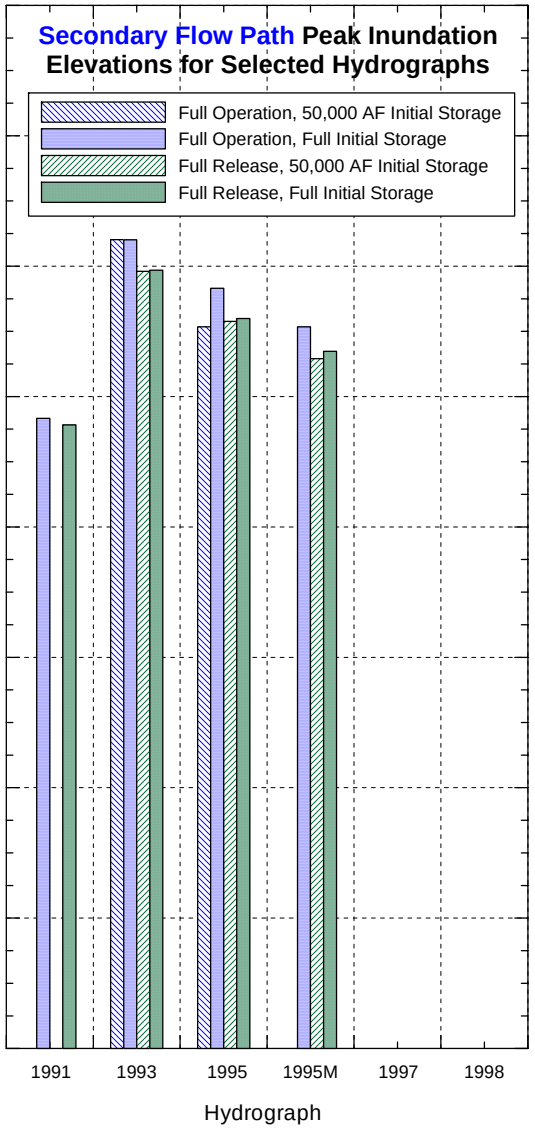

Site 3, Cross Section 1

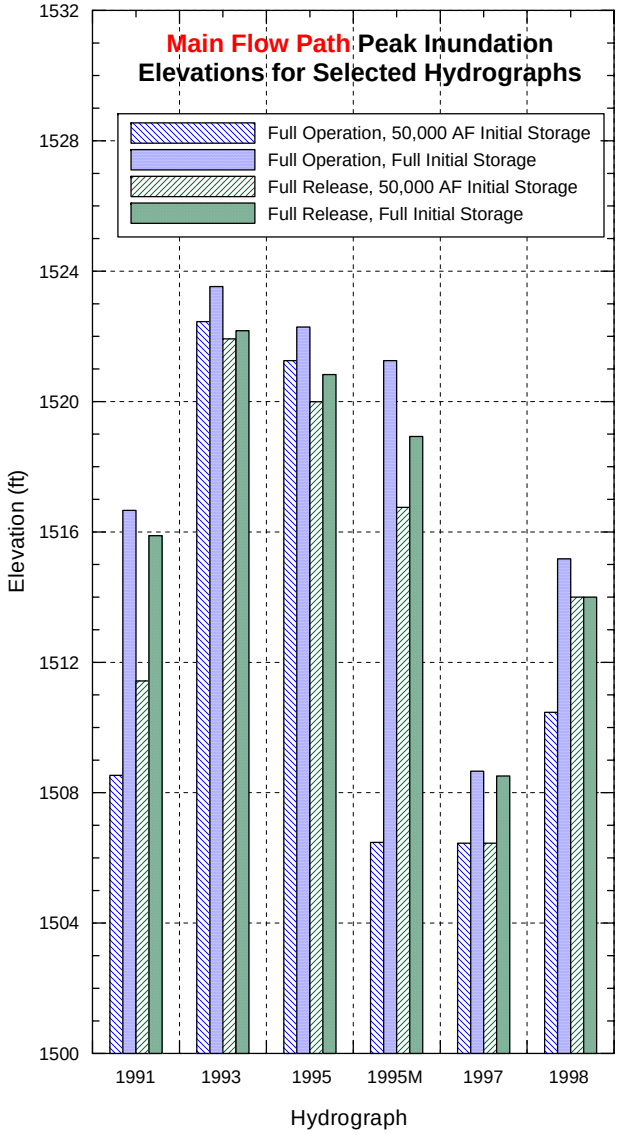

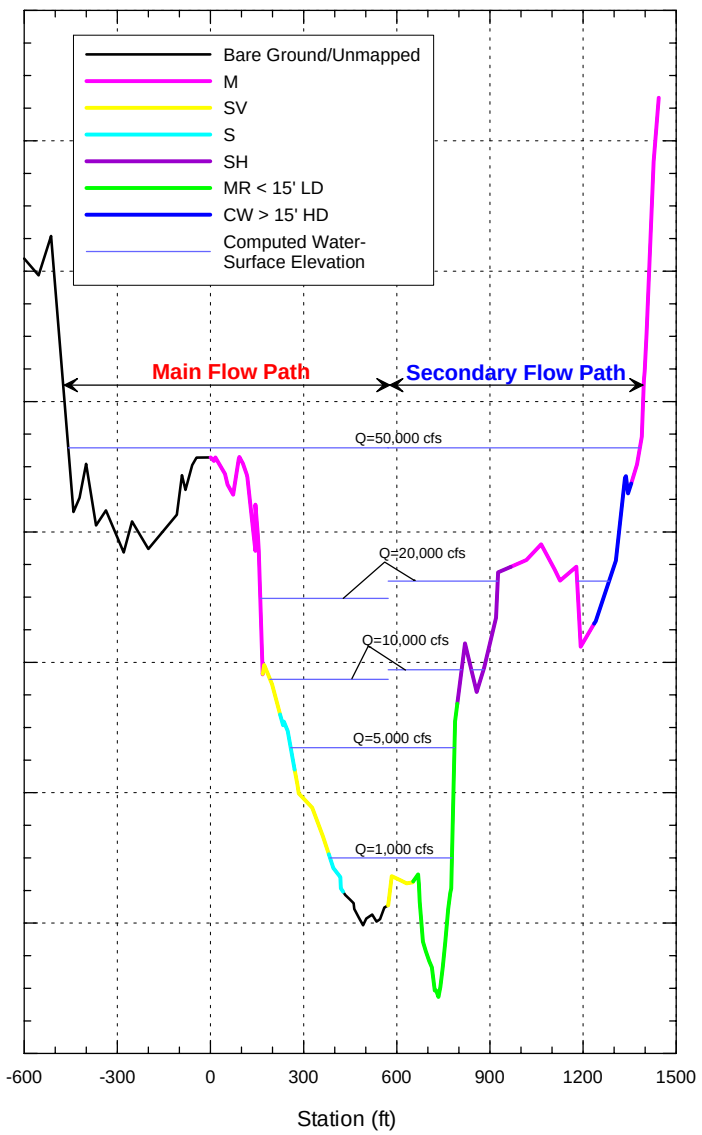

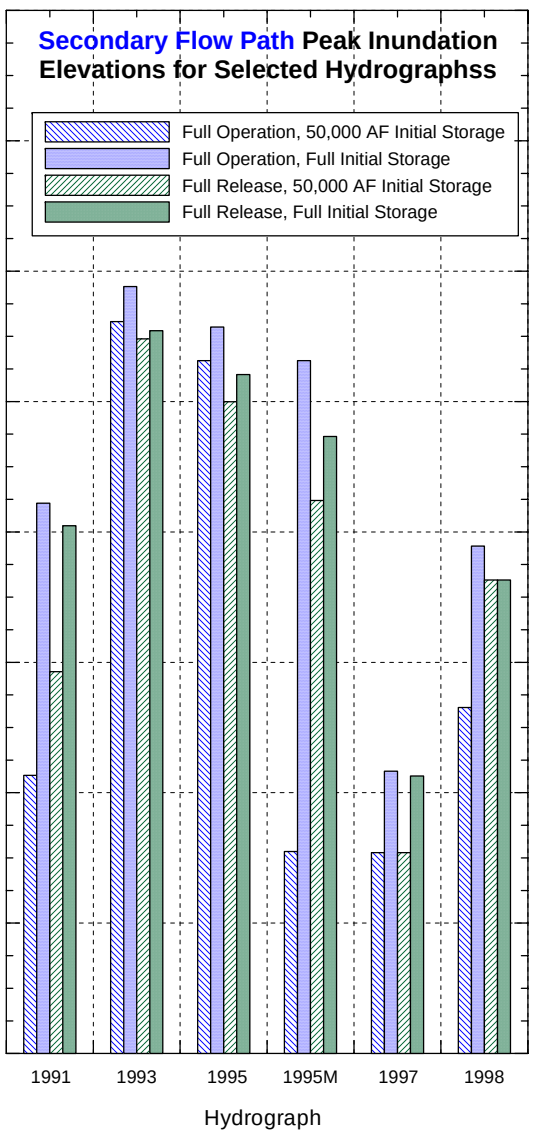

Site 3, Cross Section 2

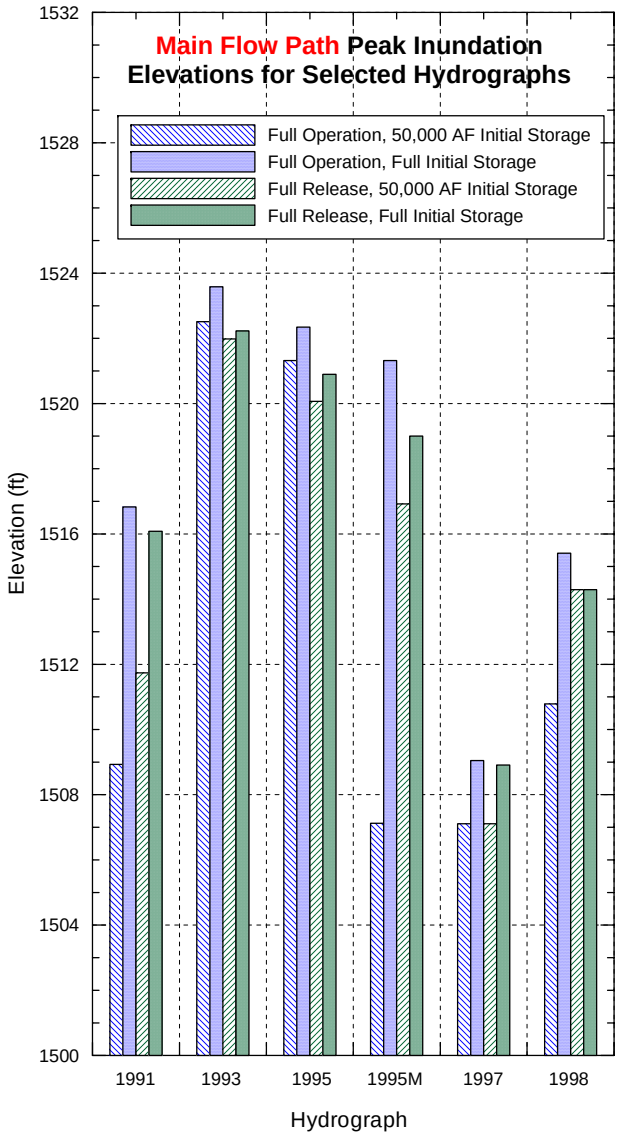

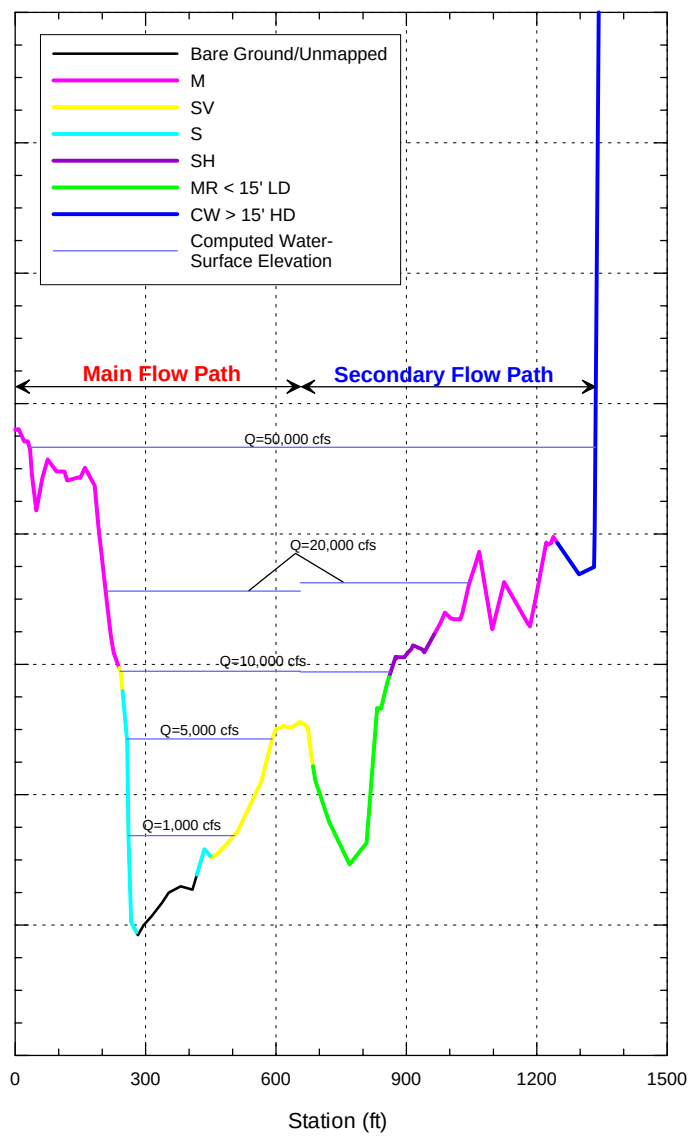

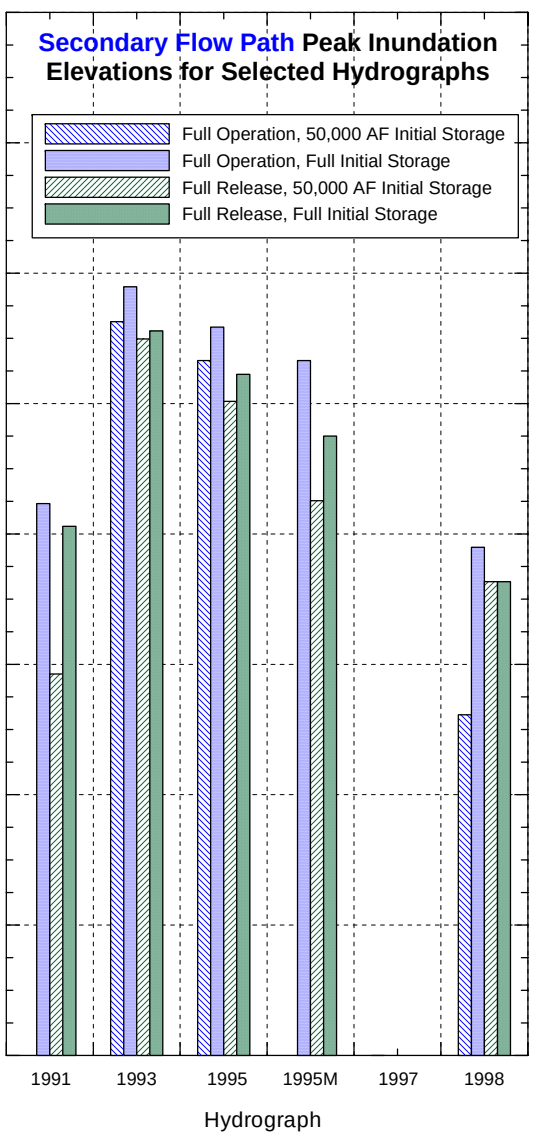

Site 3, Cross Section 3

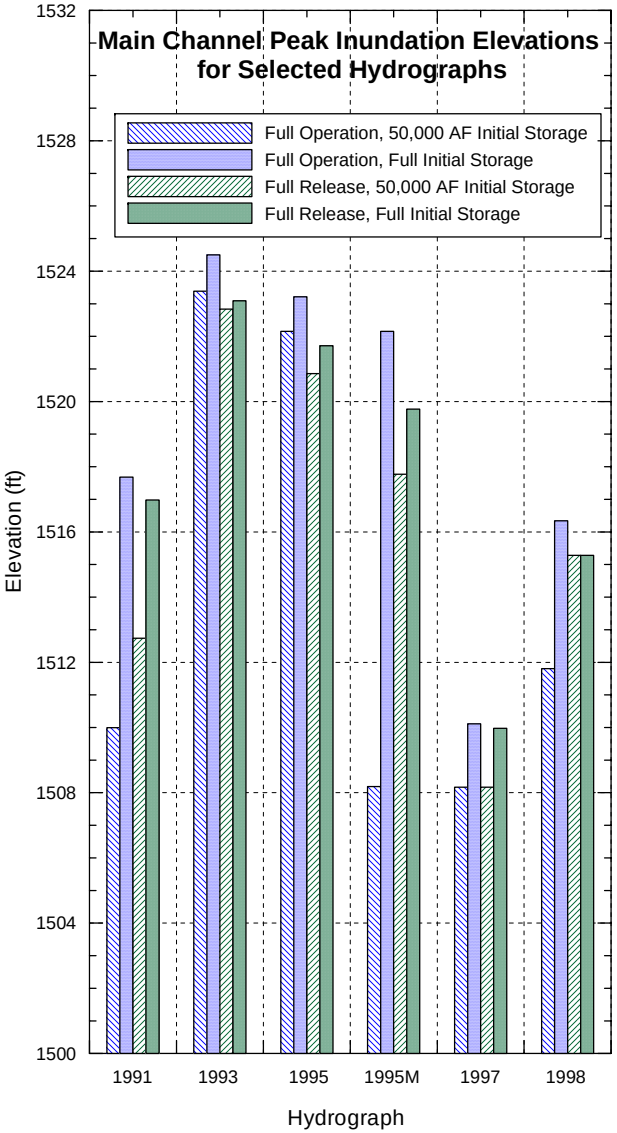

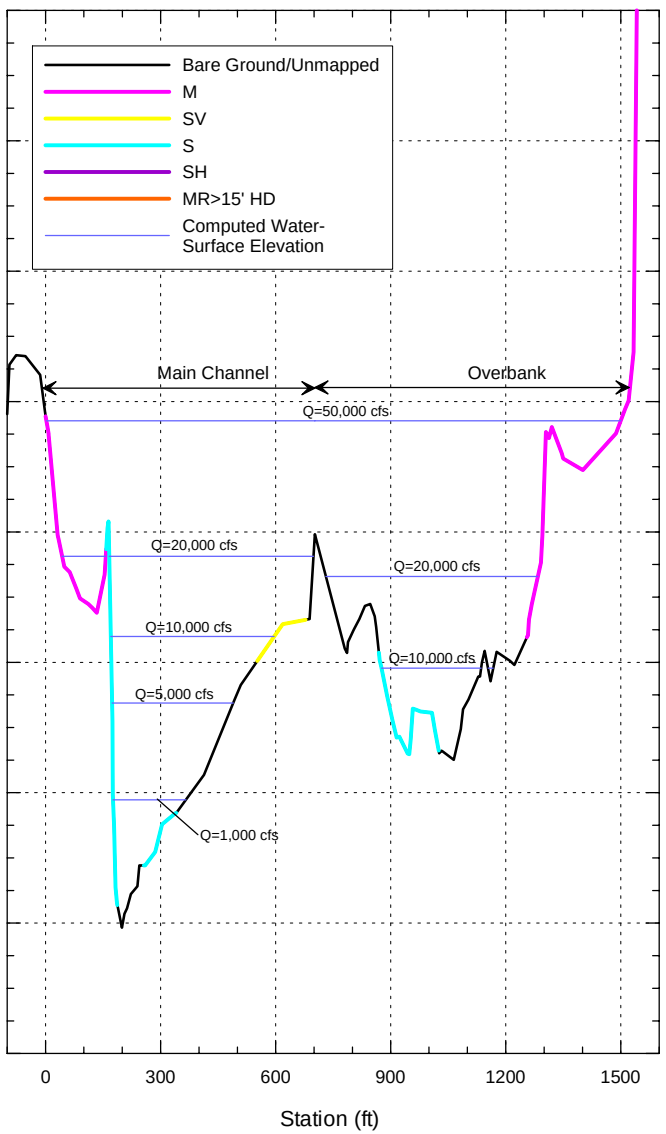

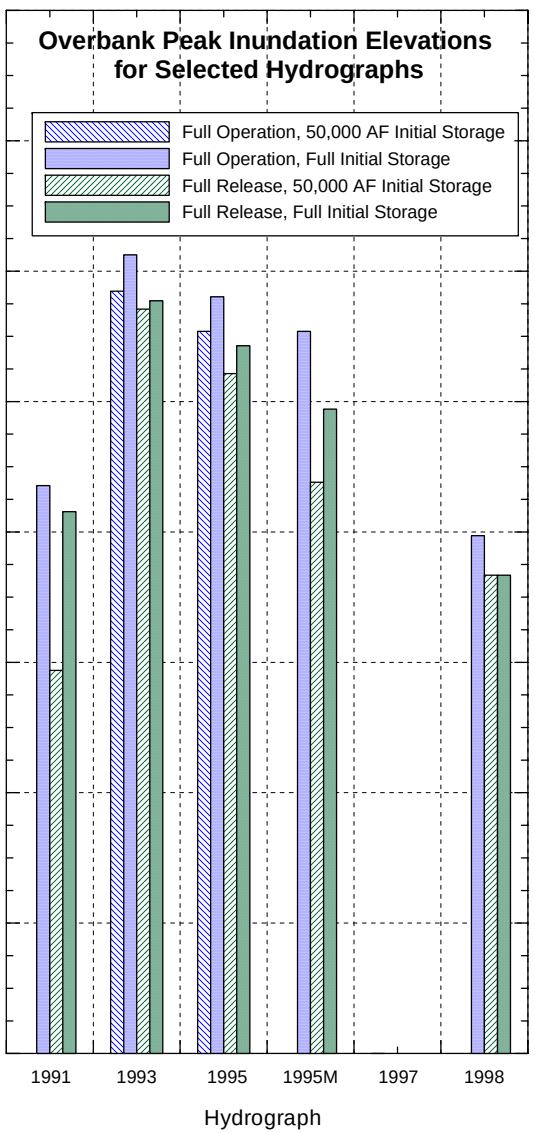

Site 3, Cross Section 4

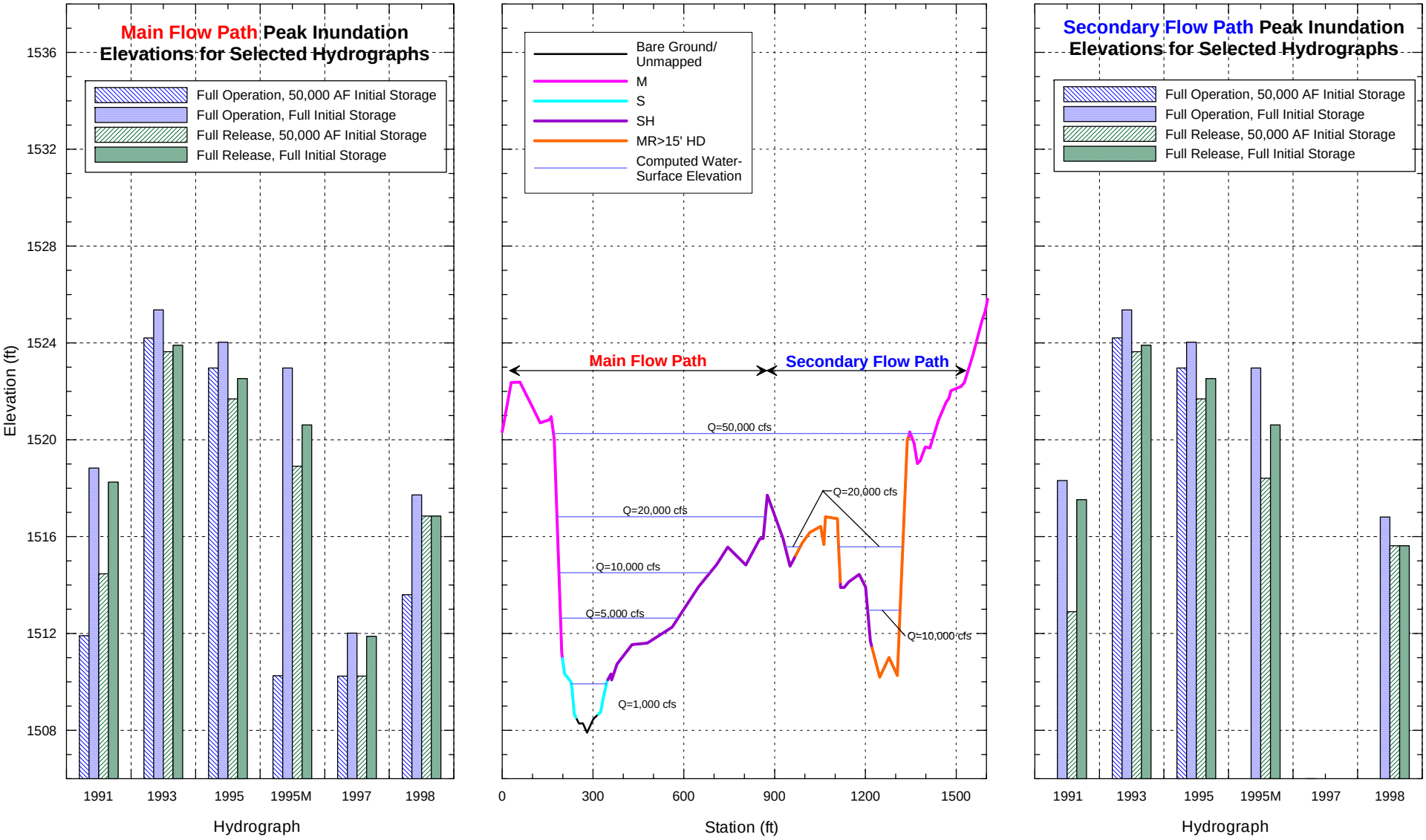

Site 3, Cross Section 5

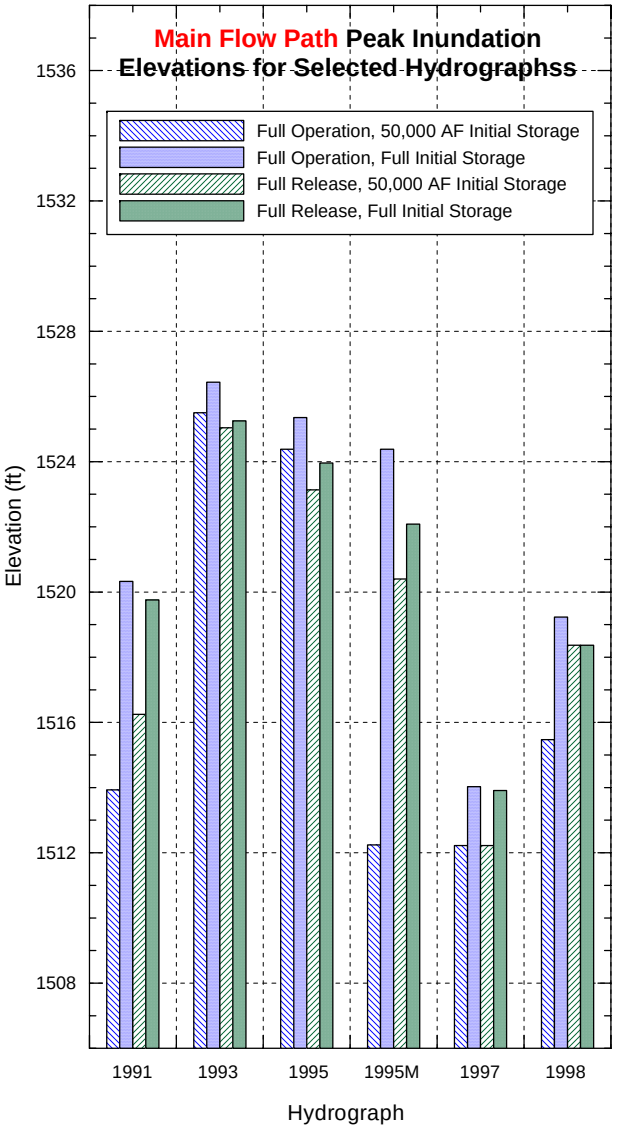

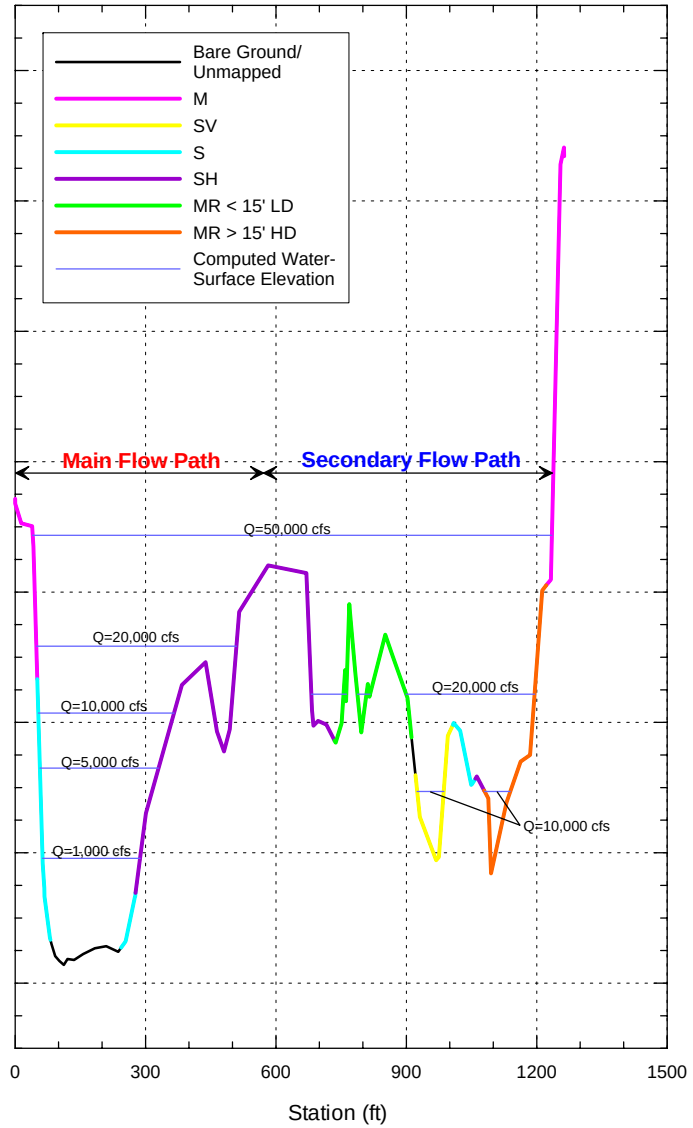

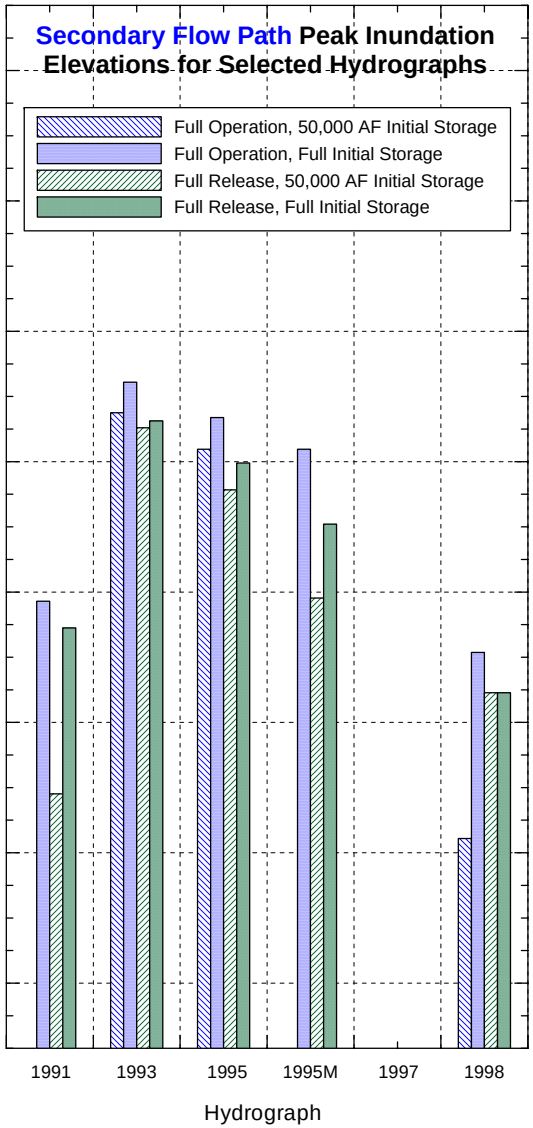

Site 3, Cross Section 7

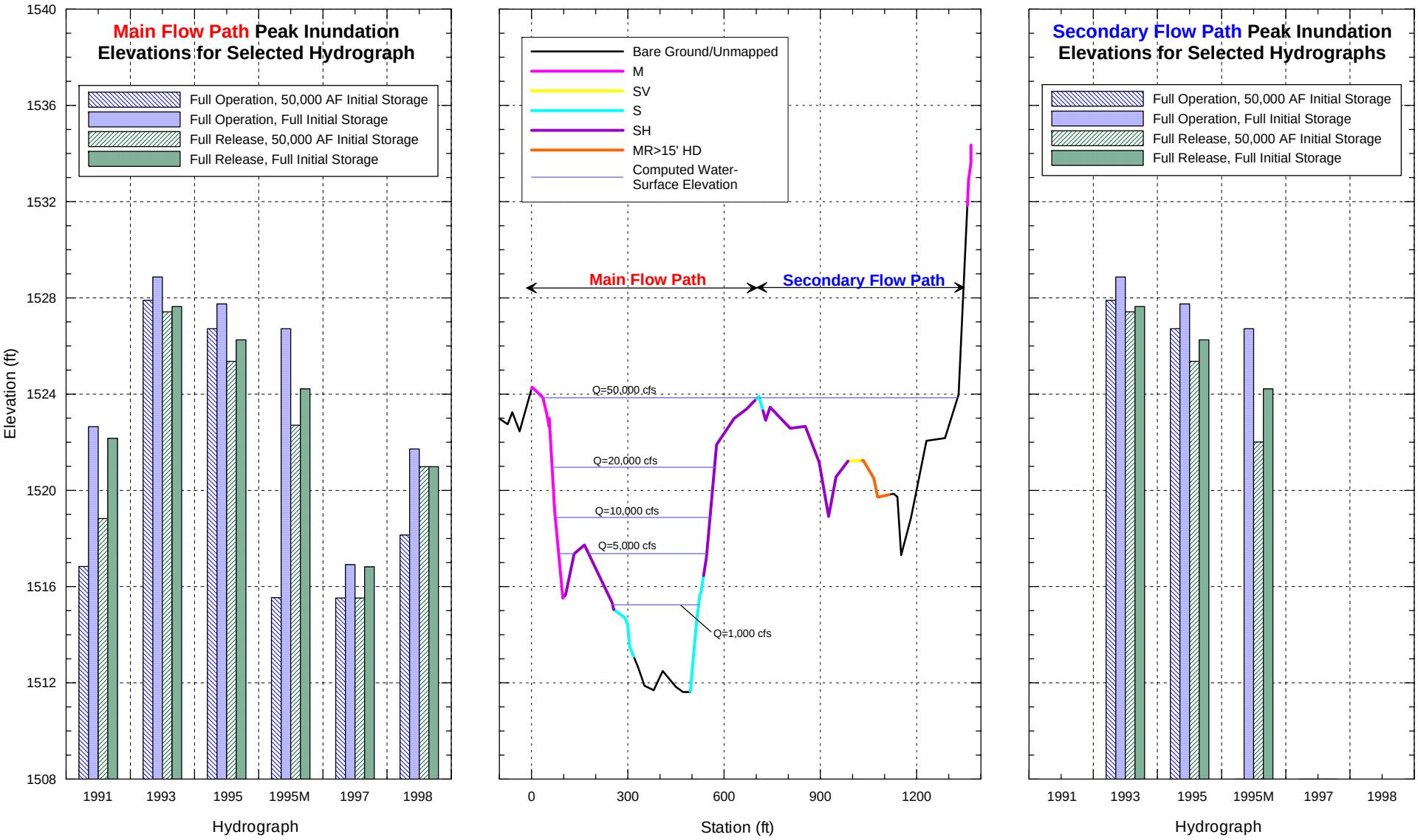

Site 3, Cross Section 8

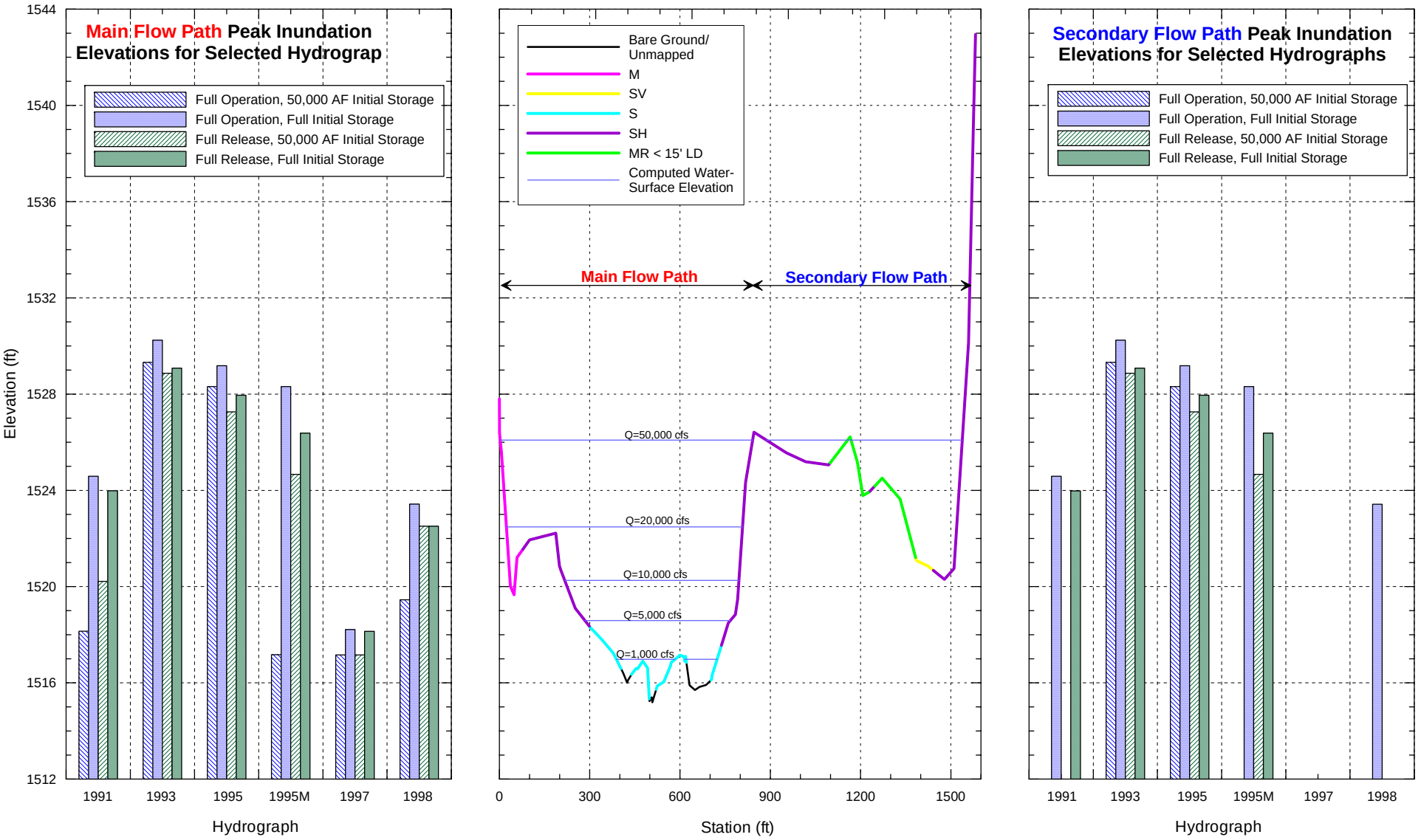

APPENDIX E

Inundation, Critical Discharge, and Sediment Mobilization Duration Data for Various Geomorphic Surfaces for the Modeled Operational Scenarios

Site 1 - Main Channel - Inundation
16,000 cfs - 2.1yr RI

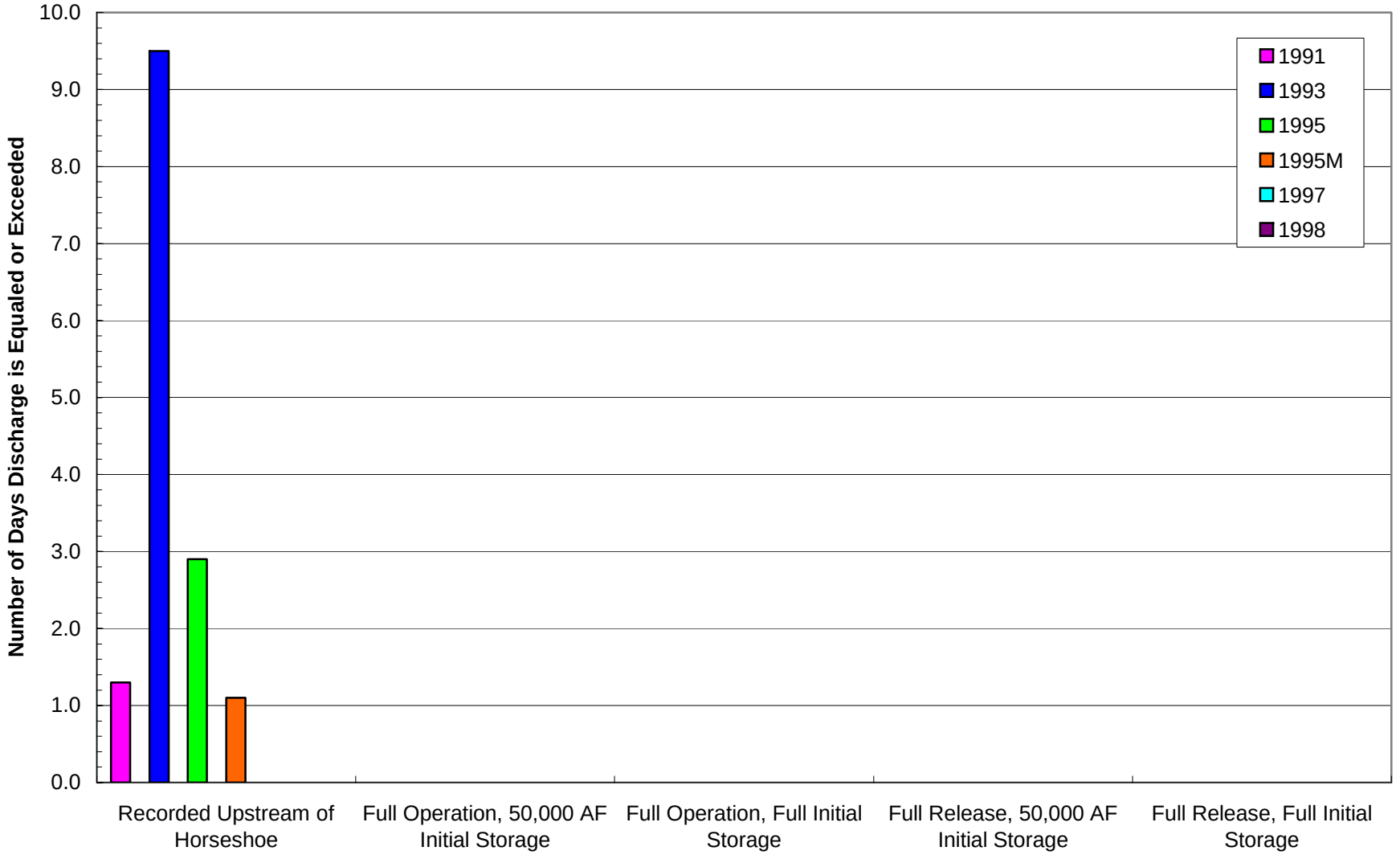

Site 1 - Low Bar - Inundation
16,000 cfs - 2.1yr RI

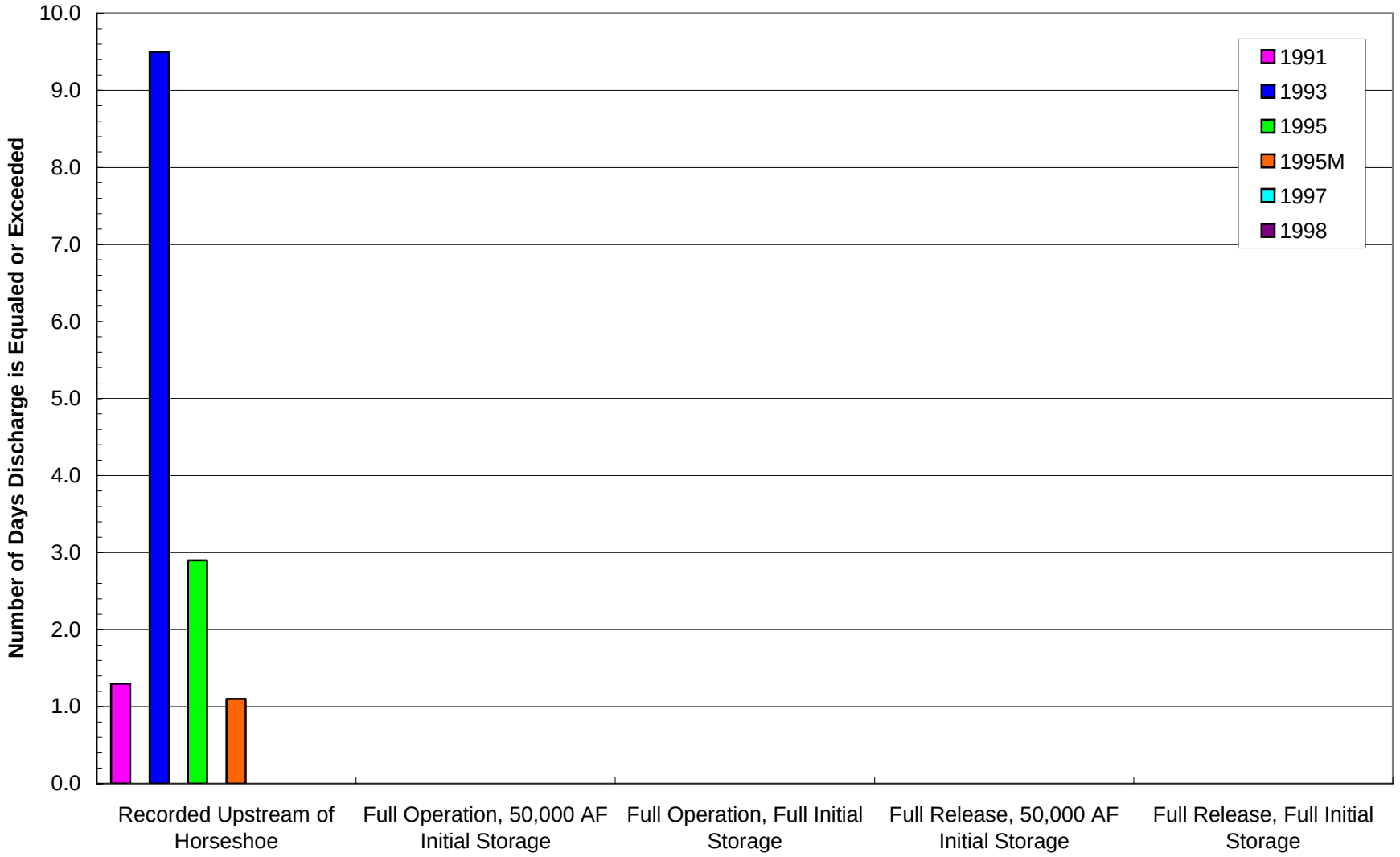

Site 1 - High Bar - Inundation
67,000 cfs - 8.6yr RI

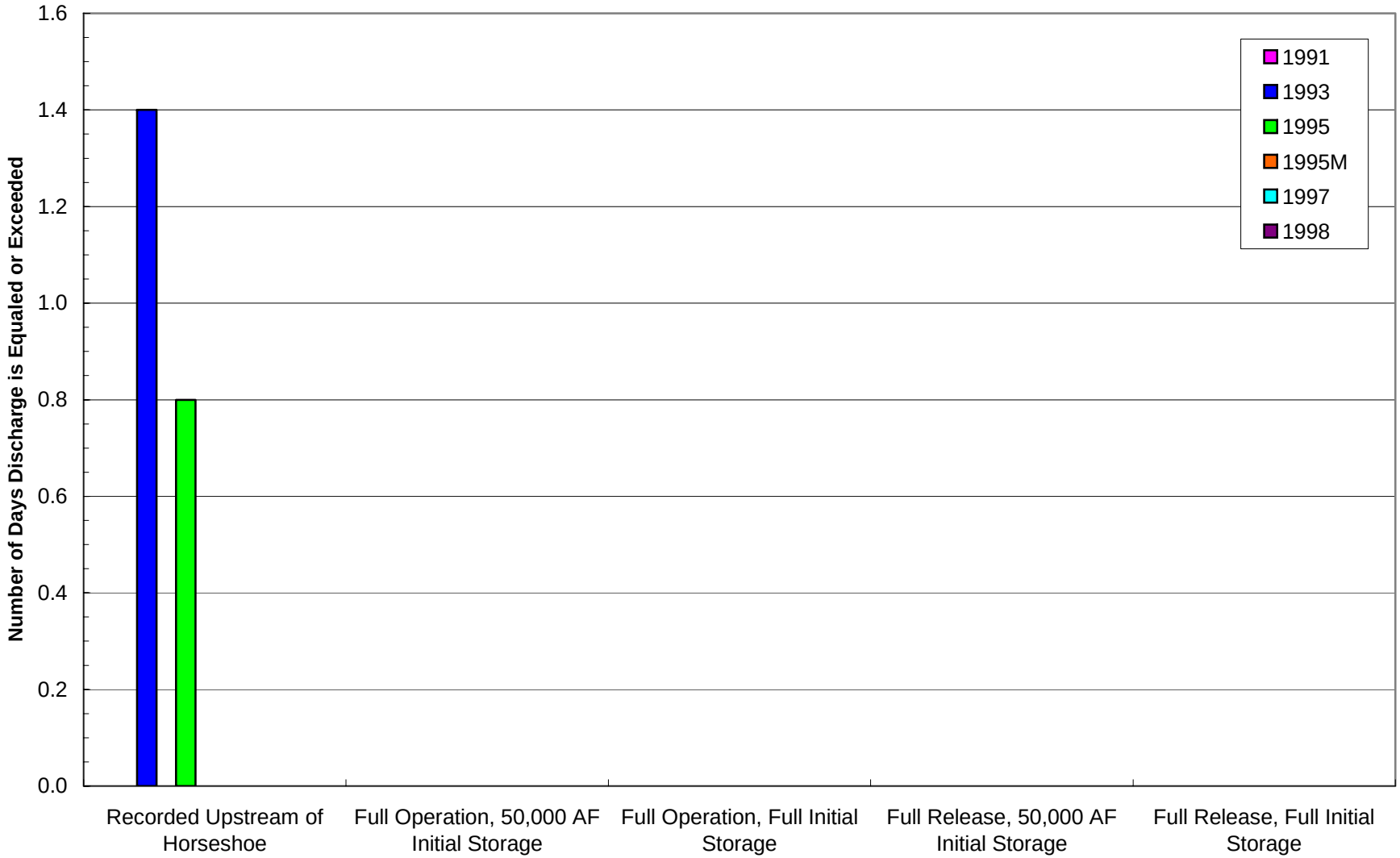

Site 1 - Chute Channels - Inundation
16,000 cfs - 2.1yr RI

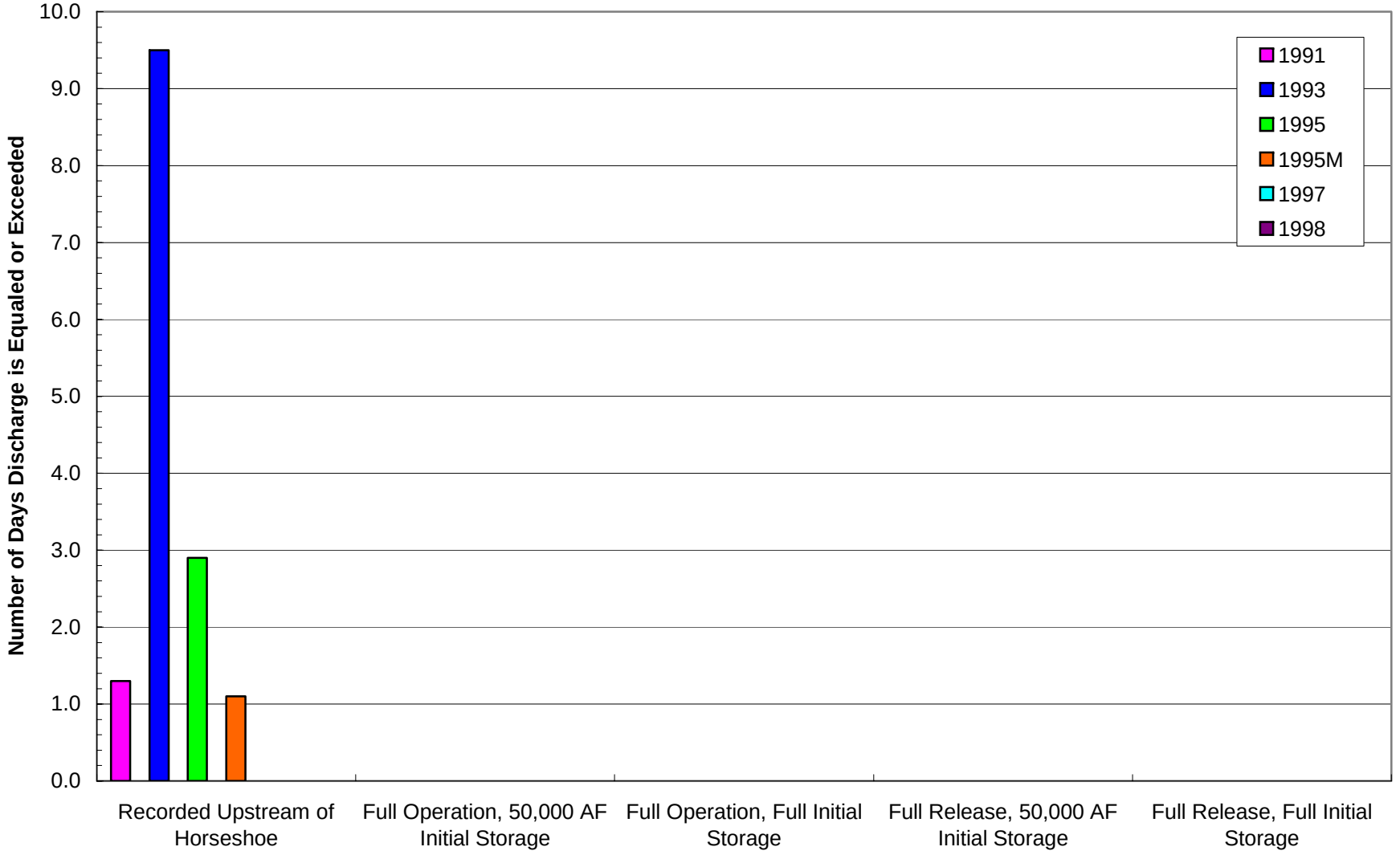

Site 1 - Main Channel - Incipient Motion
4,600 to 28,000 cfs - 1.3 to 3.5yr RI

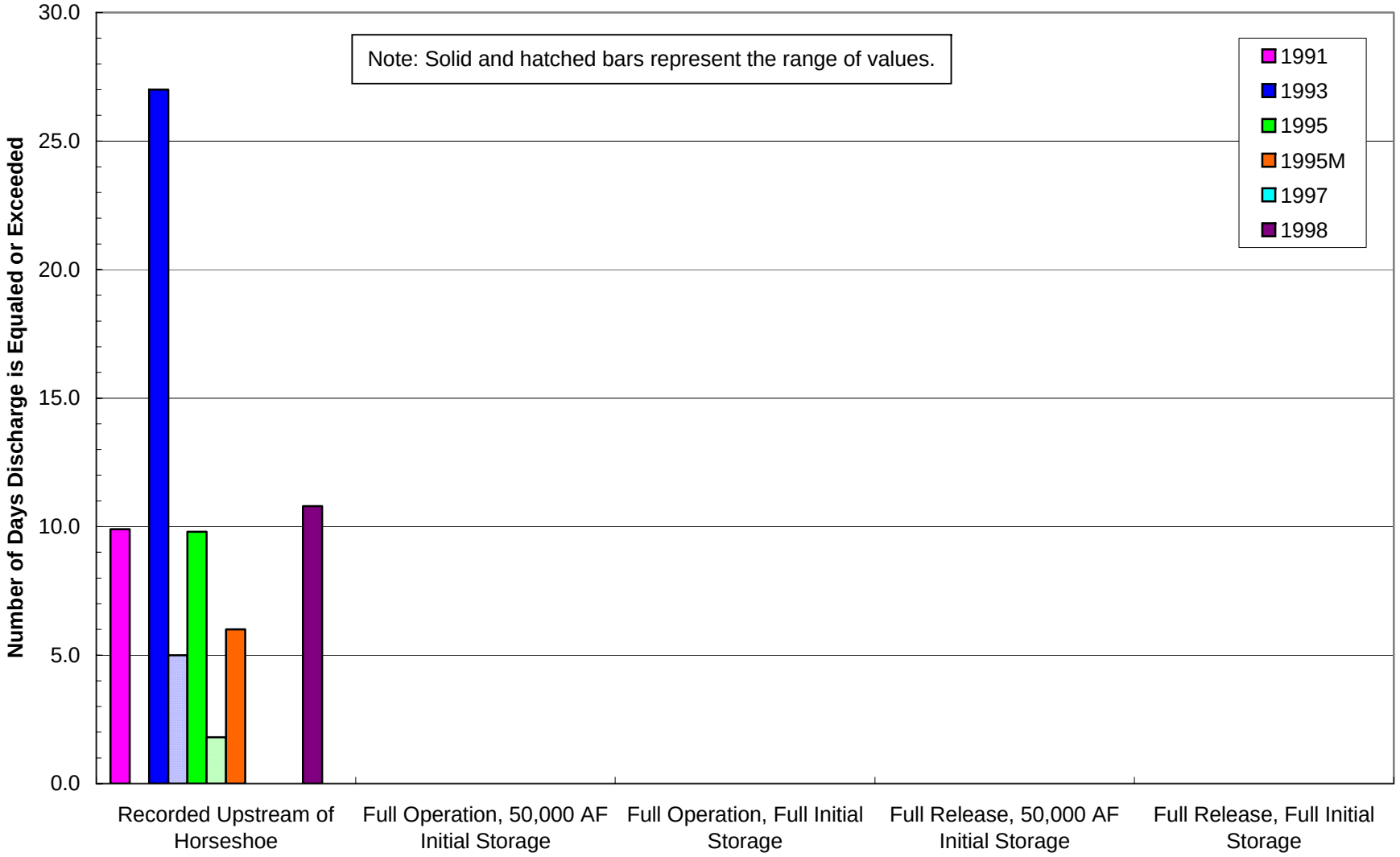

Site 1 - Low Bar - Incipient Motion
35,000 to 60,000 cfs - 4.2 to 7.1yr RI

Site 1 - Main Channel - Measurable Transport
10,000 to 60,000 cfs - 1.6 to 7.1yr RI

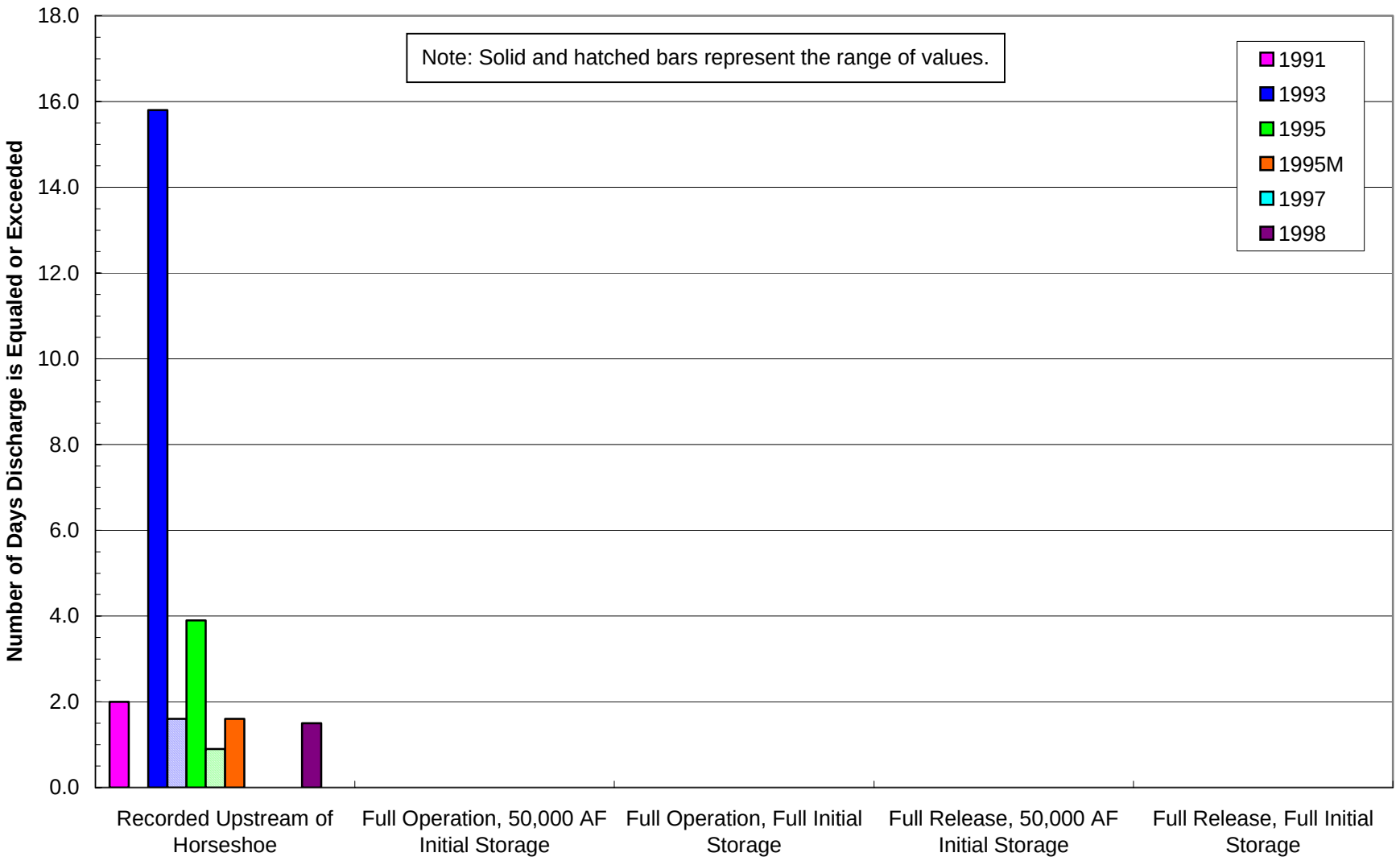

Site 1 - Low Bar - Measurable Transport
50,000 to 110,000 cfs - 6.2 to >30yr RI

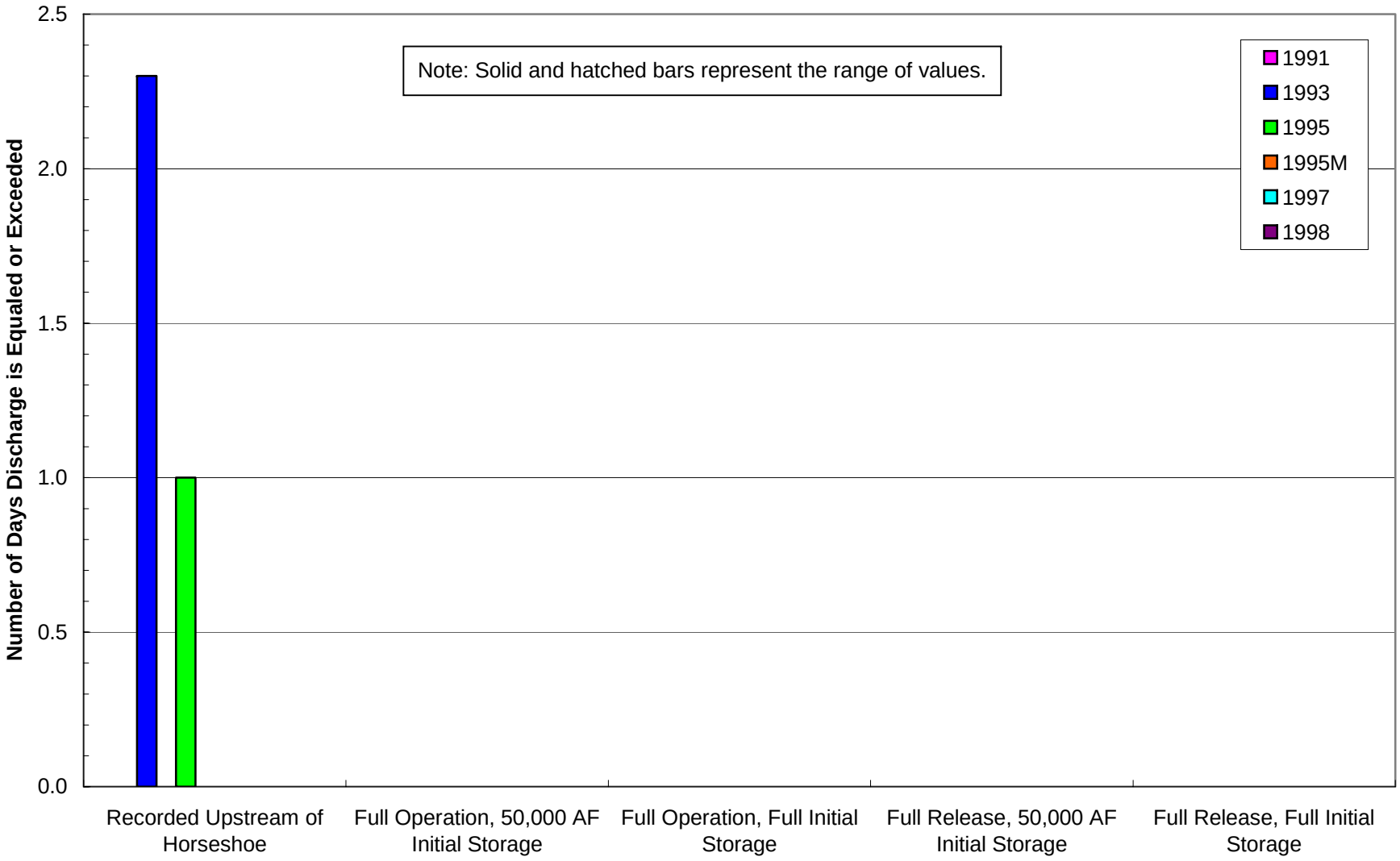

Site 2 - Main Channel - Inundation
20,000 cfs - 4yr RI

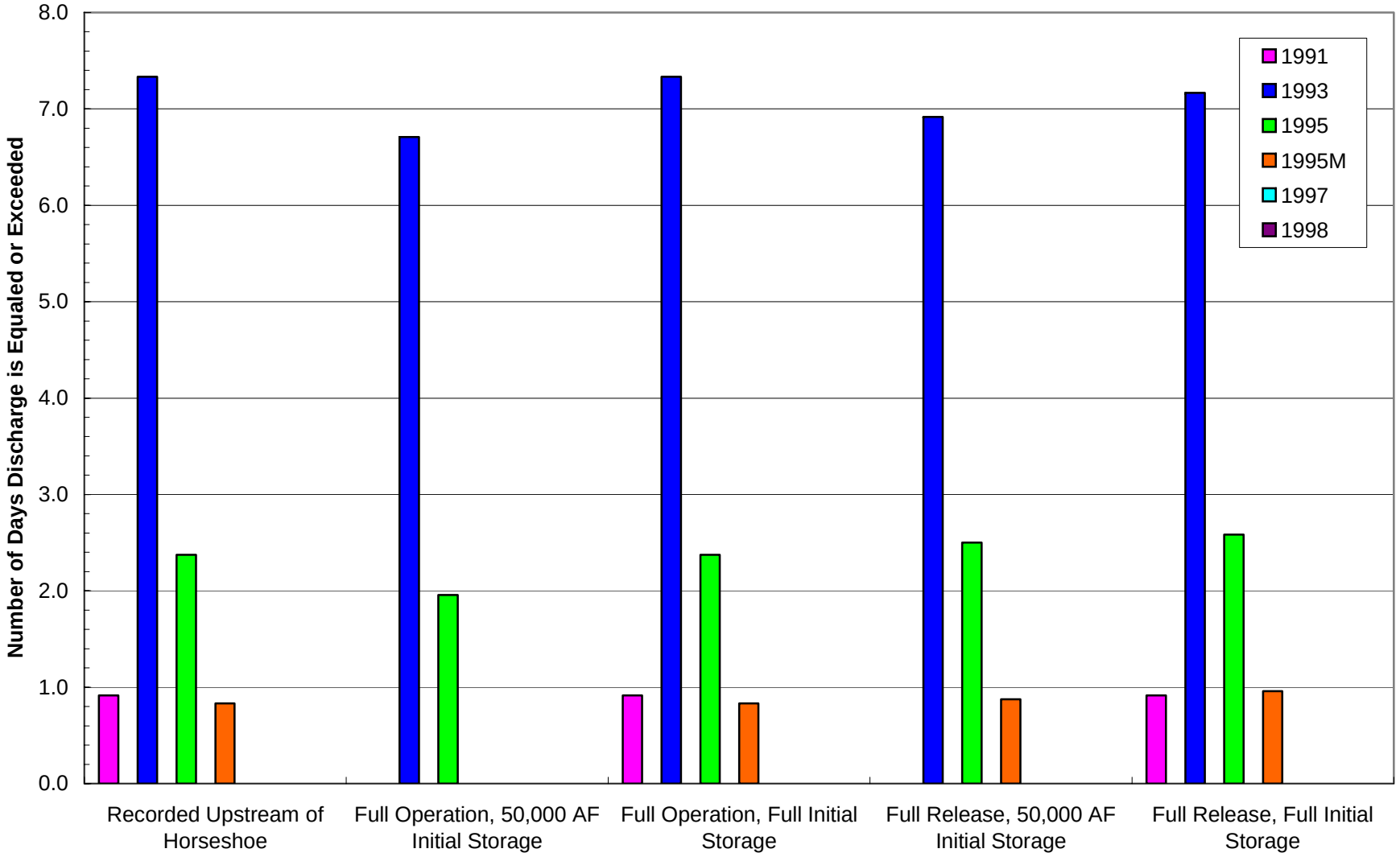

Site 2 - Low Bar - Inundation
10,000 to 20,000 cfs - 2.5 to 4yr RI

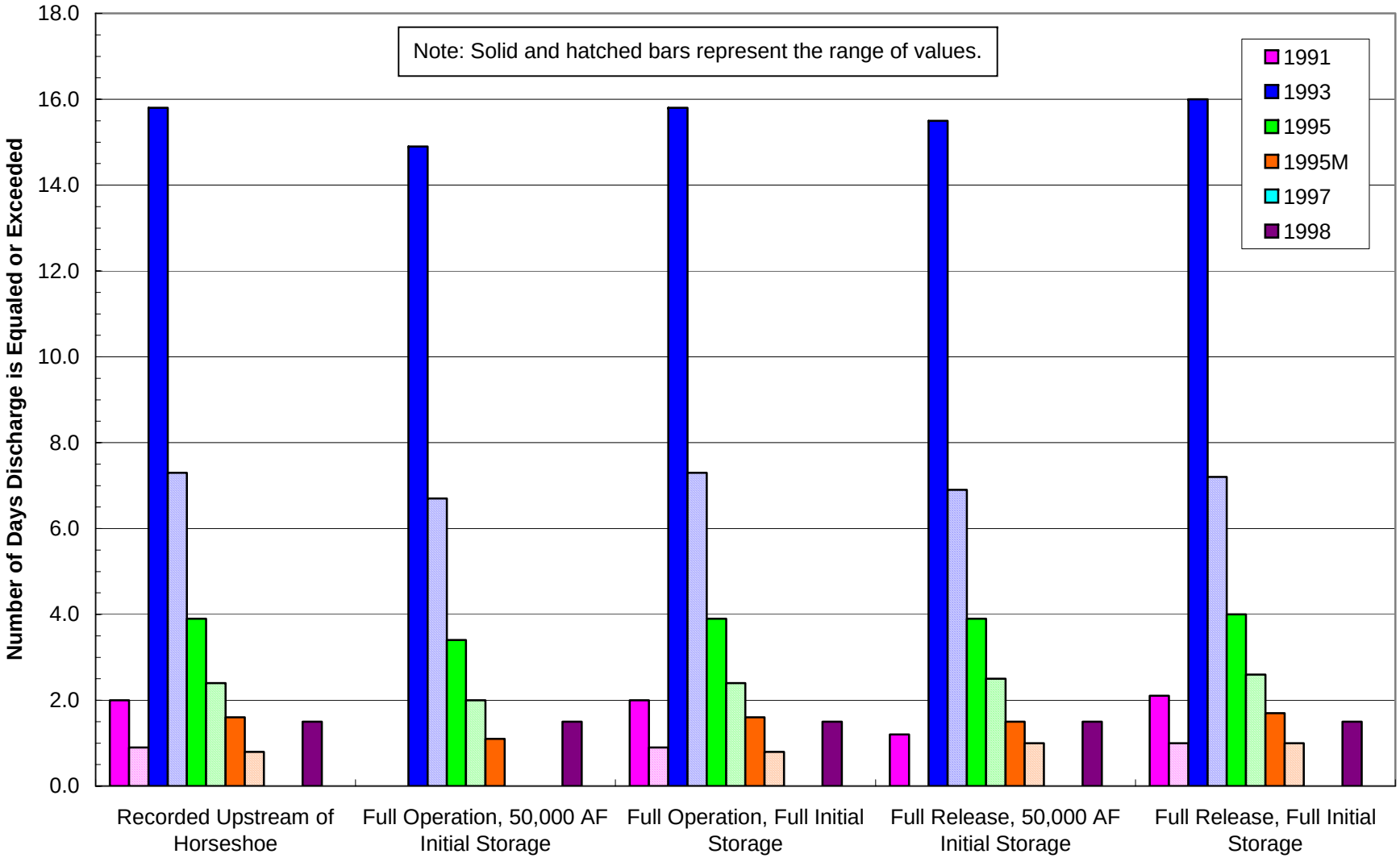

Site 2 - High Bar - Inundation
55,000 cfs - 10yr RI

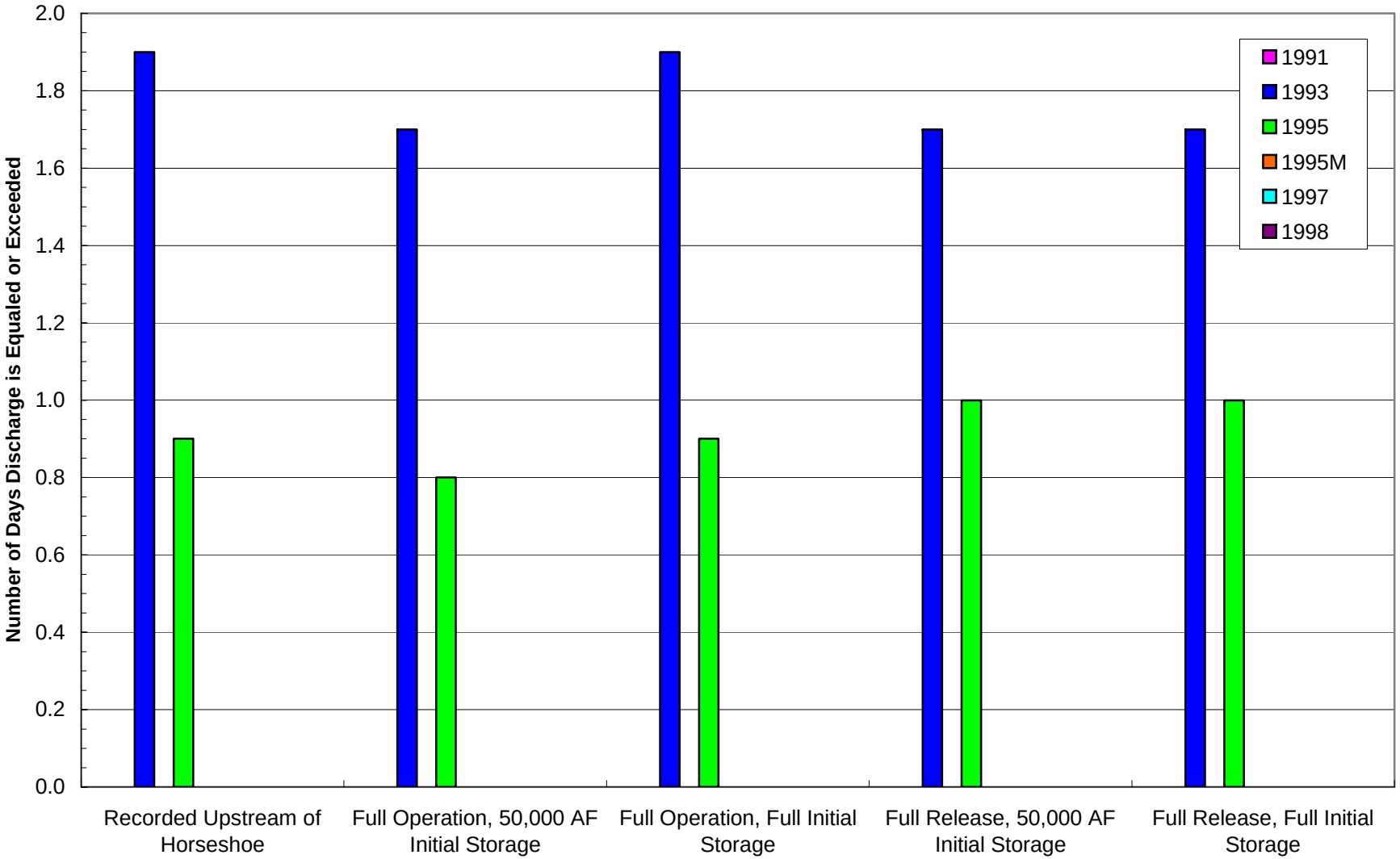

Site 2 - Chute Channels - Inundation
30,000 to 55,000 cfs - 6 to 10yr RI

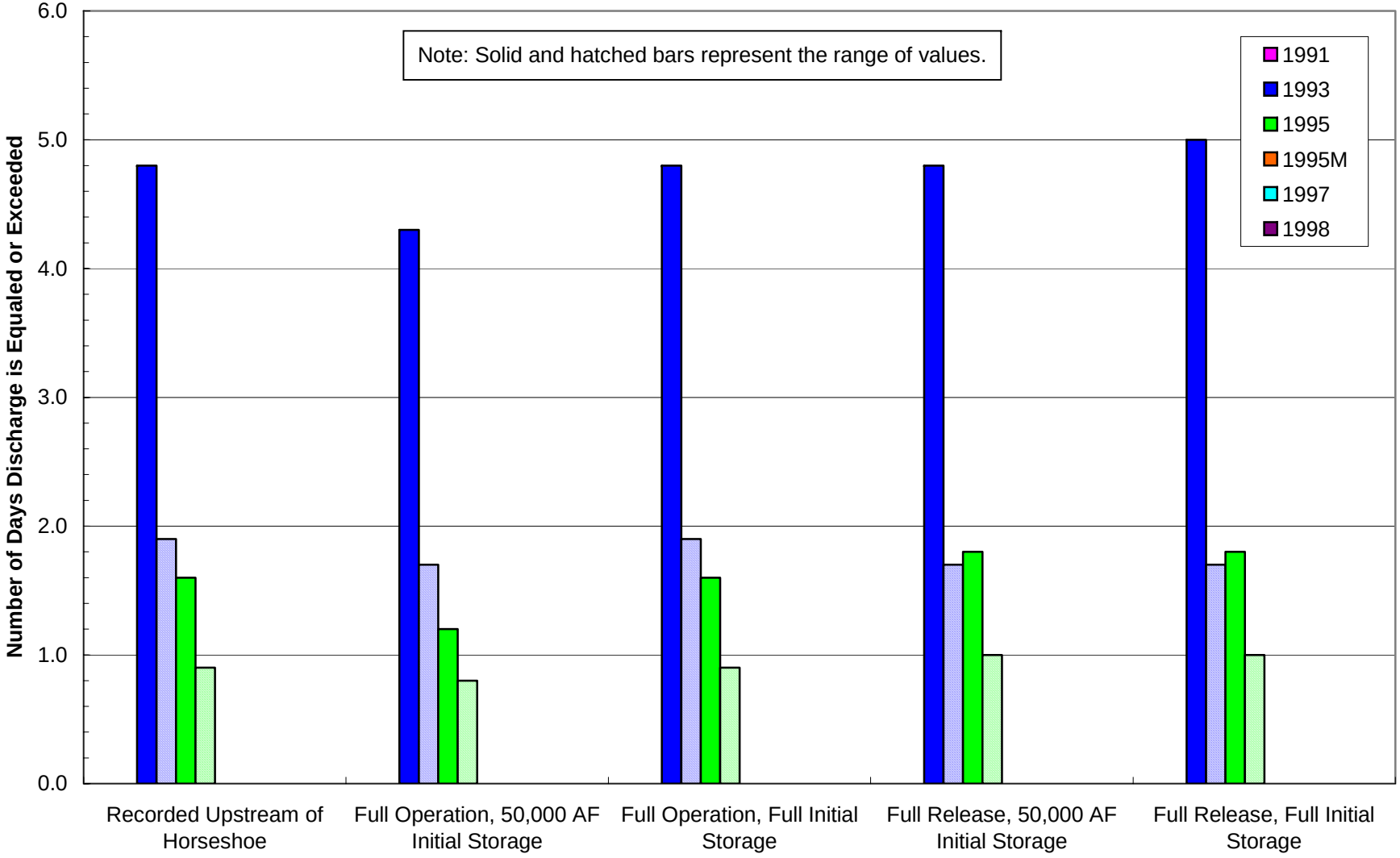

Site 2 - Main Channel - Incipient Motion
2,400 to 55,000 cfs - 1.1 to 10yr RI

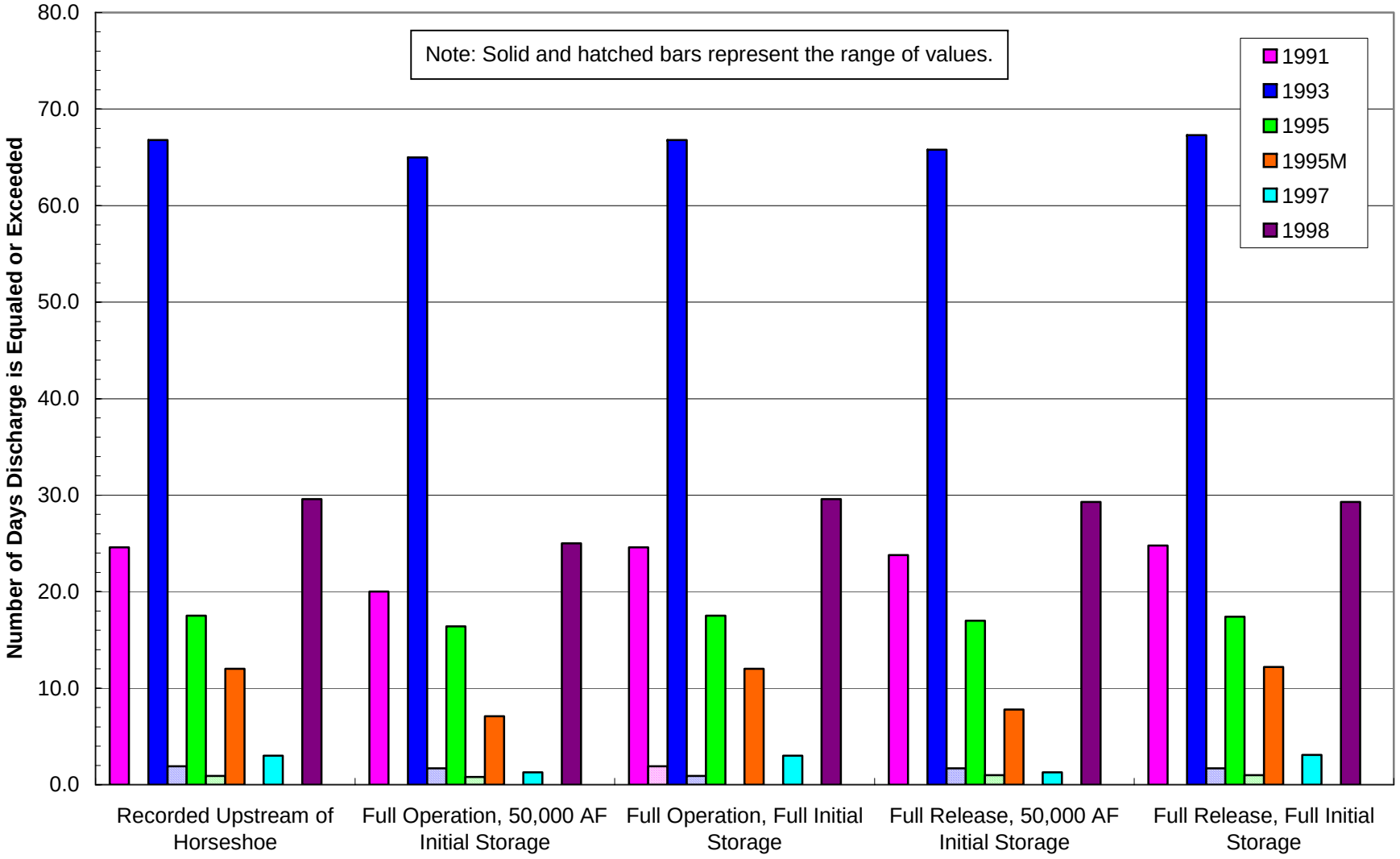

Site 2 - Low Bar - Incipient Motion
32,000 to 50,000 cfs - 6 to 8yr RI

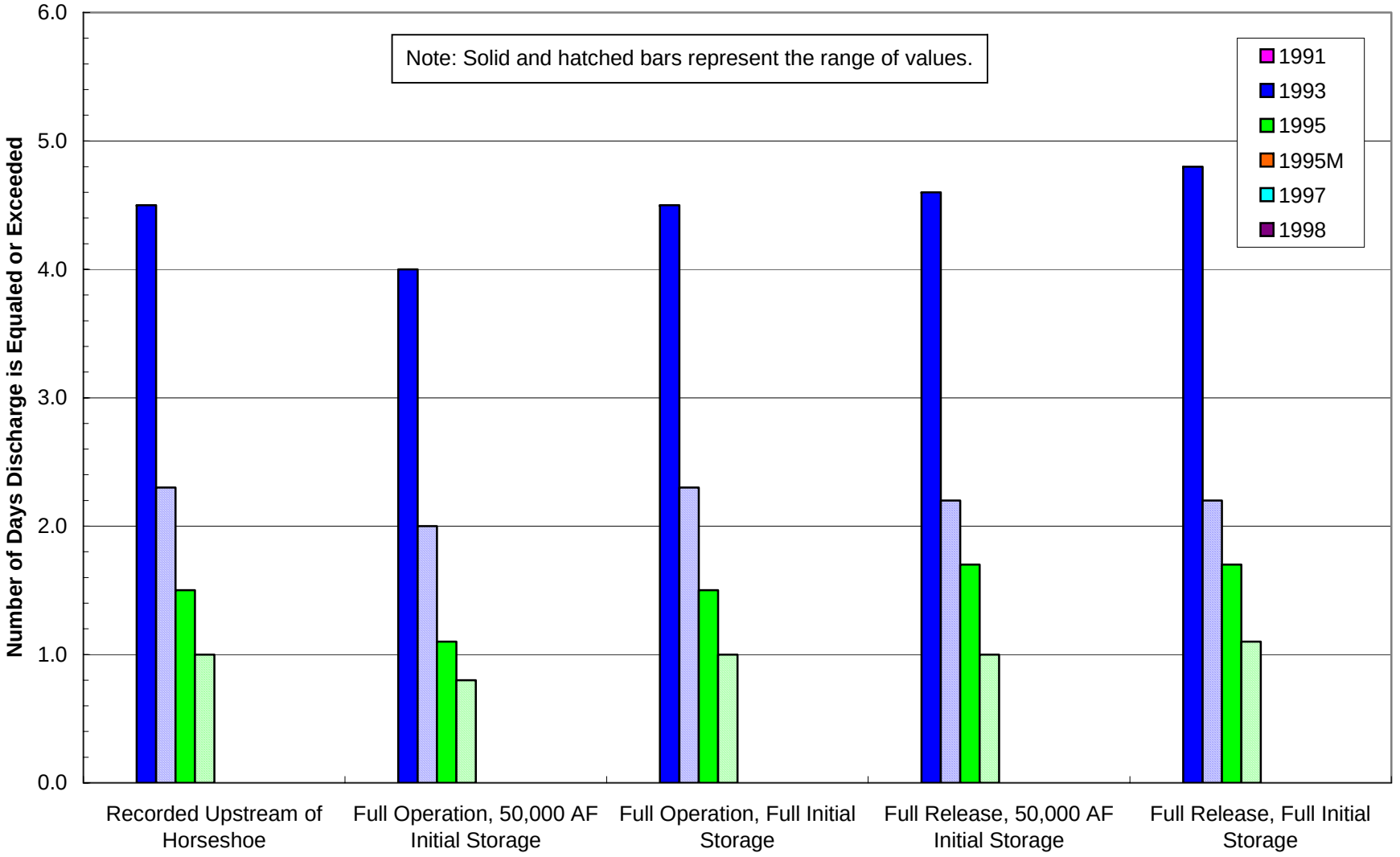

Site 2 - Main Channel - Measurable Transport
3,200 to 120,000 cfs - 1.3 to >57yr RI

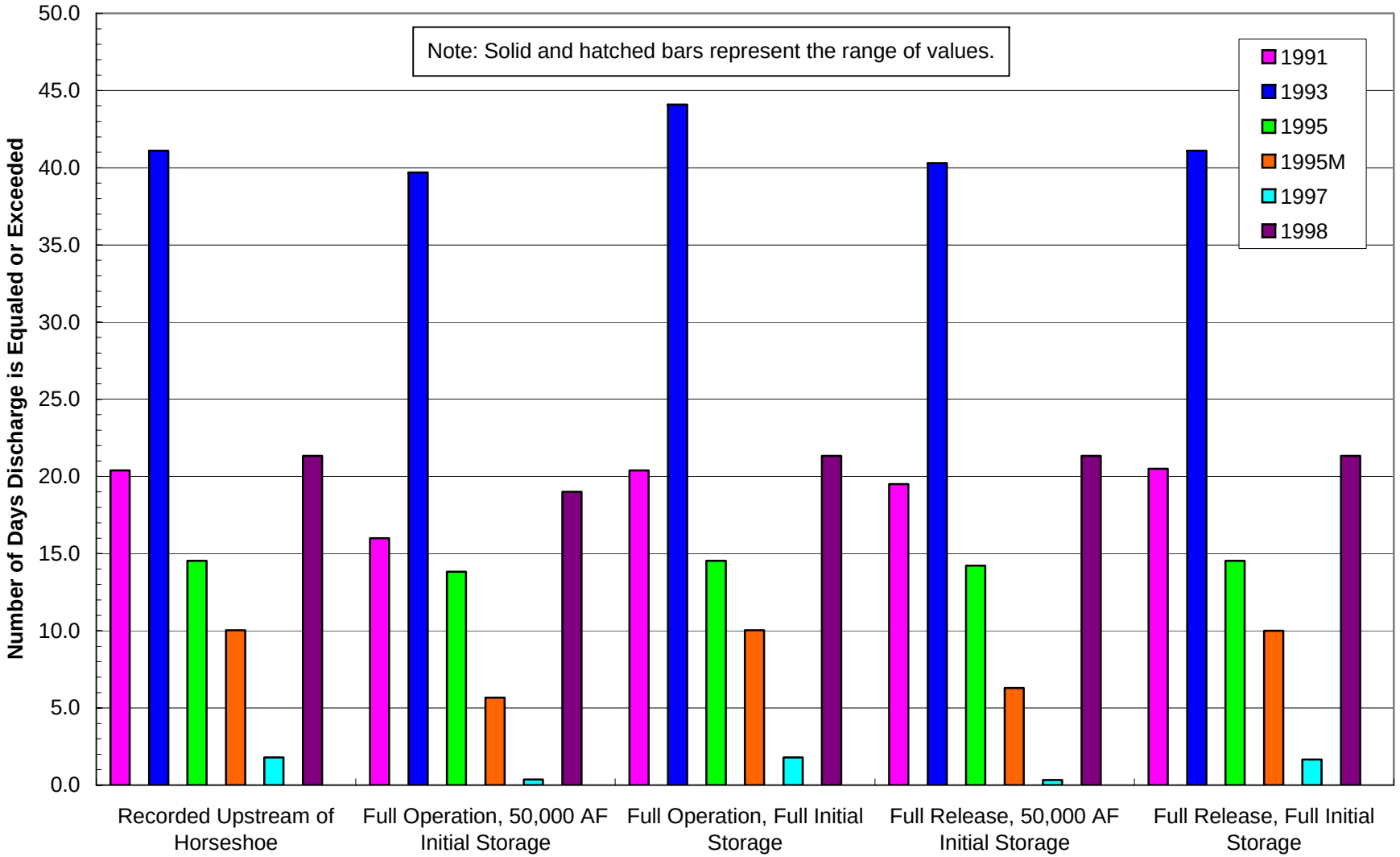

Site 2 - Low Bar - Measurable Transport
42,000 to 170,000 cfs - 7 to >57yr RI

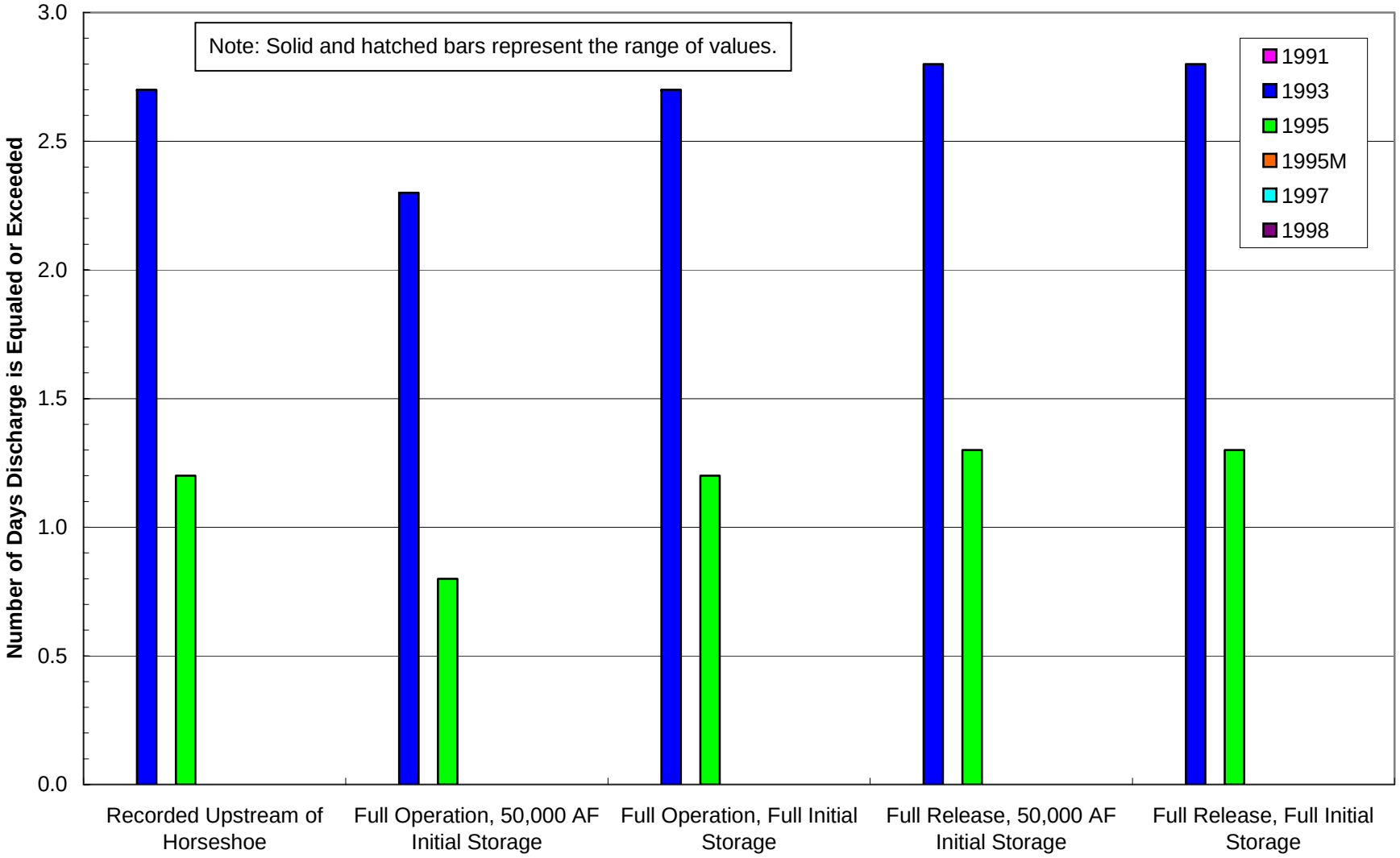

Site 3 - Main Channel - Inundation
20,000 cfs - 8.4yr RI

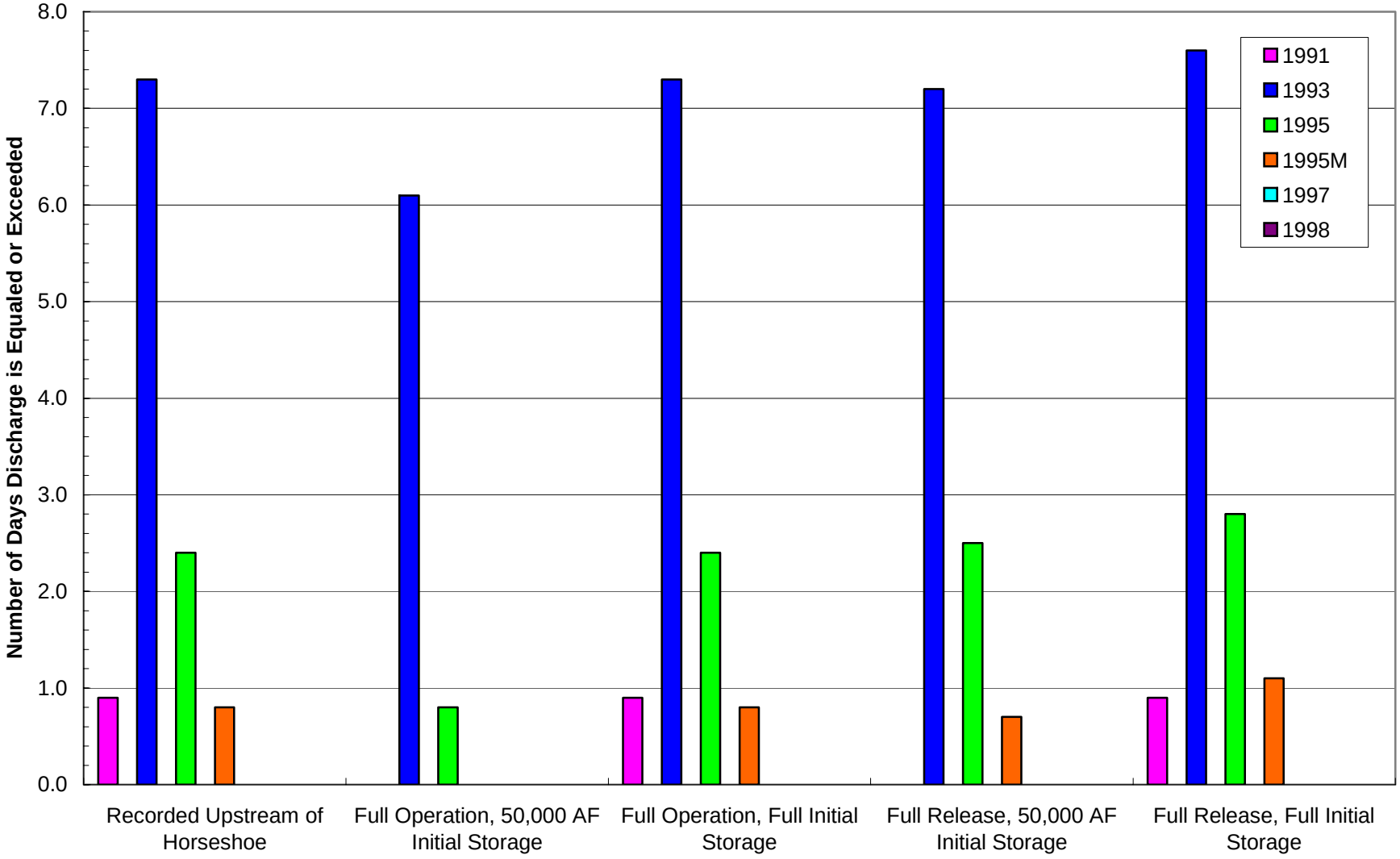

Site 3 - Low Bar - Inundation
10,000 to 20,000 cfs - 4.8 to 8.4yr RI

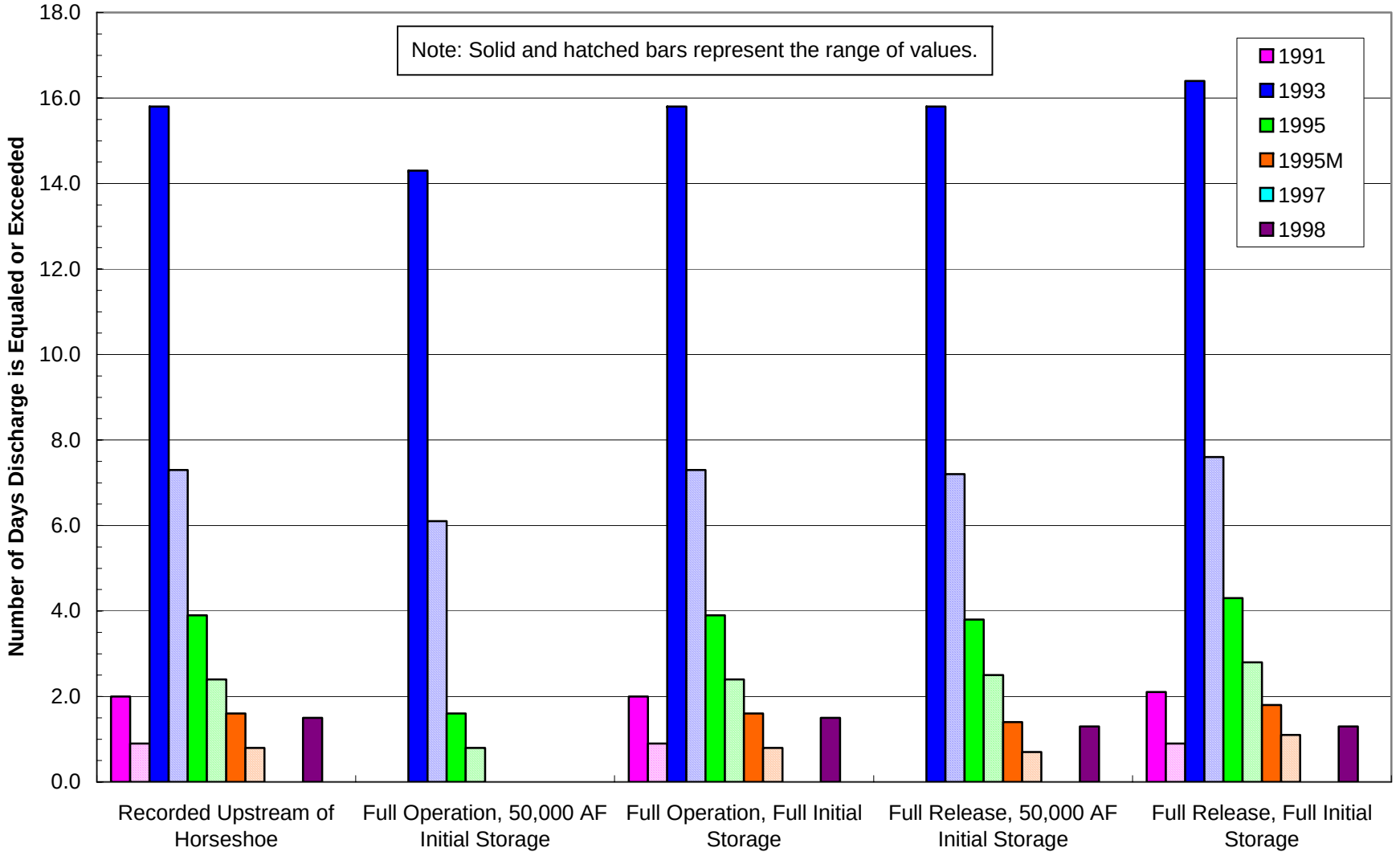

Site 3 - High Bar - Inundation
50,000 cfs - 10.6yr RI

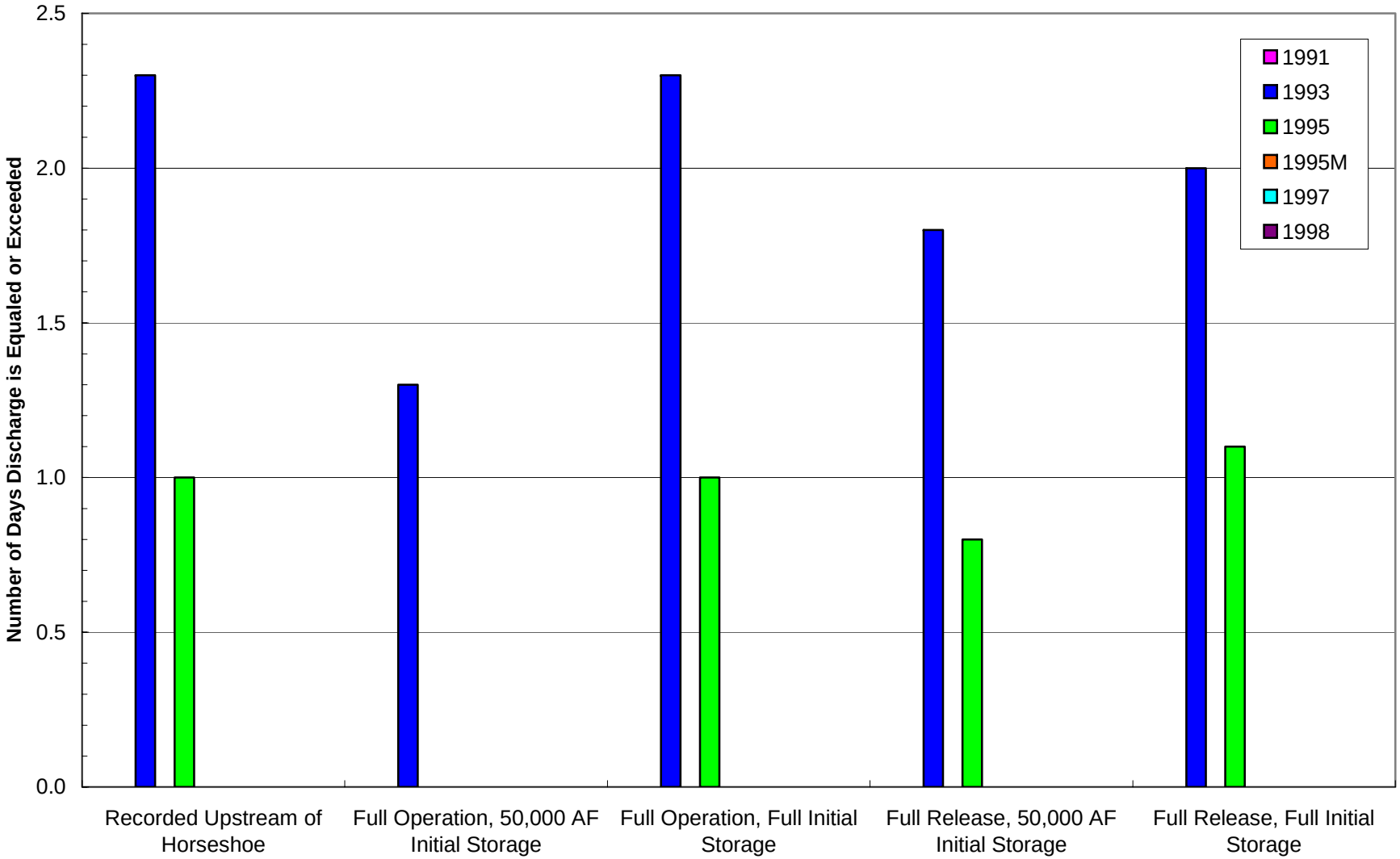

Site 3 - Chute Channels - Inundation
10,000 to 50,000 cfs - 4.8 to 10.6yr RI

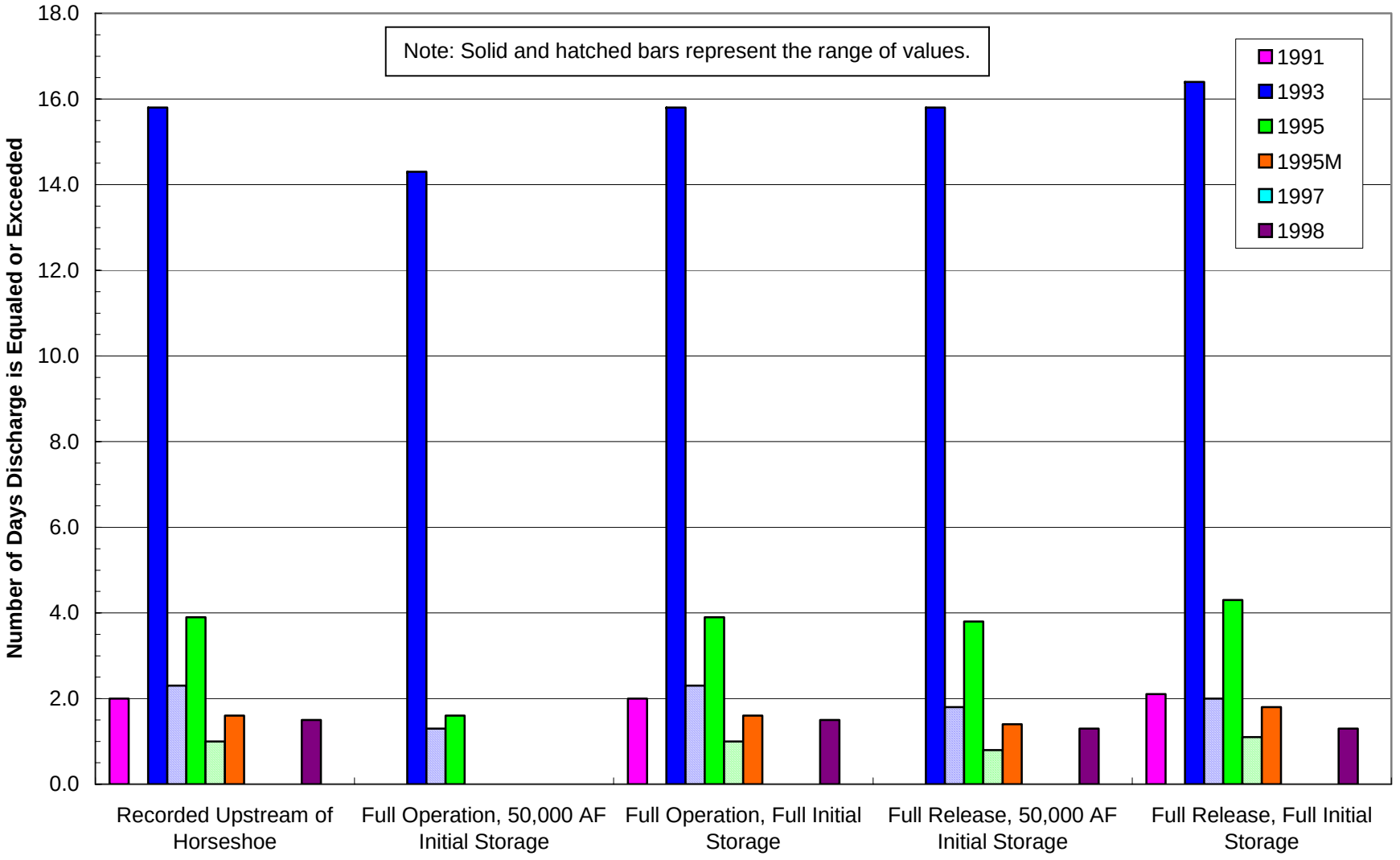

Site 3 - Main Channel - Incipient Motion
2,200 to 16,000 cfs - 1.9 to 7.7yr RI

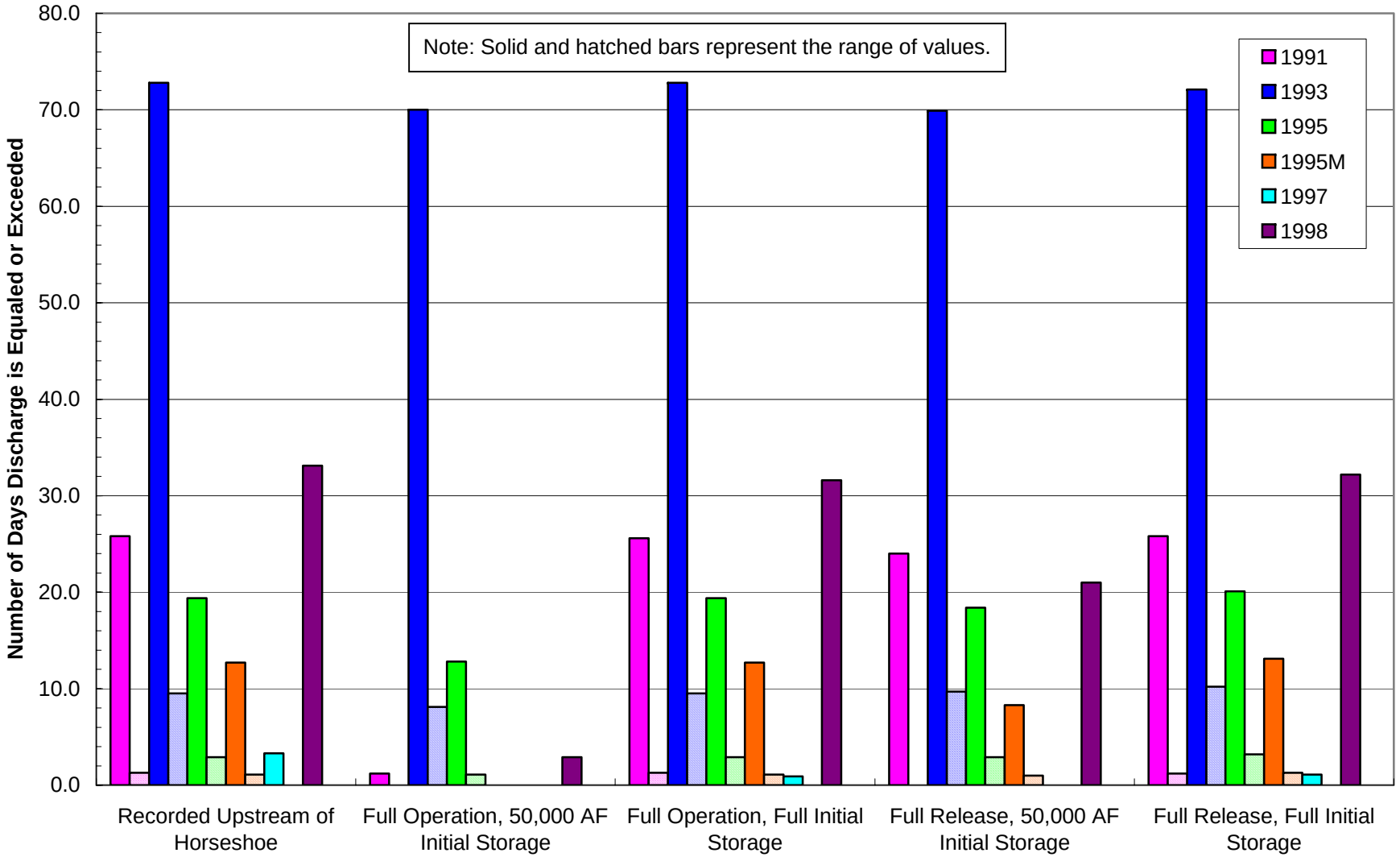

Site 3 - Low Bar - Incipient Motion
20,000 to 150,000 cfs - 8.4 to 47yr RI

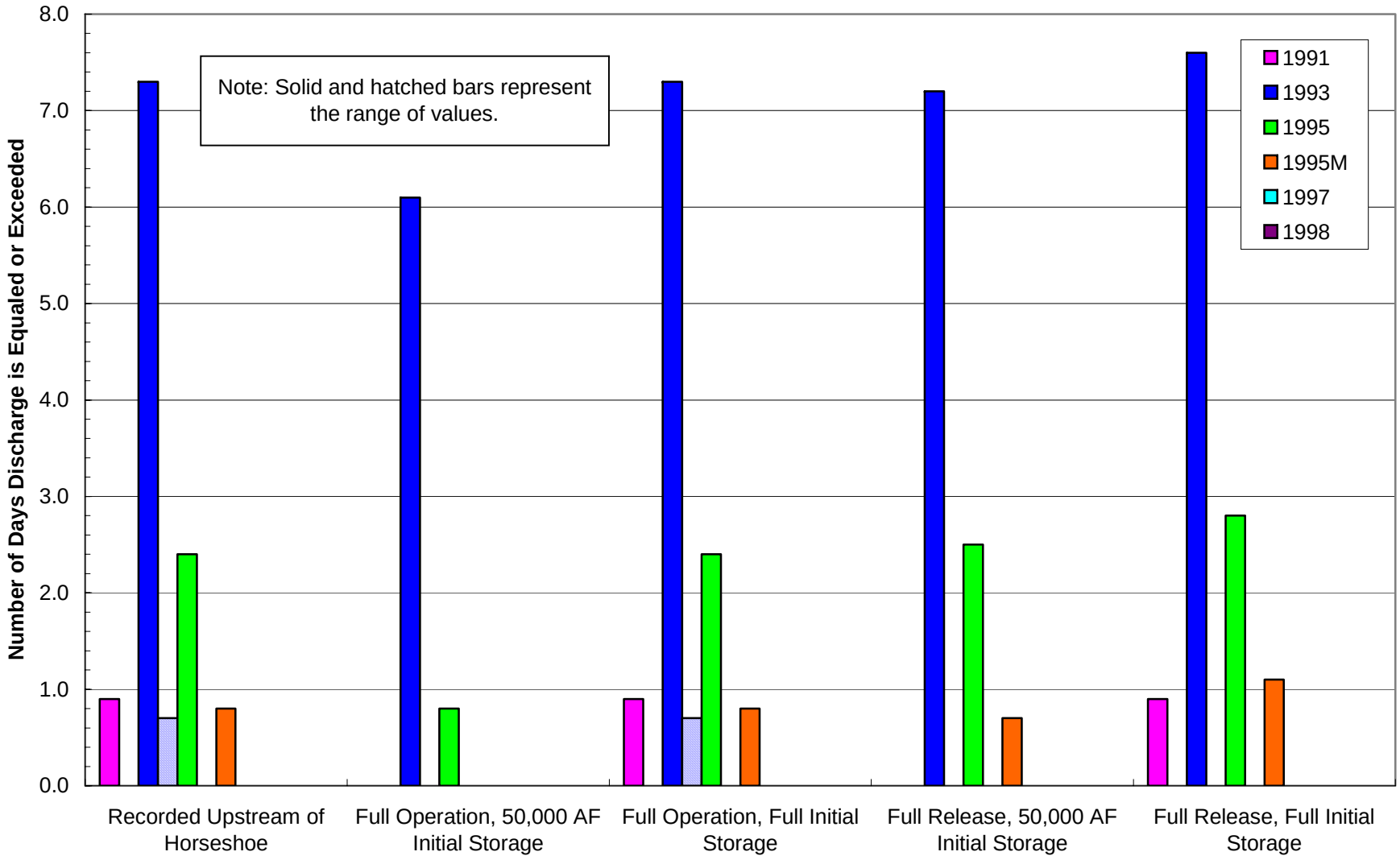

Site 3 - Chute Channels - Incipient Motion
40,000 to 180,000 cfs - 9 to >57yr RI

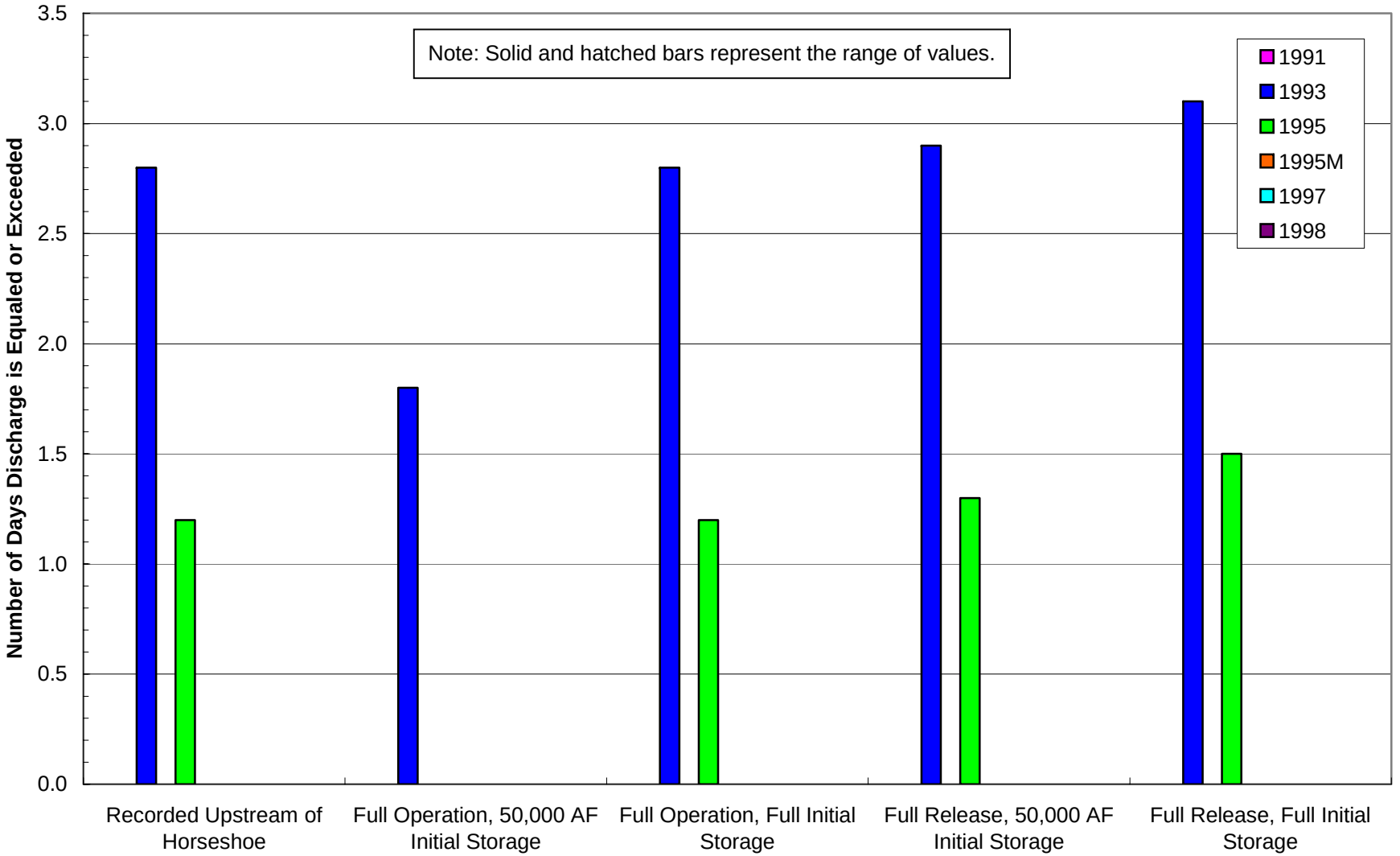

Site 3 - Main Channel - Measurable Transport
5,000 to 90,000 cfs - 3.5 to 22.6yr RI

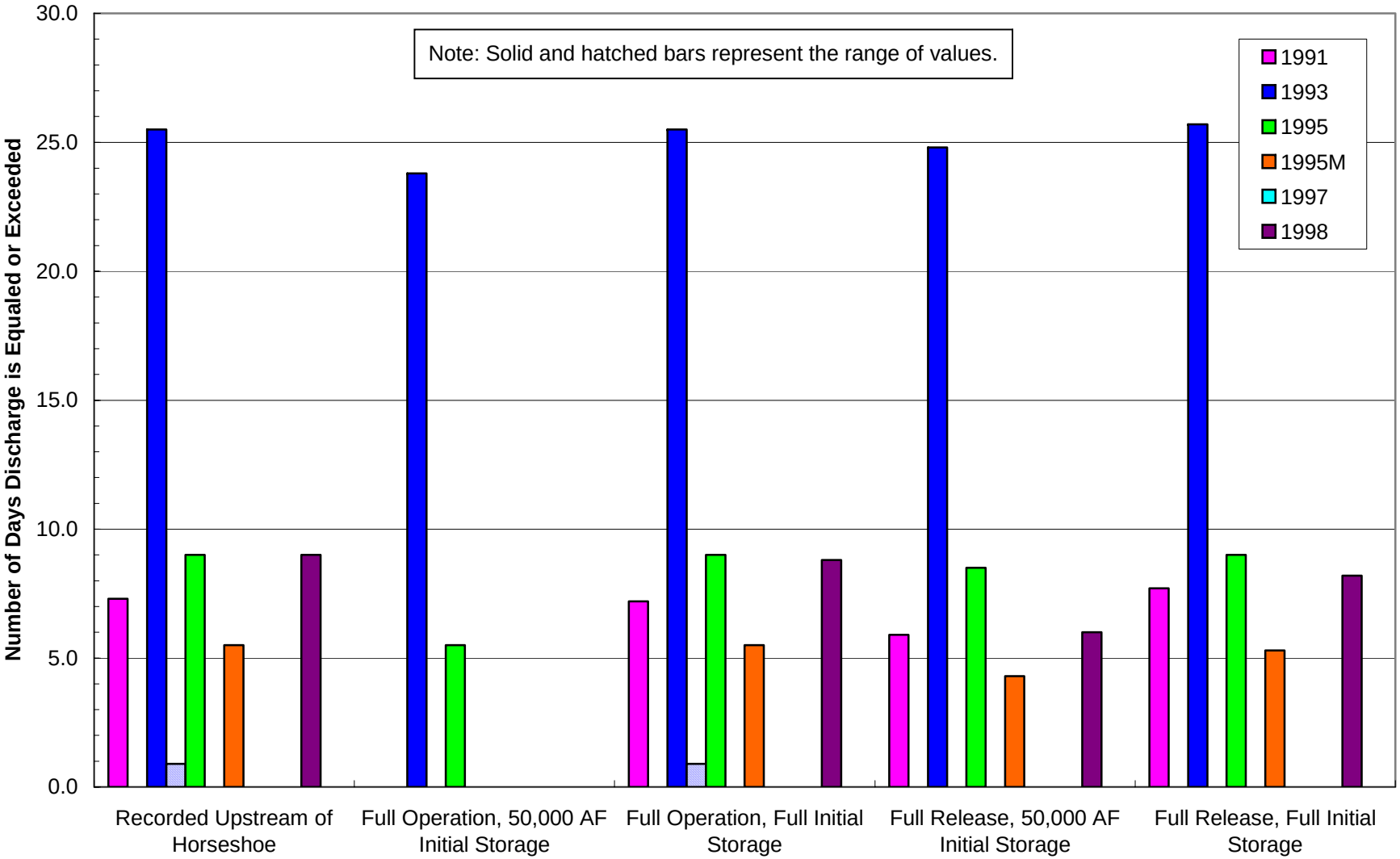

Site 3 - Low Bar - Measurable Transport
40,000 to 190,000 cfs - 9 to >57yr RI

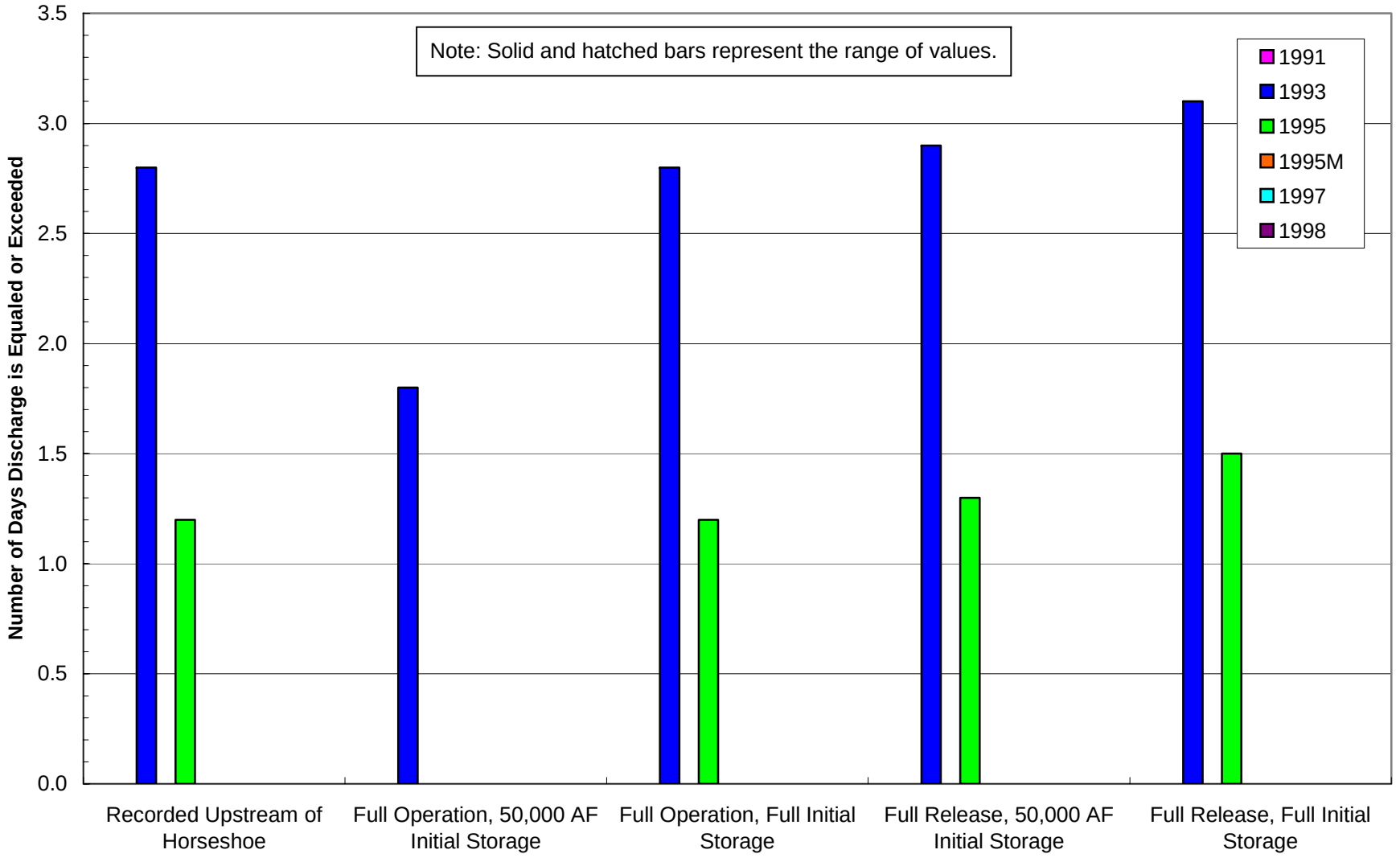

Site 3 - Chute Channels - Measurable Transport
55,000 to 150,000 cfs - 12 to >57yr RI